

# The Assignment of Absolute Configuration by NMR<sup>†</sup>

José Manuel Seco, Emilio Quiñoá, and Ricardo Riguera\*

Departamento de Química Orgánica and Unidad de RMN de Biomoléculas Asociada al CSIC, Universidad de Santiago de Compostela, E-15782, Santiago de Compostela, Spain

Received November 18, 2002

## Contents

|  |    |   |     |
|--|----|---|-----|
| 1. Introduction and Scope  | 17 | 3.9. Application to Chiral Polyhydroxylated Compounds   | 92  |
| 2. Methods Based on Chiral Derivatizing Reagents (CDAs): General Characteristics       | 19 | 3.9.1. MPA and 9-AMA  | 94  |
| 2.1. Description of the Method   | 19 | 3.9.2. MTPA   | 96  |
| 2.2. Characteristics of the Auxiliary Reagents   | 20 | 4. Methods Based on a Single Derivatization   | 99  |
| 2.3. The NMR Spectra of the Derivatives  | 20 | 4.1. Application to $\alpha$ -Chiral Secondary Alcohols   | 101 |
| 2.4. Importance of the Conformational Equilibrium                                      | 21 | 4.1.1. 9-AMA Esters: Esterification Shifts  | 101 |
| 2.5. Substrates and Derivatives  | 22 | 4.1.2. Glycosidation Shifts   | 103 |
| 3. Methods Based on Double Derivatization  | 22 | 4.1.3. Low-Temperature NMR of MPA Esters  | 105 |
| 3.1. Application to $\alpha$ -Chiral Secondary Alcohols                                | 22 | 4.1.4. Complexation of MPA Esters with Barium(II)   | 107 |
| 3.1.1. Methoxytrifluoromethylphenylacetic Acid (MTPA): Mosher's Reagent                | 22 | 4.2. Application to $\alpha$ -Chiral Primary Amines: Complexation of MPA Amides with Barium(II)                         | 108 |
| 3.1.2. Methoxyphenylacetic Acid (MPA)  | 33 | 5. New Trends   | 109 |
| 3.1.3. 9-Anthrylmethoxyacetic Acid (9-AMA) and Related AMAAs                           | 40 | 5.1. Hyphenated High-Pressure Liquid Chromatography (HPLC) NMR-MS Techniques for Automatization and Microscale Analysis | 109 |
| 3.1.4. Other Reagents  | 45 | 5.2. Resin-Bound Auxiliaries: The "Mix and Shake" Method  | 111 |
| 3.2. Application to $\beta$ -Chiral Primary Alcohols                                   | 57 | 6. Concluding Remarks: A Critical Assessment  | 113 |
| 3.2.1. MTPA  | 58 | 7. Acknowledgment   | 114 |
| 3.2.2. 9-AMA   | 61 | 8. References   | 114 |
| 3.3. Application to $\alpha$ -Chiral Tertiary Alcohols                                 | 63 |   |     |
| 3.3.1. MTPA  | 63 |   |     |
| 3.3.2. Methoxy-(2-naphthyl)acetic Acid (2-NMA)   | 63 |   |     |
| 3.3.3. The Fucofuranoside Method   | 64 |   |     |
| 3.4. Application to $\alpha$ -Chiral Primary Amines                                    | 65 |   |     |
| 3.4.1. MTPA  | 65 |   |     |
| 3.4.2. MPA   | 68 |   |     |
| 3.4.3. AMAAs   | 70 |   |     |
| 3.4.4. Boc-phenylglycine (BPG)   | 70 |   |     |
| 3.4.5. Other Reagents  | 74 |   |     |
| 3.5. Application to Secondary Amines: MTPA   | 77 |   |     |
| 3.6. Application to $\alpha$ -Chiral Carboxylic Acids                                  | 79 |   |     |
| 3.6.1. Ethyl 2-(9-anthryl)-2-hydroxyacetate (9- $\Delta$ HA) and Related Aryl Alcohols | 80 |   |     |
| 3.6.2. Arylcyclohexanols   | 82 |   |     |
| 3.6.3. ( <i>S</i> )-Methyl Mandelate.  | 84 |   |     |
| 3.6.4. Phenylglycine Dimethyl Amide (PGDA) and Phenylglycine Methyl Ester (PGME)       | 85 |   |     |
| 3.6.5. 1,1'-Binaphthalene-8,8'-diol (BNDO)   | 88 |   |     |
| 3.7. Application to $\beta$ -Chiral Carboxylic Acids                                   | 89 |   |     |
| 3.7.1. Arylethylamines   | 89 |   |     |
| 3.7.2. PGME  | 90 |   |     |
| 3.8. Application to Chiral Sulfoxides: MPA   | 92 |   |     |

## 1. Introduction and Scope

The interest in determining the absolute stereochemistry of a chiral organic compound stems from the widely recognized fact that the stereochemistry often determines important properties in the chemical, physical, biological, and pharmaceutical aspects of the compounds. The need to obtain enantiomerically pure pharmaceuticals and chemicals generally has produced a fantastic growth of fields such as asymmetric synthesis, asymmetric catalysis, and other processes where the availability of simple and reliable methods for the determination of enantiomeric purity and absolute configuration is a must.

Several instrumental methods exist for the determination of absolute configuration. The most widely known are X-ray crystallography, followed by chiroptical methods (e.g., circular dichroism<sup>1a</sup> (CD), optical rotatory dispersion (ORD), or specific optical rotation); however, their use is not devoid of some inconveniences and limitations related to the equipment, which is very specific to the method and requires special training for operation, and to the sample, which, in the case of X-ray diffraction (XRD), requires monocrystals of good quality. Other methods include specific rotation,<sup>1b</sup> infrared (IR) vibrational CD,<sup>1c</sup> and vibrational Raman optical activity.<sup>1d</sup>

\* Author to whom correspondence should be addressed. E-mail: ricardo@usc.es.

<sup>†</sup> R.R. dedicates this review to the memory of his beloved wife M. Carmen.



José Manuel Seco was born in Dodro (La Coruña, Spain) in 1968. He received his B.Sc. (1991), M. Sc. (1992), and Ph.D. (1997) degrees in Chemistry from the University of Santiago de Compostela, the latter under the supervision of Profs. Ricardo Riguera and Emilio Quiñoá. He was awarded with the Ph.D. Extraordinary Prize in 1998. In 2001, he became Assistant Professor in Organic Chemistry. His current research interest is focused in the development of new reagents and methods for the determination of absolute stereochemistry of organic compounds by NMR.



Emilio Quiñoá, a native of Lugo (Spain), obtained his Ph.D. degree (1985) in Chemistry from the University of Santiago de Compostela, for work on marine natural products from the Galician Coast, under the supervision of Prof. Ricardo Riguera. From 1985 to 1988, he worked as a postdoctoral fellow with Prof. Phillip Crews at the University of California, Santa Cruz, where he participated in the study of bioactive metabolites from marine organisms of tropical waters. He returned to Santa Cruz in 1989 and 1990 as Visiting Associate Professor. After his return to the University of Santiago, he became Associate Professor in Organic Chemistry in 1989 and Full Professor in 1998. His current research interests include marine natural products, solid-phase synthesis, and the stereochemistry of organic compounds. Among other recognition, he has received the Real Academia Gallega de Ciencias Award.

Recently, different approaches to the problem of determining absolute configuration have emerged, based on NMR spectroscopy. These techniques are very appealing, because of the undoubted advantages, which include the following: (a) the instrument is available in most laboratories; (b) an in-depth understanding of the fundamentals of the method is not necessary to apply this method; (c) a small amount of sample is needed, and this can be recovered; and (d) because the analysis is conducted in solution, it is applicable to both solid and liquid samples.

Two general approaches are known. The first approach involves those procedures where derivati-



Professor Ricardo Riguera was born in Lugo (Spain) in 1948. He received his M. S. degree in Chemistry from the University of Santiago de Compostela in 1971 and the Ph.D. degree in 1973 under the supervision of the late Prof. I. Ribas. From 1974 to 1976, he stayed at the University College London as a postdoctoral fellow under the supervision of Prof. Peter J. Garratt. After returning to the University of Santiago de Compostela, he was appointed Lecturer of Organic Chemistry in 1978 and became Full Professor in 1990. As academic, he has served the university as Chairman of the Department, Dean of the Faculty of Chemistry, and Vice-Chancellor. He also has authored textbooks for students. His research interests have involved the fields of bioactive natural products from terrestrial and marine organisms, in regard to new synthetic methods and some aspects of medicinal chemistry. In the past few years, he has focused on the development of methods for determination of the absolute configuration by NMR.

zation of the substrate whose absolute configuration is studied is not necessary. The sample (i.e., a pure enantiomer) is analyzed by NMR in a chiral environment that is provided by a chiral solvent or by the addition of a chiral solvating agent<sup>2</sup> (CSA) to a nonchiral standard NMR solvent. In this approach, there is no covalent linkage between the substrate and the chiral "reagent", and this advantage is the origin of its main limitation: The chiral environment produces very small differences in chemical shifts for the two enantiomers whose NMR are very similar; many times, the two enantiomers must be available for comparison and no clear-cut correlations between the absolute configuration and the NMR spectra can be established. For those reasons, the usefulness of this method is practically restricted to the determination of enantiomeric purity.<sup>3</sup>

A clear distinction between those two objectives should be established at this point. For the enantiomeric purity measurement, we usually work with a mixture of both enantiomers in unknown ratio and just need to obtain separate signals in NMR (or peaks in high-pressure liquid chromatography (HPLC), gas-liquid chromatography (GLC), or similar techniques) that are amenable to quantification. Determination of the absolute configuration is a much more difficult task, because it is performed on a single enantiomer and, usually, we have no other enantiomer for comparison; in addition, even if we had both and could produce different spectra, we must have criteria to assign the absolute configuration separately for each enantiomer, not just its ratio.

The second approach involves derivatization of the substrate (i.e., a pure enantiomer) with the two

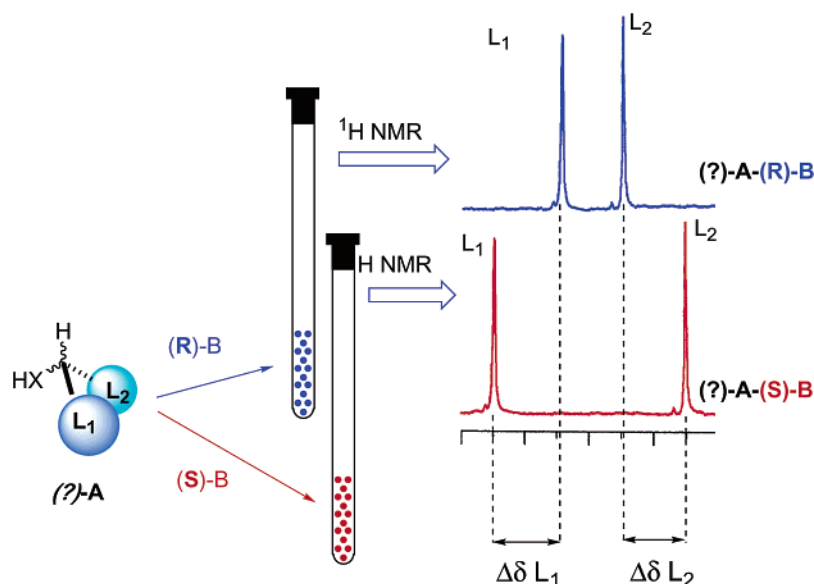


**Figure 1.**

enantiomers of a chiral derivatizing agent<sup>4</sup> (CDA), producing two diastereomeric derivatives. In this case, the chiral environment is provided by the auxiliary reagent; the association with the substrate is covalent and leads to much-greater differences in chemical shifts than those obtained when CSAs are used. Although, in certain cases, a combination of the two approaches has been used<sup>5</sup> (i.e., the addition of lanthanide shift reagents to the CDA derivatives), the derivatization with chiral auxiliary reagents is, by far, the method of choice for the assignment of absolute configuration by NMR and constitutes the main object of this review.

Many efforts to develop CDAs that are useful to assign the absolute configuration of different substrates have been described;<sup>6</sup> however, since its implementation in 1973, the so-known “Mosher’s method”, which uses MTPA (methoxytrifluorophenylacetic acid) as the reagent in its original description, has been the most successful, giving way in its evolution to many new and more-efficient reagents that are useful for different substrates and are based on the same principle.

The importance of this method can be evaluated from the ever-increasing number of papers where it is mentioned; however, in contrast to the determination of enantiomeric purity by NMR, which has been widely covered in the literature,<sup>3</sup> exhaustive reviews of this topic are absent. This absence of a comprehensive coverage means that the researcher often uses inadequate reagents for the problem being addressed or performs a nonrigorous evaluation of the experimental data, making the assignment of absolute configuration a risky exercise.

In this review, we will cover the principles and foundations of the use of CDAs and the practical aspects that are most relevant for its application to the different substrates. It is intended that this information will be of particular use to researchers who are not necessarily specialists in this field, and the purpose of this study is to provide a critical view of the methods available.

## 2. Methods Based on Chiral Derivatizing Reagents (CDAs): General Characteristics

### 2.1. Description of the Method

All the NMR-based methods for the determination of absolute configuration require the transformation of the chiral substrate to two different species that can be differentiated by NMR spectroscopy (i.e., diastereoisomers or conformers). This is achieved by derivatization of the substrate with the CDA, followed by comparison of the <sup>1</sup>H NMR spectra of those two species. Two main procedures exist, depending on the number of derivatives that should be prepared: (a) those in which the substrate (a pure enantiomer) is separately derivatized with the two enantiomers of the chiral auxiliary (Figure 1) and (b) those that require the preparation of a single derivative, using one enantiomer of a chiral auxiliary only (Figure 2).

In the first case, the chiral substrate [(?)-A] is coupled separately with the two enantiomers of the chiral auxiliary ((R)- and (S)-CDA), and the NMR spectra of the resulting diastereoisomers ((?)-A-(R)-CDA and (?)-A-(S)-CDA) are compared.

In the second possibility, the chiral substrate [(?)-A] is combined with only one enantiomer of the chiral auxiliary (either (R)- or (S)-CDA). In this way, one diastereoisomer is obtained and the spectrum of this compound is recorded. A certain conformational change is then induced (e.g., by a change in temperature of the probe or by formation of a complex) and a second spectrum is taken (Figure 2). Analysis of the differences and comparison with the conformational changes allows the configuration of the substrate to be correlated with that of the reagent. Another option that does not require the aforementioned conformational change relies simply on comparison of the spectrum of the derivative with that of the substrate prior to derivatization.

Regardless of the chosen procedure, two different spectra always must be obtained for comparison. The assignment of configuration is based on the use of the NMR to correlate the absolute stereochemistry

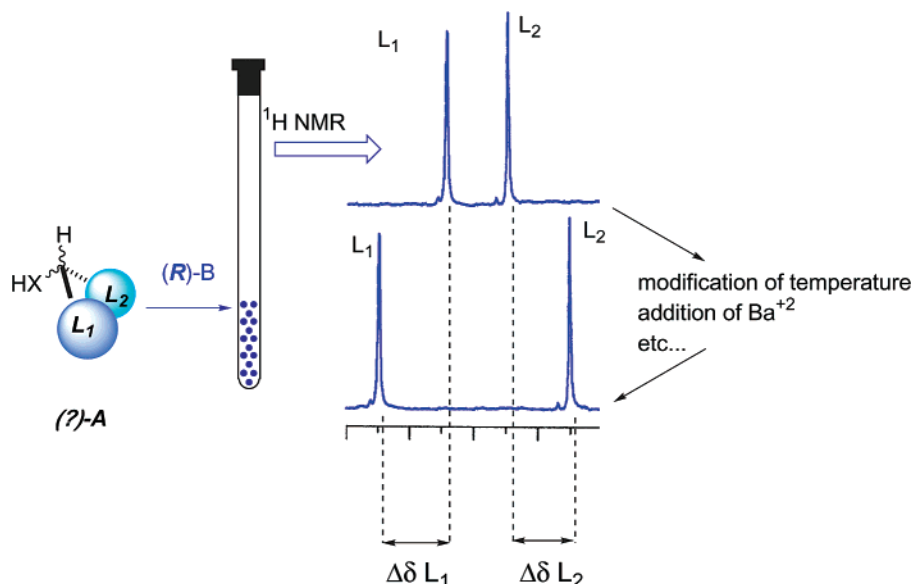


**Figure 2.**

of the chiral center of the auxiliary ( $C\alpha$ ; configuration known) with that of the substrate ( $C(1')$ , configuration unknown). To this end, the changes in the chemical shifts of the substituents of the asymmetric carbon of the substrate ( $L_1$  and  $L_2$ ) in the two derivatives (or conformational species) are considered.

These differences in the chemical shifts are represented by  $\Delta\delta$ , and it is the sign of this parameter (+ or -) that provides information about the configuration. For a particular substituent (e.g.,  $L_1$ ),  $\Delta\delta$  is defined as the difference of chemical shifts of a given signal of the substituent ( $\delta_{L_1}$ ) in the two spectra under consideration (diastereoisomers or conformers, depending on the routine chosen). As will be described in this paper, there is a variety of ways to express the differences in chemical shifts, their significance, and their characteristics. For example, in Mosher's method, a chiral secondary alcohol (i.e., 2-pentanol; see Figure 3) is derivatized with the two enantiomers of an arylmethoxyacetic acid (AMAA) i.e., (*R*)- and (*S*)- $\alpha$ -methoxy- $\alpha$ -phenylacetic acid (MPA), the  $^1\text{H}$  NMR spectra of the two derivatives are recorded, and the  $\Delta\delta^{RS}$  value is calculated for the substituents  $L_1$  ( $\Delta\delta^{RS}L_1$ ) and  $L_2$  ( $\Delta\delta^{RS}L_2$ ). In each case,  $\Delta\delta^{RS}$  is the difference between the chemical shift in the (*R*)-MPA ester derivative [ $\delta(R)$ ] and in the (*S*)-MPA derivative [ $\delta(S)$ ] (see Figure 3).

## 2.2. Characteristics of the Auxiliary Reagents

In general, the structure of the chiral auxiliary reagent (**B**) must incorporate groups with specific functions:

(a) A polar or bulky group (**R**<sub>1</sub>) to fix a particular conformation.

(b) A functional group (**Z**) (e.g., carboxylic acid) that provides a site for covalent attachment of the substrate.

(c) A group (**Y**) that is able to produce an efficient and space-oriented anisotropic effect (e.g., aromatic, carbonyl) that selectively affects substituents  $L_1$  and  $L_2$  of the substrate. This shielding/deshielding will

ensure that the chemical shifts of  $L_1$  and  $L_2$  are different in the two species (diastereoisomers or conformers) that are used for the determination of the conformation.

For example, in the case of MPA, **R**<sub>1</sub> is a methoxy group, **Z** is a carboxylic acid, and **Y** is a phenyl group (Figure 4).

## 2.3. The NMR Spectra of the Derivatives

As we have said, comparison of the NMR spectra of the two derivatives and evaluation of the differences in the chemical shifts of the signals for the substituents  $L_1$  and  $L_2$  (i.e.,  $\Delta\delta^{RS}$ ) must be performed. The signs of those parameters contain the information necessary for the configurational assignment, because they indicate the relative position of  $L_1/L_2$ , with respect to the anisotropic group **Y**; therefore, the observed differences must not be uncertain and must be clearly predictable.

In the methods that are based on the formation of two derivatives, it is important that both diastereoisomers show a certain preference for a particular conformation (NMR-significant conformer) independent of the particular substrate, and the **Y** group must project its magnetic anisotropy in a selective way, i.e., on  $L_1$  in one derivative and on  $L_2$  in the other.

For example, in the MPA esters (Figure 3), it is assumed that the representative conformer in terms of NMR is the one in which the methoxy, carbonyl, and  $C(1')\text{H}$  groups are situated in the same plane. In this way, in the (*R*)-MPA derivative, the phenyl group shields  $L_1$  ( $-\text{CH}_2\text{CH}_2\text{CH}_3$ ), whereas, in the (*S*)-MPA derivative, the shielded group is  $L_2$  ( $-\text{CH}_3$ ). The comparison of both spectra leads to  $\Delta\delta^{RS}L_1 < 0$  and  $\Delta\delta^{RS}L_2 > 0$  ( $-0.14$ ,  $-0.23$ ,  $-0.09$ , and  $+0.013$  ppm, respectively).

If the absolute configuration of the alcohol were the opposite, the signs of  $\Delta\delta^{RS}$  will also be reversed (i.e.,  $\Delta\delta^{RS}L_1 > 0$ ,  $\Delta\delta^{RS}L_2 < 0$ ).

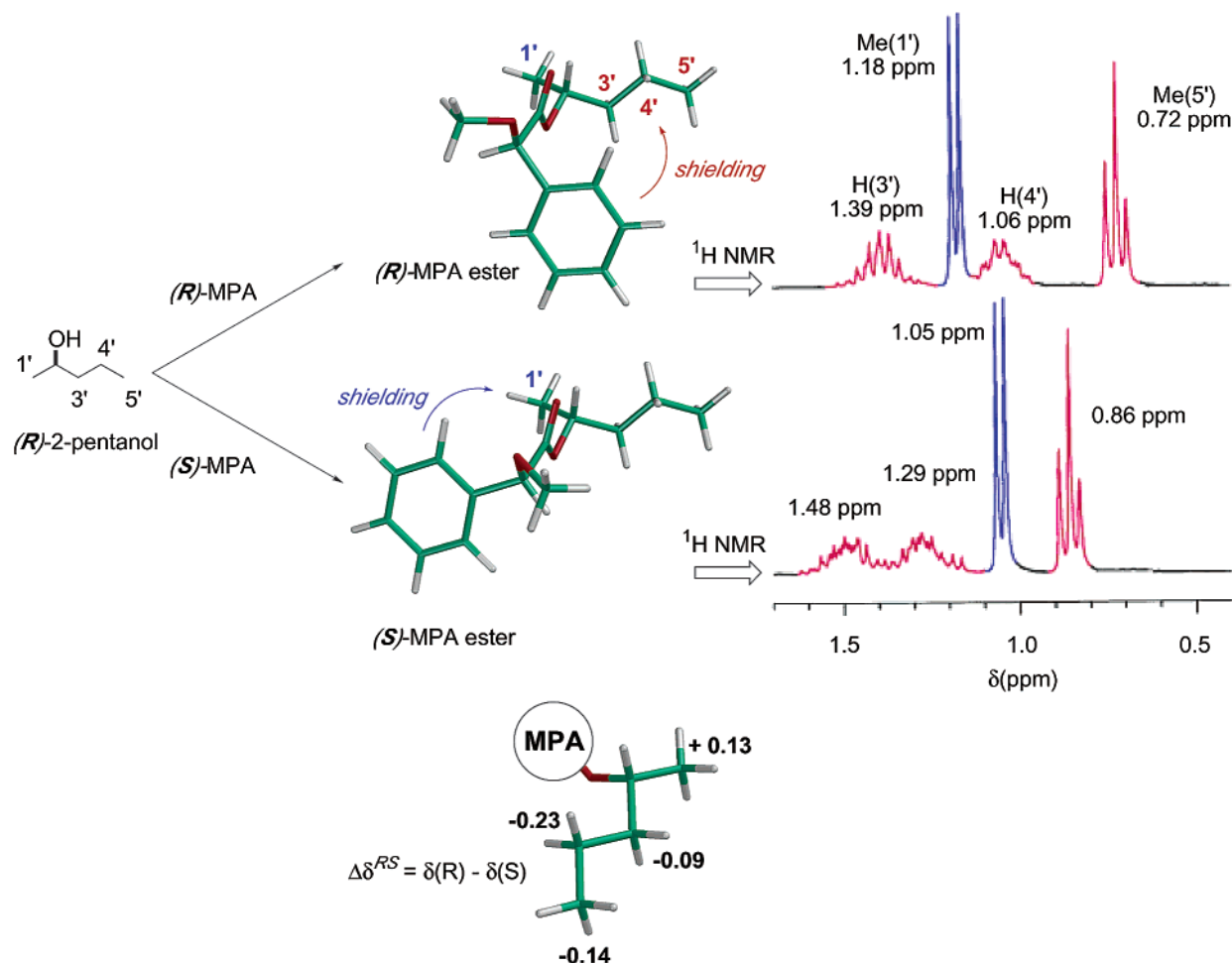


Figure 3.

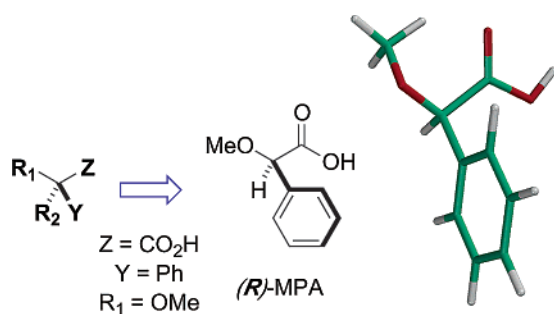


Figure 4.

## 2.4. Importance of the Conformational Equilibrium

Naturally, the key for the success of these methods lies in the assumption that a certain conformer is the most representative in both derivatives and that it remains so when different substrates are derivatized.

In solution, the CDA-derived diastereoisomers exist in a conformational equilibrium (Figure 5). This equilibrium is often very complex, because several bonds are involved and the final balance has a substantial influence on the ability of the anisotropic group **Y** to shield/deshield the substituents  $L_1/L_2$  selectively.

The balance between the relative populations of each conformer and the strength of the effect of **Y** on each conformer will be reflected (as an average) in

the resulting NMR chemical shift. Therefore, to correlate the information gained from the NMR spectra (the  $\Delta\delta$  values) with the absolute configuration, a detailed understanding of the structure and energy of the main conformers, as well as the strength and direction of the anisotropic effect of **Y** on  $L_1$  and  $L_2$  in each conformation is necessary. Naturally, for the direct use of the method, models that simplify the equilibrium, showing only the most representative conformer, are preferred (i.e., sp conformer for MPA esters; see Figure 5).

In general, the models described in the literature have been formulated as empirical rules. That is, the NMR behavior of the CDA derivatives from several substrates of known absolute configuration are analyzed and a conformational model that could explain the experimental NMR shifts is devised. In a few cases, the model proposed is claimed to be supported by XRD data; however, the differences between solution and solid state can be so big that not much support can come from that.

It is only in the past decade that extensive studies, fundamentally theoretical calculations of structure and energy, and experimental dynamic NMR and shielding effect calculations have been performed to know the contribution of each conformer and that of the average to the NMR shift that is observed.

This understanding of the fundamentals of the methods has allowed us to rationally explain not only

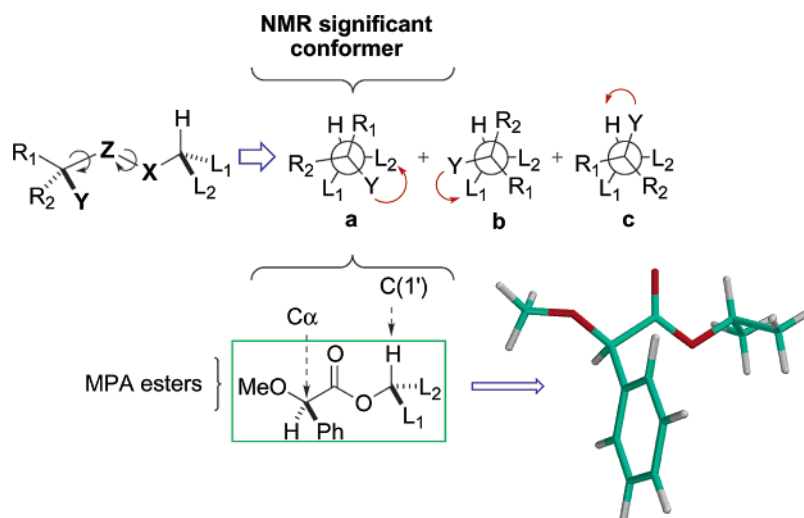


**Figure 5.**

the way in which the CDAs work but also led to the development of new and more-efficient CDA reagents and methodologies giving a plus of reliability to the absolute configuration assignment process that is now based on both empirical and theoretical results.

## 2.5. Substrates and Derivatives

The ranges of substrates whose configuration can be assigned by these methods have increased significantly recently and include primary, secondary, and tertiary alcohols, diols, carboxylic acids, primary and secondary amines, and sulfoxides. Appropriate chiral auxiliary reagents have been developed for each case that produces derivatives such as esters, amides, hemiacetals, phosphonates, etc. This review covers all those chiral substrates, the reagents and methods most commonly used and attempts to offer a critical assessment of each method.

## 3. Methods Based on Double Derivatization

### 3.1. Application to $\alpha$ -Chiral Secondary Alcohols

#### 3.1.1. Methoxytrifluoromethylphenylacetic Acid (MTPA): Mosher's Reagent

$\alpha$ -Methoxy- $\alpha$ -trifluoromethyl- $\alpha$ -phenylacetic acid (MTPA; see Figure 6) has been the most commonly used derivatizing reagent for the determination of the absolute configuration of secondary alcohols by NMR

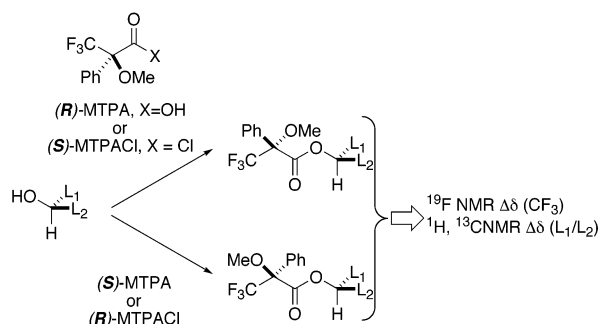


**Figure 6.**

ever since Mosher first reported<sup>7,8</sup> its use in 1973. The procedure starts with the esterification of the alcohol with the two enantiomers of MTPA. After the two diastereomeric esters have been prepared, their NMR spectra are acquired and compared. MTPA is available both as the acid and the acid chloride, and users must remember that, although derivatization of the alcohol with the (*R*)-MTPA acid leads to the corresponding (*R*)-MTPA ester, the (*R*)-MTPA chloride leads to the (*S*)-MTPA ester, which has led to confusion and some erroneous assignments.<sup>9</sup>

In his first study, Mosher used <sup>19</sup>F NMR spectroscopy—particularly, the chemical shifts of the CF<sub>3</sub> groups—for the assignment. In later studies, however, <sup>1</sup>H and <sup>13</sup>C NMR were utilized, and the chemical shifts of the protons and C atoms of the chiral alcohol under examination were used, respectively. The absolute configuration of the substrate is deduced by interpretation of the signs of  $\Delta\delta$  values, using certain empirical models. A description of those models, classified according to the NMR technique used, follows.

**3.1.1.1. The Use of <sup>19</sup>F NMR.** <sup>19</sup>F NMR was used by Mosher to determine the absolute configuration of secondary alcohols.<sup>8a</sup> The procedure is based on the anisotropic effect that the carbonyl group of the auxiliary MTPA exerts on the CF<sub>3</sub> group. For this purpose, Mosher assumed that the (*R*)- and (*S*)-MTPA esters of secondary alcohols exist in a conformation in which C(1')H, the carbonyl, and the CF<sub>3</sub> groups are situated in the same plane (Figure 7) in the derivative where the phenyl ring is opposite to the least bulky substituent of the alcohol. In the derivative in which the phenyl ring is situated on the same side as the most bulky substituent, the coplanarity is lost and, as a consequence, the CF<sub>3</sub> moves from the deshielding zone to the shielding zone of the carbonyl group.

When the bulkier substituent (e.g., L<sub>1</sub>) is on the same side as the phenyl group, the CF<sub>3</sub> resonates at a higher field—because of greater shielding (Figure 7b)—than if L<sub>1</sub> were on the side of the methoxy group (Figure 7a). These differences in chemical shifts are

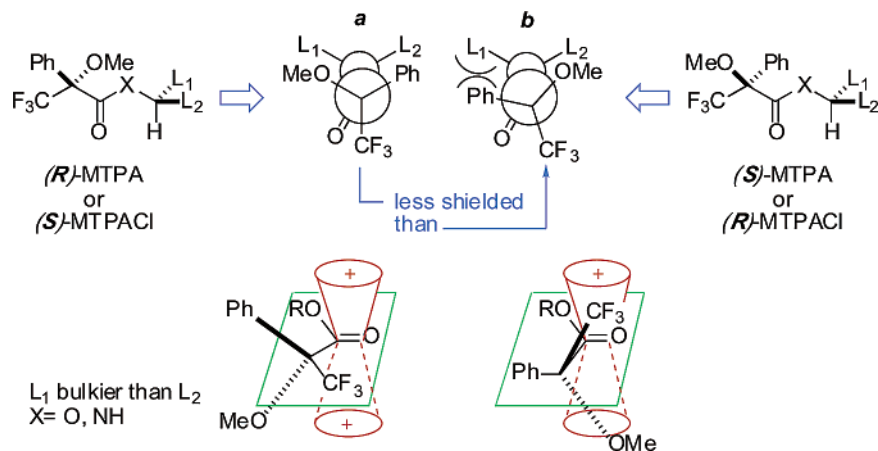


**Figure 7.** Model for the correlation of configuration/NMR for  $^{19}\text{F}$  and NMR spectra of MTPA esters.

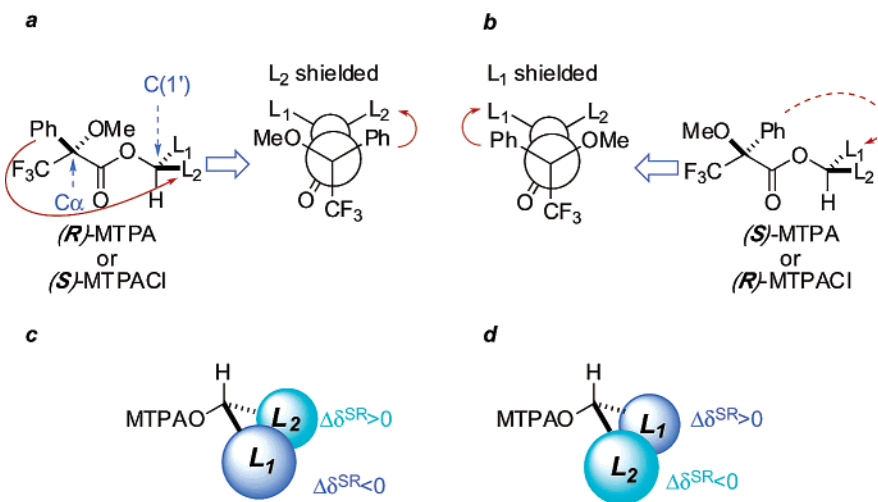


**Figure 8.** Models proposed by the Mosher model for (a, b) the assignment of configuration by  $^1\text{H}$  NMR and (c, d) the expected sign of  $\Delta\delta^{SR}$ .

expressed in terms of the parameter  $\Delta\delta^{SR(19\text{F})\text{CF}_3}$ , which is defined as the difference in the chemical shift of the trifluoromethyl signal in the  $(S)$ -MTPA ester ( $\delta\text{CF}_3(S)$ ) and the chemical shift of the same signal in the  $(R)$ -MTPA ester ( $\Delta\delta^{SR(19\text{F})\text{CF}_3} = \delta\text{CF}_3(S) - \delta\text{CF}_3(R)$ ).

For example, an alcohol with the configuration represented in Figure 7, in which  $\text{L}_1$  is more bulky than  $\text{L}_2$ , gives a negative value of  $\Delta\delta^{SR(19\text{F})\text{CF}_3}$  ( $< 0$ ). If the configuration of the alcohol were the opposite, or the size of the substituent  $\text{L}_2$  was much greater than that of  $\text{L}_1$ , the sign of  $\Delta\delta^{SR}$  would be positive.

An advantage of this procedure lies in the cleanliness of the  $^{19}\text{F}$  NMR spectra, which generally only contain signals that are due to the  $\text{CF}_3$  groups and eliminates the possibility of overlapping signals that often complicate proton spectra. Its application for the configurational assignment will be discussed later in this review.

**3.1.1.2. The Use of  $^1\text{H}$  NMR.** The use of  $^1\text{H}$  NMR spectroscopy is undoubtedly more common for the assignment of the configuration of secondary alcohols<sup>10</sup> than the use of  $^{19}\text{F}$  NMR that has been described previously. This approach is based on the anisotropic effect that the phenyl group of the chiral auxiliary MTPA exerts on the substituents ( $\text{L}_1/\text{L}_2$ ) of the alcohol. This effect allows a correlation to be

made, regarding the spatial position of  $\text{L}_1$  and  $\text{L}_2$ , with respect to the phenyl group of the MTPA moiety on the basis of the signs of  $\Delta\delta^{SR}$  of the substituents. In this case, Mosher assumed that the most representative conformation is that in which  $\text{C}(1)\text{H}$ , the carbonyl group, and the  $\text{CF}_3$  group are situated in the same plane (Figure 8a).

Accordingly, the protons of substituent  $\text{L}_2$  are shielded by the phenyl ring in the  $(R)$ -MTPA ester, whereas those on  $\text{L}_1$  remain unaffected (Figure 8a). In the  $(S)$ -MTPA derivative, on the other hand, it is  $\text{L}_1$  and its protons that are shielded while  $\text{L}_2$  is unaffected (Figure 8b). Therefore, the substituent  $\text{L}_1$  will be more shielded in the  $(S)$ -MTPA ester than in the  $(R)$ -MTPA ester and the substituent  $\text{L}_2$  will be more shielded in the  $(R)$ -MTPA than in the  $(S)$ -MTPA ester derivative.

These selective shieldings are expressed using the parameter  $\Delta\delta^{SR}$ , which is defined as the difference between the chemical shift of a certain proton in the  $(S)$ -MTPA ester and the chemical shift of the same proton in the  $(R)$ -MTPA derivative. All the protons shielded in the  $(R)$ -MTPA will present a positive  $\Delta\delta^{SR}$  value, whereas those shielded in the  $(S)$ -MTPA derivative will present a negative  $\Delta\delta^{SR}$  value.

In the case of the alcohol shown in Figure 8c, for example, the signs for each proton in  $\text{L}_1$  and  $\text{L}_2$  are

as follows:

$$\Delta\delta^{SR}L_1 = \delta L_1(S) - \delta L_1(R) < 0$$

$$\Delta\delta^{SR}L_2 = \delta L_2(S) - \delta L_2(R) > 0$$

If the configuration of the alcohol shown in Figure 8c were opposite, then the signs of  $\Delta\delta^{SR}L_1$  and  $\Delta\delta^{SR}L_2$  would also be opposite (see Figure 8d). An analysis of the results obtained with this technique, its scope, and its limitations are included in the corresponding section of this review.

**3.1.1.3. The Use of  $^{13}\text{C}$  NMR.** This approach for the assignment of the absolute configuration of the alcohol is similar to that previously described for  $^1\text{H}$  NMR spectroscopy but using the  $^{13}\text{C}$  NMR chemical shifts<sup>11</sup> of the substituents  $L_1$  and  $L_2$  ( $(C)L_1$ ,  $(C')L_2$ ) in the  $(S)$ - and  $(R)$ -MTPA esters. In the example shown in Figure 8c, the substituent that results in negative signs of  $\Delta\delta^{SR}$  occupies the place of  $L_1$ , whereas the substituent whose C atoms result in a positive  $\Delta\delta^{SR}$  value is  $L_2$ .

**3.1.1.4. Scope and Limitations in the Use of  $^{19}\text{F}$ ,  $^1\text{H}$ , and  $^{13}\text{C}$  NMR of MTPA Esters.** The NMR method for assignment of the absolute configuration of alcohols using MTPA, as described by Mosher,<sup>8d</sup> is entirely empirical, and the models represent no more than a convenient way to correlate the experimental NMR with the absolute configuration of the compounds. This means that the quality of the assignment is indicated by the number and structural variety of the substrates of known absolute stereochemistry used as test compounds. In addition, the NMR data used for assignment should adhere to several prerequisites:

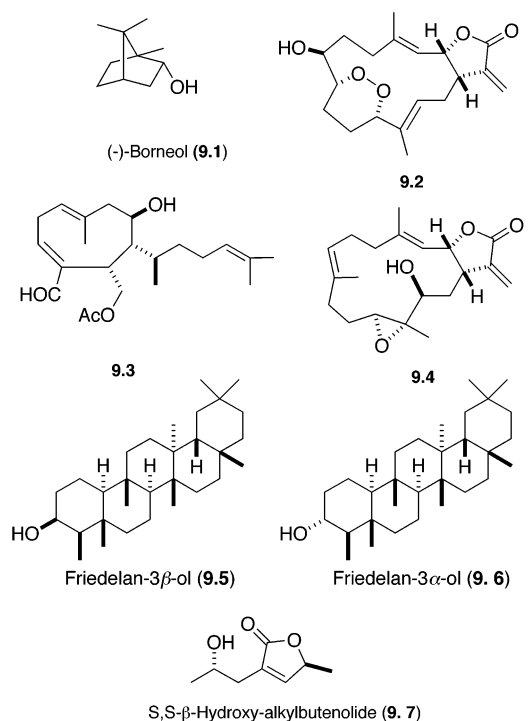
(a) The  $\Delta\delta^{SR}$  values must be sufficiently large and be above the level of experimental error,

(b) The distribution of the signs of the parameter  $\Delta\delta^{SR}$  must be uniform for a given substituent (i.e., all the protons on the same side of the plane of the MTPA ester should have the same sign), and, finally,

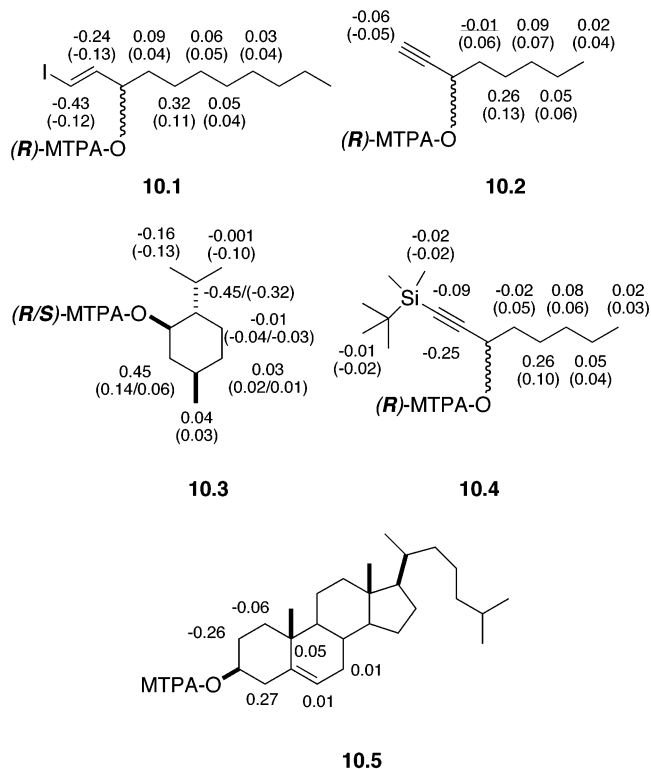
(c) If the sign of  $\Delta\delta^{SR}$  is negative for one substituent (e.g.,  $L_1$ ), then the sign of  $\Delta\delta^{SR}$  for the other substituent (i.e.,  $L_2$ ) must be positive.

Unfortunately, MTPA derivatives frequently do not seem to comply with those criteria, leading to a loss of confidence in the assignment that clearly overcome the alleged advantages of MTPA as an auxiliary reagent. In this section, we will present a critical account of the models described, the scope of each procedure, and its anomalies and limitations.

In regard to using  $^{19}\text{F}$  NMR spectroscopy, the researcher must remember that the assignment is made on the basis of a single piece of data:  $\Delta\delta^{SR}(^{19}\text{F})\text{-CF}_3$  is the difference in the chemical shifts of the  $\text{CF}_3$  group in the two derivatives. In contrast, the use of the proton or C chemical shifts from the two substituents of the alcohol involves the recording of many signals and allows any anomaly to be easily detected, because it will produce a nonhomogeneous distribution of  $\Delta\delta^{SR}$  signs. This check is not possible using  $^{19}\text{F}$  NMR, because only one data point is obtained; the data point can be either positive or negative and, as such, will always give a certain configuration.



**Figure 9.** Selection of compounds that do not conform to the  $^{19}\text{F}$  NMR Mosher model for assignment.<sup>12</sup>

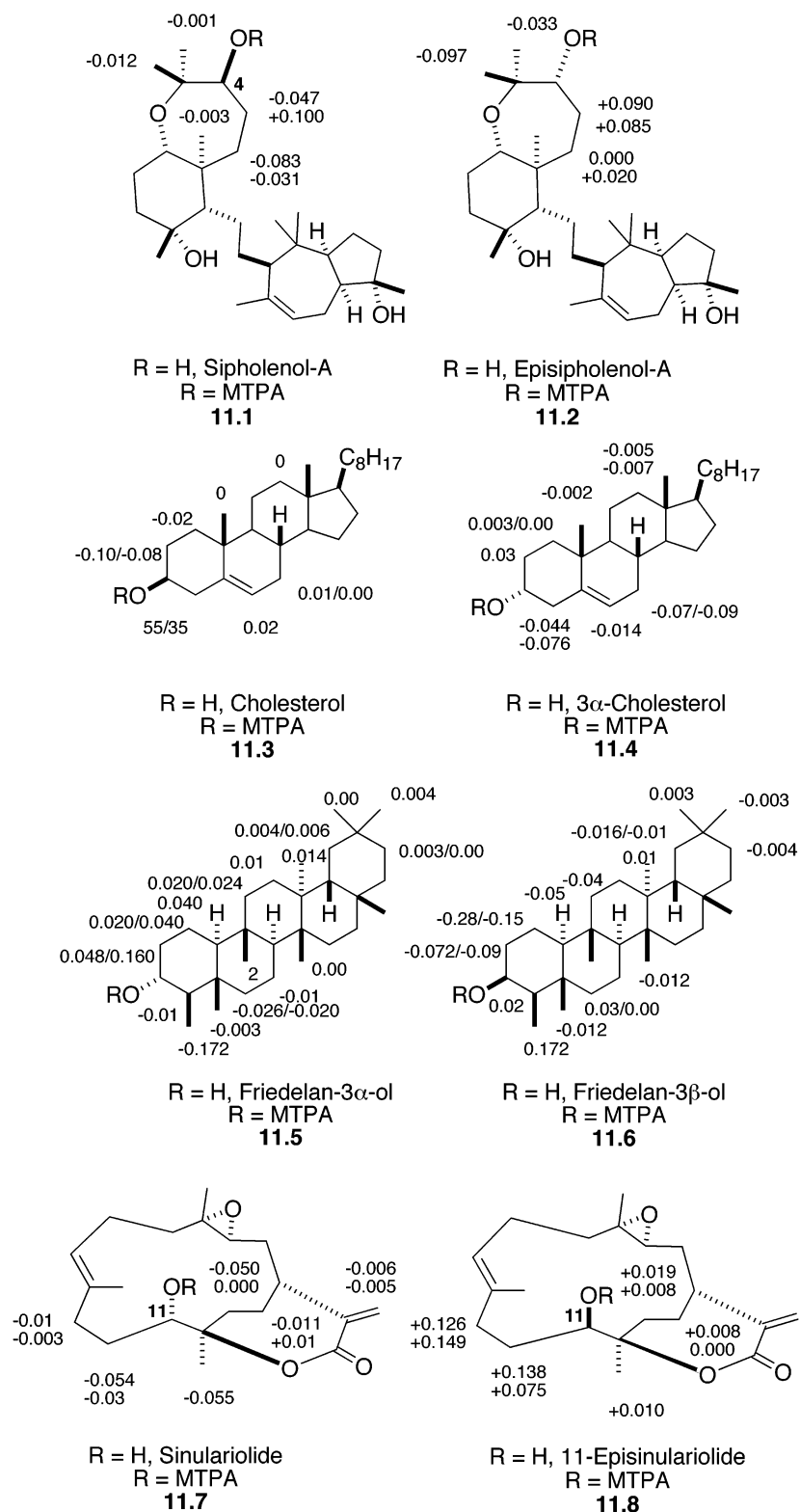


**Figure 10.**  $\Delta\delta^{SR}$  values from the  $^{13}\text{C}$  (and  $^1\text{H}$ ) NMR spectra of different MTPA esters. Anomalous values are underlined.

Indeed, many configurations that had been assigned on the basis of  $^{19}\text{F}$  NMR have since been corrected.<sup>12</sup> A selection of these cases is given in Figure 9.

Apart from that phenomenon,  $^{19}\text{F}$  NMR of the MTPA esters is frequently performed with complete success for the enantiomeric excess calculation of alcohols.



**Figure 11.**

Application of  $^{13}\text{C}$  NMR for the assignment of configuration of alcohols presents some advantages but also some important limitations.

Although the use of  $^{13}\text{C}$  NMR requires a greater amount of sample than does  $^1\text{H}$  NMR, this technique could be especially interesting in cases where  $^1\text{H}$  NMR is not useful because one of the substituents  $\text{L}_1/\text{L}_2$  has no protons. Nevertheless, those wishing to use it as a general method for assignment should

remember the following points that greatly limit its application on a general basis:

(a) The number of alcohols of known configuration (Figure 10) that have been used to test the validity of the correlations is rather small; therefore, the accuracy of the configuration assigned to a certain substrate has some uncertainty.

(b) The  $\Delta\delta^{SR}$  values obtained are very small, in comparison to the  $^{13}\text{C}$  chemical shift scale.

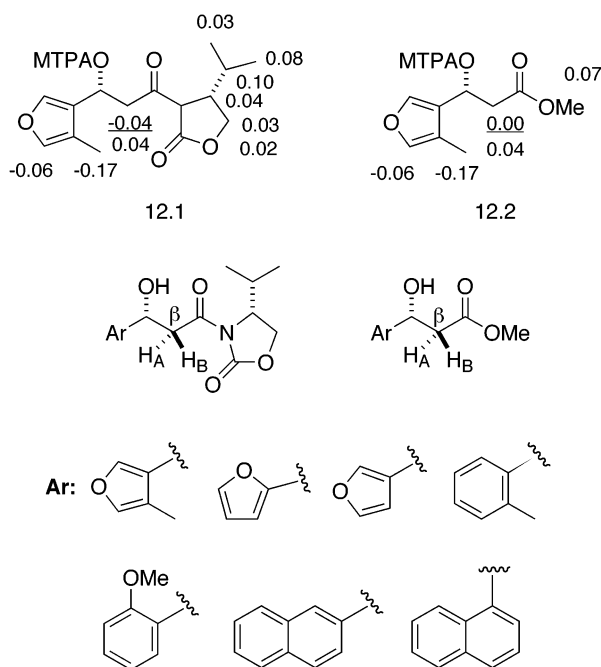


**Figure 12.**  $\alpha$ -Aryl-substituted secondary alcohols that present anomalies in the  $\Delta\delta^{SR}$  signs of the  $\beta$ -protons (data underlined).

(c) Nonhomogeneous distributions of the signs of  $\Delta\delta^{SR}$  have been obtained for some secondary alcohols (data underlined in compounds 10.2 and 10.4 in Figure 10).

The most numerous examples of application of MTPA for the assignment of configuration of alcohols have been described using  $^1\text{H}$  NMR. The method has been tested with a fair number of alcohols of known absolute configuration; nevertheless, numerous cases have been described in which the  $\Delta\delta^{SR}$  values obtained from the MTPA esters do not allow a safe assignment, in accordance with the criteria discussed previously,<sup>13</sup> either because (a) the magnitude of the shifts is very similar to the experimental error or (b) the distribution of signs is not consistent.

Both the small shifts and the irregular distribution of signs can lead to erroneous assignment of configuration. This has been demonstrated in certain cases by XRD<sup>12</sup> or other methods; however, in other cases, the configuration that is assigned has remained unchecked.

For example, the MTPA derivatives of siphnenol A<sup>14a</sup> (Figure 11) result in  $\Delta\delta^{SR}$  values with the same sign for both substituents ( $L_1$  and  $L_2$ ), which is a fact that makes the assignment impossible, whereas its epimer, epi-siphnenol A<sup>14b</sup> (Figure 11), gives opposite signs for each substituent. Similar situations have been described for other cyclic alcohols<sup>12b</sup> that give irregular distribution of the signs of  $\Delta\delta^{SR}$ , including 3- $\alpha$ -cholesterol and friedelan-3 $\beta$ -ol, which possess axial hydroxyl groups. In contrast, the epimers of these two compounds, cholesterol and friedelan-3 $\alpha$ -ol, with equatorial hydroxyl groups give a perfectly homogeneous distribution of signs for  $\Delta\delta^{SR}$  (Figure 11).

The anomalous behavior of siphnenol A, 3- $\alpha$ -cholesterol, and friedelan-3 $\beta$ -ol has been explained in terms of the steric hindrance of the axial hydroxyl

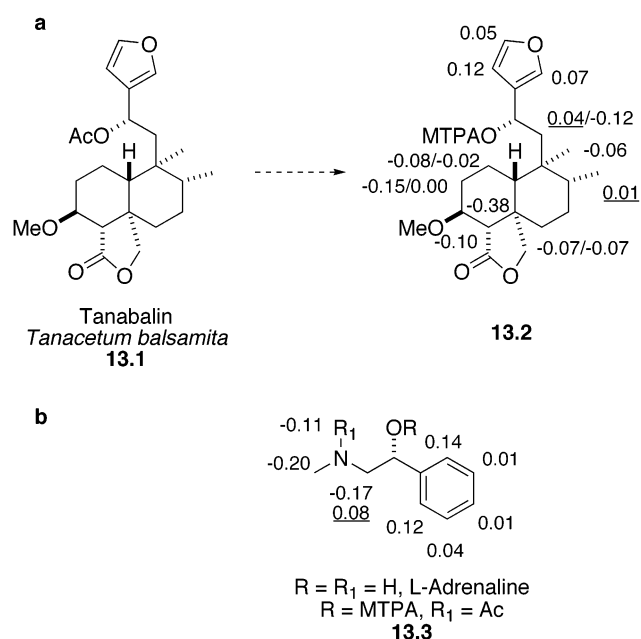


**Figure 13.** (a) Structure of tanabalin (**13.1**) and  $\Delta\delta^{SR}$  values for the MTPA esters; (b)  $\Delta\delta^{SR}$  values for the MTPA esters of *N*-acetyl-L-adrenalin.

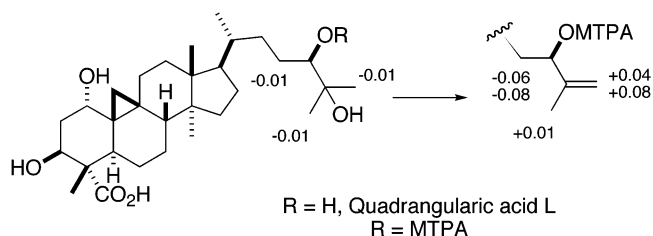


**Figure 14.** Structure of quadrangularic acid L and  $\Delta\delta^{SR}$  values of the MTPA esters.

group modifying the conformation of the MTPA esters. However, similar cases are known in which this explanation is not applicable, such as sinulariolide and its epimer 11-episinulariolide,<sup>15</sup> which both produce anomalous  $\Delta\delta^{SR}$  sign distributions and, thus, cannot be assigned a configuration with any degree of certainty by this method.

Given the frequency with which MTPA esters lead to irregular sign distributions, Kakisawa and co-workers<sup>10,12b,16</sup> proposed a new way to evaluate the  $\Delta\delta^{SR}$  data; this methodology is called the "Modified Mosher Method." This procedure involves the analysis of all (or the vast majority) of the protons in the molecule, so that a representative sign for  $\Delta\delta^{SR}$  of substituents  $L_1$  and  $L_2$  can then be adopted based on the majority of the protons for each substituent. In our opinion, however, the elimination of those resonances that produce anomalous signs can only be justified if (a) those proton(s) are located at a long distance from the chiral center and (b) there is a sufficiently large number of protons close to the asymmetric C atom producing the expected homogeneous sign distribution.

Another class of compounds in which irregular  $\Delta\delta^{SR}$  signs have been observed is alcohols with aromatic rings in the  $\alpha$ -position.<sup>17</sup> This situation is illustrated in Figure 12 by the MTPA esters of the alcohols derived from tautomycin,<sup>17a</sup> in which irregular  $\Delta\delta^{SR}$  values are found exclusively for the  $\beta$ -protons (un-

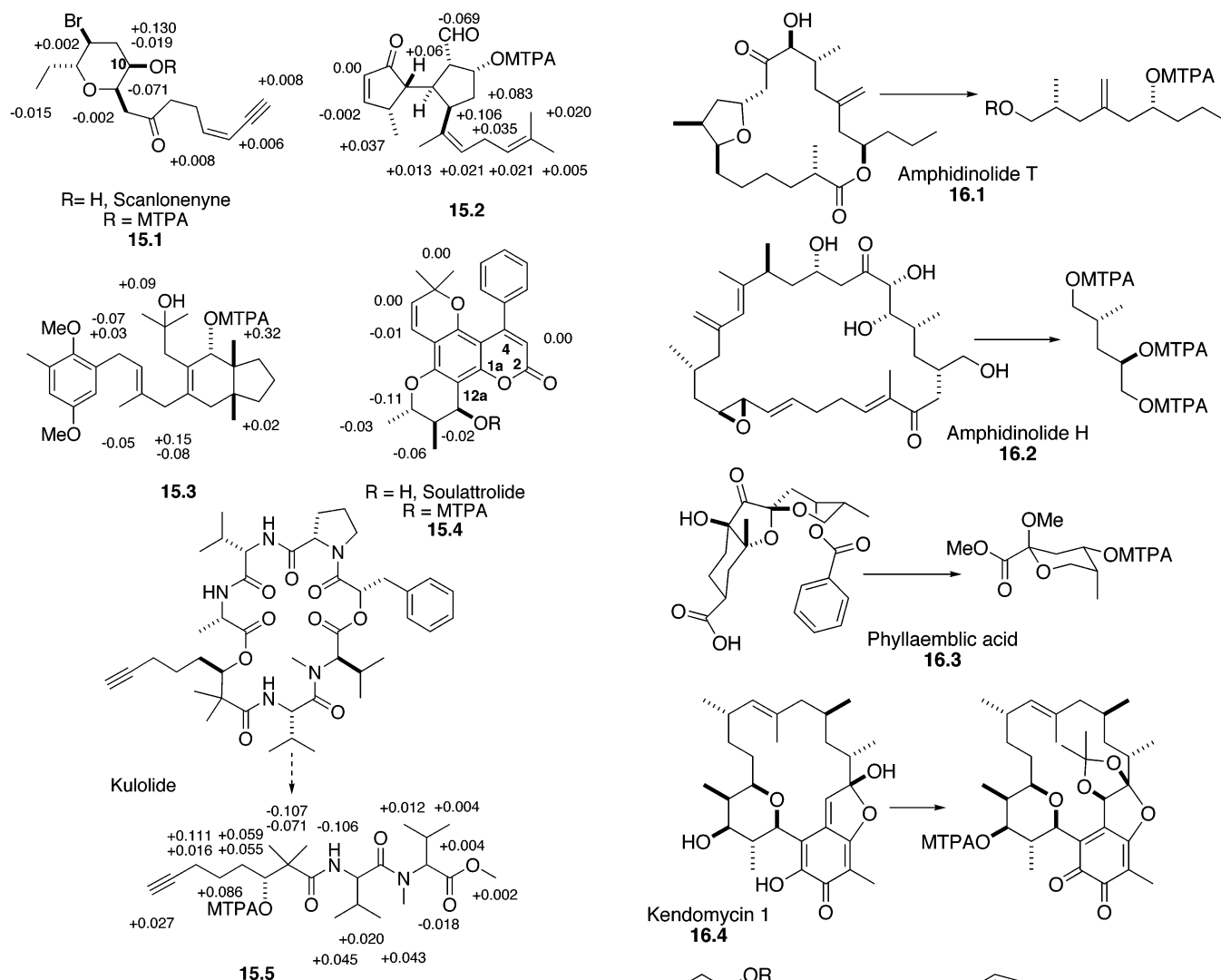


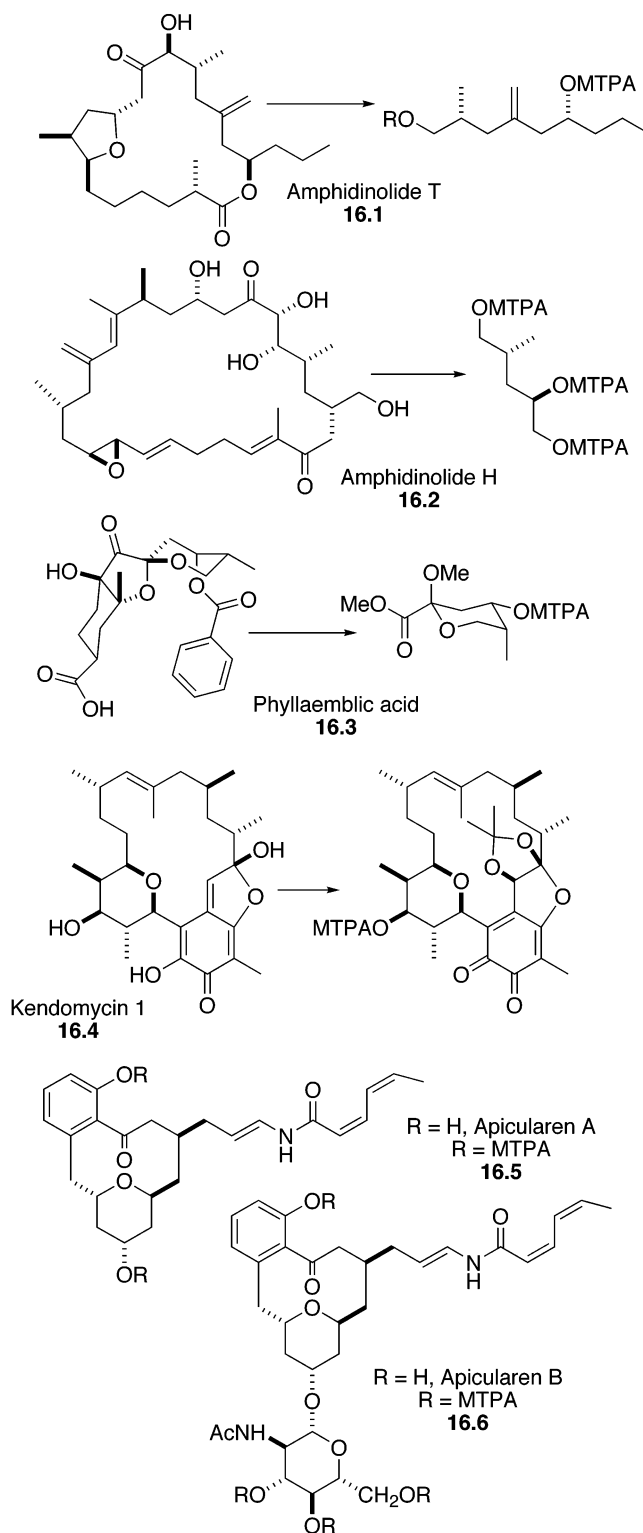
**Figure 15.**  $\Delta\delta^{SR}$  values obtained for the MTPA esters shown.

derlined in Figure 12) whereas the rest of the protons give regular sign distributions. The authors suggest<sup>17a</sup> that the cause of these irregular sign distributions could be the fact that these protons are affected not only by the phenyl ring of the MTPA but also by the aromatic ring at the  $\alpha$ -position in the alcohol, which is a view supported by Molecular Mechanics calculations.

Other examples include tanabalin<sup>17b</sup> (13.1, Figure 13), which is an insect antifeedant isolated from *Tanacetum balsamita*, and *N*-acetyl-L-adrenalin (13.3, Figure 13).

Irregular distributions in the signs of  $\Delta\delta^{SR}$  have also been found in substrates that do not contain aromatic groups competing with MTPA. Quadrangularic acid L<sup>18</sup> (Figure 14) is one such example that produces negative signs for  $\Delta\delta^{SR}$  of both substituents L<sub>1</sub> and L<sub>2</sub>. The fact that the dehydro-derivatives of these compounds give the correct sign distribution has led to the belief that the presence of a neighboring polar group should be responsible for that anomalous sign distribution.

Unfortunately, the explanation for that incoherence is not so simple, and there are many other compounds that produce nonhomogeneous sign distribution but

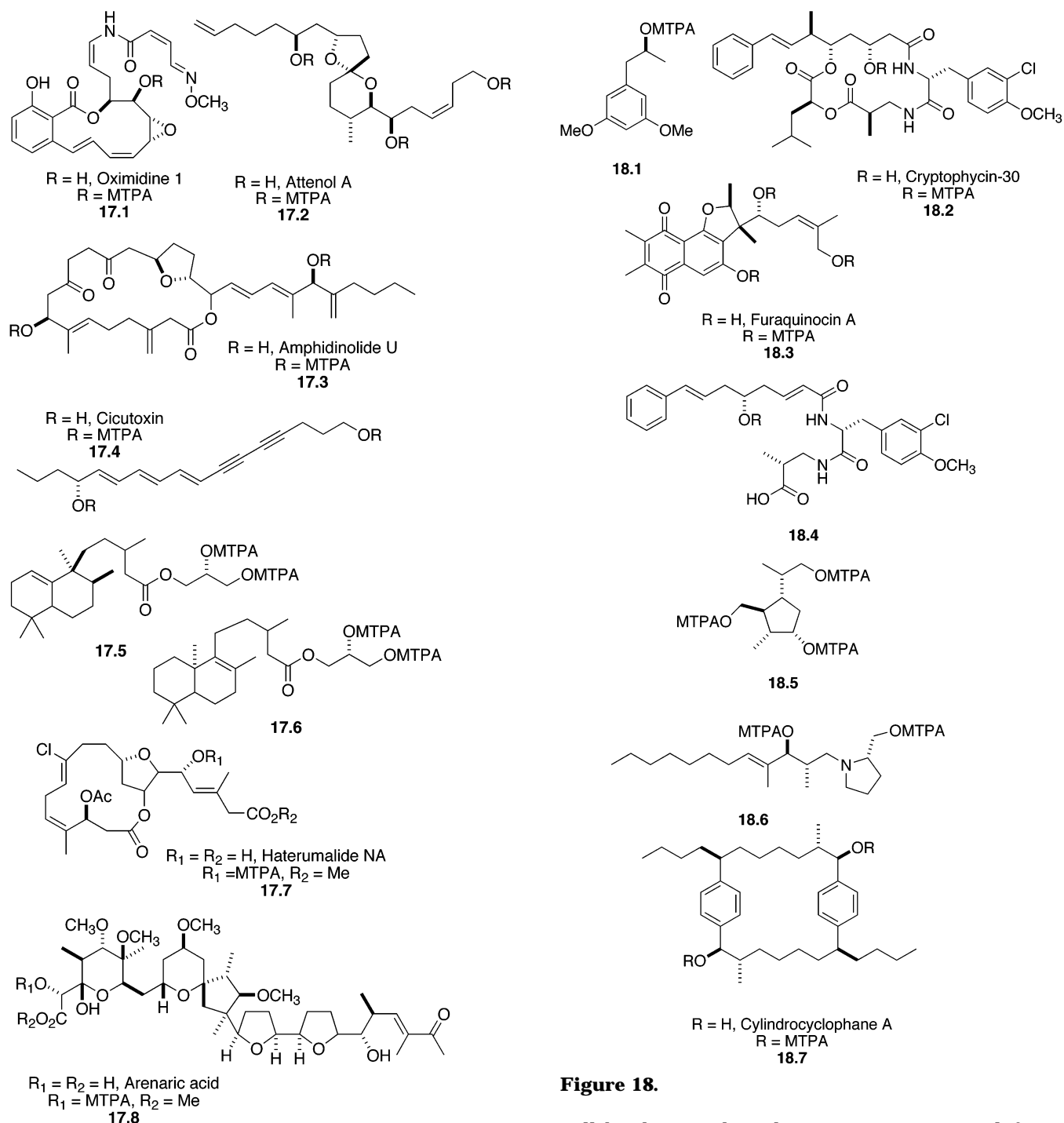


**Figure 16.**

have no polar groups or neighboring aromatic rings in their structures. Some examples are shown in Figure 15.<sup>19</sup>

Many compounds have been reported whose MTPA esters produce sign distributions in good agreement with Mosher's model, despite the presence of hindered hydroxyl groups, polar groups, or other aromatic rings. Their structures are shown in Figures 16,<sup>20</sup> 17,<sup>21</sup> and 18.<sup>22</sup>

One specific class of compounds in which irregular sign distributions are obtained from the MTPA esters

**Figure 17.**

warrants special mention. Those are the polyalcohols that have been completely derivatized with MTPA. Examples of such systems include penaresidin A and B,<sup>23</sup> pyripropene A,<sup>24</sup> and other compounds<sup>25</sup> shown in Figure 19. The anomalies observed in these compounds have been identified as being due to the presence of several MTPA units whose effects interfere with each other. Such crossed effects cause sign distributions that bear no relation to Mosher's predictions for monoalcohols where only the effect of a single aromatic ring must be considered. The assignment of the configuration of polyalcohols by NMR spectroscopy must be analyzed in a different way and

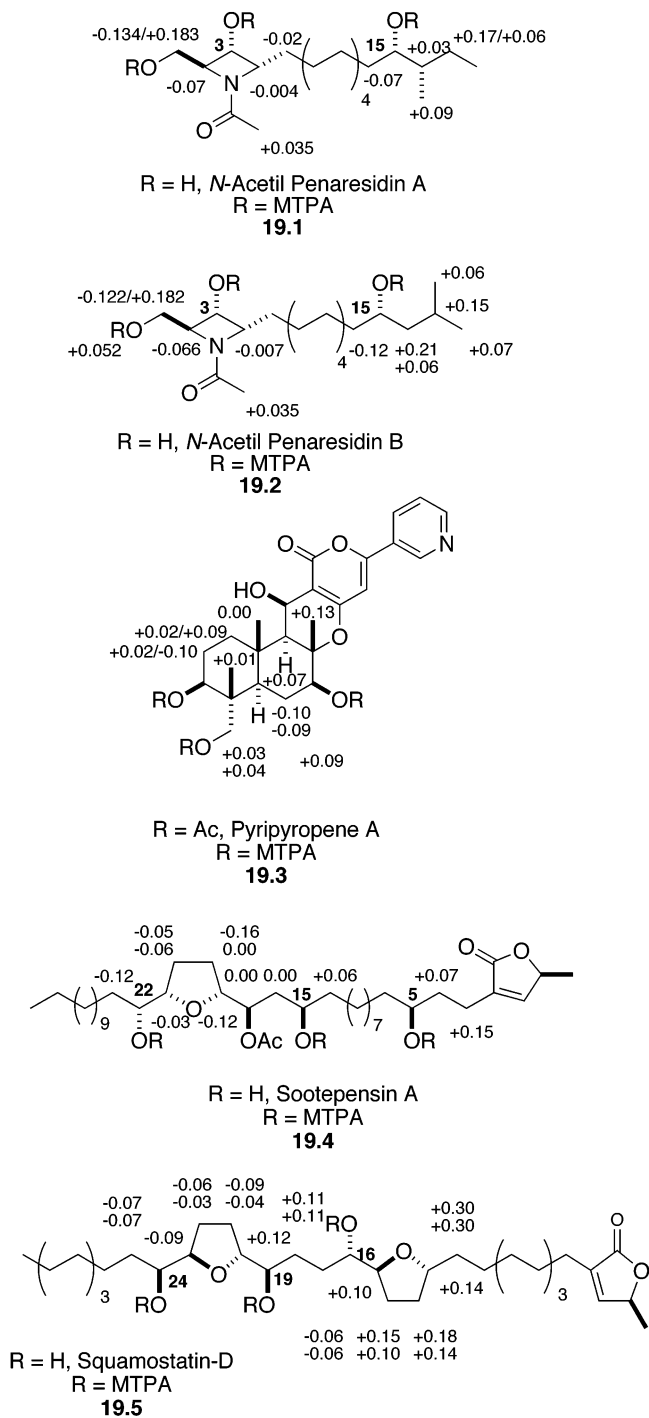
**Figure 18.**

will be discussed in the section covering polyfunctional compounds.

**3.1.1.5. Special Models for Special Cases.** It is obvious that no prediction of configuration is possible by the method described if one of the substituents of the substrate has no resonances to examine or if those peaks cannot be clearly distinguished because of overlapping.

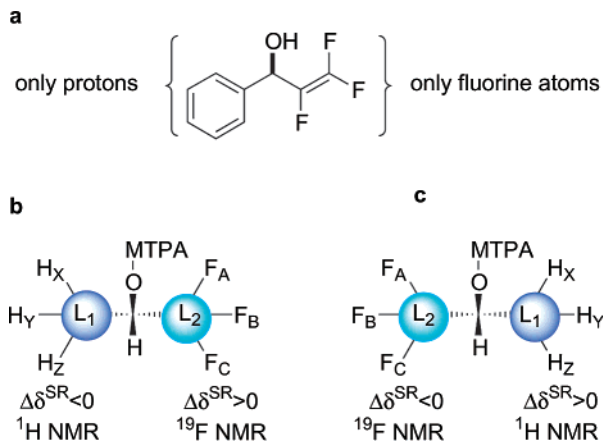
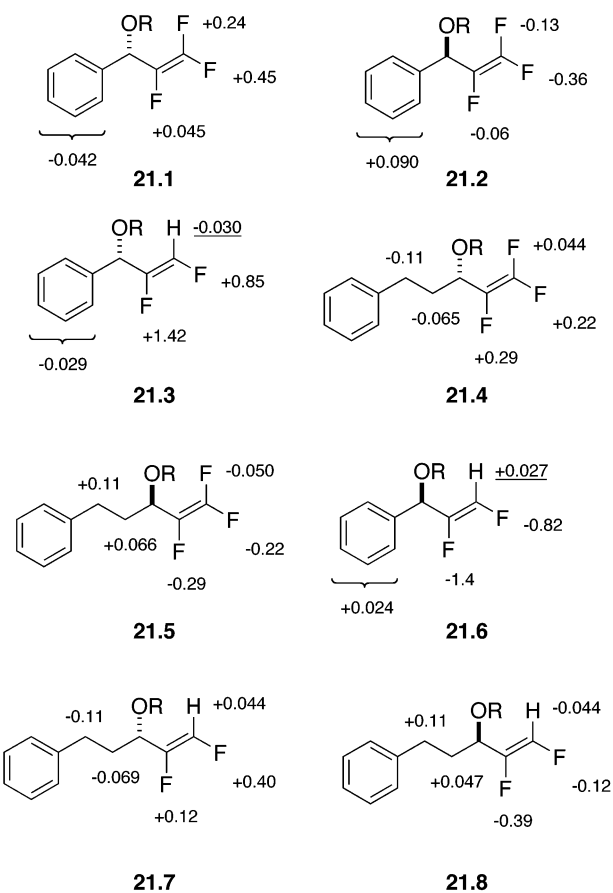
Alternatives have been proposed<sup>26</sup> to overcome these limitations in two particular classes of compounds.

Thus, for fluoro-substituted secondary alcohols such as the 1,2-difluoroallyl alcohols shown in Figures 20 and 21, where one substituent contains protons and the other contains only F atoms, the combined use of <sup>1</sup>H and <sup>19</sup>F NMR spectroscopy has

**Figure 19.**

been described.<sup>26a</sup> The  $^1\text{H}$  and  $^{19}\text{F}$  NMR spectra of the two MTPA esters are recorded and the  $\Delta\delta^{SR}$  values calculated for the protons on one substituent and for the fluoro-substituents of the other substituent. The model proposed assumes that if the configuration of the alcohol is that shown in Figure 20b, then the protons in  $L_1$  must produce a negative  $\Delta\delta^{SR}$  value, whereas the fluoro-substituents in  $L_2$  must have a positive  $\Delta\delta^{SR}$  value. When the configuration is the opposite, the signs of  $\Delta\delta^{SR}$  then will be reversed (see Figure 20c).

Figure 21 shows the alcohols of known absolute configuration that have been used as support of the mixed proton–fluorine NMR approach. Although

**Figure 20.****Figure 21.**

most of the  $\Delta\delta^{SR}$  signs are in good agreement with the configuration, some compounds (21.3 and 21.6) exhibit signals (underlined in the figure) that are inconsistent with their configuration and put a limit on the validity of the method.

The purpose of the second alternative described<sup>26b</sup> is to solve the difficulties presented by overlapping signals for  $L_1/L_2$  in aromatic and heteroaromatic alcohols. It is based on the combined use of the anisotropic effect caused by the aromatic ring of the alcohol on the methoxy group of the auxiliary MTPA and that of the phenyl ring of the auxiliary on the substituents  $L_1/L_2$  of the alcohol.

According to the author, in the (*R*)-MTPA ester of the alcohol shown in Figure 22a, both aryl rings are

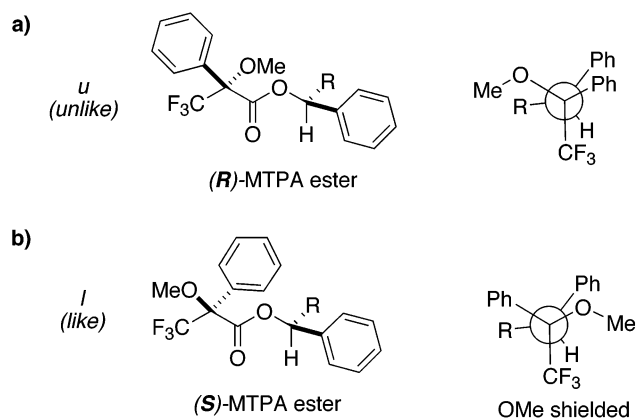


Figure 22.

on the same side of the plane of the MTPA, and, consequently, neither the signals of the MeO nor those of substituent (*R*) of the alcohol are affected by the anisotropy of the rings. For its part, in the (*S*)-MTPA ester (Figure 22b), the aromatic groups are on opposite sides and both the MeO and substituent (*R*) are under their shielding influence. Application of this method requires the derivatization of the alcohol with the two enantiomers of MTPA and comparison of their NMR spectra.

Negative  $\Delta\delta^{SR}$  values for the MeO group result when the configuration is that indicated in Figure 22, and positive  $\Delta\delta^{SR}$  values are to be obtained if the configuration of the alcohol were the opposite.

This model has been tested with 50 alcohols of known absolute configuration. The prediction of the configuration was correct in 46 cases and incorrect in just 1. In 3 examples, the  $\Delta\delta^{SR}$  values were negligible and did not allow the assignment of configuration.

In summary, the data presented indicates that MTPA frequently presents severe limitations in its use for the assignment of configuration of secondary alcohols: small  $\Delta\delta^{SR}$  values, which are very much affected by the presence of anisotropic groups in the substrate, and irregular sign distributions.

In addition, the explanations that have been put forth for these inconsistencies—usually centered on the particular characteristics of the substrates—are not satisfactory. They are neither general nor do they allow the researcher to predict whether this method could be used to assign, with complete certainty, the absolute configuration of a new substrate. We will show in the next section that the problem is not with the substrate but rather with the characteristics and limitations of the MTPA itself.

**3.1.1.6. The Mode of Action of MTPA: A Revision of the Model.** As we have seen, the assignment of absolute configuration by  $^1\text{H}$  NMR of MTPA esters rests with the detection by NMR of the relative position of substituents  $L_1$  and  $L_2$ , with respect to the phenyl ring of the auxiliary MTPA. It is this spatial information that is contained in the  $\Delta\delta^{SR}$  signs of the substituents.

The anomalies observed in the use of MTPA suggested that perhaps the empirical model described by Mosher in 1973 is not fully representative of the

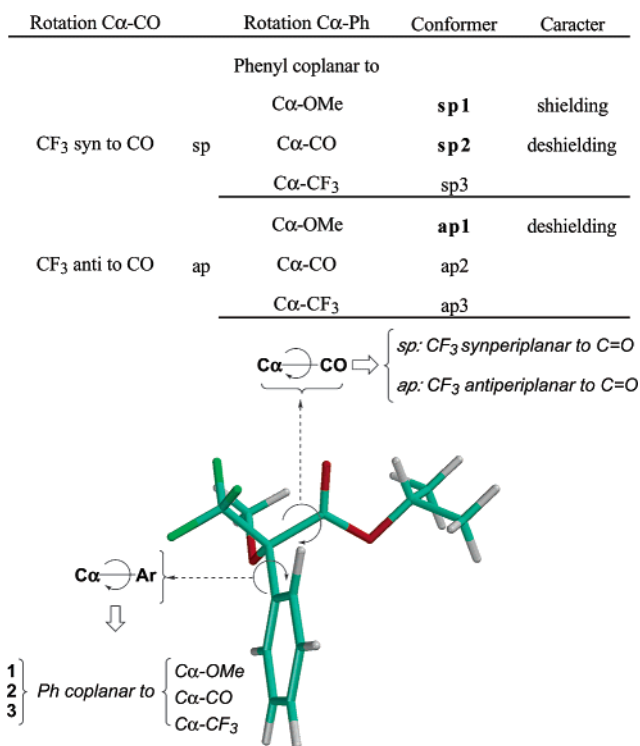
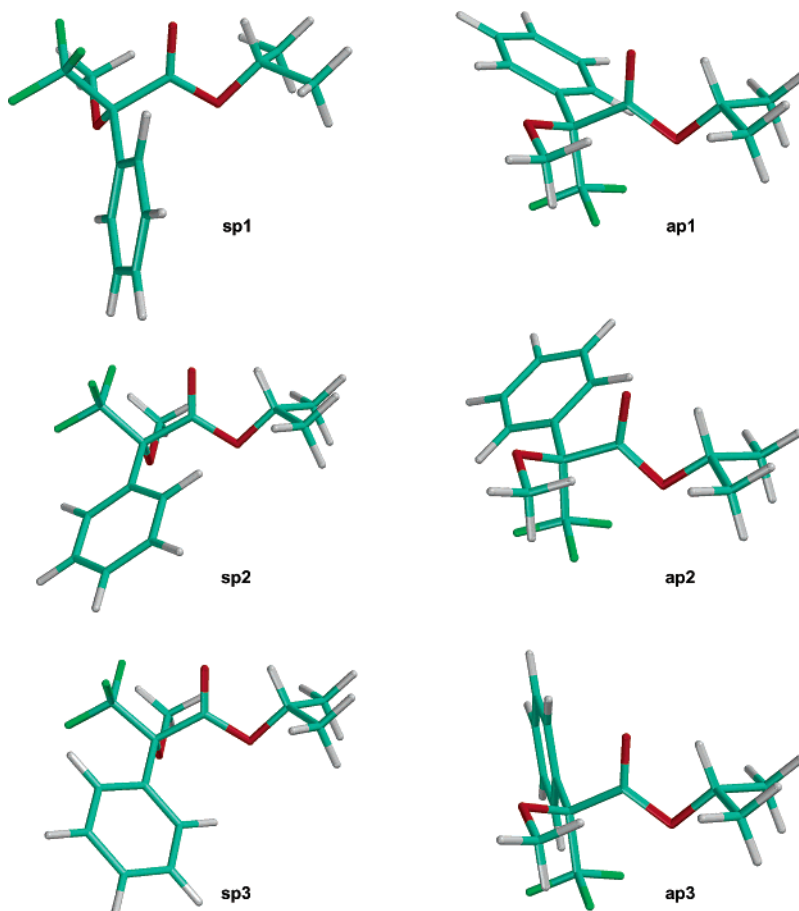


Figure 23. Generation of conformers in MTPA esters and the most-significant characteristics of each.

real position of the phenyl ring, with respect to the substituents, and stressed the need to study the conformational composition and the exact direction of the anisotropic effect in MTPA esters.

In fact, theoretical calculations on the conformations (molecular mechanics, semiempirical and *ab initio*) and shielding/deshielding contributions (aromatic ring current increments) were performed<sup>27</sup> in conjunction with variable-temperature NMR and dynamic NMR experiments that allowed the full understanding of the fundamentals of the MTPA action and of the correlation between NMR spectra and absolute configuration.<sup>27</sup>

The results indicate that the conformational composition of MTPA esters is very complex and that the situation cannot be fully represented by the empirical model proposed by Mosher (Figure 8). According to those studies,<sup>27</sup> the main conformational processes involve rotation about the C $\alpha$ -CO and C $\alpha$ -Ph bonds (Figure 23). The first generates two conformers: the sp conformer, in which the CF<sub>3</sub> has a syn-periplanar disposition, with respect to the carbonyl group, and the ap conformer, in which these groups have an anti-periplanar disposition. Rotation about the C $\alpha$ -Ph bond generates three conformers that differ in the orientation of the phenyl ring (coplanar with the C $\alpha$ -CO, C $\alpha$ -CF<sub>3</sub>, and C $\alpha$ -OMe bonds, respectively). Consideration of their relative energies indicates that only three of the six possible forms (Figure 24) are really representative: ap1, sp1, and sp2. Their order of stability is ap1 > sp1 > sp2, although the energy differences are so small (0.40 and 0.63 kcal/mol, respectively) that they are present in similar populations, and, therefore, significant contribution of each one to the average spectrum must be expected.



**Figure 24.**

Conformer ap1 is the most stable conformer and has the CF<sub>3</sub> group anti-periplanar, with respect to the carbonyl group; its phenyl ring produces a deshielding effect on the substituents of the alcohol. The next conformer, in terms of energy, is sp1; it has the CF<sub>3</sub> and carbonyl groups in a syn-periplanar disposition, as in the empirical Mosher's model, and its phenyl ring produces a shielding effect on the alcohol part. The third conformer is sp2, and this conformer also has a syn-periplanar disposition that results in deshielding on the alcohol substituents. The conformers are shown in Figure 24.

In accordance with that composition, the final chemical shift of substituents L<sub>1</sub> and L<sub>2</sub> in the average spectrum will be the result of the combined action of those three similarly populated forms. Each conformer contributes a different shielding/deshielding effect; therefore, some cancellations may result, causing small  $\Delta\delta^{SR}$  values.

For example, in the ester that is derived from (*R*)-MTPA (Figure 25a), substituent L<sub>1</sub> is deshielded in conformer ap1, whereas substituent L<sub>2</sub> is shielded in conformer sp1 and deshielded in conformer sp2. Therefore, the net effect on substituent L<sub>2</sub> will range from slight shielding/deshielding to a mutual cancellation of effects.

For its part, in an ester that is derived from (*S*)-MTPA (Figure 25b), substituent L<sub>2</sub> is deshielded in conformer ap1, whereas substituent L<sub>1</sub> is shielded in conformer sp1 but deshielded in conformer sp2. As in the previous example, the net result is a total or

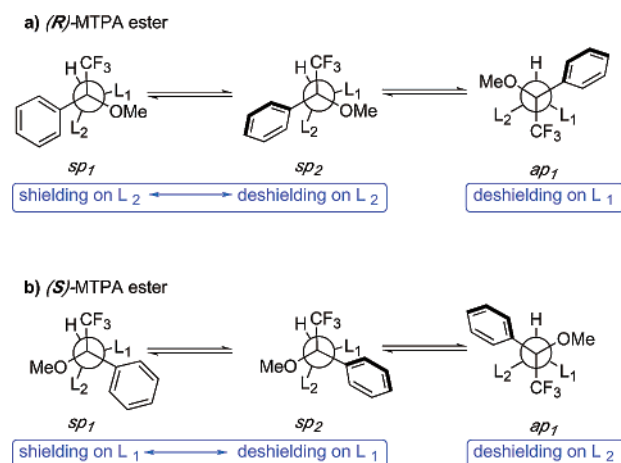


**Figure 25.** Shielding/deshielding effects in the three most-representative conformers of the MTPA esters.

partial cancellation of effects and this results in substituent L<sub>1</sub> being slightly shielded/deshielded or remaining unaffected by the phenyl ring of the reagent.

The final results for substituent L<sub>1</sub> will be deshielding in the ester-derived form (*R*)-MTPA, and either slightly shielding or just a null effect in the (*S*)-MTPA derivative. Substituent L<sub>2</sub>, on the other hand, is deshielded in the (*S*)-MTPA derivative but only slightly shielded or unaffected in the (*R*)-MTPA derivative. Negative signs for  $\Delta\delta^{SR}$  are then expected for all the protons on substituent L<sub>1</sub> and positive

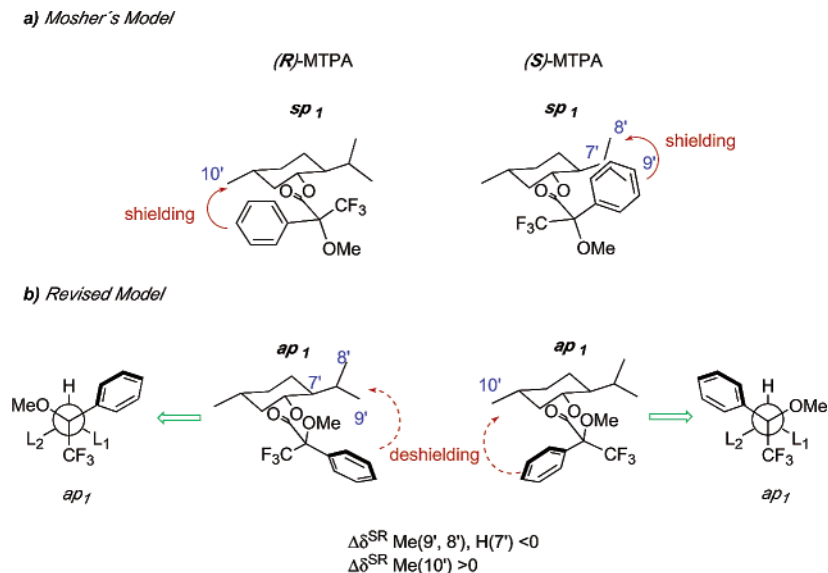


**Figure 26.** Mosher's model<sup>8</sup> and the revised model<sup>27</sup> for the assignment of absolute configuration of MTPA esters.

signs are expected for those on substituent  $L_2$ :

$$\Delta\delta^{SR}L_1 = \delta L_1(S) - \delta L_1(R) < 0$$

$$\Delta\delta^{SR}L_2 = \delta L_2(S) - \delta L_2(R) > 0$$

As indicated, experimental support for those conclusions has been obtained from the evolution of the NMR spectra, with temperature, of the MTPA esters that showed the shift of the equilibrium toward conformer *ap*1 at lower temperatures. Similarly, good agreement was observed between the experimental chemical shifts and those expected from the calculated aromatic shielding effect of the phenyl ring on  $L_1$  and  $L_2$  in each individual conformer and in the average mixture.<sup>27</sup> Interestingly, both calculations and experiments demonstrate that the effect on substituents  $L_1$  and  $L_2$  of the phenyl ring of MTPA is net deshielding rather than shielding, as suggested by Mosher in its empirical rule.<sup>8</sup>

On that basis, a simplified model representative of the NMR behavior of the MTPA esters and useful for the assignment has been formulated.<sup>27</sup> It has the  $\text{CF}_3$  group, the carbonyl group, and the H atom on the chiral C atom of the alcohol in the same plane and the  $\text{CF}_3$  anti-periplanar to the carbonyl group. In this way, the phenyl ring deshields the substituent on the same side of the plane, i.e.,  $L_1$  in the (*R*)-MTPA ester and  $L_2$  in the (*S*)-MTPA analogue (Figure 26).

### 3.1.1.7. The Conformations of MTPA Esters.

The existence of three main conformers that have similar energy and contribute to the chemical shifts with both shielding and deshielding effects serves to explain the origin of the two most important limitations of this reagent: the small  $\Delta\delta^{SR}$  values and the frequent surge of irregular distributions of the signs of  $\Delta\delta^{SR}$ .

The origin of the reduced  $\Delta\delta^{SR}$  values has been already advanced and resides in the eventual cancellation in the average spectrum of the shielding/deshielding that is associated with each individual conformer.

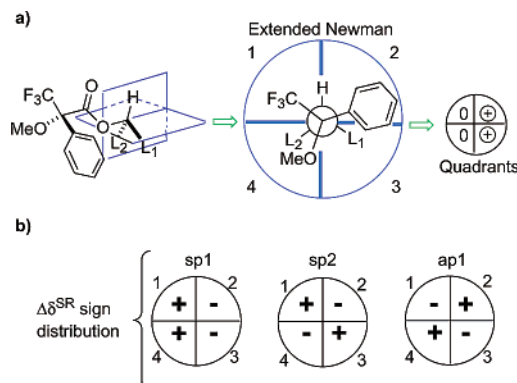


**Figure 27.** Spatial distributions of (a) the shielding effect on a MTPA ester and (b) the resulting signs of  $\Delta\delta^{SR}$  in the conformers of a MTPA ester.

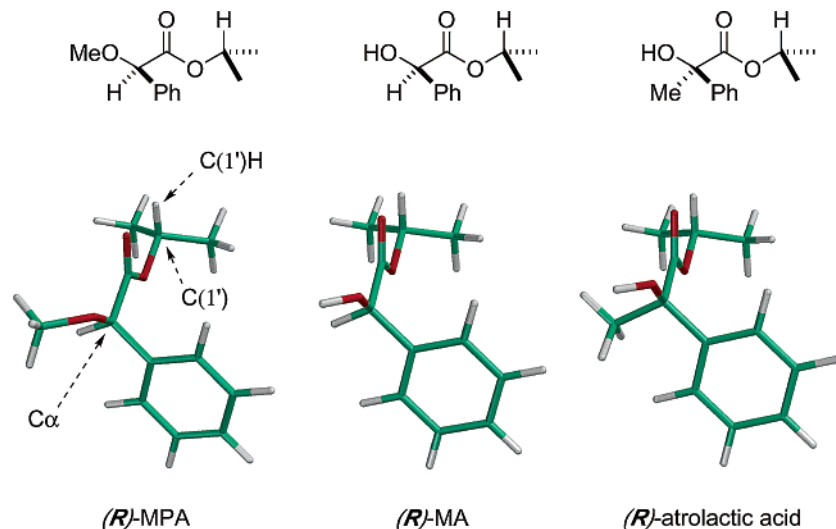
Another consequence of this same fact is reflected in the case of the  $\alpha$  aryl alcohols in Figures 12 and 13, where anisotropic groups in the alcohol substituents effectively overcome the reduced shielding/deshielding produced by the MTPA, leading to  $\Delta\delta^{SR}$  signs that do not necessarily reflect the configuration of the substrate.

Figure 27a illustrates how the magnetic field of the phenyl ring affects the space occupied by the alcohol substituents. When we consider the three main conformers of a MTPA ester, the space distribution of the magnetic field is different for each conformer and leads to the signs of the  $\Delta\delta^{SR}$  value that are indicated in Figure 27b.

As can be observed, it is perfectly possible for a substituent such as  $L_1$  to possess protons located in the space determined by quadrant 2 and other protons in quadrant 3. If this were the case, different  $\Delta\delta^{SR}$  signs will result in the average spectra and, therefore, an irregular distribution of signs will result for the protons in  $L_1$ .

Furthermore, if one considers the role of the conformational equilibrium in the average spectra, it is easy to understand that small changes in the balance of conformers may produce certain protons to pass from a net shielding area to a net deshielding area. In fact, even if we assume that conformer *ap*1





**Figure 28.** Isopropyl esters of MPA, MA, and atrolactic acid.

remains the most significant conformer in all circumstances, small variations in the ratio of the other two forms could eventually lead to a different shielding/deshielding balance, because each conformer has a different shielding/deshielding effect.

**3.1.1.8. Summary.** In summary, the use of MTPA for the assignment of the absolute configuration of alcohols is restricted by the conformational limits imposed by the reagent. Three conformations of similar population are present, and these simultaneously cause shielding/deshielding effects on the same substituent. This situation explains many of the observations regarding this method,<sup>13</sup> including (a) the frequency with which small values of  $\Delta\delta^{SR}$  are found that are of little use for the assignment of configuration and (b) irregular sign distributions.

The conformational flexibility of MTPA esters and the magnetic field distribution facilitates small structural or experimental changes (e.g., NMR solvent or temperature) to change the balance between the conformers, causing the sign distributions of  $\Delta\delta^{SR}$  to follow patterns that are different from those predicted by the original Mosher model.

Overall, Mosher's reagent, although still useful for the determination of enantiomeric purity by NMR spectroscopy, is not recommended for the determination of the absolute configuration of secondary alcohols by NMR. Such assignments should be made using other, more-reliable reagents.

### 3.1.2. Methoxyphenylacetic Acid (MPA)

**3.1.2.1. Classical Models for MPA Esters.**  $\alpha$ -Methoxy- $\alpha$ -phenylacetic acid (MPA; see Figures 4 and 28), along with MTPA, has been one of the most frequently used auxiliary reagents for the assignment of the absolute configuration of secondary alcohols by NMR. The application of this reagent, together with the use of mandelic acid (MA) and atrolactic acid (Figure 28), was described by Mosher in 1973.<sup>8c</sup> However, the utility of this reagent was not fully accepted at the time, mainly because of problems associated with racemization found during the derivatization of the alcohol. It was later found that this problem could be easily circumvented if different derivatization conditions are used.<sup>28</sup>

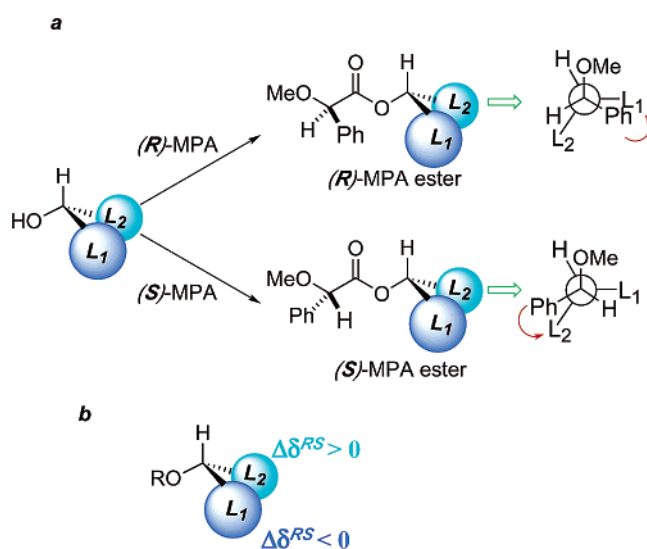


**Figure 29.** Model for configurational correlation of MPA esters.

The procedure for the determination of absolute configuration with this reagent is the same as that already described for MTPA and can be summarized as follows (Figure 29): (a) derivatization of the alcohol in question with the two enantiomers of the reagent, (b) examination of the NMR spectra of the (*R*)- and (*S*)-MPA ester derivatives and evaluation of the corresponding differences in the chemical shifts of the substituents of the alcohol ( $\Delta\delta^{RS}L_1 = \delta L_1(R) - \delta L_1(S)$  and  $\Delta\delta^{RS}L_2 = \delta L_2(R) - \delta L_2(S)$ ). As noted previously, the configuration is deduced from the signs of these differences and their comparison with an empirical model (see Figure 29b).

In this model, the most representative conformer has the methoxy group of MPA (the hydroxyl group in MA and atrolactic acid) and the carbonyl and C(1')H proton of the alcohol in the same plane (see Figure 29a). These groups are arranged in such a way that, in the (*R*)-MPA ester, substituent  $L_1$  is shielded by the phenyl ring while  $L_2$  is unaffected, whereas, in the (*S*)-MPA ester, substituent  $L_2$  is the shielded group and  $L_1$  remains unaffected (Figure 29a).

In this way, the alcohols in the figure show  $\Delta\delta^{RS}L_1 < 0$ , because substituent  $L_1$  is more shielded in the

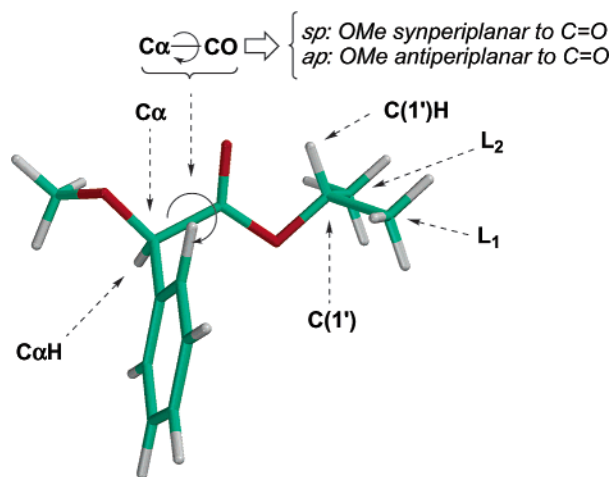


**Figure 30.** Main conformers of the MPA esters.

(*R*)-MPA ester than in the (*S*)-MPA ester, and  $\Delta\delta^{RS}L_2 > 0$ , because substituent  $L_2$  is more shielded in the (*S*)-MPA ester than in the (*R*)-MPA ester (see Figure 29b).

The relative position of the phenyl group of the auxiliary, with respect to  $L_1$  and  $L_2$  of the same alcohol, is opposite in the MPA and MTPA esters, thus producing opposite signs for the same chirality (see Figure 8). To obtain the same signs with the two reagents, the differences in chemical shifts are calculated as  $\Delta\delta^{RS}$  in MPA esters, whereas  $\Delta\delta^{SR}$  is used with MTPA esters.

**3.1.2.2. Conformational Analysis.** Historically, the first model used to correlate the absolute configuration of alcohols with the NMR shifts and signs of the  $\Delta\delta^{RS}$  values of the MPA esters was proposed by Mosher<sup>8c</sup> and is, as in the case of MTPA derivatives, empirically generated from the study of several alcohols of known stereochemistry. For this reason, the validity of the method is related to the representativity and scope of the series of alcohols initially studied.<sup>8c</sup>

To evaluate the limitations of this model, studies have been conducted<sup>29</sup> that are comprised of (a)

theoretical structure calculations (molecular mechanics, semiempirical (AM1) and ab initio), (b) shielding-effect calculations on the contribution of the phenyl group to the chemical shift, and (c) dynamic NMR to elucidate the conformational characteristics of the compounds.

As a result, the main conformers of the MPA esters were identified. Their populations and the role of the phenyl ring were determined, and this determination allowed a complete understanding of the fundamentals of the method and provided the basis for the design of more-efficient reagents.<sup>30</sup>

It was found<sup>29</sup> that the MPA esters of secondary alcohols are mainly composed of two conformers that are formed by hindered rotation around the  $C\alpha$ -CO bond (see Figures 30 and 31). The most stable one (by 0.6–1.0 kcal/mol) is the *sp* conformer, in which the methoxy group, the  $C\alpha$  carbon, and the carbonyl group of the MPA portion and the  $C(1)H$  hydrogen of the alcohol portion are in the same plane, with the methoxy and the carbonyl groups in a *syn* (synperiplanar) disposition. In this conformation, the phenyl ring is coplanar with the  $C\alpha$ -H bond, which is the best arrangement to effectively transmit aromatic shielding to the substituent ( $L_1$  or  $L_2$ ) located in the same side of the plane (see Figure 31).

The next conformer, in terms of energy (the *ap* conformer), has the same coplanar arrangement of the aforementioned groups, but, in this case, the methoxy and carbonyl groups are in an anti-periplanar relationship and the phenyl group is rotated so it cannot transmit the shielding effect to substituents  $L_1/L_2$  as efficiently as in the example discussed previously (see Figure 31). Thus, in the (*R*)-MPA ester derivative, substituent  $L_1$  is shielded by the phenyl ring in the *sp* conformation while substituent  $L_2$  is unaffected (see Figure 32a). In contrast, substituent  $L_2$  should be slightly shielded in the *ap* conformation while substituent  $L_1$  remains unaffected (see Figure 32a). The opposite situation occurs in the (*S*)-MPA ester: substituent  $L_2$  is shielded and substituent  $L_1$  remains unaffected in the

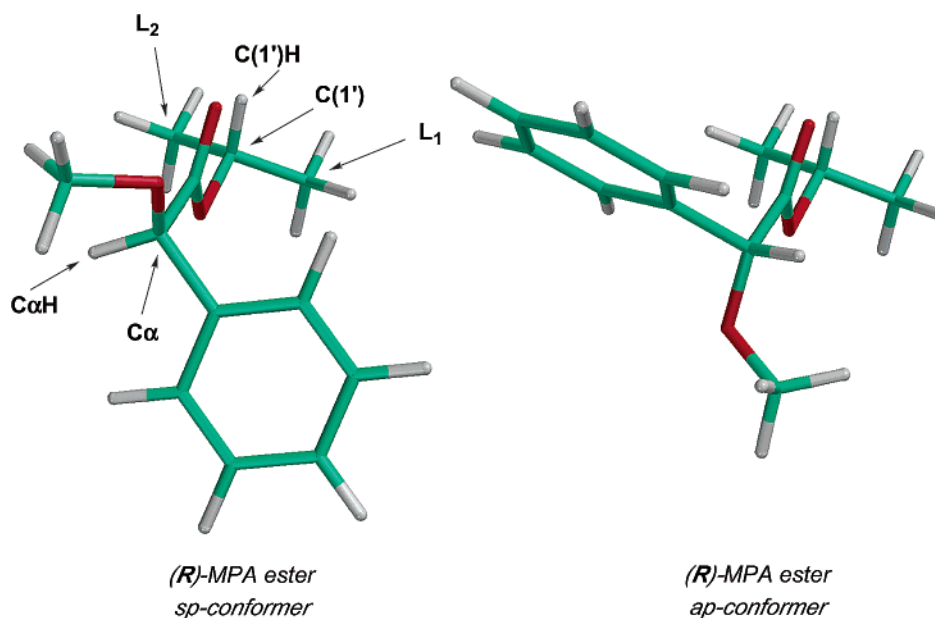


**Figure 31.** Conformers *sp* and *ap* of the isopropyl (*R*)-MPA ester.

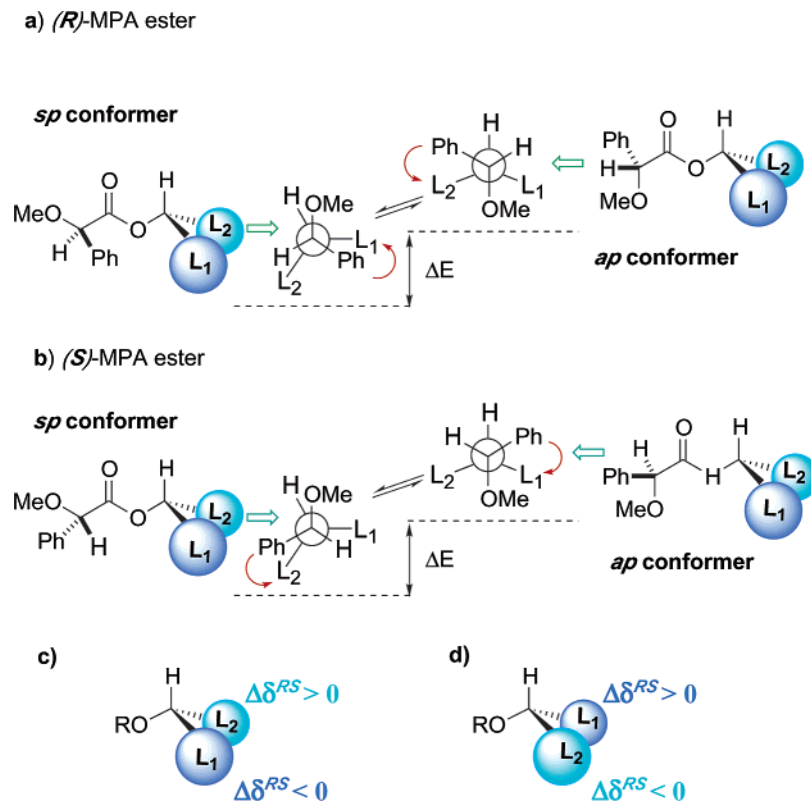


**Figure 32.** Conformational equilibrium in MPA esters.

*sp* conformer, whereas substituent  $L_1$  is slightly shielded and substituent  $L_2$  is unaffected in the *ap* conformer (Figure 32b).

As a result of the characteristics discussed above, the aromatic group of the reagent will modify the chemical shifts of substituents  $L_1$  and  $L_2$  in a very selective way: In the (*R*)-MPA ester, it is expected that strong shielding will be experienced by substituent  $L_1$  but only on the proportion of the molecules in which substituent  $L_1$  is beside the phenyl group (conformer *sp*). On the other hand, in the (*S*)-MPA ester, substituent  $L_1$  will be slightly shielded, but only for those molecules in the *ap* conformation. Given that the *sp* conformer is more abundant than the *ap* conformer, substituent  $L_1$  is more shielded in the (*R*)-MPA ester than in the (*S*)-MPA ester. Similar reasoning for substituent  $L_2$  leads to the conclusion that it will be more shielded in the (*S*)-MPA ester than in the (*R*)-MPA ester. Thus, the differences in chemical shifts ( $\Delta\delta^{RS}$ ) will be positive in one case and negative in the other (see Figure 32c). If the opposite configuration is considered for the alcohol (i.e., substituent  $L_1$  in place of substituent  $L_2$ ), then the opposite distribution of signs is obtained (see Figure 32d), thus demonstrating that the sign of  $\Delta\delta^{RS}$  is a reliable indicator of the spatial arrangement of the substituents.

$$\Delta\delta^{RS}L_1 = \delta L_1(R) - \delta L_1(S) < 0$$

$$\Delta\delta^{RS}L_2 = \delta L_2(R) - \delta L_2(S) > 0$$

The model proposed by Mosher<sup>8c,28a</sup> for the assignment of the configuration of MPA esters is, in fact, a representation of the most stable conformer of the

equilibrium, which is also the most important, from the standpoint of NMR, and is therefore suitable to predict the correct configuration. Figure 33 shows a selection of compounds studied using that model.<sup>31</sup>

Note that this is not the case for MTPA esters, where the model used by Mosher is not truly representative of the conformational composition.<sup>27</sup>

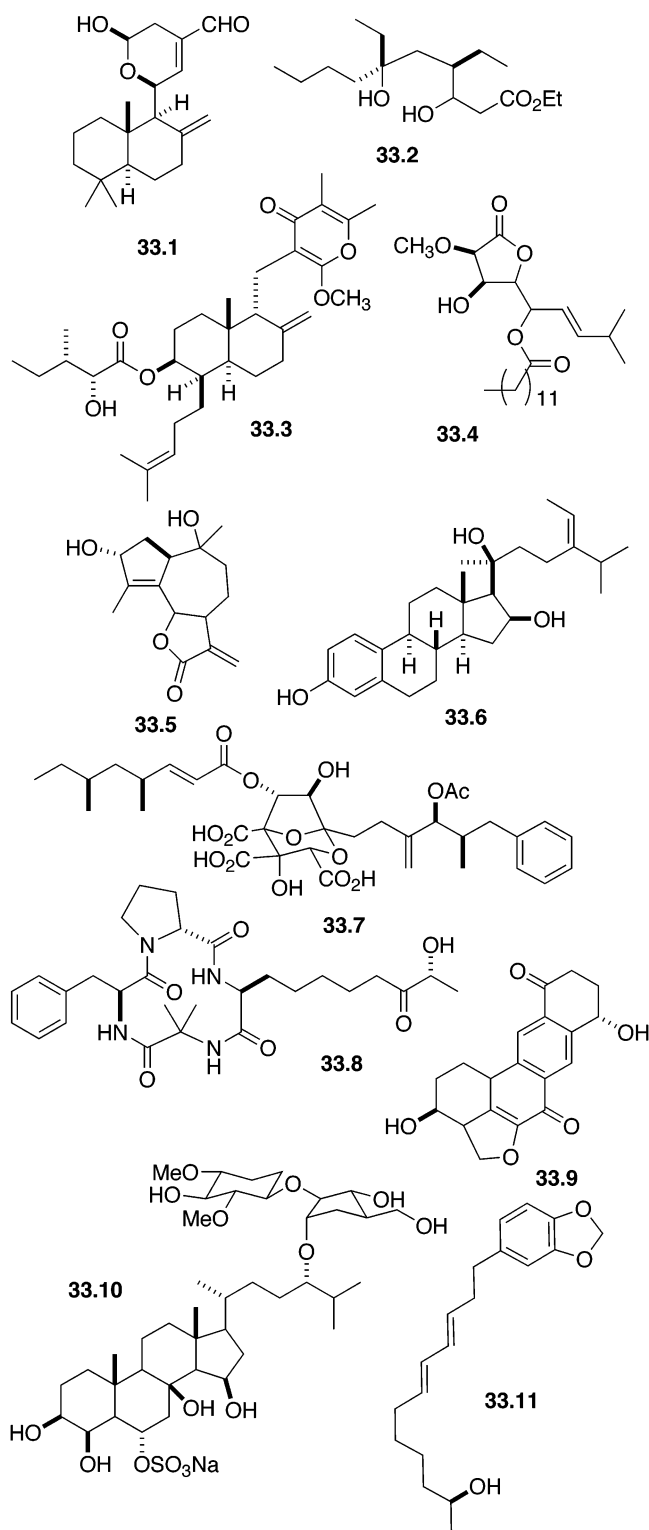
**3.1.2.3. MPA versus MTPA.** In general, researchers have not been very critical when choosing between MPA and MTPA for the assignment of secondary alcohols. Quite frequently, they have overlooked the anomalies detected with MTPA<sup>13</sup> that were mentioned in the previous chapter.

In the case of MTPA esters of secondary alcohols, two factors contribute to these limitations:<sup>27,32</sup> (a) the presence of three main conformers with similar populations and (b) the fact that some of these conformers produce shielding effects and others produce deshielding effects on substituents  $L_1/L_2$  (see Figure 25), the combination of which produces very small  $\Delta\delta^{SR}$  values and sometimes unexpected signs.

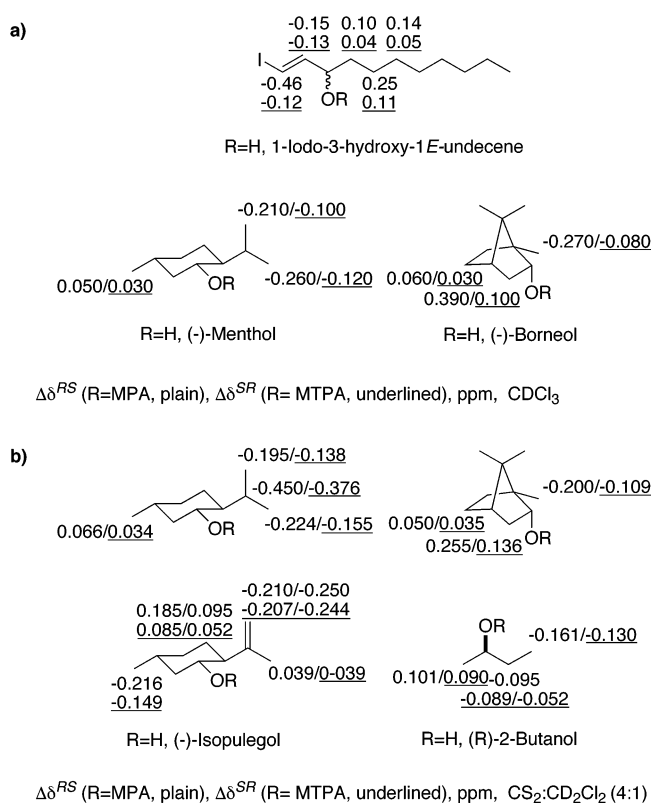
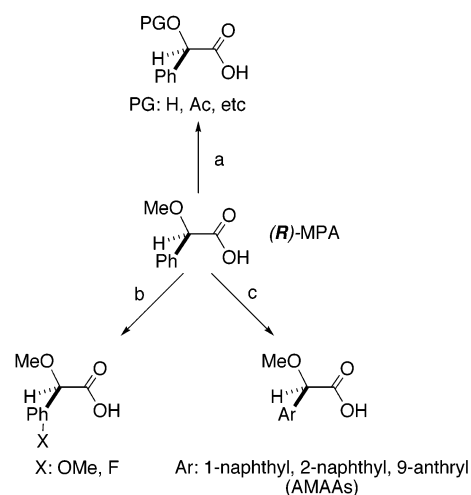
In contrast, the MPA esters present a simpler conformational composition (see Figure 32) with only two conformers (*sp/ap*) and a clearer preference for one of those (*sp*), which, in turn, transmits a shielding effect to the substituents to give higher  $\Delta\delta^{RS}$  values that are more reliable and homogeneous in terms of distribution of the signs (Figure 34).

On the basis of the aforementioned discussion, the choice between MTPA and MPA as a derivatizing agent for secondary alcohols should be clearly in favor of MPA.

**3.1.2.4. New MPA Analogues: The Effect of Structural Modifications.** In the search for more efficient and reliable reagents, a variety of modifica-

**Figure 33.**

tions of the structure of MA have been performed (Figure 35), leading to a series of arylmethoxyacetic acids<sup>30,33</sup> (AMAAs). Some of these compounds are interesting from the practical standpoint and others are interesting because of the information they provide regarding our understanding of the method. The most revealing modifications have been (a) the introduction of different *O*-substituents on MA,<sup>34</sup> (b) the introduction of different substituents on the phenyl ring<sup>30,33</sup> of MPA, and (c) the replacement of that phenyl ring by other aryl ring systems.<sup>29,30,33</sup>

**Figure 34.**  $\Delta\delta^{RS}$  and  $\Delta\delta^{SR}$  values (in ppm) for a selection of MPA and MTPA esters of secondary alcohols obtained in (a)  $\text{Cl}_3\text{CD}$  and (b)  $\text{CS}_2:\text{CD}_2\text{Cl}_2$  (4:1). MTPA data are noted by an underline.**Figure 35.**

**3.1.2.5. *O*-Substituted Mandelic Acids.** Table 1 shows the structures of several *O*-substituted MAs and the ability of their enantiomers to differentiate the NMR signals<sup>34a</sup> of (-)-menthol expressed as  $\Delta\delta^{RS}$ . As can be seen, the values are very similar in all cases, being somewhat greater in MA and its acetyl derivative (see Figure 36). In addition to similar  $\Delta\delta^{RS}$  values, the same distribution of the signs as that observed with MPA itself is obtained, indicating that their mode of action and conformational composition is quite probably the same, suggesting that no real improvement can be expected by changing the *O*-substituent in MA.

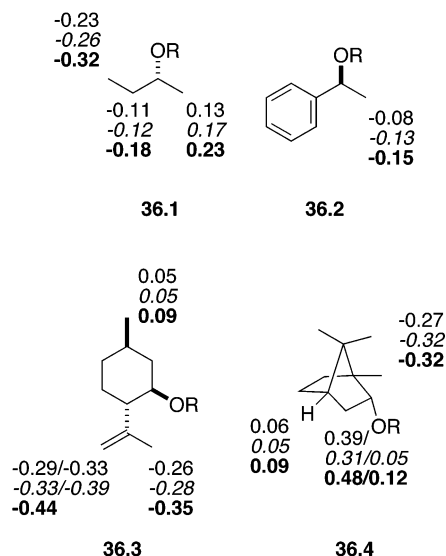


**Figure 36.**  $\Delta\delta^{RS}$  values obtained for *O*-substituted mandelic esters with a selection of secondary alcohols. Data for R = AcMA is given in italic type, and data given for R = MA is given in boldface type.

**Table 1.**  $\Delta\delta^{RS}$  Values of *O*-Substituted Mandelic Esters of (-)-Menthol

| R group                        | $\Delta\delta\text{Me}(8)$ | $\Delta\delta\text{Me}(9)$ | $\Delta\delta\text{Me}(10)$ |
|--------------------------------|----------------------------|----------------------------|-----------------------------|
| Me (MPA)                       | <b>-0.22</b>               | <b>-0.26</b>               | <b>0.05</b> ←               |
| Bn                             | -0.21                      | -0.26                      | 0.05                        |
| <i>tert</i> -Bu                | -0.12                      | -0.11                      | 0.03                        |
| H (MA)                         | <b>-0.25</b>               | <b>-0.40</b>               | <b>0.01</b> ←               |
| CH <sub>3</sub> CO (AcMA)      | <b>-0.28</b>               | <b>-0.32</b>               | <b>0.04</b> ←               |
| <i>tert</i> -BuCO              | -0.19                      | -0.27                      | 0.02                        |
| <i>p</i> -NO <sub>2</sub> PhCO | -0.23                      | -0.33                      | 0.07                        |
| PhCO                           | -0.22                      | -0.33                      | 0.01                        |
| <i>p</i> -BrPhCO               | -0.20                      | -0.29                      | 0.02                        |

A different case is constituted by the THP ether of MA, which has been investigated<sup>34b</sup> as a reagent for the assignment of the absolute configuration of cyclic alcohols (see Figure 37). Unfortunately, an irregular distribution of  $\Delta\delta^{RS}$  signs were obtained in the two compounds tested, which makes the reagent useless for the intended purpose. Only two open-chain secondary alcohols (Figure 37) were studied with this reagent and showed the same distribution of signs as that for MPA.

**3.1.2.6. The Role of the Substituents in the Aromatic Ring.** Similar studies have been conducted<sup>30,33</sup> to ascertain whether the introduction of substituents into the phenyl ring of MPA will produce an increase in the  $\Delta\delta^{RS}$  values.

The results obtained for some of these new reagents with (-)-menthol as the substrate are shown in Table 2. These data indicate that, in general, the presence of fluoro or methoxy groups in several different positions does not produce any improvement in the capability of MPA to separate the signals of enantiomers. In the case of the pentafluorophenyl

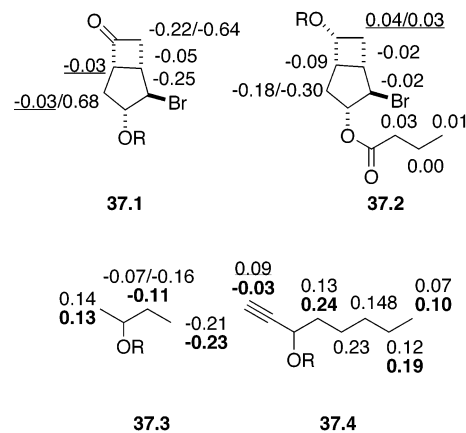


**Figure 37.**  $\Delta\delta^{RS}$  values of *O*-substituted mandelic esters. Data for R = MPA is given in boldface type; underlined data present anomalous signs.

**Table 2.**  $\Delta\delta^{RS}$  Values Obtained for Phenyl-Substituted MPA Esters of (-)-Menthol

| Aryl | $\Delta\delta^{RS}$ |         |        |        |
|------|---------------------|---------|--------|--------|
|      | Acid                | Me(10') | Me(8') | Me(9') |
|      |                     | 0.07    | -0.040 | -0.10  |
|      |                     | 0.05    | -0.021 | -0.25  |
|      |                     | 0.06    | -0.022 | -0.25  |
| Ph   | <b>MTPA</b>         | 0.07    | -0.017 | -0.04  |
| Ph   | <b>MPA</b>          | 0.05    | -0.022 | -0.26  |

derivative, the  $\Delta\delta^{RS}$  values are, in fact, smaller than those obtained with MPA and similar to those obtained with MTPA, whereas the methoxy-substituted reagents give  $\Delta\delta^{RS}$  values that are greater than those for MTPA and equivalent to those of MPA.

Conformational studies were performed and revealed that the introduction of those substituents shifts the equilibrium between the *sp* and *ap* conformers and changes the orientation of the phenyl ring to a less favorable arrangement for shielding. It is the combination of these two facts that result in smaller  $\Delta\delta^{RS}$  values.

**3.1.2.7. Arylmethoxyacetic Acids (AMAAs).** The structural modifications discussed in the preceding lines have shown that no improvement of  $\Delta\delta$  can be expected by introduction of substituents on MPA. As will be fully discussed in the corresponding section (Section 3.1.3), the replacement of the phenyl ring of MPA by a naphthyl or anthryl ring has been shown to produce the most efficient reagents to date.<sup>29,30,33,35-37</sup> More specifically,  $\alpha$ -(2-naphthyl)- $\alpha$ -methoxyacetic acid (2-NMA),  $\alpha$ -(1-naphthyl)- $\alpha$ -methoxyacetic acid (1-NMA),  $\alpha$ -(9-anthryl)- $\alpha$ -methoxyacetic acid (9-AMA), and  $\alpha$ -(2-anthryl)- $\alpha$ -methoxyacetic acid (2-ATMA) are effective reagents (see Figure 38).

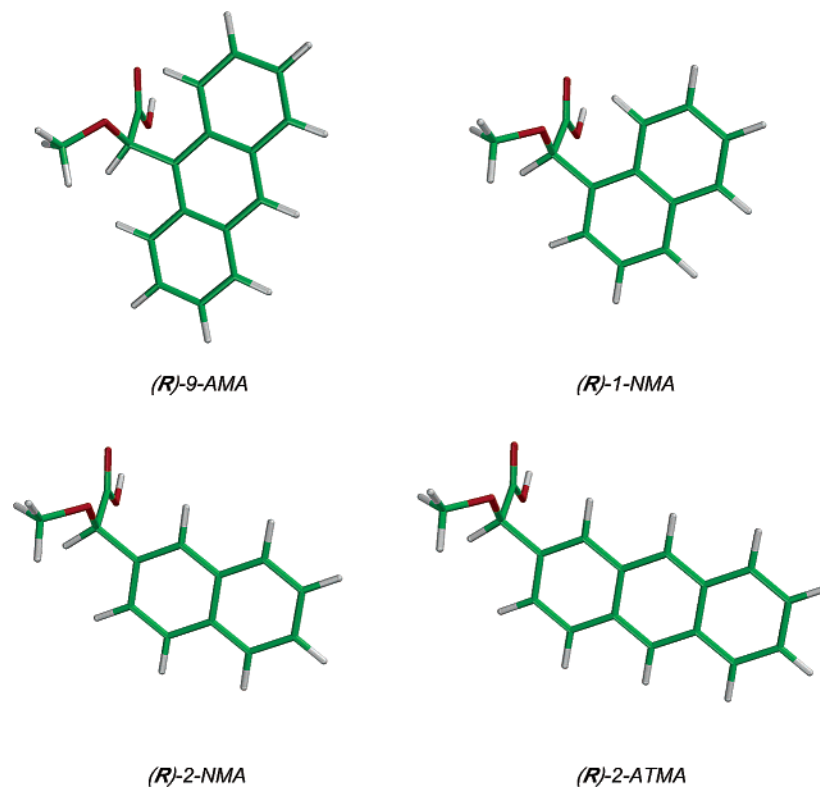


**Figure 38.** Molecular structure of the arylmethoxyacetic acids (AMAAs).

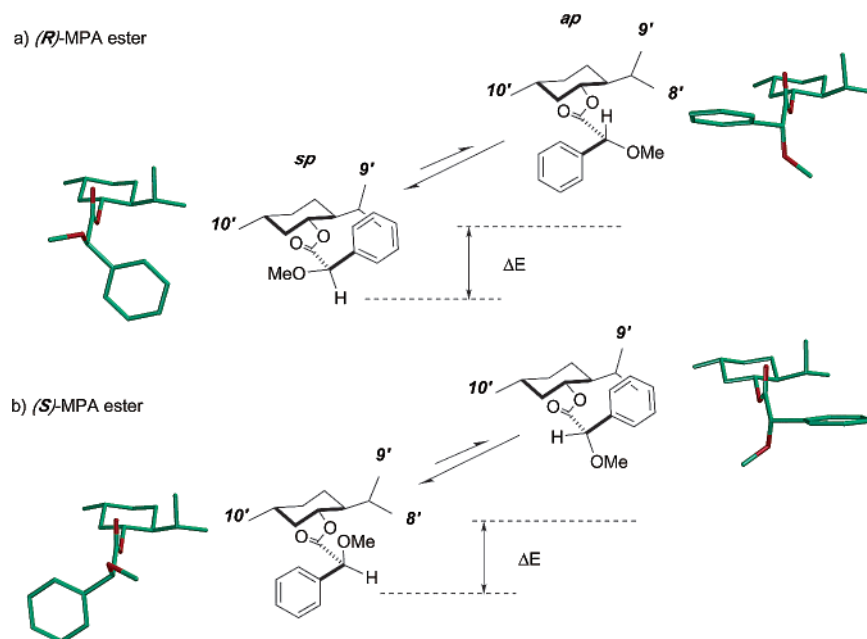


**Figure 39.** Conformational composition of the MPA esters of (–)-menthol.

**3.1.2.8. The Effect of the Temperature on the NMR of MPA Esters.** A different and successful approach to obtain the best  $\Delta\delta^{RS}$  values without modification of the structure of the auxiliary reagent consists of the controlled modification of the relative populations (conformer *sp/ap*) of the MPA esters by directly acting on the thermodynamic parameters governing the equilibrium,<sup>38</sup> namely the polarity of the NMR solvent and the temperature of the NMR probe.

Although changes in the NMR solvent<sup>30</sup> did not lead to any significant improvement of the  $\Delta\delta^{RS}$  values obtained for MPA esters of several secondary

alcohols, when their NMR spectra were recorded at different temperatures, the changes in chemical shifts consistently produced higher  $\Delta\delta^{RS}$  values<sup>38</sup> of practical interest.

Thus, in the (*R*)-MPA ester of (–)-menthol, the Me(8) and Me(9) protons are strongly shielded by the phenyl ring in the *sp* conformer (see Figure 39a, resonances at 0.651 and 0.418 ppm, respectively), whereas Me(10') is slightly shielded in the *ap* conformer (0.888 ppm). A decrease of the probe temperature should produce an increase in the number of molecules in the *sp* conformation (the most stable one) and a corresponding decrease in the *ap* popula-

**Table 3. Chemical Shifts of MPA Esters of (-)-Menthol at Different Temperatures<sup>a</sup>**

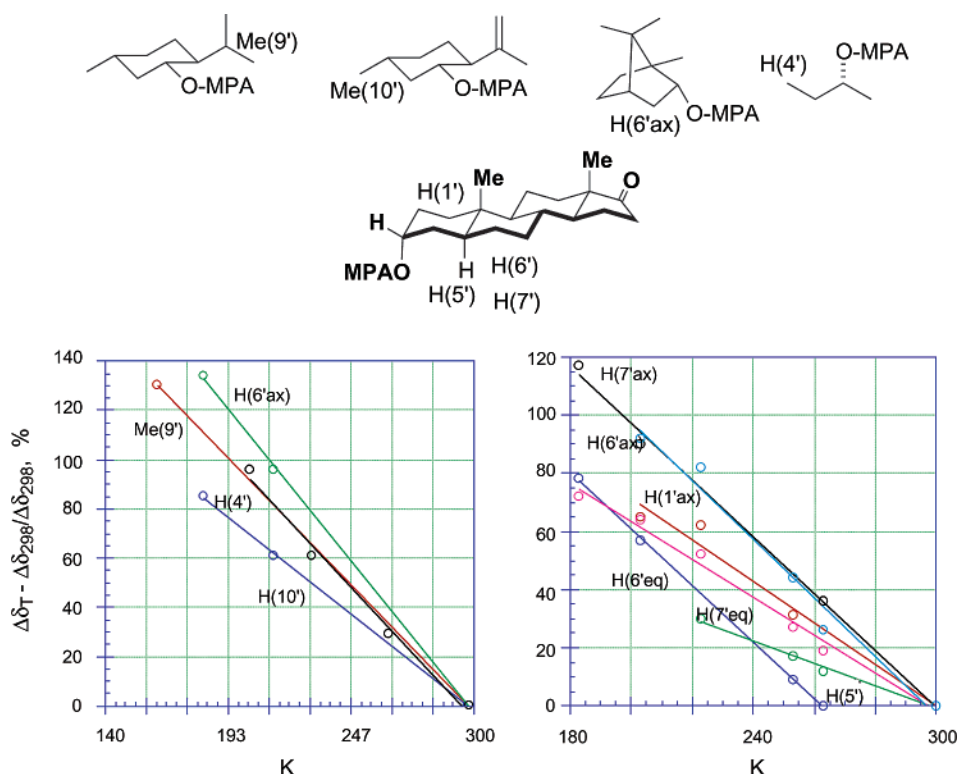
| ester               | chemical shift   |        |         |
|---------------------|------------------|--------|---------|
|                     | Me(8')           | Me(9') | Me(10') |
|                     | <i>T</i> = 296 K |        |         |
| ( <i>R</i> )-MPA    | 0.651            | 0.418  | 0.888   |
| ( <i>S</i> )-MPA    | 0.846            | 0.642  | 0.822   |
| $\Delta\delta^{RS}$ | -0.195           | -0.224 | 0.066   |
|                     | <i>T</i> = 153 K |        |         |
| ( <i>R</i> )-MPA    | 0.561            | 0.165  | 0.898   |
| ( <i>S</i> )-MPA    | 0.895            | 0.681  | 0.785   |
| $\Delta\delta^{RS}$ | -0.334           | -0.516 | 0.113   |

<sup>a</sup> CS<sub>2</sub>:CD<sub>2</sub>Cl<sub>2</sub> ratio = 4:1.

tion (the least stable one). For this reason, as shown in Table 3, at lower temperatures, more molecules

have their Me(8') and Me(9') groups shielded (increased shielding in the average spectrum; resonances at 0.561 and 0.165 ppm) and fewer molecules have their Me(10') shielded by the phenyl group (increased shielding in the average spectrum; resonance at 0.898 ppm).

Similarly, in the (*S*)-MPA ester, the Me(8') and Me(9') groups become less shielded at lower temperatures and the signals are shifted from 0.846 and 0.642 ppm to 0.895 and 0.681 ppm, respectively, whereas Me(10') is more intensely shielded at lower temperatures, with a change in chemical shift from 0.822 to 0.785 ppm for the corresponding signal (see Figure 39b).

**Figure 40.** Evolution with temperature of the  $\Delta\delta^{RS}$  values of MPA esters of secondary alcohols.**Table 4.  $\Delta\delta^{RS}$  Values for a Selection of MPA Esters at Different Temperatures<sup>a</sup>**

| temp.<br><i>T</i> (K) | $\Delta\delta^{RS}$ (ppm) |        |        |       |        |        |         |        |        |        |        |         |
|-----------------------|---------------------------|--------|--------|-------|--------|--------|---------|--------|--------|--------|--------|---------|
|                       | H(1')                     | H(3')  | H(4')  | H(5') | H(6'a) | H(6'e) | H(6'ax) | H(7')  | H(8')  | Me(8') | Me(9') | Me(10') |
|                       | (-)-Isopulegol            |        |        |       |        |        |         |        |        |        |        |         |
| 298                   |                           |        |        |       |        | 0.050  | 0.085   |        | -0.210 | -0.250 | -0.216 | 0.039   |
| 213                   |                           |        |        |       |        | 0.100  | 0.175   |        | -0.319 | -0.373 | -0.348 | 0.049   |
| 183                   |                           |        |        |       |        | 0.100  | 0.175   |        | -0.346 | -0.403 | -0.40  | 0.049   |
|                       | (-)-Menthol               |        |        |       |        |        |         |        |        |        |        |         |
| 298                   |                           |        |        |       |        |        |         | -0.45  |        | -0.195 | -0.224 | 0.066   |
| 153                   |                           |        |        |       |        |        |         | -1.170 |        | -0.334 | -0.516 | 0.103   |
|                       | (-)-Borneol               |        |        |       |        |        |         |        |        |        |        |         |
| 298                   |                           |        |        | 0.050 | 0.255  | 0.080  |         |        |        |        | -0.200 |         |
| 213                   |                           |        |        | 0.104 | 0.499  | 0.138  |         |        |        |        | -0.312 |         |
| 183                   |                           |        |        | 0.125 | 0.596  | 0.162  |         |        |        |        | -0.331 |         |
|                       | <i>(R)</i> -2-Butanol     |        |        |       |        |        |         |        |        |        |        |         |
| 298                   | 0.101                     | -0.095 | -0.161 |       |        |        |         |        |        |        |        |         |
| 263                   | 0.120                     | -0.127 | -0.207 |       |        |        |         |        |        |        |        |         |
| 230                   | 0.138                     | -0.137 | -0.259 |       |        |        |         |        |        |        |        |         |
| 203                   | 0.156                     | -0.166 | -0.316 |       |        |        |         |        |        |        |        |         |

<sup>a</sup> CS<sub>2</sub>:CD<sub>2</sub>Cl<sub>2</sub> ratio = 4:1.

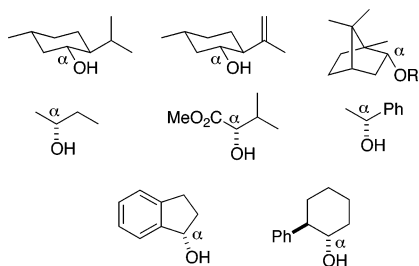


**Figure 41.** Alcohols tested with this method.

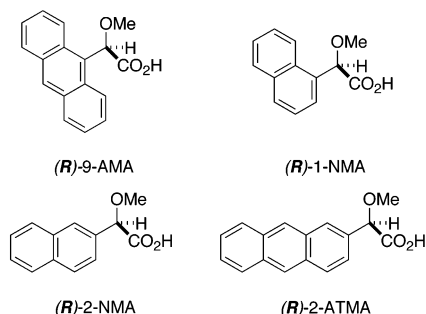


**Figure 42.** Structure of the arylmethoxyacetic acids (AMAAs).

In accordance with those results, the  $\Delta\delta^{RS}$  values of MPA esters of secondary alcohols become higher as the probe temperature is reduced (see Table 4 and Figure 40).

This trend reflects a general behavior that is well illustrated by the variety of structures shown in Figure 40. This technique is particularly useful when the  $\Delta\delta^{RS}$  values obtained at room temperature are so small that reliable e.e. or absolute configuration cannot be derived. In these cases, simply repeating the spectrum at a lower temperature can be sufficient to obtain well-separated signals and large  $\Delta\delta^{RS}$  values.

**3.1.2.9. Other Models for MPA Esters.** A new application of MPA in the determination of the absolute configuration of secondary alcohols has been described recently,<sup>39</sup> based in the exclusive use of the chemical shifts of the  $C\alpha H$  protons of the substrate in the corresponding (*R*)- and (*S*)-MPA esters. To assign the configuration, interactions between the reagent and substrate moieties of the diastereomeric esters must be estimated in the two main forms in the equilibrium (sp and ap) and compared with the chemical shifts of the  $C\alpha H$  protons. The diastereomer with the greater relative population of the most stable conformer in the equilibrium (sp form) should resonate at lower field. This behavior was experimentally proven for six alcohols and two amines (see Figure 41).

This method presents some limitations. One of them lies in the fact that it is based on the analysis of data from a single group ( $\Delta\delta^{RS}$  of the  $C\alpha H$ ), analogous to Mosher's Method for  $^{19}F$  NMR ( $\Delta\delta^{SR}$  of the  $CF_3$ ). The sign will always be correlated to a certain configuration, so if an anomaly arises, it will not be detected. In some cases, another restriction comes from the need of a combined use of NMR data and theoretical studies (i.e., semiempirical calculations) to evaluate the difference of energy between both conformers to compare them with the experi-

mental  $\Delta\delta^{RS}$  value. Nevertheless, and despite the aforementioned limitations, the method may be useful to analyze structures that lack protons in one of the substituents.

### 3.1.3. 9-Anthrylmethoxyacetic Acid (9-AMA) and Related AMAAs

The results described to date for MPA, along with the discovery of the role played by the phenyl ring in influencing the NMR shifts, have led to a search for more-efficient reagents by replacement of the phenyl ring by other aryl systems that are able to produce a more intense aromatic shielding effect on the substrate.<sup>29,30,33,35–37</sup> The most widely studied systems in this respect are the arylmethoxyacetic acids (AMAAs; see Figures 38 and 42), which contain naphthyl or anthryl systems. In general, all these compounds produce more-intense shielding than MPA and, consequently, better separation of the signals is observed for the enantiomers of the substrate. This effect is particularly important when 9-AMA is used as the reagent with secondary alcohols: the  $\Delta\delta^{RS}$  values obtained are 3–4 times higher than those with MPA.<sup>29,30</sup> In fact, this more pronounced separation of the signals for the substrate results from the combination of two factors: the intense aromatic magnetic field of the anthracene system and the greater conformational rigidity of 9-AMA, which is a factor that leaves the anthracene ring particularly well-oriented, with respect to the substrate.<sup>29</sup>

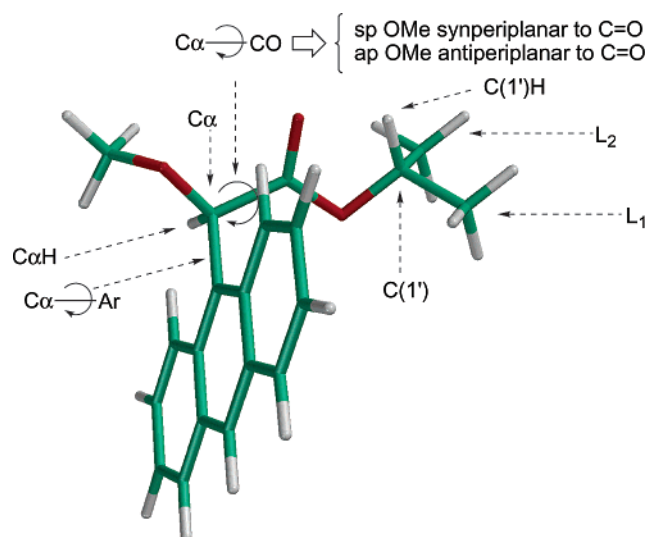


**Figure 43.** Main conformational processes in AMAA esters.

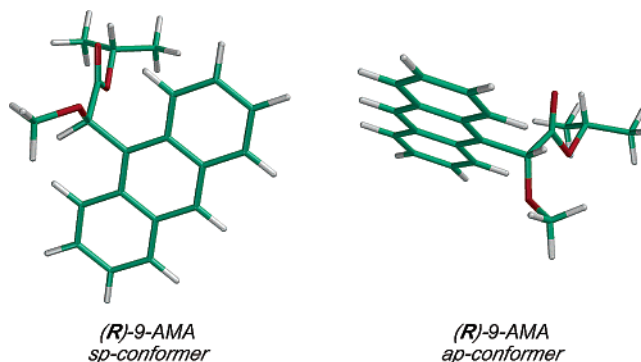


**Figure 44.** Main conformers of the 9-AMA esters.



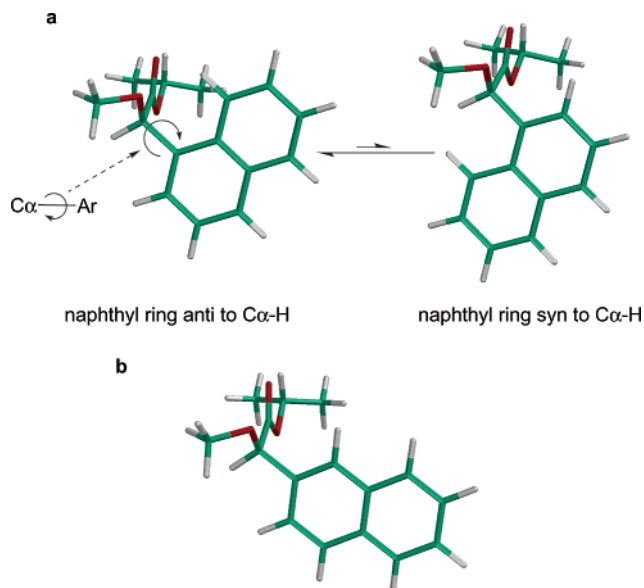


**Figure 45.** Main conformers generated by rotation around the C $\alpha$ -Ar bond (a) for 1-NMA and (b) for 2-NMA.

**3.1.3.1. Conformational Analysis.** Conformational studies<sup>29</sup> (theoretical and experimental) based on structure minimizations (molecular mechanics, semiempirical and *ab initio*, and shielding-effect calculations) and NMR studies (variable temperature) on the auxiliaries 9-AMA, 1-NMA, and 2-NMA

(no such information is available on 2-ATMA<sup>37</sup>) have revealed that, in a way similar to that for the MPA esters, the main conformational process is rotation around the C $\alpha$ -CO bond, and this process generates the same types of conformers as already described for MPA esters:<sup>29</sup> conformer *sp*, with the MeO group syn to the carbonyl group, is the most stable conformer and conformer *ap*, where the MeO group is anti, with respect to the carbonyl group, is the least stable (see Figures 43 and 44).

In regard to rotation around the C $\alpha$ -Ar bond, calculations indicate that the most stable conformer is that in which the C $\alpha$ -H bond is coplanar with the aryl plane, as shown in Figure 44. In those reagents where the aromatic substitution is asymmetric (e.g., 1-NMA, 2-NMA, and probably 2-ATMA), the main portion of the aryl ring is anti, with respect to the C $\alpha$ -H bond (see Figure 45).

Therefore, in the more stable conformer (*sp*), the C $\alpha$ -Ar bond is almost perpendicular to the C=O bond and the plane of the aromatic ring is parallel to the C=O bond. This arrangement makes the orientation of the aryl ring particularly effective, in terms of transmission of the shielding effect to the alcohol substituents L<sub>1</sub>/L<sub>2</sub>.

From the conformational standpoint, the equilibrium between the *sp* and *ap* conformations is, in all cases, shifted toward the *sp* conformer, which is the most stable conformer and the most representative

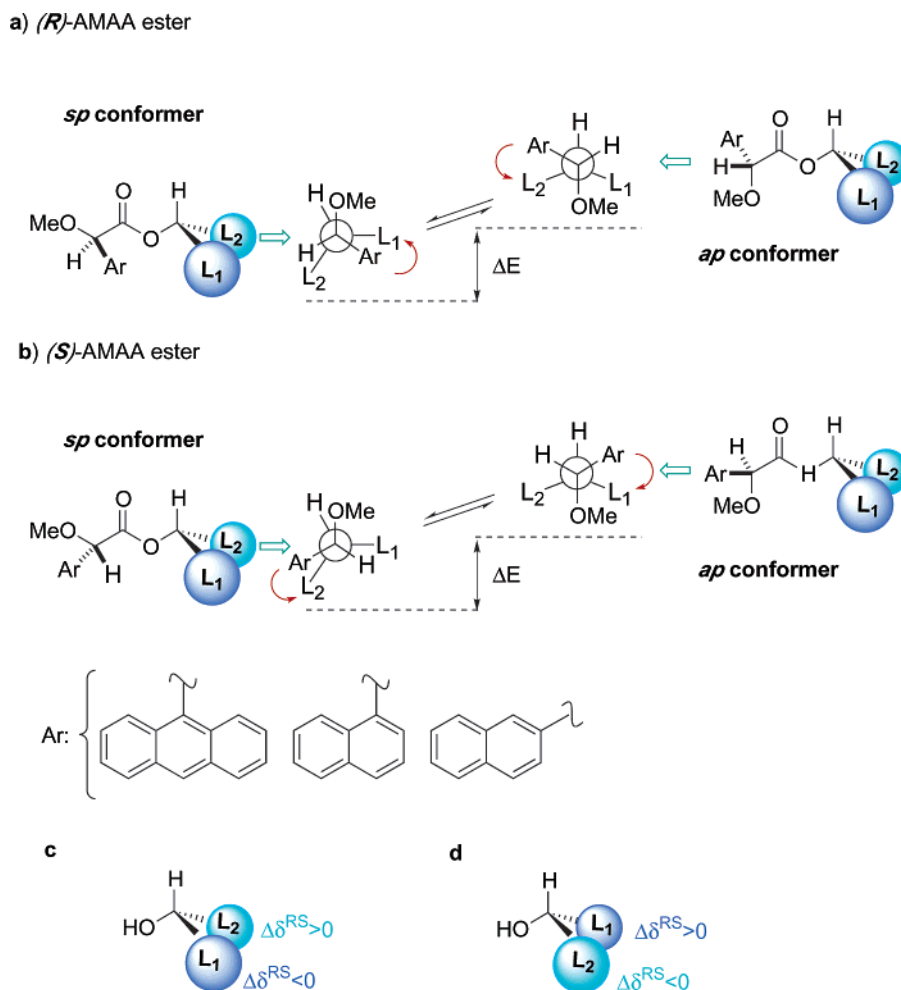


**Figure 46.** Conformational equilibrium in the AMAA esters.

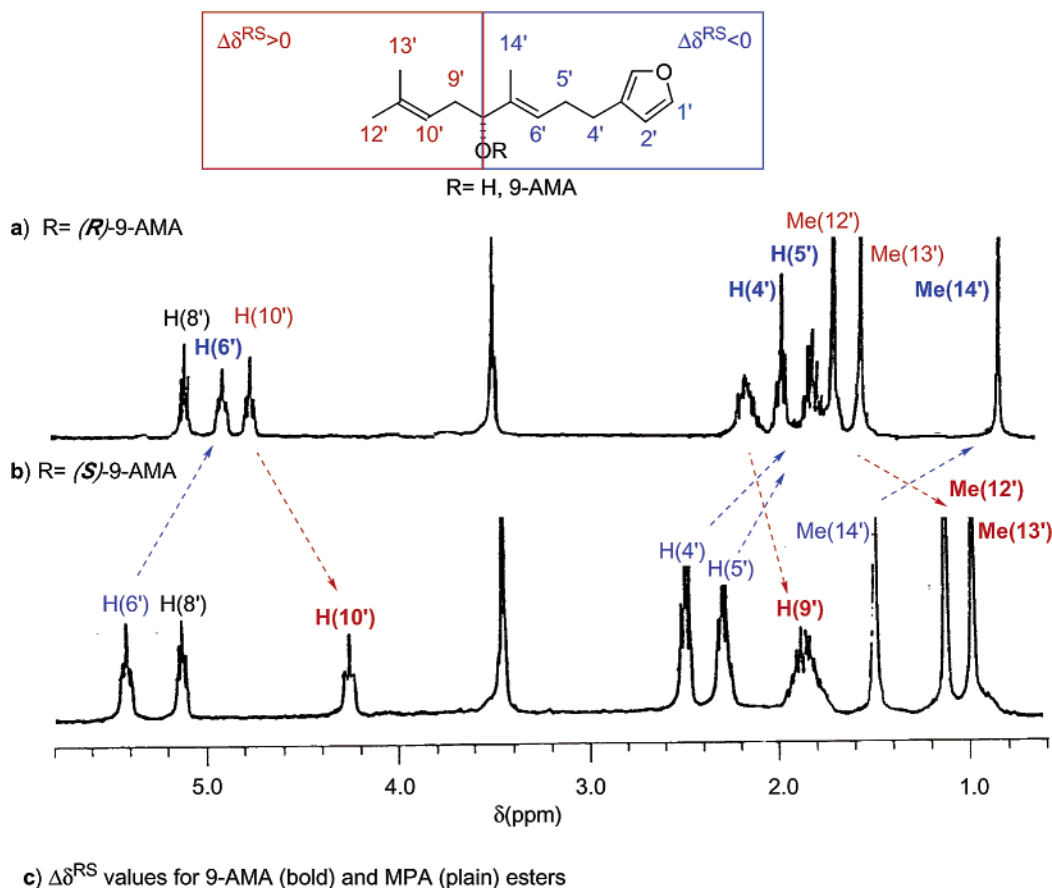


**Figure 47.** (a, b) NMR spectra of the (*R*)- and (*S*)-9-AMA esters of a marine metabolite and (c) comparison of the  $\Delta\delta^{RS}$  values of the 9-AMA esters with those of the MPA esters.

in the NMR process. However, the difference in energy<sup>29</sup> varies with the nature of the aryl ring and follows the order 9-AMA > 1-NMA > 2-NMA > MPA.

Thus, changing the aromatic ring plays a double role, because it affects both the intensity of the aromatic magnetic current and the conformational orientation of the ring, with respect to the substrate. In fact, the larger the ring, the more intense the aromatic shielding effect and the greater the resulting difference of energy between the *sp* and *ap* conformers. The combined effect of these two factors makes 9-AMA the most useful reagent of all, producing  $\Delta\delta^{RS}$  values that are much greater than those caused by other reagents.

The substitution pattern of the ring is also important because the rotational barriers for the  $C\alpha$ -Ar and  $C\alpha$ -CO bonds will be different. For example, the barrier in 1-NMA is greater than that for 2-NMA and this, in turn, affects the NMR results.

**3.1.3.2. NMR Spectra of AMAA Esters.** The NMR spectra of the AMAA esters are similar to those of the MPA esters, and the contribution of each conformer to the average NMR spectra also follows the same trend. Thus, in the (*R*)-AMAA ester, sub-

stituent  $L_1$  is shielded in conformer *sp* and substituent  $L_2$  remains unaffected, whereas in the *ap* conformer, substituent  $L_2$  is shielded and substituent  $L_1$  is not affected (see Figure 46a). In the ester derived from the (*S*)-AMAA auxiliary, the opposite situation occurs:  $L_2$  is shielded in the *sp* conformer and  $L_1$  is shielded in the *ap* conformer (see Figure 46b).

Comparison of the spectra of the (*R*)- and the (*S*)-AMAA esters, and considering the greater population of the *sp* conformer in comparison to that of the *ap* conformer, leads to the following signs for  $\Delta\delta^{RS}$  (these are the same as those obtained in the MPA esters with the same configuration):

$$\Delta\delta^{RS}L_1 = \delta L_1(R) - \delta L_1(S) < 0$$

$$\Delta\delta^{RS}L_2 = \delta L_2(R) - \delta L_2(S) > 0$$

Naturally, if the absolute configuration of the alcohol is opposite to that shown above, then the signs should be reversed (see Figure 46c and d).

Figure 47 illustrates the power of 9-AMA as a reagent for the assignment of the absolute configuration. The NMR spectra of the (*R*)- and (*S*)-9-AMA

esters of a marine metabolite<sup>40</sup> show that the signals for protons H(1'), H(2'), H(4'), H(5'), H(6'), and Me(14') result in negative  $\Delta\delta^{RS}$  values and, therefore, take the place of substituent L<sub>1</sub> in the model shown in Figure 47. On the other hand, protons H(9'), H(10'), Me(12'), and Me(13') give positive  $\Delta\delta^{RS}$  values and are therefore represented by substituent L<sub>2</sub>. As can be seen in Figure 47c, the  $\Delta\delta^{RS}$  values obtained with 9-AMA are far superior to those obtained using MPA as the auxiliary (in some cases, by a factor of >4), although the signs are the same.

An experimental demonstration of the reliability of the configurational assignment obtained with these AMAAs, and, consequently, of the model described in Figure 46, was achieved by examination of a series of alcohols of known absolute configuration. In all the cases described<sup>41</sup> in Figures 48 and 49, the  $\Delta\delta^{RS}$  signs are in accordance with the stereochemistry of the alcohol examined. The magnitude of the  $\Delta\delta^{RS}$  values follows the order 9-AMA > 1-NMA > 2-NMA > MPA > MTPA.

The number of alcohols of known absolute configuration used to validate 2-ATMA<sup>37</sup> as the reagent is much lower than for the other reagents. In addition, neither structure calculations nor conformational analyses have been presented,<sup>37</sup> although it does not seem unreasonable to believe that the model should be the same as that presented for the other AMAAs.

On the basis of the nature and orientation of the aromatic ring in the AMAAs and its associated magnetic field, it was proposed that some of these reagents should be particularly suited for study linear alcohols and others should be suited for cyclic systems.<sup>37b</sup> In this respect, the reagents 2-NMA and 2-ATMA were proposed<sup>36,37</sup> as being the most suitable for the study of long-chain alcohols, on the basis of the expectation that, in the esters, the aromatic rings of the reagent would lie over the chain of the substrate and thus cause significant shift changes on the protons of a large portion of the chain (see Figure 50). Reagent 9-AMA, on the other hand, was expected to be more efficient when used in conjunction with cyclic alcohols.<sup>30</sup>

Nevertheless, comparison of the  $\Delta\delta^{RS}$  values obtained<sup>30,36,37</sup> for the esters of 9-AMA, 2-NMA, and 2-ATMA with the linear long-chain alcohols shown in Figure 51 demonstrates that the highest  $\Delta\delta^{RS}$  values are always obtained when 9-AMA is used as the reagent, whereas 2-NMA is the least-efficient reagent of the three.

A graphical representation of the  $\Delta\delta^{RS}$  values obtained for protons at different distances from the asymmetric C atom for the 9-AMA esters<sup>42</sup> derived from **51.1**, **51.2**, and **51.3**, and of the 2-NMA and 2-ATMA esters derived from **51.4** and **51.5**, is shown in Figure 51. The spatial zone of maximum shielding is much more concentrated in the 9-AMA esters than in the other. In the 9-AMA esters, it is experienced by protons 2–3 carbon bonds away from the asymmetric C atom, decreases rapidly with distance, and at approximately the fifth bond away shows  $\Delta\delta^{RS}$  values equivalent to those produced by 2-NMA and 2-ATMA.

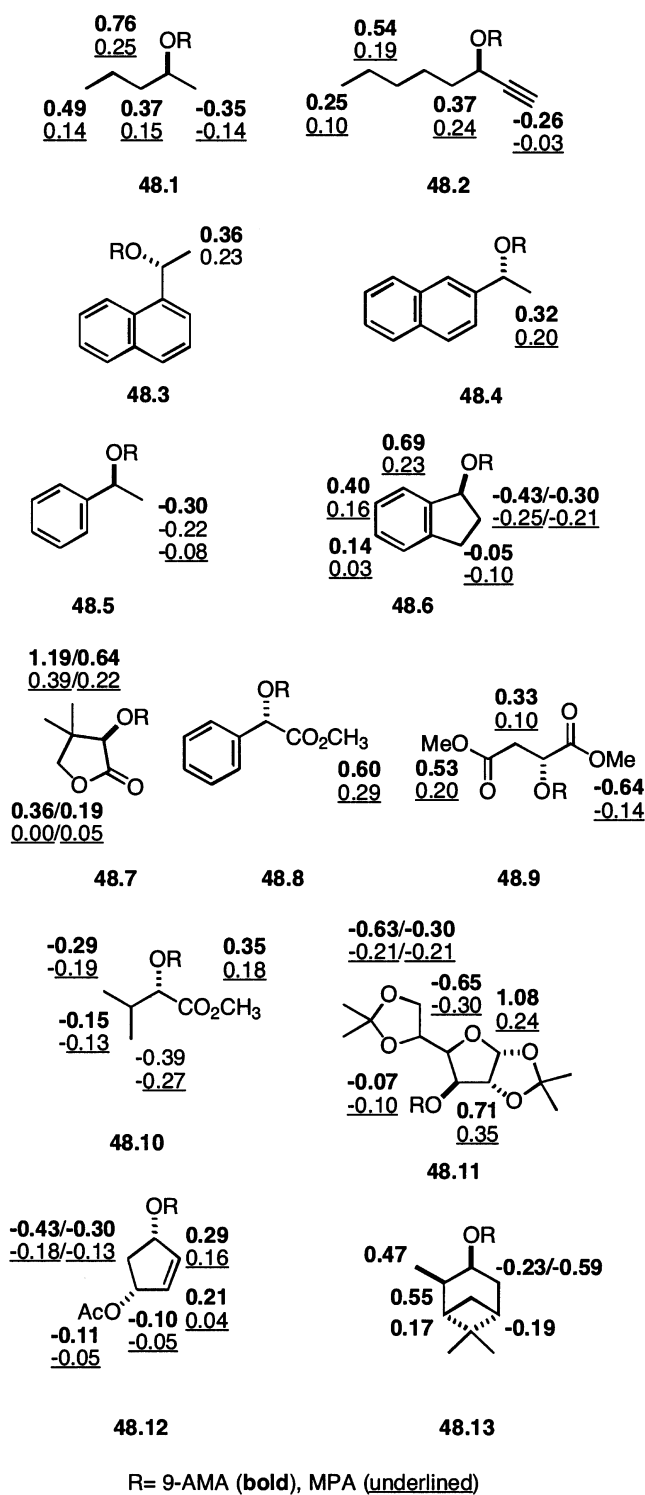


**Figure 48.**  $\Delta\delta^{RS}$  values for selected 9-AMA and MPA esters.

In the esters formed with 2-NMA and 2-ATMA, the variation of shielding intensity with distance is much more uniform and the maximum shielding zone covers the region from approximately two carbon bonds away from the asymmetric C atom up to approximately six bonds away.

In practice, when the assignment of the configuration of an alcohol is made difficult by substantial overlap of the NMR signals, 9-AMA is better than both 2-NMA and 2-ATMA, because the intense, yet rapidly decaying, shielding zone ensures a wide

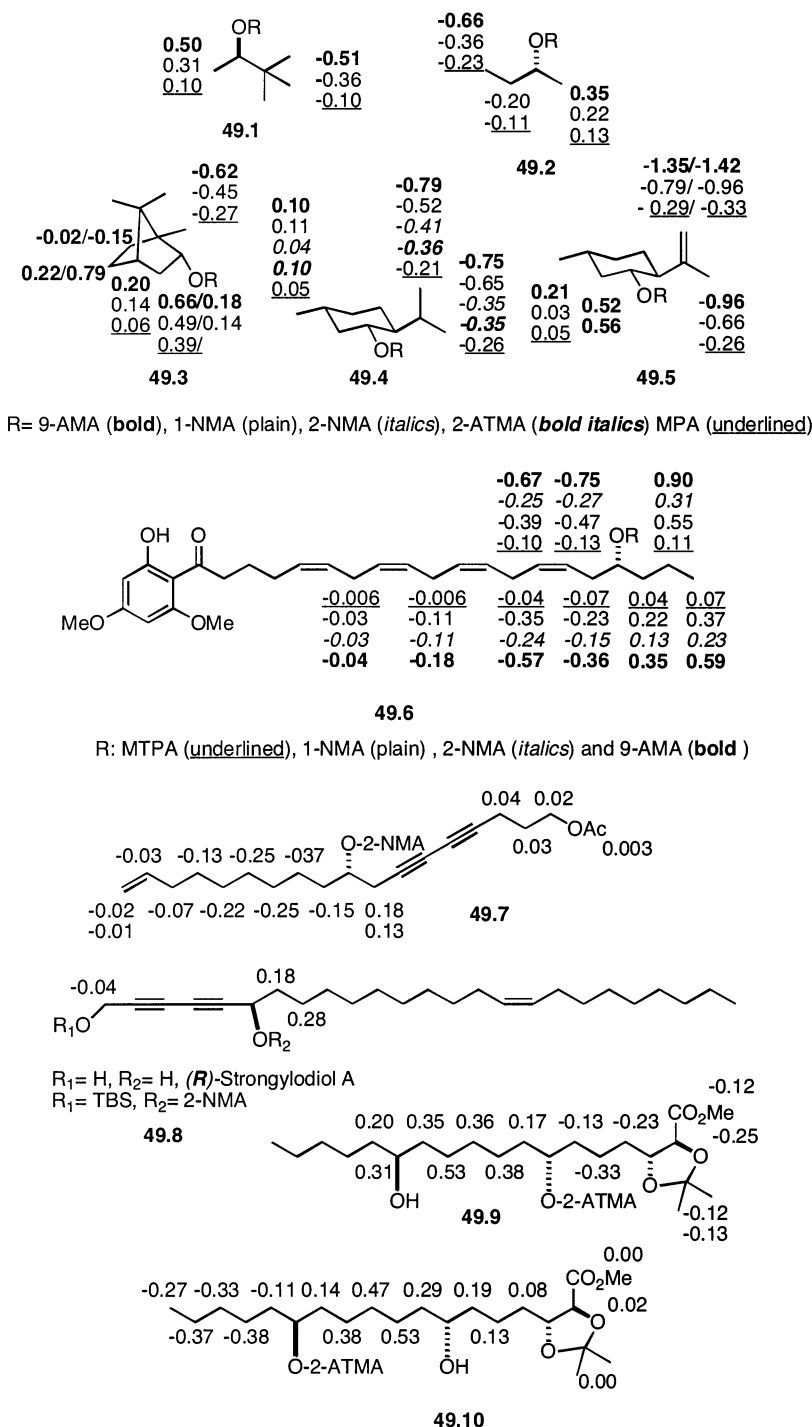


**Figure 49.**  $\Delta\delta^{RS}$  values for selected 9-AMA, 1-NMA, 2-NMA, 2-ATMA, MPA, and MTPA esters of secondary alcohols.

signal distribution across the spectrum for the relevant protons and eliminates signal overlap. The reagents 2-NMA and 2-ATMA<sup>37</sup> are less effective in this respect, because a large number of protons in the chain will be shielded to approximately the same extent and, therefore, considerable signal overlap is likely.

This ability of 9-AMA to separate the signals of the alcohol portion is essential for the correct assignment of the protons and calculation of the  $\Delta\delta^{RS}$  values and is not limited to linear substrates but can also be of use for cyclic alcohols.<sup>30</sup> An illustrative example of such a case is represented by *cis*-androsterone.

The 500 MHz NMR spectrum of *cis*-androsterone<sup>30</sup> is shown in Figure 52b and those of its (*R*)- and (*S*)-9-AMA ester derivatives in Figure 52a and c, respectively. It is clear that an unambiguous assignment of the signals in Figure 52b is impossible, because most of the signals are overlapped in a narrow range of  $\sim 1$  ppm. In contrast, the 9-AMA esters present an extraordinary dispersion of these signals, and this phenomenon allows the complete assignment of all the protons in the molecule.

As predicted, the maximum shielding is located in the region near to the asymmetric center (rings A and B of the steroid) and is so intense that the chemical

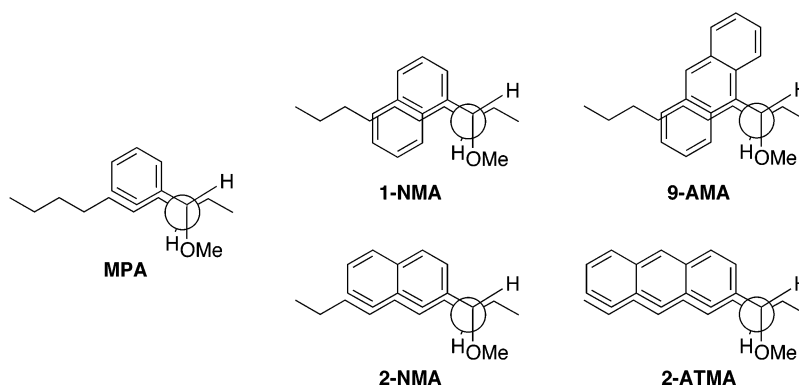
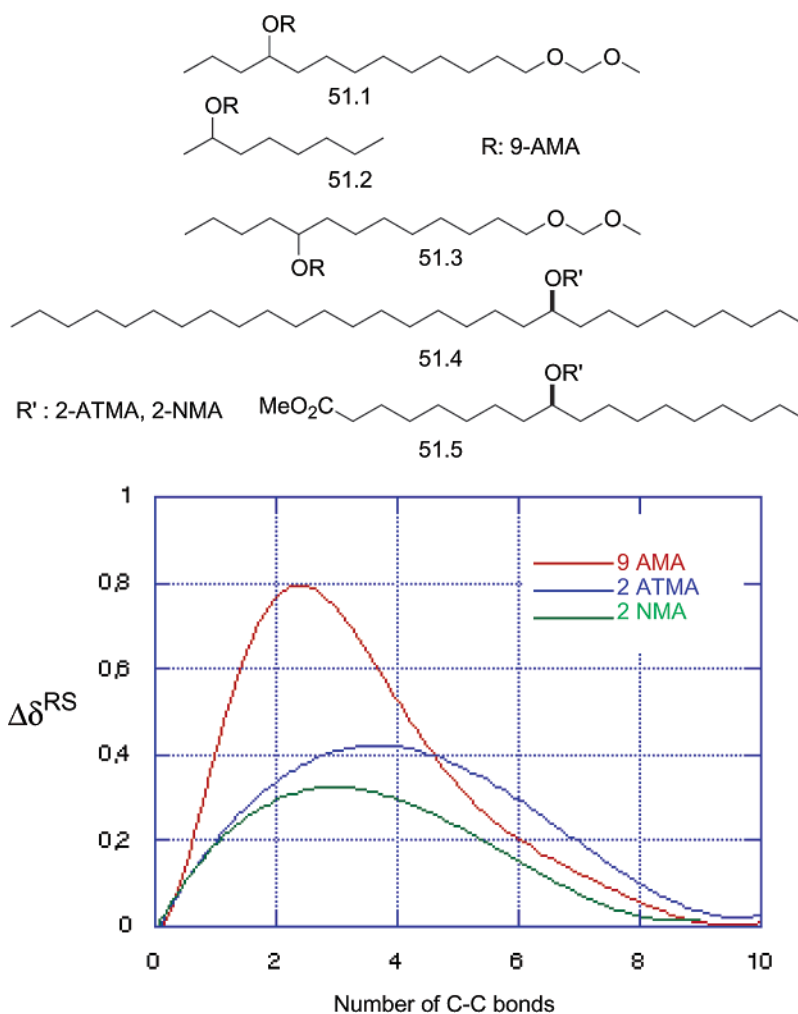


Figure 50.



**Figure 51.** Variation of  $\Delta\delta^{RS}$  with the distance to the asymmetric C atom in 9-AMA, 2-NMA, and 2-ATMA esters of lineal alcohols.

shifts of protons H(1'), H(9'), H(6'), H(5'), and H(7'), which are indistinguishable in *cis*-androsterone itself, are moved to the right of TMS and is enough to move protons in the C ring.

In conclusion, replacement of the phenyl ring of MPA by naphthyl or anthryl rings is shown to be a useful way to modify these reagents. Of all the AMAAs investigated, 9-AMA is the one that produces the most marked changes in shifts and  $\Delta\delta^{RS}$  values, because (a) its aromatic system produces the most intense magnetic field and (b) the population of the

*sp* conformer in its esters is greater than that in the other AMAAs.

#### 3.1.4. Other Reagents

In addition to the reagents described thus far, many other compounds have been proposed as CDAs for the assignment of configuration of secondary alcohols by NMR. Most of the methods reported in this section use  $^1\text{H}$  and  $^{13}\text{C}$  NMR, with only a few—mostly those devoted to e.e. calculations rather than absolute configuration assignment—involving  $^{19}\text{F}$

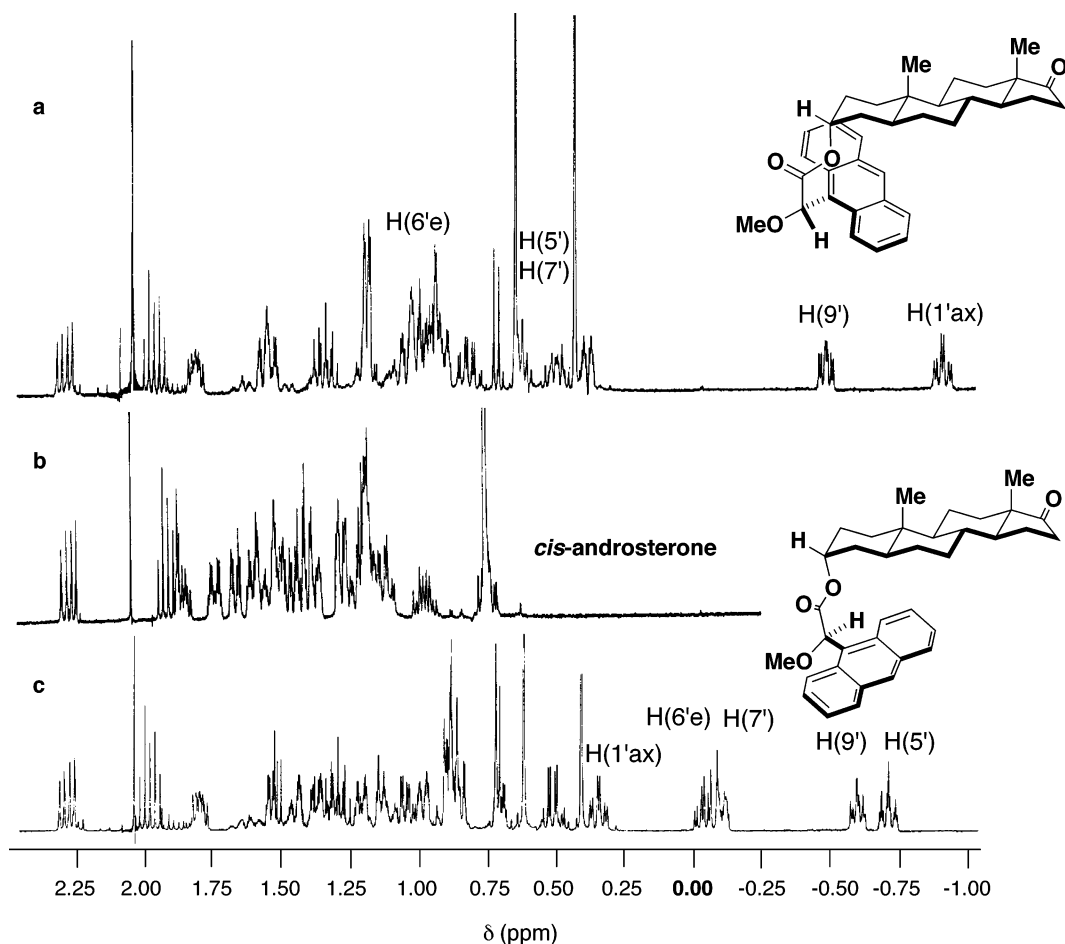


**Figure 52.** <sup>1</sup>H NMR spectra of *cis*-androsterone (b) and its (*R*)-9-AMA (a) and (*S*)-9-AMA esters (c).

NMR. Generally, these reagents contain a magnetically anisotropic group (e.g., phenyl, naphthyl), which is responsible for the shifts experienced by substituents  $L_1/L_2$ , a polar group (e.g., OMe, F) that favors a certain conformation, and an additional functional group for bonding to the substrate. This linkage is, in most cases, an ester bond, although there are examples where an ether, a glycoside, or a phosphamide bond have been used.

In contrast to the cases described for MPA, MTPA, and 9-AMAA, only a few of the procedures described in this section involve conformational analysis and/or theoretical calculations to support the results. For this reason, the reliability of the configuration assigned by these procedures relies essentially on the number and structural variety of the alcohols of known absolute configuration used to validate the method/reagent.

**3.1.4.1. 2-Phenylbutyric Acid: Helmchen's Method.** The commercially available (*R*)- and (*S*)-2-phenylbutyric acids ((*R*)- and (*S*)-PBA, respectively; see Figure 53a), which are well-known in the kinetic method described by Horeau,<sup>43</sup> have been proposed by Helmchen et al.<sup>44</sup> as CDAs for secondary alcohols, and this method has since been extended to assign the stereochemistry of amines and thiols.

Helmchen's procedure is similar to that described by Mosher and consists of the preparation of the esters of the alcohols with the two enantiomers of the reagent (PBA) and subsequent comparison of the <sup>1</sup>H

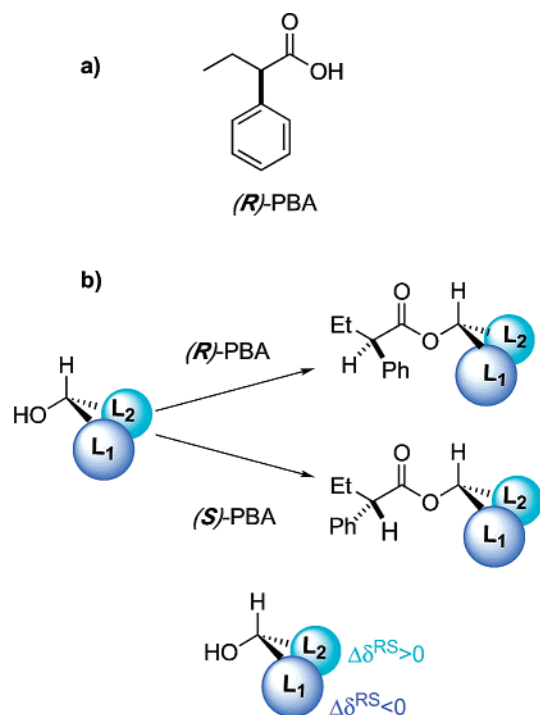


**Figure 53.** (a) Structure of (*R*)-PBA and (b) model for the assignment of the configuration of secondary alcohols from the NMR spectra of the PBA esters.

NMR spectra of the diastereomeric esters. The signs of the resulting  $\Delta\delta^{RS}$  values are then used to locate, in space, the substituents  $L_1$  and  $L_2$ , in accordance

**Table 5.**  $\Delta\delta^{RS}$  Values Obtained for the (*R*)- and (*S*)-PBA Esters of a Selection of Secondary Alcohols of Known Configuration

| L <sub>1</sub>                              |                |             | L <sub>2</sub>  |                |      | PBA      |
|---|----------------|-------------|-----------------|----------------|------|----------|
| C <sub>6</sub> H <sub>13</sub> <sup>a</sup> | $\delta$       | 1.11        | CH <sub>3</sub> | $\delta$       | 1.16 | <i>R</i> |
|   | $\delta$       | 1.28        |                 | $\delta$       | 1.05 | <i>S</i> |
|   | $\Delta\delta$ | -0.17       |                 | $\Delta\delta$ | 0.11 |          |
| C <sub>6</sub> H <sub>5</sub>               | $\delta$       |             | CH <sub>3</sub> | $\delta$       | 1.45 | <i>R</i> |
|   | $\delta$       |             |                 | $\delta$       | 1.35 | <i>S</i> |
|   | $\Delta\delta$ |             |                 | $\Delta\delta$ | 0.10 |          |
| COOEt                                       | $\delta$       | 1.09/4.04   | CH <sub>3</sub> | $\delta$       | 1.41 | <i>R</i> |
|   | $\delta$       | 1.23/4.15   |                 | $\delta$       | 1.36 | <i>S</i> |
|   | $\Delta\delta$ | -0.14/-0.11 |                 | $\Delta\delta$ | 0.05 |          |
| bornyl <sup>b</sup>                         | $\delta$       | 0.63        |                 |                |      | <i>R</i> |
|   | $\delta$       | 0.81        |                 |                |      | <i>S</i> |
|   | $\Delta\delta$ | -0.18       |                 |                |      |          |

<sup>a</sup> Shift of the CH<sub>2</sub> group. <sup>b</sup> Signal corresponding to Me(10).

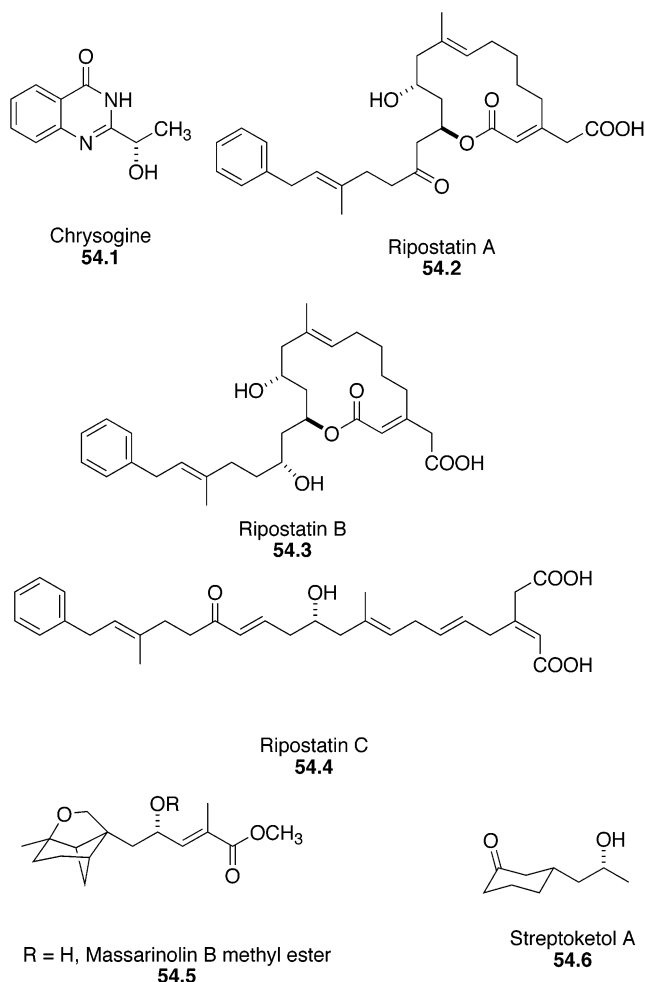
with an empirical model (see Figure 53b). The empirical model was designed to correlate the NMR results of many secondary alcohols of known absolute configuration with the stereochemistry. Table 5 shows a selection of secondary alcohols of known absolute configuration, along with the resulting  $\Delta\delta^{RS}$  values, that have been used to validate this procedure. This model has also been applied, without modifications, to the assignment of the configurations of amines<sup>45a</sup> and thiols.<sup>45b</sup>

Despite the very small number of substrates of known absolute configuration originally used for the validation of PBA as a CDA,<sup>45</sup> as well as the absence of other studies that could lend support to the model, PBA has been frequently used to deduce the configuration of natural products.<sup>46</sup> Examples (Figure 54) include the following: the fungus metabolites chryso-gine, which is isolated from *Fusarium sambucinum*;<sup>46a</sup> ripostatin A, B, and C, which is isolated from *Sorangium cellulosum*;<sup>46b</sup> massarinolin B methyl ester<sup>46c</sup> (from *Massarina tunicata*); and streptoketol A<sup>46d</sup> (from an *Streptomyces sp.*)

The applicability of this reagent for the assignment of the configuration of secondary alcohols using <sup>13</sup>C NMR instead of <sup>1</sup>H NMR has also been investigated.<sup>47</sup> However, in this case, the number of alcohols of known absolute configuration studied as test compounds is very limited and more examples should be analyzed before the procedure is recommended.

More recently, the possibility of using the isomer 3-phenylbutyric acid (3-PBA) as a CDA has been evaluated<sup>48</sup> (Figure 55a). However, the presence of the phenyl group and asymmetric center at position  $\beta$ , rather than at position  $\alpha$  (as in PBA, MPA, MTPA, or 9-AMA), and the higher conformational freedom inherent in this system leads to a reduction of the aromatic shielding/deshielding on substituents L<sub>1</sub>/L<sub>2</sub>, which is a situation that gives smaller  $\Delta\delta^{RS}$  values. In fact, comparison of the  $\Delta\delta^{RS}$  values obtained for the ester derivatives of diacetone-D-glucose and 2-butanol with 3-PBA, MPA, and MTPA as reagents showed that the smallest shifts were obtained with 3-PBA.

The model presented in Figure 55b is empirical and was designed to correlate the NMR spectra of the 3-PBA esters of just five alcohols of known absolute configuration with their stereochemistry.

**Figure 54.** Natural products of microbial origin studied by Helmchen's method.

The authors assume that the most representative conformation is the one in which the H atoms at the  $\beta$ -carbon of the acid, the carbinol, and the carbonyl group are syn-periplanar. In accordance with this model, substituent L<sub>1</sub> should be shielded in the (*R*)-ester, while substituent L<sub>2</sub> is shielded in the (*S*)-ester; therefore,  $\Delta\delta^{RS}$  must be negative for substituent L<sub>1</sub> and positive for substituent L<sub>2</sub>.

In conclusion, the applicability of both PBA and 3-PBA as CDAs is limited by several considerations: (a) the small number of substrates of known absolute configuration that have been used to validate the assignment, (b) the absence of other experimental or theoretical studies that might support the correlation models, and (c) (in the case of 3-PBA) the small  $\Delta\delta^{RS}$  values.

**3.1.4.2. Naphthylpropionic Acids.** In the past few years, several naphthylpropionic acids have been investigated as CDAs.<sup>49</sup> One of the most commonly used is 2-methoxy-2-(1-naphthyl)propionic acid (M $\alpha$ NP; see Figure 56), which is already known as a derivatizing agent for HPLC resolution of alcohols.<sup>50</sup>

In the (*R*)-M $\alpha$ NP ester of the alcohol shown in Figure 57, substituent L<sub>1</sub> experiences a shielding influence from the naphthyl group, whereas, in the (*S*)-M $\alpha$ NP ester, the shielded group is substituent L<sub>2</sub>. Therefore, substituent L<sub>1</sub> results in a negative  $\Delta\delta^{RS}$  value and substituent L<sub>2</sub> yields a positive  $\Delta\delta^{RS}$  value.

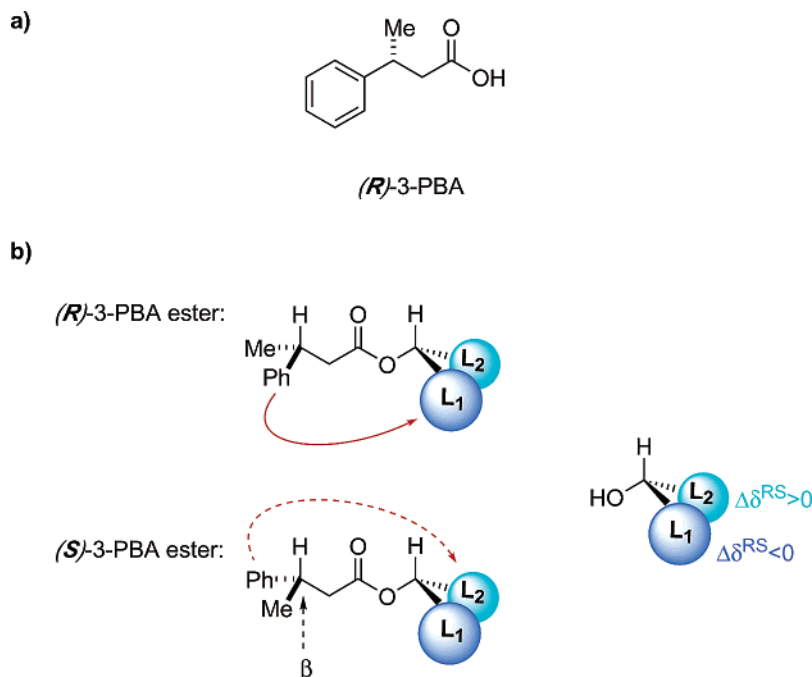


**Figure 55.** (a) Structure of *(R)*-3-PBA and (b) model for the assignment of the configuration of secondary alcohols from the NMR spectra of the 3-PBA esters.

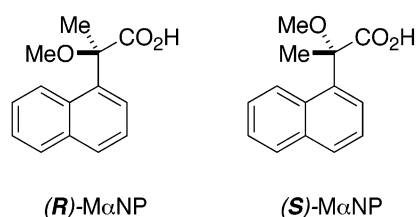


**Figure 56.** Structure of the 2-methoxy-2-(1-naphthyl)propionic acids.

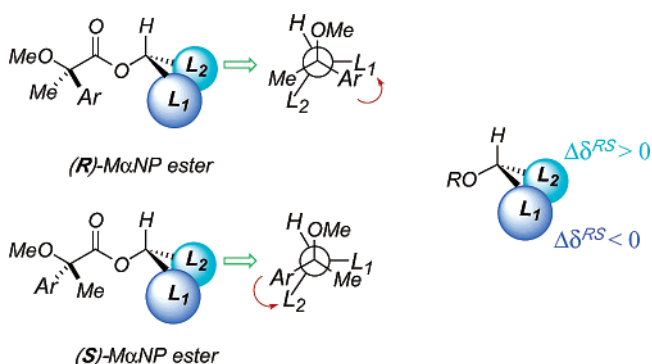


**Figure 57.** Model for the assignment of configuration by NMR of M $\alpha$ NP esters.

This model was derived from the study of just five alcohols of known absolute configuration, and the structures and  $\Delta\delta^{RS}$  values for these are shown in Figure 58.<sup>49a</sup>

The authors proposed a variant using the racemic mixture of the auxiliary ( $\pm$ )-M $\alpha$ NP. In this case, the mixture of M $\alpha$ NP esters first should be separated and a small sample of one diastereoisomer transformed to the corresponding methyl ester. Inspection of the CD spectra allows the identification of the *(R)*- and *(S)*-M $\alpha$ NP esters (the *(S)*-M $\alpha$ NP has a negative CD band and the *(R)*-M $\alpha$ NP has a positive band at 280 nm). After the *(R)*- and the *(S)*-M $\alpha$ NP esters have been identified, their NMR spectra are recorded and

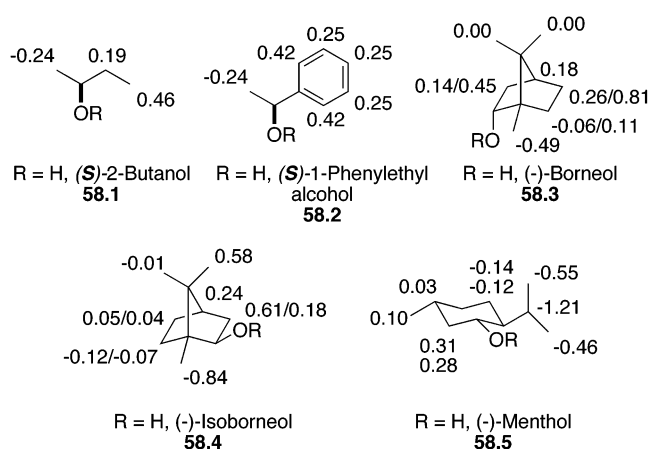


**Figure 58.** Alcohols of known configuration studied by NMR of their M $\alpha$ NP esters and the resulting  $\Delta\delta^{RS}$  values.

the model shown in Figure 57 allows the configuration to be assigned.<sup>49a</sup>

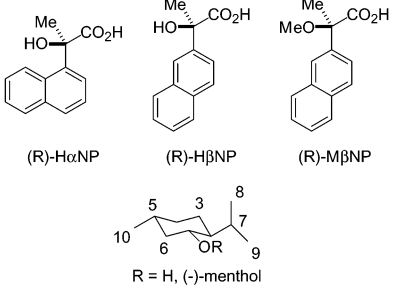
In addition to M $\alpha$ NP, the potential of some other naphthylpropionic acids to act as CDAs has been evaluated using (-)-menthol as a test compound, on the assumption that the correlation model of M $\alpha$ NP is still valid.

Table 6 shows the  $\Delta\delta^{RS}$  values obtained for the (-)-menthol esters of 2-hydroxy-2-(1-naphthyl)propionic acid<sup>49c</sup> (H $\alpha$ NP), 2-hydroxy-2-(2-naphthyl)propionic acid (H $\beta$ NP), and 2-methoxy-2-(2-naphthyl)propionic acid<sup>49d</sup> (M $\beta$ NP), as well as, for comparative purposes, those obtained with several AMAA reagents described previously in this review—including MPA and MTPA.

Examination of the data shows that the  $\Delta\delta^{RS}$  values of the naphthylpropionic acids mentioned in this section follow the order H $\alpha$ NP > M $\alpha$ NP > H $\beta$ NP > M $\beta$ NP, and, in fact, the values for M $\beta$ NP are very small and the distribution of the signs is irregular (for example, see H(10')).



**Table 6. Structure of the Naphthylpropionic Acids Evaluated as CDA Reagents and the  $\Delta\delta^{RS}$  Values Obtained for Their Esters with (-)-Menthol and Those of Other AMAAs**



| Aryl       | CDA    | $\Delta\delta^{RS}$ (ppm) |         |          |           |        |
|------------|--------|---------------------------|---------|----------|-----------|--------|
|            |        | Me (8')                   | Me (9') | Me (10') | H (6')    | H (5') |
| 1-naphthyl | MαNP   | -0.45                     | -0.55   | 0.11     | 0.28/0.32 | 0.03   |
|            | HαNP   | -0.51                     | -0.54   | 0.11     | 0.25/0.36 | 0.03   |
| 2-naphthyl | MβNP   | -0.05                     | -0.04   | 0.00     | 0.04/0.01 | 0.00   |
|            | HβNP   | -0.31                     | -0.32   | 0.09     | 0.14/0.19 | 0.03   |
| 9-anthryl  | 9-AMA  | -0.75                     | -0.79   | 0.10     |           |        |
| 2-anthryl  | 2-ATMA | -0.36                     | -0.35   | 0.10     |           |        |
| 1-naphthyl | 1NMA   | -0.52                     | -0.65   | 0.11     |           |        |
| 2-naphthyl | 2NMA   | -0.41                     | -0.35   | 0.04     |           |        |
| phenyl     | MPA    | -0.21                     | -0.26   | 0.05     |           |        |
| phenyl     | MTPA   | 0.12                      | 0.10    | -0.03    |           |        |

Comparison of these reagents with the AMAA systems discussed previously shows that the anthryl reagent 9-AMA produces the highest  $\Delta\delta^{RS}$  values of all, with the second-highest values resulting from the naphthyl acid, 1-NMA. In addition, comparison between the 1-naphthyl-substituted reagents MαNP and 1-NMA indicates that 1-NMA is the more effective reagent. Similarly, among the 2-naphthyl-substituted systems, it is evident that 2-NMA is more effective than MβNP and this clearly suggests that the replacement of the H atom in the  $\alpha$ -position by a methyl group (as in MαNP and MβNP) leads to a significant loss of efficacy of the reagents—probably a consequence of a reduction in the energy difference between the conformers.

In conclusion, the use of naphthylpropionic acids as CDAs is limited by (a) the small number of substrates of known absolute configuration used to validate the method and (b) the absence of information about their conformational characteristics. The shifts obtained are smaller than those observed for other, better-known naphthyl-substituted reagents and, therefore, do not provide any advantage.

**3.1.4.3. Axially Chiral CDAs (MBNC and MNCB).** Several compounds of the binaphthyl and biphenyl classes with axial chirality have been proposed as CDA reagents.<sup>51</sup> The most important

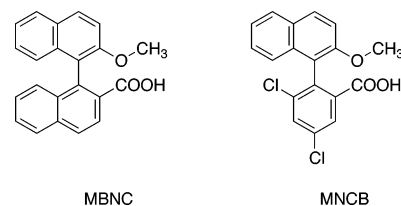


**Figure 59.** Structure of axially chiral acids MBNC and MNCB.

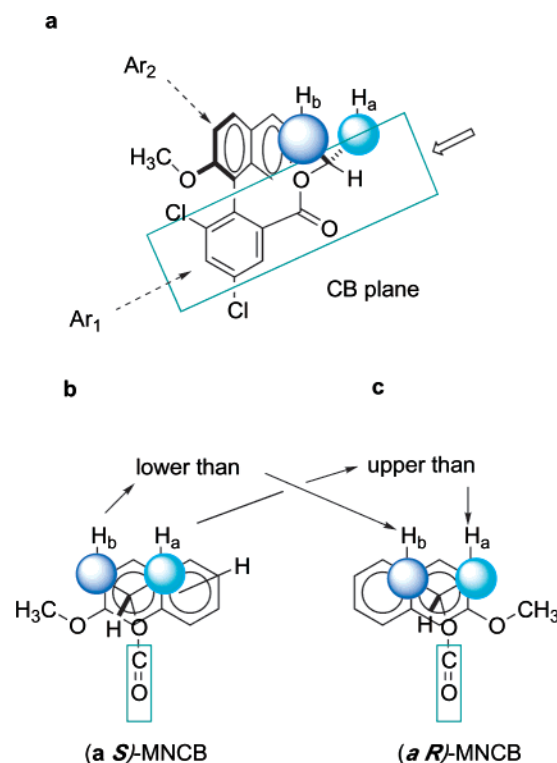


**Figure 60.** Model for the assignment of the configuration of alcohols using the NMR of their MBNC and MNCB esters.

examples are 2'-methoxy-1,1'-binaphthyl-2-carboxylic acid (MBNC) and 2-(2'-methoxy-1'-naphthyl)-3,5-dichlorobenzoic acid (MNCB). These compounds have been evaluated for the assignment of the configuration of secondary alcohols by means of  $^1\text{H}$  and  $^{13}\text{C}$  NMR spectroscopy<sup>51a,b</sup> (see Figure 59).

This protocol is not unusual in any respect and consists of the derivatization of the substrate with the two enantiomers of the reagent and subsequent comparison of their  $^1\text{H}$  or  $^{13}\text{C}$  NMR spectra.

The interpretation of the NMR data follows the model shown in Figure 60. Thus, in the case of the esters of MNCB (Figure 60a), the most representative conformer is assumed to be that which the phenyl group of the acid (Ar1), the carbonyl group, and the hydrogen bond to the chiral center of the alcohol are in the same plane (plane "CB"). In addition, the Ar1–Ar2 bond and the C=O group should be anti-periplanar, with the aromatic rings (Ar1, Ar2) perpendicular to each other.

This geometry allows the naphthyl ring to transmit its shielding to the substituents of the alcohol but, unfortunately, not in a very selective manner, because both substituents in each conformer are shielded, although one is slightly more affected than the other.

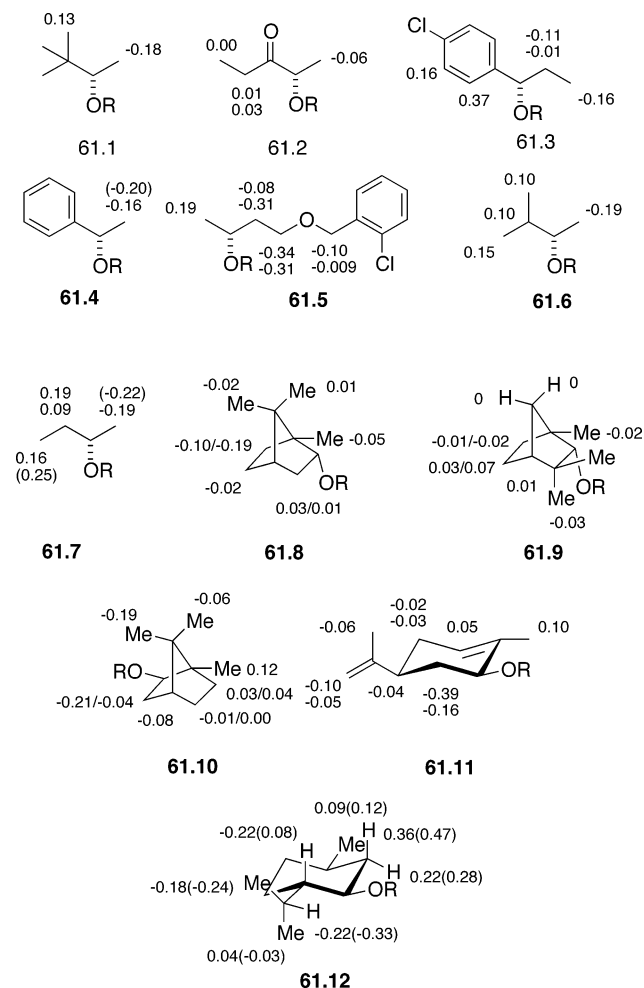


**Figure 61.** Secondary alcohols and  $\Delta\delta$  ( $^1\text{H}$  NMR) values obtained from their MNCB (plain,  $\Delta\delta^{SR}$ ) and MBNC (in parentheses,  $\Delta\delta^{RS}$ ) esters.

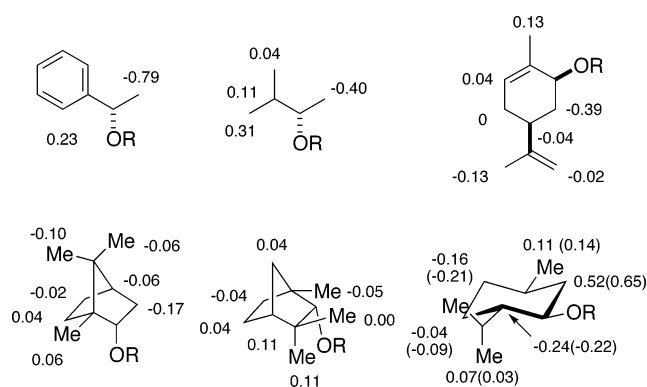


**Figure 62.** Secondary alcohols and  $\Delta\delta$  ( $^{13}\text{C}$  NMR) values obtained from their MNCB ( $\Delta\delta^{SR}$ ) and MBNC ( $\Delta\delta^{RS}$ ) esters. MBNC data given in parentheses.

The signal for Ha appears in the (a*S*)-MNCB ester at higher field than in the (a*R*)-MNCB ester; the reverse situation is observed for Hb. In this way, the resulting differences ( $\Delta\delta = \delta_{aS} - \delta_{aR}$ ) are  $\Delta\delta_{\text{Hb}}^{SR} > 0$  and  $\Delta\delta_{\text{Ha}}^{SR} < 0$ .

Figures 61 and 62 show the structures of the alcohols of known configuration used to validate the model and the corresponding  $\Delta\delta^{SR}$  values ( $^1\text{H}$  and  $^{13}\text{C}$  NMR data). The proton NMR data of the lineal alcohols are in good agreement with the model; however, the use of cyclic alcohols results in an

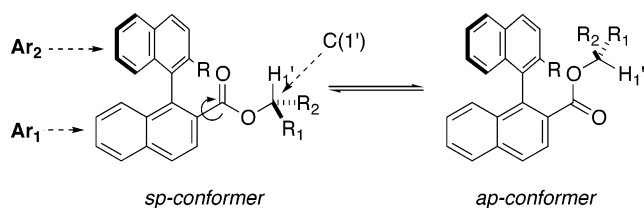


**Figure 63.** Conformational equilibrium in the esters of MNCB.

irregular distribution of signs for  $\Delta\delta^{SR}$  (see 61.8, 61.9, and 61.12).

In regard to the  $^{13}\text{C}$  NMR data (Figure 62), the resulting  $\Delta\delta^{SR}$  values are too small to ensure a safe assignment. A similar situation had been observed previously with other reagents (MTPA; see Section 3.1.1.4) and this is not surprising, given the low sensitivity of  $^{13}\text{C}$  chemical shifts to the anisotropic effect.

The  $\Delta\delta$  values shown in Figure 61 are clearly smaller than those obtained with other naphthyl-containing reagents described in this review, such as the AMAAs (1-NMA and 2-NMA). The explanation for this less-marked effect is evident after performing calculations<sup>51c</sup> on the structure and conformation of the compounds in question. For example, molecular mechanics (MM), semiempirical (PM3 and AM1), and ab initio calculations have revealed that these compounds exist in solution as two main conformers in equilibrium: the *sp* conformer (with the  $\text{Ar}_1$ - $\text{Ar}_2$  bond and the  $\text{C}=\text{O}$  group syn-periplanar; see Figure 63) and the *ap* conformer (where the aforementioned groups are anti-periplanar). In both cases, the  $\text{Ar}_1$  ring, the  $\text{C}=\text{O}$  group, and the  $\text{C}(1')$ - $\text{H}$  bond remain coplanar, whereas  $\text{Ar}_2$  is perpendicular to  $\text{Ar}_1$ .

Although the *ap* conformer has a better geometry than the *sp* conformer, in terms of transmission of the effect of  $\text{Ar}_2$  to the substituents of the alcohol ( $\text{R}_1/\text{R}_2$ ), the calculations reveal that the most stable form is the *sp* conformer, in which the aromatic ring is poorly oriented for transmission purposes.

Despite the fact that the *ap* conformer is less abundant, it is considered to be the most important conformer, in terms of NMR shifts, and its use in the correlation model shown in Figure 60 is justified by the results of NMR studies at low temperature and by aromatic shielding calculations. A second aspect that must be considered concerns the fact that in neither of the two conformers can the aromatic ring produce selective shielding on just one of the substituents ( $\text{R}_1/\text{R}_2$ ), which is a situation that is contrary to that observed for the AMAA derivatives. In the case in question here, both substituents are moderately shielded in the *ap* conformer, whereas in the *sp* conformer, they are only slightly shielded.

These two points explain the small shifts obtained with these reagents and the need for more efforts to improve their performance. With this intent in mind, the reagent 1-(10-bromo-1-anthryl)-2-naphthoic acid (BANA, Figure 64) was prepared and its ability to produce separate signals for diastereomeric (-)-menthol esters was evaluated. Although the  $\Delta\delta^{SR}$  values obtained are slightly better than those obtained with MNCB, they are still too small to justify

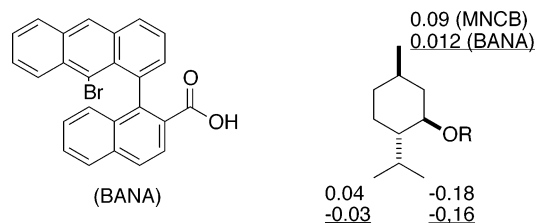


Figure 64.

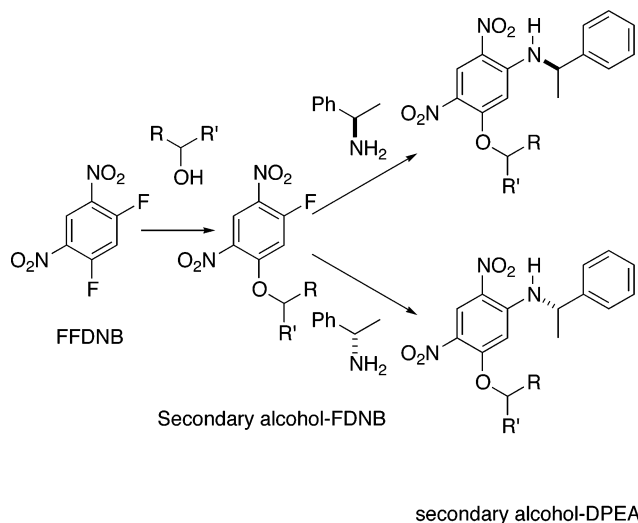


Figure 65. Derivatization procedure for secondary alcohols.

the extensive use of these reagents for the assignment of secondary alcohols.

**3.1.4.4. Difluorodinitrobenzene.** An empirical method based on the use of 1,5-difluoro-2,4-dinitrobenzene (FFDNB) as a CDA for the assignment of secondary alcohols and primary amines has been described.<sup>52</sup> In the case of alcohols<sup>52</sup> (the application to amines is reviewed in Section 3.4.5.1), the substrate and the difluorodinitrobenzene reagent are linked through an ether bond and a second auxiliary reagent is then introduced. Therefore, the procedure for derivatization entails the reaction of the chiral alcohol with FFDNB and the resulting fluoro-dinitrobenzene (FDNB) ether is subsequently made to react separately with the two enantiomers of 1-phenylethylamine (second auxiliary). The resulting diastereomeric alcohol-DPEA derivatives are then examined by NMR (Figure 65).

Interpretation of the NMR spectra of the derivatives and the assignment of the configurations of the alcohols are based on a model proposed by the authors (based on fast atom bombardment (FAB), UV and <sup>2</sup>D NMR spectra, and NOE experiments) in which the proton on the asymmetric C atom of the alcohol and H(6) on the benzene ring are coplanar (see Figure 66). According to this conformation, the DPEA derivative containing (*R*)-1-phenylethylamine has substituent L<sub>2</sub> shielded by the phenyl group of the amine, whereas, in the derivative containing the (*S*)-1-phenylethylamine fragment, it is substituent L<sub>1</sub> that is shielded. Consequently, the difference in the chemical shifts ( $\Delta\delta = \delta_R - \delta_S$ ) for an alcohol with the stereochemistry shown in Figure 66 is negative for substituent L<sub>2</sub> and positive for substituent L<sub>1</sub>.

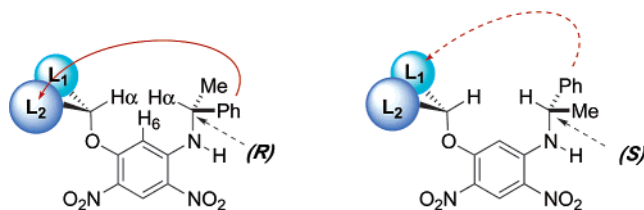


Figure 66. Conformational model and predicted  $\Delta\delta$  signs for the assignment of the configuration of secondary alcohols from the NMR of their alcohol-DPEA derivatives.

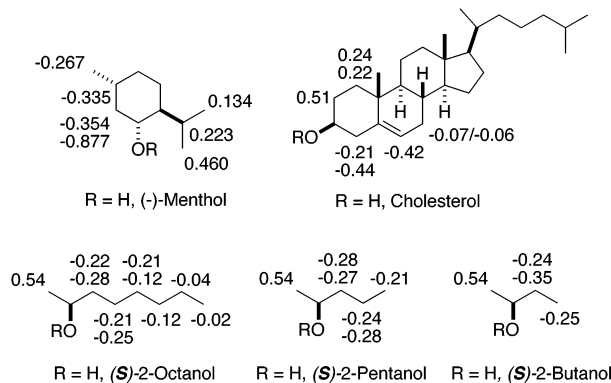


Figure 67. Secondary alcohols of known absolute configuration and  $\Delta\delta$  values obtained from their alcohol-DPEA derivatives.

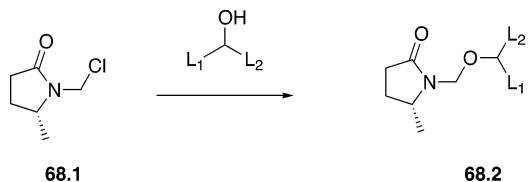
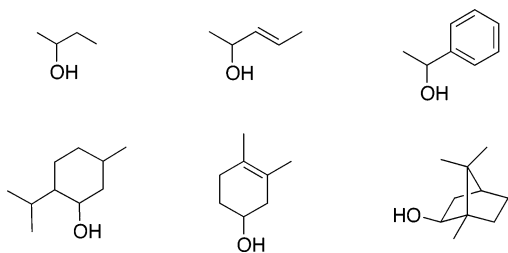


Figure 68. Preparation of *N*-(alkoxymethyl)-2-pyrrolidinone derivatives.

This model has been experimentally assessed with five alcohols of known absolute configuration (Figure 67). The signs of  $\Delta\delta$  are in good agreement with the stereochemistry and the shifts are large. However, note that the number and structural variety of compounds used to validate the method are too small to guarantee its general applicability to other substrates. This fact, together with the two-step derivatization procedure, represents the main limitation of this reagent.

**3.1.4.5. 5(*R*)-Methyl-1-(chloromethyl)-2-pyrrolidinone.** 5(*R*)-Methyl-1-(chloromethyl)-2-pyrrolidinone (**68.1**) has been proposed<sup>53</sup> as an auxiliary reagent for absolute configuration (and % ee) determinations of chiral secondary alcohols by the formation of the corresponding *N*-(alkoxymethyl)-2-pyrrolidinone derivative **68.2** (see Figure 68).

Theoretical calculations have shown that those derivatives exist in equilibrium between two conformational forms obtained by rotation of the CH<sub>2</sub>OR unit around the C-N bond. The more stable one has an NCOC angle of  $\sim 90^\circ$ , whereas the conformation with a linear arrangement (NCOC angle of  $\sim 180^\circ$ ) has greater energy. In both, the lactam ring is



**Figure 69.** Alcohols of known absolute configuration studied by this method.

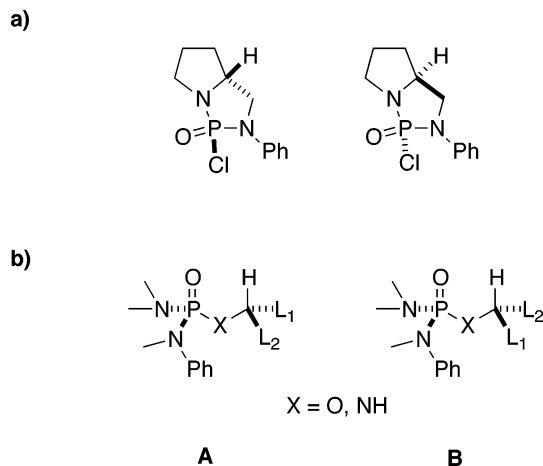


**Figure 70.** Structure of the diazacyclopophosphamide chlorides and correlation model for configurational assignment of alcohols.

essentially planar and the methyl group has a pseudo-axial orientation.

In accordance with that prediction, experimental data indicated that the NMR shifts of the NCH<sub>2</sub>O protons are determined by the anisotropic effect of the C=O bond and the polar effect of the O atom in each conformer. Under those conditions, a relationship between the chemical shifts and the relative position of those protons, with respect to the carbonyl group, and the absolute stereochemistry of the derivatives can be established. In fact, application of the proposed model to six chiral alcohols (Figure 69) predicted the correct configuration.

The authors warn about the convenience of working with both diastereomeric derivatives; that is to say, both enantiomers of the chiral alcohol are necessary. This is a clear limitation of the method, and the report explicitly says that if only one enantiomer of the alcohol is available for derivatization, assignment of the correct absolute configuration is risky. Nevertheless, the procedure works well when substituents L<sub>1</sub> and L<sub>2</sub> are clearly different in size.

**3.1.4.6. Diazacyclopophosphamides.** The use of diazacyclopophosphamide chlorides as reagents for secondary alcohols and primary amines has been described<sup>54</sup> (see Figure 70a). In this procedure, the linkage between the substrate and the reagent is a phosphate or phosphamide bond and the configuration of the substrate is determined by <sup>1</sup>H NMR on the basis of the models indicated in Figure 70b.

This method is totally empirical and conformational studies have not been performed to support the model shown. In addition, the number of substrates used to validate this model is extremely small and

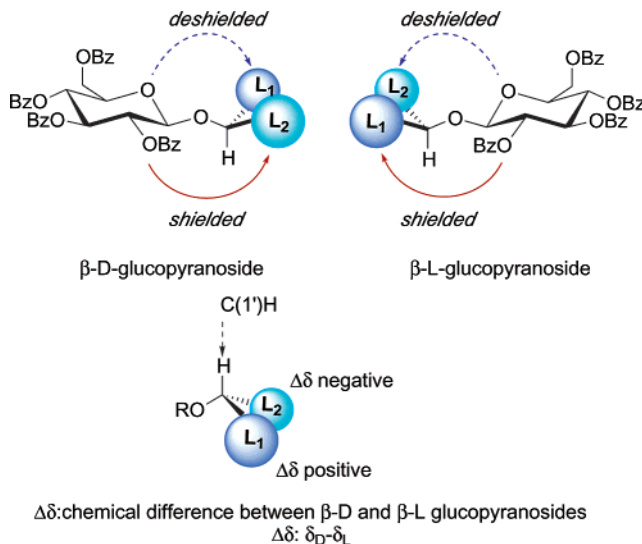


**Figure 71.** Structure and correlation models of  $\beta$ -D- and  $\beta$ -L-glucopyranosides.

the NMR data are very limited: Only two alcohols—one primary and the other secondary—and seven amines have been studied, and, even then, only the shift of one of the substituents of the substrate (L<sub>1</sub> or L<sub>2</sub>) is considered.

A model for the correlation of the <sup>31</sup>P NMR shifts with the configuration is not proposed by the authors; therefore, the best application of this method is in the field of e.e. calculation rather than the assignment of configuration.

**3.1.4.7. Tetra-O-benzoylglucosyl Bromides: The Glucosylation Method.** There have been several attempts to use sugars as CDAs for the assignment of the configuration of alcohols that are derivatized as glycosides<sup>55–57</sup> and examined by <sup>13</sup>C and <sup>1</sup>H NMR. In a few cases, a single derivative is used<sup>55</sup> (comparison of the spectra of the alcohol with that of the derivative) and these will be discussed in the corresponding section (Section 4.1.2). In this part of the review, however, we are only concerned with cases in which the assignment is performed by comparison of the L and D glycosides.<sup>56</sup>

The most commonly used of these procedures consists of the preparation of the tetra-O-benzoyl- $\beta$ -D-glucopyranoside and tetra-O-benzoyl- $\beta$ -L-glucopyranoside of the alcohol and comparison of their <sup>1</sup>H NMR spectra.<sup>56</sup>

The interpretation of the spectra and the configurational assignment is based on the observation that, in both derivatives, protons anti to the endocyclic oxygen (substituent L<sub>2</sub> in  $\beta$ -D-glucopyranoside; see Figure 71) are shielded, probably because of the effect of the benzoyl group at C-2, whereas those with the syn arrangement (substituent L<sub>1</sub> in  $\beta$ -D-glucopyranoside) are deshielded, presumably because they are close to the endocyclic O atom (O-5).

In this way, the differences in the chemical shifts ( $\Delta\delta = \delta_D - \delta_L$ ) for an alcohol with the configuration shown in Figure 71 are negative for substituent L<sub>2</sub> and positive for substituent L<sub>1</sub>.

Nine alcohols of known absolute configuration were studied, and these are shown in Figure 72. The results obtained are in agreement with the predic-

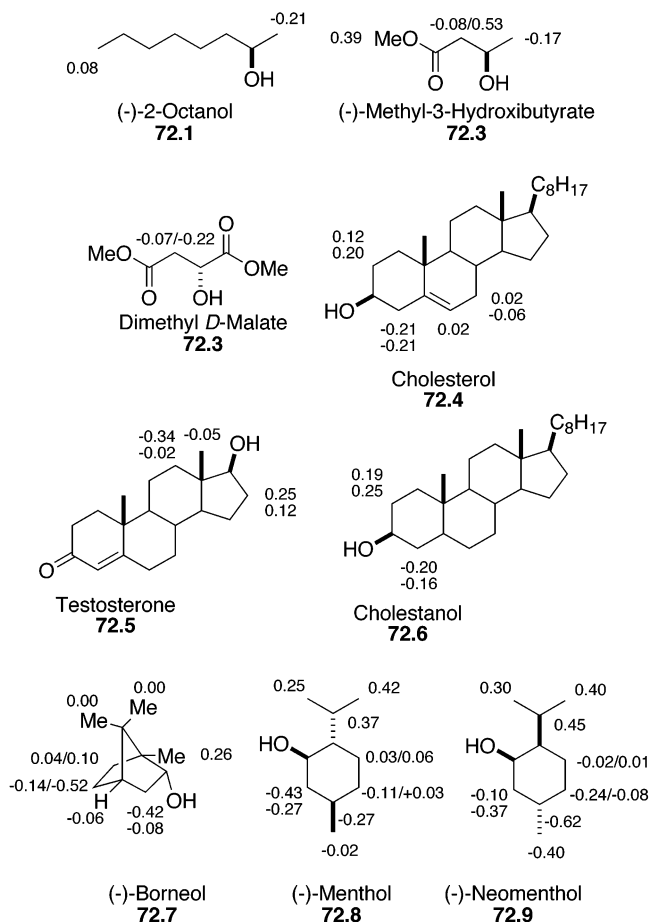
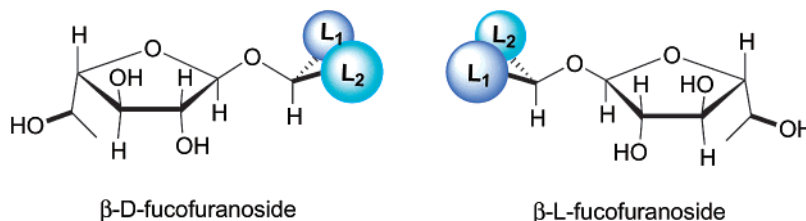


**Figure 72.** Secondary alcohols of known absolute configuration studied as tetra-*O*-benzoyl- $\beta$ -glucopyranosyl derivatives and the corresponding  $\Delta\delta$  values.

tions and, therefore, validate the method. Only in the methylene group of (-)-methyl-3-hydroxybutyrate are the signs unexpected, and this is probably due to the anisotropic action of the two carbonyl groups.

The authors also mention that a correlation apparently exists between the chemical shift of the proton at C(1')H, the "carbinyl carbon", and the absolute configuration: For the derivatives with the *R* configuration,  $\Delta\delta$  is positive, whereas  $\Delta\delta$  is negative when the configuration at that C atom is *S* (see Table 7). Unfortunately, cholesterol and cholestanol are two exceptions to this rule, and the authors explain this phenomenon as being due to the absence of substituents in the  $\beta$  position.

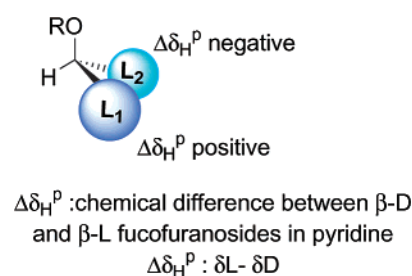
**3.1.4.8. Fucufuranose Tetra-*O*-acetate: The Fucufuranoside Method.** A procedure has been described<sup>57</sup> that involves comparison of the NMR spectra of the  $\beta$ -D- and  $\beta$ -L-fucufuranosides (Figure 73) in chloroform or pyridine as the solvent and the application of totally empirical rules (see Figure 74).



**Figure 73.**

**Table 7. Relationship between the Absolute Configuration of the Carbinyl Carbon and the Sign of  $\Delta\delta$**

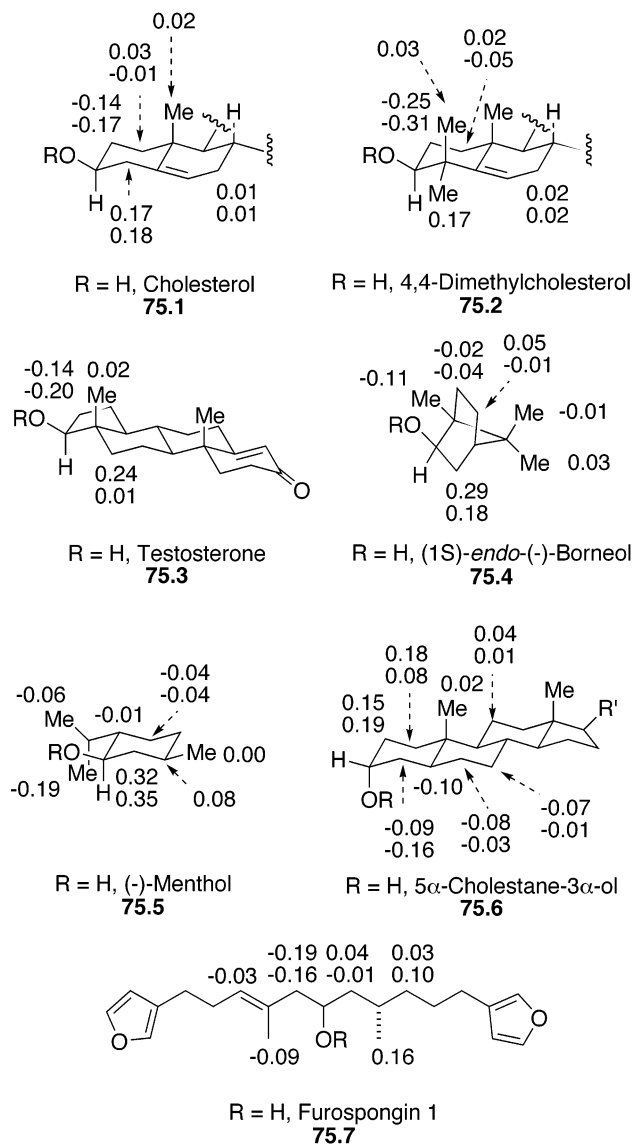
| alcohol                       | carbinyl carbon configuration (C1') | $\delta_D - \delta_L$ |
|-------------------------------|-------------------------------------|-----------------------|
| (-)-2-octanol                 | <i>R</i>                            | +0.09                 |
| (+)-2-octanol                 | <i>S</i>                            | -0.09                 |
| (-)-menthol                   | <i>R</i>                            | +0.16                 |
| (+)-menthol                   | <i>S</i>                            | -0.16                 |
| (-)-neomenthol                | <i>R</i>                            | +0.16                 |
| (+)-neomenthol                | <i>S</i>                            | -0.16                 |
| (-)-borneol                   | <i>R</i>                            | +0.23                 |
| (+)-borneol                   | <i>S</i>                            | -0.23                 |
| (3b)-cholesterol              | <i>S</i>                            | 0.00                  |
| (3b)-cholestanol              | <i>S</i>                            | 0.00                  |
| (17b)-testosterone            | <i>S</i>                            | -0.03                 |
| dimethyl-D-malate             | <i>R</i>                            | -0.14                 |
| dimethyl-L-malate             | <i>S</i>                            | +0.14                 |
| (-)-methyl 3-hydroxy-butyrate | <i>R</i>                            | +0.02                 |
| (+)-methyl 3-hydroxy-butyrate | <i>S</i>                            | -0.02                 |



**Figure 74.**

These rules are based on the study of seven examples of known absolute configuration (Figure 75), although the range of structures is not very diverse (six are cyclic alcohols and just one is an open-chain alcohol) and, as such, the use of this reagent for the assignment of the configuration of a secondary alcohol is not yet fully established. In addition, the preparation of the auxiliary reagent and the derivatization of the alcohol are more complex and time-consuming than that with glucopyranosides or AMAAs. Finally, the shifts obtained with the fucufuranosides are smaller than those obtained with the tetra-*O*-benzoylglucosides, and, for this reason, its use does not offer any advantages.

If the configurational assignment is to be performed using  $^1\text{H}$  NMR spectroscopy, the spectra of the  $\beta$ -L-fucufuranoside and the  $\beta$ -D-fucufuranoside are taken in pyridine and the differences between the chemical shifts ( $\Delta\delta_{H^P}$ ) is calculated ( $\Delta\delta = \delta_L - \delta_D$ ). In the case where the alcohol has the configuration shown in Figure 74, substituent  $L_1$  should result in a positive  $\Delta\delta_{H^P}$  and substituent  $L_2$  should result in a negative value. In this procedure, only the signs for the protons on the  $\beta$ -carbon of substituents  $L_1/L_2$  are considered.



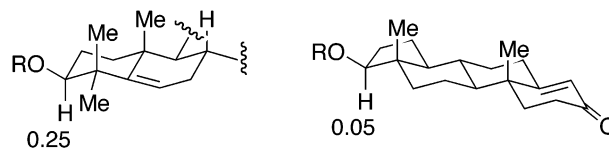
**Figure 75.**  $\Delta\delta_{H^P}$  values observed for  $\beta$ -D- and  $\beta$ -L-fucuranoside derivatives.

Figure 75 shows the structures of the compounds studied by this method, along with the corresponding  $\Delta\delta_{H^P}$  data. It can be seen that, with the exception of furospingonin 1, the signs of  $\Delta\delta_{H^P}$  for the protons on the  $\beta$ -carbons correlate well with the stereochemistry. However, the other protons do not show any correlation and different signs are obtained for protons in the same substituent.

A study by the same authors on a series of just four compounds (Figure 76) led them to suggest that there could be a correlation between the configuration and the signs of  $\Delta\delta_{H^P}$  for the protons on the asymmetric carbon of the alcohol (carbinyl protons, C(1')H): the sign of  $\Delta\delta_{H^P}$  is positive for those classified as *S*-type alcohols and negative for *R*-type alcohols. The small number of examples investigated, along with the lack of studies on the fundamental aspects of this method, represents a clear limitation for the general applicability of this approach.

A procedure very similar to that previously described but involving  $^{13}\text{C}$  NMR shifts has been described, and the results are represented in Figure 77. Once again, only the shifts of the C atoms at the

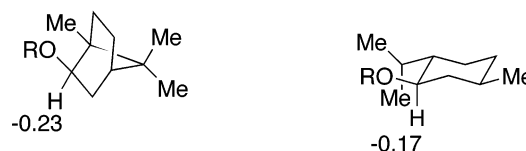
#### Unsymmetrical *S*-type alcohols



$R = H$ , 4,4-Dimethylcholesterol

$R = H$ , Testosterone

#### Unsymmetrical *R*-type alcohols



$R = H$ , (1*S*)-*endo*(-)-Borneol

$R = H$ , (-)-Menthol

**Figure 76.**  $\Delta\delta_{H^P}$  for the carbinyl protons.

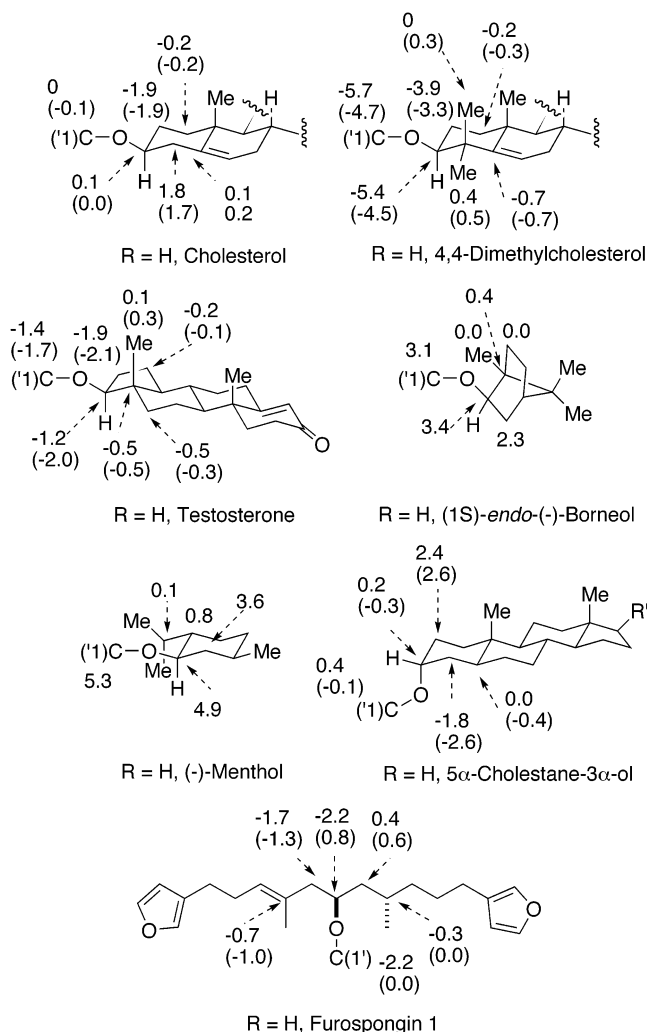


**Figure 77.** Chemical-shift differences ( $^{13}\text{C}$  NMR,  $\Delta\delta_{C^P}$ ) in pyridine- $d_5$  ( $\Delta\delta_{C^P}$ ) and  $\text{CDCl}_3$  ( $\Delta\delta_{C^C}$ ) of  $\beta$ -D- and  $\beta$ -L-fucufuranosides.  $\text{CDCl}_3$  data given in parentheses.

$\beta$ -position are considered; because the signs for the other C atoms are unreliable, the absolute values are very small and, furthermore, the degree of substitu-

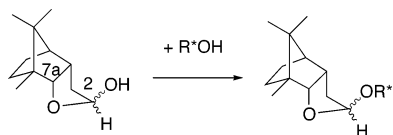


**Figure 78.**

tion at that C atom should be taken into consideration for the assignment.

**3.1.4.9. Noe Lactols.** The lactols derived from camphor are known as Noe lactols, and these have been used as CDAs for secondary alcohols<sup>58</sup> in which one of the substituents ( $L_1$  or  $L_2$ ) is a phenyl, nitrile, ethynyl, or formyl group. One example of this type of reagent is (+)- and (-)-*endo*-octahydro-7,8,8-trimethyl-4,7-4,7-methanobenzofuran-2-ol ((+)- and (-)-*endo*-MBF-OH), the structure of which is shown in Figure 78.

The method is totally empirical and consists of the derivatization of the alcohol with the two enantiomers of the reagent MBF-OH, followed by analysis of the  $^{13}\text{C}$  or  $^1\text{H}$  NMR spectra of the resulting diastereomeric lactols.

The stereochemistry at carbon 2 (Figure 78) in the starting hemiketal is not fixed; therefore, when single enantiomers of the auxiliary and the substrate are made to react, two epimers at C-2 result (types A and B). The predominant epimer in the mixture is the type-A lactol (see Figure 79).

The four stereoisomers obtained from a single enantiomer of the auxiliary and the two enantiomers (named A and B) of the alcohol are represented in Figure 79 and classified according to their origin as AA, AB, BB, and BA.

The assignment of the configuration involves determining the differences in the chemical shifts ( $\delta_{\text{AB}}$

**Table 8. The “b-pl” Rules for the Assignment of Configuration from Noe Lactols**

| pl          | $\Delta\delta = \delta\text{H}_{\text{AB}} - \delta\text{H}_{\text{AA}}$ |      |      |
|-------------|--|------|------|
|             | 2-H  | 7a-H | C*-H |
| aryl        | >0   | <0   | <0   |
| CN, CO, C≡C | <0   | >0   | <0   |

–  $\delta_{\text{AA}}$ ) of protons H(7a), H(2) in the auxiliary portion and H-C\* in the alcohol portion (Figure 79). Alternatively, the corresponding C-atom signals can be considered. The chemical-shift differences should be calculated and the signs interpreted, using the so-called “b-pl rules” (where b denotes bulky and pl denotes plane/lineal) indicated in Table 8.

For example, starting from the lactol MBF-OH of type A and a secondary alcohol of unknown configuration, we can obtain two derivatives, arbitrarily designated as A-A and A-B (see Figure 79a). If the differences  $\Delta\delta = \delta\text{H}_{\text{AB}} - \delta\text{H}_{\text{AA}}$  obtained are as shown in Table 8, derivative AA is formed from an alcohol with configuration type A and the derivative denoted as AB comes from the enantiomeric alcohol of configuration B. If the  $\Delta\delta$  signs obtained were opposite to those shown in Table 8, the configuration of the alcohol would also be opposite.

The chemical shifts ( $^1\text{H}$  and  $^{13}\text{C}$  NMR) and their differences ( $\Delta\delta$ ) are shown in Table 9 for the three most-relevant signals of a series of alcohols of known absolute configuration. The results obtained validate the rules for the assignment previously discussed and indicate that the method works well with secondary alcohols containing aryl, heteroaryl, nitrile, carbonyl, carboxyl, or ethynyl groups directly bonded to the asymmetric center (the pl substituent), as well as in cases where the substituents can be easily classified according to their “b-pl” character.

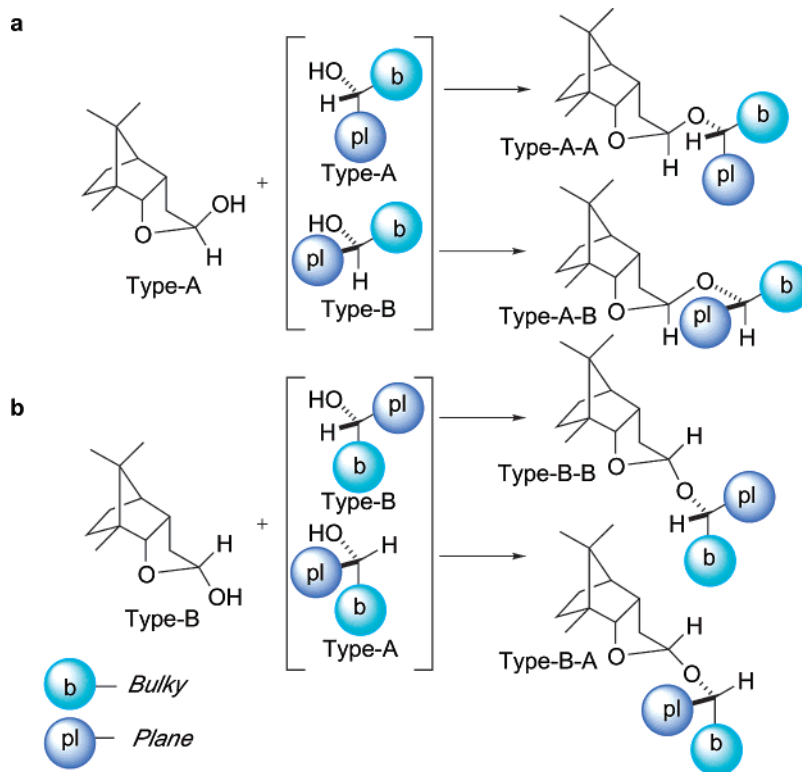


**Figure 79.**

**Table 9. Selected  $^1\text{H}$  and  $^{13}\text{C}$  NMR Data for the Noe Derivatives of Secondary Alcohols of Known Absolute Configuration<sup>a</sup>**

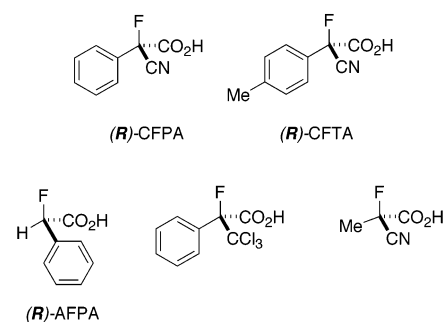
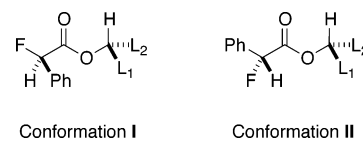
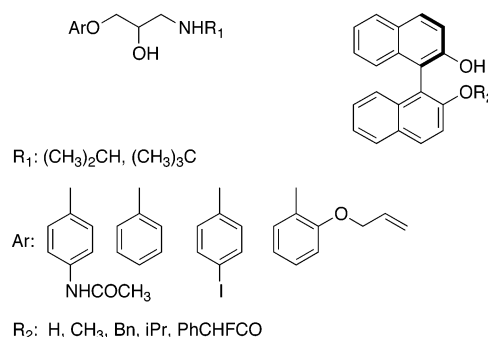
|                | hydrogen  |       | carbon |       |      |      |
|----------------|---|-------|--------|-------|------|------|
|                | 2H  | 7a-H  | C*-H   | C-2   | C-7a | C*   |
|                | b = CH <sub>3</sub> , pl = CN   |       |        |       |      |      |
| $\delta$       | 5.38  | 4.42  | 4.30   | 108.9 | 90.1 | 60.5 |
| $\delta$       | 5.51  | 4.19  | 4.54   | 106.5 | 90.3 | 59.0 |
| $\Delta\delta$ | -0.13   | 0.23  | -0.24  | 2.4   | -0.2 | 1.5  |
|                | b = C <sub>6</sub> H <sub>5</sub> <sup>b</sup> , pl = CN              |       |        |       |      |      |
| $\delta$       | 5.35  | 4.51  | 5.33   | 108.1 | 90.6 | 66.2 |
| $\delta$       | 5.71  | 4.23  | 5.51   | 107.0 | 90.8 | 65.6 |
| $\Delta\delta$ | -0.36   | 0.28  | -0.18  | 1.1   | -0.2 | 0.6  |
|                | b = CH <sub>3</sub> , pl = C≡CH                                       |       |        |       |      |      |
| $\delta$       | 5.45  | 4.38  | 4.40   | 106.6 | 89.3 | 61.4 |
| $\delta$       | 5.61  | 4.21  | 4.46   | 105.5 | 89.3 | 60.1 |
| $\Delta\delta$ | -0.16   | 0.17  | -0.06  | 1.1   | 0.0  | 1.3  |
|                | b = C <sub>6</sub> H <sub>5</sub> <sup>b</sup> , pl = C≡CH            |       |        |       |      |      |
| $\delta$       | 5.23  | 4.40  | 5.37   | 105.9 | 89.7 | 66.9 |
| $\delta$       | 5.82  | 4.22  | 5.45   | 105.7 | 89.7 | 66.2 |
| $\Delta\delta$ | -0.59   | 0.18  | -0.08  | 0.2   | 0.0  | 0.7  |
|                | b = CH <sub>3</sub> , pl = CH=O                                       |       |        |       |      |      |
| $\delta$       | 5.39  | 4.31  | 3.94   | 108.7 | 90.2 | 78.0 |
| $\delta$       | 5.44  | 4.27  | 4.17   | 107.9 | 89.9 | 76.3 |
| $\Delta\delta$ | -0.05   | 0.04  | -0.23  | 0.8   | 0.3  | 1.7  |
|                | b = C <sub>6</sub> H <sub>5</sub> <sup>b</sup> , pl = CH=O            |       |        |       |      |      |
| $\delta$       | 5.38  | 4.37  | 5.00   | 107.7 | 90.4 | 83.2 |
| $\delta$       | 5.58  | 4.07  | 5.14   | 107.6 | 90.1 | 81.6 |
| $\Delta\delta$ | -0.20   | 0.30  | -0.14  | 0.1   | 0.3  | 1.6  |
|                | b = CH <sub>3</sub> , pl = C <sub>6</sub> H <sub>5</sub> <sup>b</sup> |       |        |       |      |      |
| $\delta$       | 5.49  | 3.95  | 4.73   | 106.7 | 89.5 | 73.0 |
| $\delta$       | 5.12  | 4.32  | 4.78   | 105.6 | 89.0 | 72.9 |
| $\Delta\delta$ | 0.37  | -0.37 | -0.05  | 1.1   | 0.5  | 0.1  |
|                | b = <i>i</i> -Pr, pl = C <sub>6</sub> H <sub>5</sub> <sup>b</sup>     |       |        |       |      |      |
| $\delta$       | 5.40  | 3.61  | 4.07   | 109.1 | 89.1 | 84.7 |
| $\delta$       | 5.08  | 4.30  | 4.26   | 105.3 | 89.3 | 82.1 |
| $\Delta\delta$ | 0.32  | -0.69 | -0.19  | 3.8   | -0.2 | 2.6  |

<sup>a</sup> In the table, "b" denotes bulky and "pl" denotes plane/lineal. The first-line  $\delta$  value indicates Type AB, whereas the second-line  $\delta$  value denotes Type AA; the third line is  $\Delta\delta$ . <sup>b</sup> In this case, because both substituents are plane/lineal, the phenyl group at the  $\beta$  position is considered to be the bulky group.

These limitations certainly restrict the use of Noe's method for other alcohols but, at the same time, makes this procedure advantageous, because it allows the assignment of the configuration of alcohols that do not have protons in one of the substituents L<sub>1</sub>/L<sub>2</sub>—a case where the classical Mosher method cannot be used (see Section 3.1.1).

**3.1.4.10. Fluoroacetic Acids.** As mentioned previously in this review, with the exception of MTPA, very few reagents that contain F atoms have been explored<sup>59,60</sup> as auxiliary reagents for the assignment of the absolute configuration of substrates through  $^{19}\text{F}$  NMR. In general, the structures of these reagents are derived from that of MTPA (Figure 80) and, although some have been successfully used for the determination of the e.e. of alcohols, their application as CDAs has been hampered by the absence of a truly general model that can be applied to any other substrate.

In a study describing the application of AFPA (2-fluoro-2-phenylacetic acid) to secondary alcohols,<sup>60a-d</sup> the authors indicate that the corresponding esters exist in two conformations (I and II). However,

**Figure 80.** Structures of  $\alpha$ -fluoroacetic acids explored as CDAs.**Figure 81.** Main conformations of the esters of AFPA.**Figure 82.** Secondary alcohols studied by NMR of their AFPA esters.

although conformer I is the most representative species from the standpoint of  $^1\text{H}$  NMR, only conformer II is used as a model (see Figure 81) for the correlation of the  $^{19}\text{F}$  shifts with the configuration of the alcohol. This situation arises because it is this conformer in which the F atoms are subjected to the electronic effects of substituents L<sub>1</sub>/L<sub>2</sub> of the alcohol (the  $\gamma$ -gauche-type effect). Figure 82 shows a selection of the substrates of known absolute configuration that produce  $^{19}\text{F}$  shifts coherent with the model indicated.

Another fluorine-containing compound used for this purpose is  $\alpha$ -cyano- $\alpha$ -fluoro-*p*-tolylacetic acid<sup>60e</sup> (CFTA). The structure of this compound is shown in Figure 80, and it is used for secondary alcohols ( $^1\text{H}$  NMR) and amines ( $^{19}\text{F}$  NMR; see Section 3.4.5.1). The procedure requires the preparation of the esters from the two enantiomers of CFTA and measurement of the  $\Delta\delta^{SR}$  value ( $\delta(S) - \delta(R)$ ) for the substituents (L<sub>1</sub>/L<sub>2</sub>) of the alcohol. The assignment is based on the fact that, in the ester derived from (*S*)-CFTA, substituent L<sub>1</sub> is shielded by the fluorophenyl group whereas in the (*R*)-CFTA ester, the shielded substituent is L<sub>2</sub> (see Figure 83).

Figure 84 shows the structures of the compounds of known absolute configuration used to validate this procedure, along with the  $\Delta\delta^{SR}$  values that are obtained. The data demonstrate that, in all cases, the signs of  $\Delta\delta^{SR}$  are coherent with the configuration and the model.



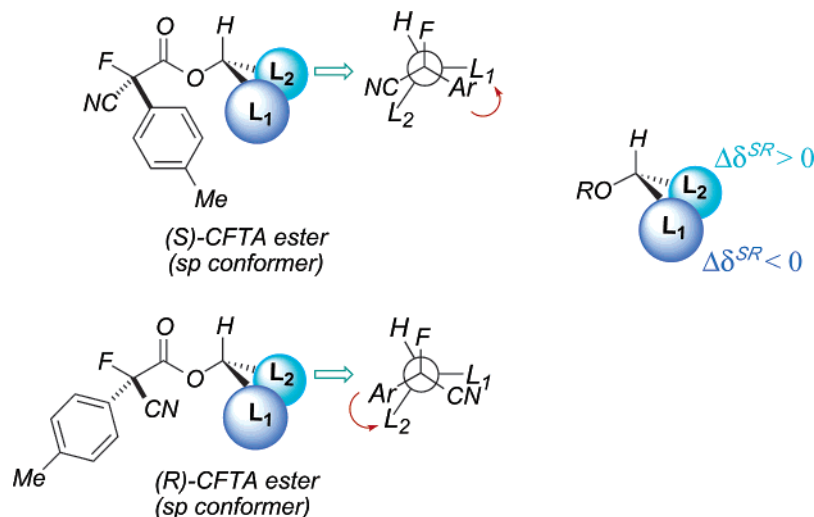


Figure 83.

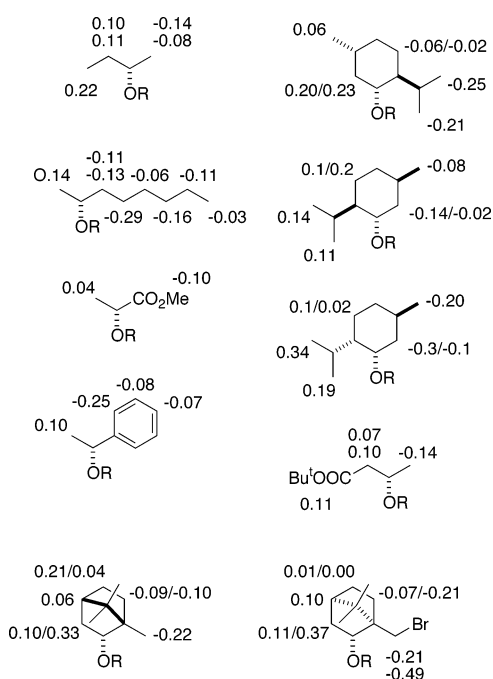


Figure 84.

Theoretical calculations on the geometry and conformational composition of these CFTA esters, using ab initio (GAUSSIAN 98, RHF/6-31+G(d)) methods, revealed that there is an equilibrium between two main rotamers around the C $\alpha$ -C=O bond. One

rotamer, denoted sp, has the C-F and CO bonds in a syn-periplanar arrangement and the other, designated ap, contains the aforementioned bonds in an anti-periplanar relation. According to the calculations, the most stable conformer is sp, and this is represented in Figure 83.

The <sup>19</sup>F NMR spectra of these esters have also been reported; however, a convincing model that allows the correlation of the absolute configuration of the alcohol with the signs of  $\Delta\delta^{SR}$  has yet to be proposed.

**3.1.4.11. Chiral Silylating Reagents.** Attempts to use chiral silylating reagents to determine the absolute stereochemistry of chiral allylic alcohols led to the proposal of (+)- and (-)-chloromenthoxydiphenylsilanes and (+)- and (-)-2-bromo- $\alpha$ -methylbenzyl-oxychlorodiphenylsilanes as CDAs.<sup>61</sup> Although they showed promising results, the small number of alcohols tested (two and one examples, respectively) prevents their use as a general method.

## 3.2. Application to $\beta$ -Chiral Primary Alcohols

The extension of the NMR methods for the assignment of the configuration of secondary alcohols described previously to other substrates is particularly appealing, because systems such as primary alcohols with the chiral center in the position  $\beta$  to the OH group, are frequently found in nature in chiral forms or are obtained by a reduction of the carboxylic acids and aldehydes.

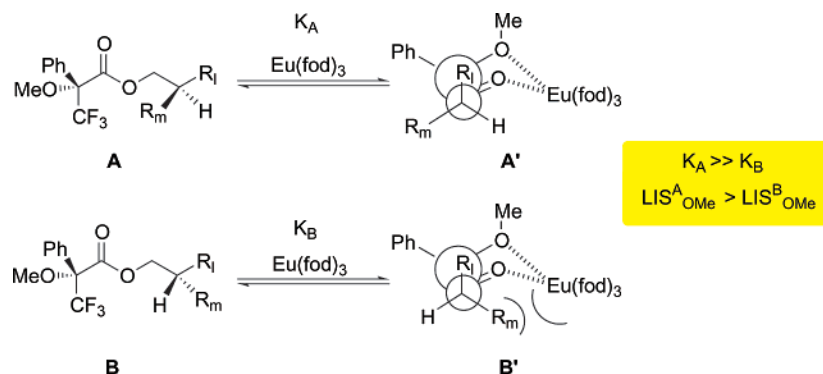
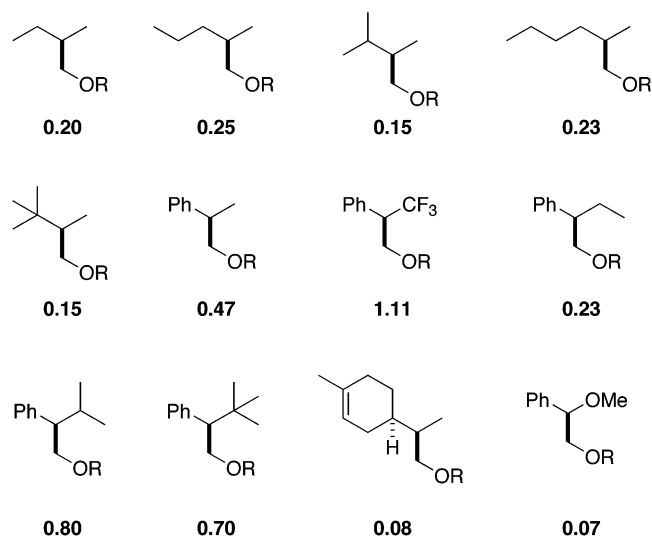


Figure 85. Empirical models for the determination of the absolute configuration of primary alcohols by NMR of their MTPA esters in the presence of  $\text{Eu}(\text{fod})_3$ .  $R_m$  represents the medium-sized group and  $R_l$  represents the large-sized group.



**Figure 86.** Lanthanide-induced shift ( $\text{Eu}(\text{fod})_3$ ;  $\Delta\text{LIS}_{\text{OMe}} = \text{LIS}^{\text{A}} - \text{LIS}^{\text{B}}$ ) obtained for the OMe group of diastereomeric (*R*)-MTPA esters.

Two main difficulties are apparent when dealing with primary alcohols:

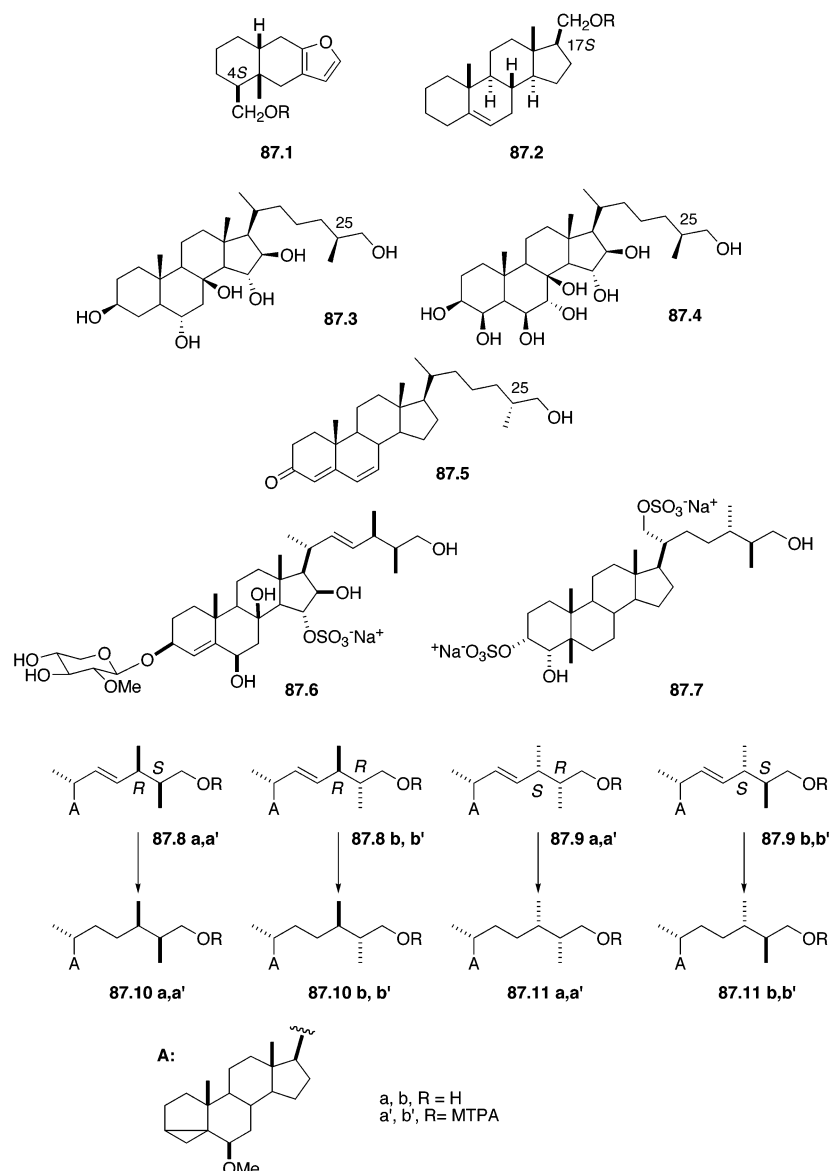
(1) The distance between groups  $\text{L}_1/\text{L}_2$  of the substrate and the aryl ring of the auxiliary reagent is greater than that in secondary alcohols, because the asymmetric center is at the  $\beta$ -position, and

(2) The presence of an extra C–C bond between the chiral center and the auxiliary reagent reduces the conformational preference by increasing the rotational freedom. As a result, the  $\Delta\delta^{\text{RS}}$  values for primary alcohols would be expected to be smaller and less reliable than those usually obtained for secondary alcohols.

Very few papers have been published on this particular subject. MTPA and recently 9-AMA are the reagents most amply used in the assignment of absolute configuration of such substrates.

### 3.2.1. MTPA

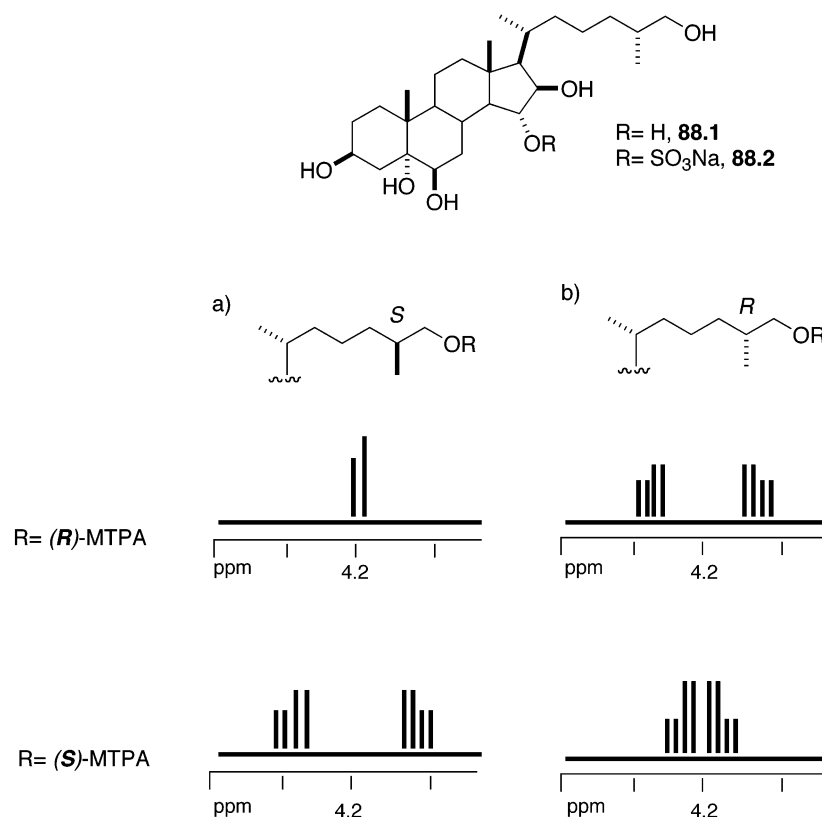
A quarter of century ago, Yasuhara and Yamaguchi<sup>62a</sup> developed a procedure that is based on the use of a shift reagent with MTPA derivatives for the determination of the absolute configuration of primary carbinols with a chiral center at the  $\beta$ -position. This approach was an extension of a previous method



**Figure 87.** Natural compounds studied with MTPA and steroidal side chains obtained by synthesis and used as models.

**Table 10. Selected NMR Data (CD<sub>3</sub>OD) for Side-Chain Signals in Synthetic 24-Methyl-26-hydroxy Steroids and in Natural Compounds 87.6 and 87.7**

| compound                             | 26-CHH <sub>2</sub> | 27-CH <sub>3</sub> | 28-CH <sub>3</sub> | C-24 | C-27 | C-28 | ( <i>R</i> )-MTPA ester<br>(26-CH <sub>2</sub> )                           |
|--------------------------------------|---------------------|--------------------|--------------------|------|------|------|--|
| $\Delta^{22}$ Series                 |                     |                    |                    |      |      |      |  |
| (87.8a) (24 <i>R</i> ,25 <i>S</i> )  | 3.28 dd, 3.60 dd    | 0.90 d             | 0.95 d             | 39.7 | 13.8 | 17.1 | 4.19 dd, 4.31 dd   |
| (87.9a) (24 <i>S</i> ,25 <i>R</i> )  | 3.29 dd, 3.59 dd    | 0.90 d             | 0.97 d             | 39.5 | 13.8 | 16.8 | 4.13 dd, 4.38 dd   |
| (87.9b) (24 <i>S</i> ,25 <i>S</i> )  | 3.34 dd, 3.53 dd    | 0.87 d             | 1.02 d             | 39.2 | 13.6 | 19.0 | 4.21 br d  |
| (87.8b) (24 <i>R</i> ,25 <i>R</i> )  | 3.34 dd, 3.52 dd    | 0.88 d             | 1.02 d             | 39.3 | 13.6 | 19.2 | 4.16 dd, 4.21 dd   |
| Saturated Series                     |                     |                    |                    |      |      |      |  |
| (87.10a) (24 <i>R</i> ,25 <i>S</i> ) | 3.38 dd, 3.55 dd    | 0.83 d             | 0.81 d             | 35.1 | 14.8 | 12.0 | 4.23 br d  |
| (87.11a) (24 <i>S</i> ,25 <i>R</i> ) | 3.38 dd, 3.49 dd    | 0.81 d             | 0.81 d             | 35.1 | 15.1 | 11.6 | 4.14 dd, 4.34 dd   |
| (87.11b) (24 <i>S</i> ,25 <i>S</i> ) | 3.36 dd, 3.58 dd    | 0.93 d             | 0.92 d             | 36.8 | 17.5 | 14.4 | 4.22 dd, 4.32 dd   |
| (87.10b) (24 <i>R</i> ,25 <i>R</i> ) | 3.37 dd, 3.57 dd    | 0.91 d             | 0.91 d             | 36.1 | 17.4 | 14.1 | 4.16 dd, 4.38 dd   |
| Natural Compounds                    |                     |                    |                    |      |      |      |  |
| (87.6) (24 <i>R</i> ,25 <i>S</i> )   | 3.46 dd, 3.58 dd    | 0.91 d             | 0.97 d             | 40.4 | 14.5 | 17.5 | ( <i>R</i> )-MTPA: 4.17 dd, 4.33 dd<br>( <i>S</i> )-MTPA: 4.06 dd, 4.46 dd |
| (87.7) (24 <i>S</i> ,25 <i>S</i> )   | 3.34 dd, 3.62 dd    | 0.92 d             | 0.92 d             | 36.7 | 17.4 | 14.3 | ( <i>R</i> )-MTPA: 4.24 dd, 4.32 dd<br>( <i>S</i> )-MTPA: 4.16 dd, 4.37 dd |

**Figure 88.** Shape of the partial NMR spectra of the 26-methylene protons in (*R*)- and (*S*)-MTPA esters of (a) a 25*S* steroid and (b) its 25*R* isomer.

used for secondary alcohols<sup>4a,62b,c</sup> and consisted of the conversion of a mixture of the two enantiomers of a primary alcohol into the corresponding mixture of (*R*)-(+)-MTPA esters. The magnitude of the lanthanide-induced shift (LIS<sub>OMe</sub>) produced by Eu(fod)<sub>3</sub> on the OMe group of the MTPA ester showed a correlation with the absolute configuration. The diastereomeric (*R*)-(+)-MTPA esters with the larger LIS<sub>OMe</sub> value had configuration A and the diastereomer with the smaller LIS<sub>OMe</sub> value had configuration B (see Figure 85).

The results were rationalized in terms of the models shown in Figure 85, where the complexation constant  $K_A$  is larger than  $K_B$ , because of the less-marked steric interaction between Eu(fod)<sub>3</sub> and the H atom at the chiral center in A' than with R<sub>m</sub> in B'. The fact that the magnitudes of  $\Delta$ LIS<sub>OMe</sub> for the

esters of 2-phenylethanols with bulky R<sub>m</sub> groups are larger than those with smaller R<sub>m</sub> groups is consistent with the model. The procedure was tested on the 12 substrates shown in Figure 86, where the chiral center is not present as part of a ring in any of the cases.

The application of this method to cyclic alcohols was explored by Takahashi et al.<sup>63a</sup> with the terpenes **87.1** and **87.2** shown in Figure 87. The compounds were transformed to the corresponding (*R*)- and (*S*)-MTPA esters and the resulting  $\Delta$ LIS<sub>OMe</sub> values indicated configurations that were in agreement with the known configurations deduced by alternative correlation procedures.

The same method has also been applied to the determination of the stereochemistry of a variety of steroidal side chains. Minale et al.<sup>63b,c</sup> assigned the

stereochemistry at C-25 of a series of polyhydroxylated steroids, such as **87.3** or **87.4** (Figure 87), which were isolated from different starfish species.

It has been observed empirically that the LIS<sub>OMe</sub> signal in the <sup>1</sup>H NMR spectrum of a primary carbinol (+)-MTPA ester with *R* chirality at the β-carbon (or a β-*S* carbinol (−)-MTPA ester) is greater than that of its diastereomer. This information was used in the assignment of the C-25 configuration of steroid **87.5** (Figure 87), which was obtained after acid methanolysis of pavoninin 1, isolated from the defense secretion of the sole *P. pavoninus*.<sup>63d</sup> The addition of an equimolar amount of Eu(fod)<sub>3</sub> to a mixture of the (+)- and (−)-MTPA esters (ca. 10:7) of **87.5** in CDCl<sub>3</sub> shifted the two OMe signals by 0.68 and 0.66 ppm, respectively, and the addition of 2.8 molar equivalents Eu(fod)<sub>3</sub> shifted them by 2.05 and 2.00 ppm, respectively. The larger downfield shift observed for the more intense OMe signal of the (+)-MTPA ester showed the configuration at C-25 to be *R*.

For those cases where the steroidal side chains had an extra chiral center at C-24, several compounds of known stereochemistry were synthesized and used as model systems. This was the case for two naturally occurring marine steroids from a starfish and an opiuroid: **87.6** and **87.7**, respectively<sup>64</sup> (see Figure 87).

Also, the stereoisomers of Δ<sup>22</sup>E and the saturated 24-methyl-26-hydroxy steroids **87.8**–**87.11** (Figure 87) were prepared by Claisen rearrangement and the relative stereochemistries (*threo* or *erythro*) were deduced by comparison of <sup>1</sup>H and <sup>13</sup>C NMR spectra (see Table 10) and application of the Yasunara–Yamaguchi method that established the configuration at C-25.

Similar NMR studies of MTPA esters showed that there was a correlation between the shape of the signals due to the CH<sub>2</sub>OH (C-26) group in the (*R*)- and (*S*)-MTPA esters and the absolute configuration at C-25. This new approach (i.e., comparison of the chemical shifts of the methylene protons at C-26 in the spectra of the (*R*)- and (*S*)-MTPA esters) has the advantage of avoiding the use of europium salts and has been widely used by researchers interested in the stereochemistry of steroid side chains.<sup>65</sup>

It can be seen from Figure 88 that, in the spectra of the MTPA esters of a 25*S* isomer, the C-26 methylene protons resonate much closer to each other in the spectrum of the (*R*)-MTPA ester than in the (*S*)-MTPA derivative, whereas the reverse situation occurs for the MTPA esters of a 25*R* isomer.

The assignment of the configuration of the marine polyhydroxylated steroids **88.1** and **88.2** was conducted using this technique. In the case of **88.1**, the signals due to the methylene at C-26 in the (*R*)-MTPA derivative appeared as two well-separated doublet of doublets (dd) at δ 4.14 (*J* = 6.6 and 10.8 Hz) and 4.28 ppm (*J* = 6.4 and 10.8 Hz) (Δδ ca. 0.14 ppm). The (*S*)-MTPA derivative, on the other hand, exhibited very similar dd signals, at 4.19 and 4.23 ppm (Δδ ca. 0.04 ppm), thus indicating an *R* configuration for the compound in question. The same procedure was applied to **88.2**; however, unfortunately, the presence of the bulky sulfate group at C-15 made the differ-

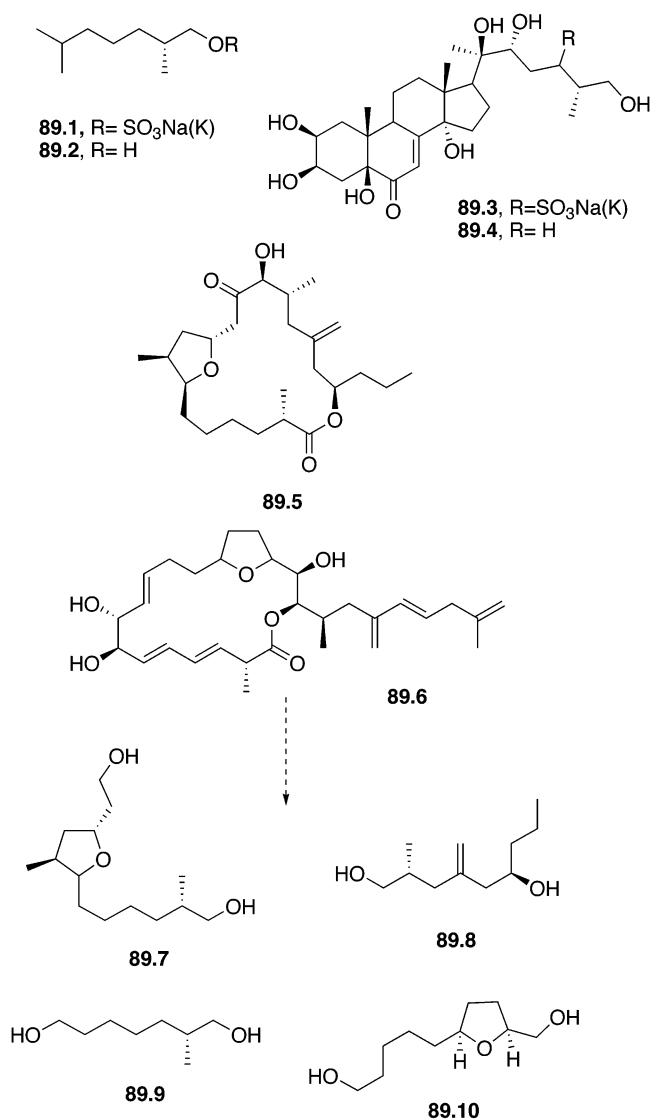


**Figure 89.** Chiral primary alcohols used in these studies.

ences between the methylene group in the (*R*)- and (*S*)-MTPA esters very small (δ 4.15/4.25 and 4.15/4.23, respectively). Removal of the sulfate group produced the expected sets of doublet of doublets at δ 4.14/4.27 and 4.19/4.23, respectively. This case illustrates the limitations imposed by the presence of bulky substituents in ring D of steroids.<sup>66a</sup>

Other examples of the use of this technique include 2,6-dimethylheptyl sulfate, **89.1** (see Figure 89), which was isolated from marine ascidians and its configuration at C-2 was inferred as *R*, from the application of the same method to its desulfated derivative **89.2**.<sup>66b</sup> Kobayashi et al. also used this technique on a variety of marine metabolites such as the ecdysteroids palythoalones A (**89.3**) and B (**89.4**)<sup>66c</sup> and the amphidinolides T (**89.5**)<sup>66d</sup> and E (**89.6**)<sup>66e</sup>. In these latter cases, the absolute configuration was deduced after degradation of the natural product (**89.7**, **89.8**, **89.9**, and **89.10**), subsequent derivatization with MTPA, and the use of compounds with known absolute configuration, obtained by synthesis, as models for comparison of the NMR spectra.

|  | Conf.    | $\delta(F)$ of MTPA |              | Empirical models |
|--|----------|---------------------|--------------|------------------|
|  |          | ( <i>S</i> )        | ( <i>R</i> ) |                  |
|  | <i>R</i> | -71.97              | -72.02       |                  |
|  | <i>R</i> | -71.58              | -71.87       |                  |
|  | <i>R</i> | -71.51              | -71.84       |                  |
|  | <i>R</i> | -71.76              | -71.98       |                  |
|  | <i>R</i> | -71.76              | -72.00       |                  |
|  | <i>R</i> | -71.81              | -71.98       |                  |
|  | <i>S</i> | -72.10              | -72.07       |                  |
|  | <i>S</i> | -72.12              | -72.10       |                  |

**Figure 90.**  $^{19}\text{F}$  NMR chemical shifts of MTPA esters of primary hydroxy-sulfonamides and empirical models.

In 1996, Seebach and co-workers<sup>67</sup> proposed a method based on  $^{19}\text{F}$  NMR analysis of the MTPA esters and, more specifically, directed toward the determination of the absolute configuration of hydroxy-sulfonamides. The study was comprised of six cyclic hydroxy-sulfonamides, one cyclic hydroxy-ester, and just one acyclic primary alcohol (2-methylbutanol) of known configuration. A correlation between the relative configuration of the MTPA esters with the  $^{19}\text{F}$  NMR chemical shift of the  $\text{CF}_3$  group was deduced. Figure 90 shows the structures, chemical shifts, and the empirical model used to explain the correlation.

### 3.2.2. 9-AMA

The most general approach to the assignment of the absolute configuration of primary alcohols is based on the use of 9-AMA,<sup>68,69</sup> because this reagent

has been shown<sup>29,30</sup> to possess two very important features: (a) a higher conformational preference (the syn-periplanar form, *sp*), than other AMAA reagents, and (b) the anthryl ring in the main conformer (*sp*) is particularly well-oriented, in terms of projecting its strong aromatic magnetic cone on substituent  $\text{L}_1$  or  $\text{L}_2$ .

No such advantages are expected from MPA or MTPA, because they have lower conformational preferences, less-favorable orientation of the phenyl ring (MTPA), and a weaker magnetic cone (phenyl versus anthryl). Indeed, when these three reagents were tested using 2-methylpropan-1-ol as a model compound, completely separate signals for the diastereotopic methyl groups were obtained only in the 9-AMA esters<sup>69</sup> ( $\Delta\delta^{RS} = 0.033$  versus  $\Delta\delta^{RS} = 0.002$  ppm for 9-AMA and MPA respectively, and no separation for MTPA).

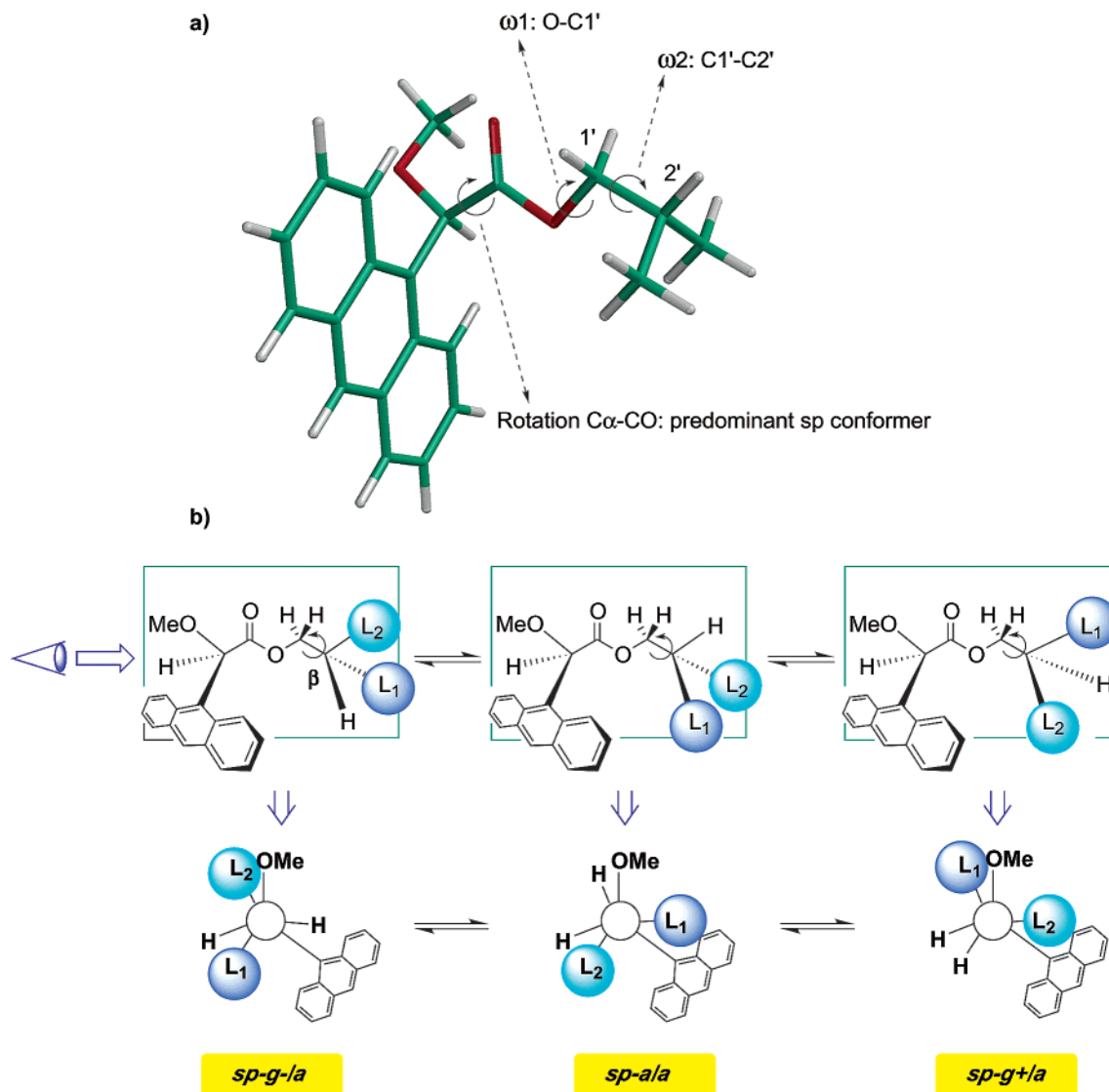


**Figure 91.** Low-energy conformers (perspective and Newman projections) for (*R*)-9-AMA esters of primary alcohols. In most cases, *sp-a/a* is the most populated and relevant for NMR studies.

Complex theoretical studies (including molecular mechanics, semiempirical, *ab initio*, and aromatic shielding-effect calculations), complemented by D NMR, were performed<sup>69</sup> with simple model compounds to assess the viability of 9-AMA esters for this purpose. The results of these studies indicated that the main conformational processes involve rotation around  $\omega_1$  and  $\omega_2$  bonds (see Figure 91 a), generating three main low-energy conformations (syn-periplanar-gauche+/anti (*sp-g+/a*), syn-periplanar-anti/anti (*sp-a/a*), and syn-periplanar-gauche-/anti (*sp-g-/a*); see Figure 91b), with one of these (*sp-a/a*) becoming the most significant, in terms of NMR spectroscopy in most cases. In all these conformations, the 9-AMA substructure maintains its most-stable *sp* form.

Because conformer *sp-a/a* is the more stable and representative, from the standpoint of NMR, for a primary alcohol with the stereochemistry shown in Figure 92, substituent  $L_1$  will be more shielded in the (*R*)-9-AMA ester, whereas substituent  $L_2$  will be in the (*S*)-9-AMA ester. Therefore, a negative  $\Delta\delta^{RS}$  sign is expected for substituent  $L_1$  and a positive  $\Delta\delta^{RS}$  sign is expected for substituent  $L_2$ .

Sixteen 9-AMA esters of primary alcohols were studied,<sup>69</sup> and, in most cases (**93.1–93.13**; see Figure 93), the conformational preferences and the model previously described do, in fact, apply. This observation means that the NMR spectra of this set of 9-AMA esters could be reliably interpreted on the basis of the corresponding model, and NMR spectroscopy can be used to correlate the absolute configuration at the asymmetric center of the 9-AMA and that of the alcohol.

Unfortunately, in three examples involving cyclic structures or bulky substituents (**93.14–93.16**), the calculations showed that the *sp-a/a* forms were not the preferred forms and that the *sp-g-/a* and *sp-g+/a* forms make a very significant contribution. In these cases, it is clear that the *sp-a/a* model is not valid for interpretation of the NMR spectra of the 9-AMA esters.

In conclusion, to assign the absolute configuration of a primary alcohol by this method, a preliminary calculation must be performed (being the best force field, PCff), especially when the chiral center is part of a ring, or when strong steric interactions could be in operation, to confirm that the anti form is the most

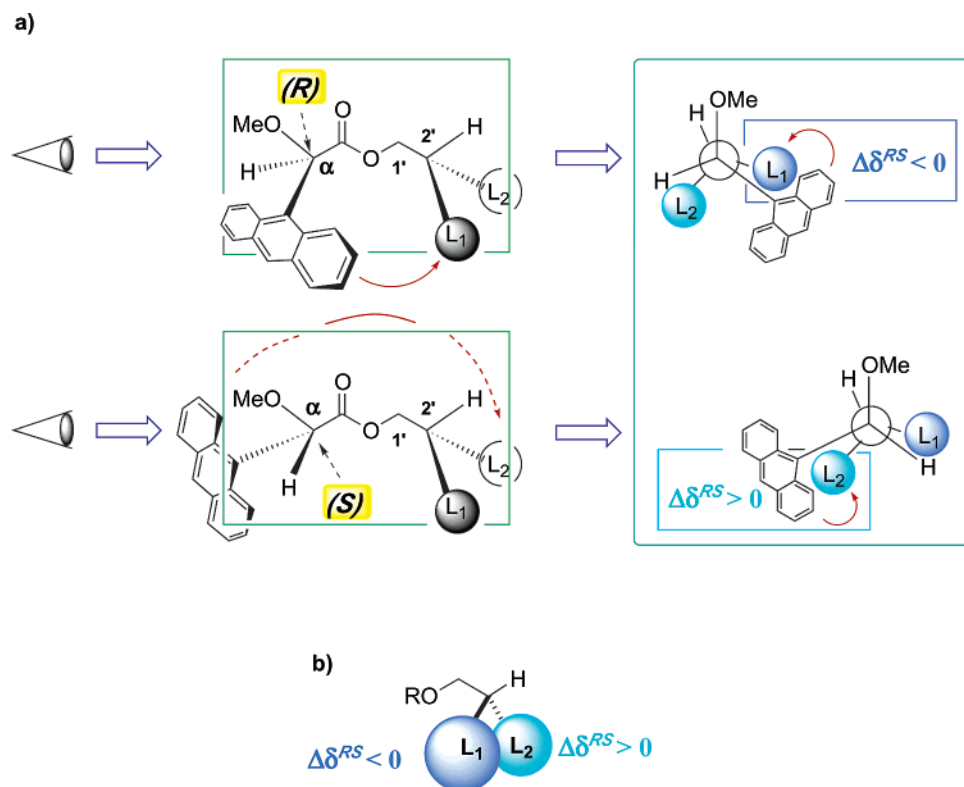


**Figure 92.** Conformational model for the determination of the absolute configuration of  $\beta$ -chiral primary alcohols by NMR of their 9-AMA esters.

stable one and, consequently, that the model shown in Figure 92 is representative and can be applied to the interpretation of the chemical shifts.

The use of the auxiliary reagents MTPA and MPA did not generate either the required  $\Delta\delta^{RS}$  values or homogeneity in the sign distribution, and this situation confirmed that these compounds could not be used as auxiliary reagents with chiral primary alcohols.

A good example of the application of this procedure for the determination of the configuration of a complex substance is shown in Figure 94, which depicts oxazinin-1, a cytotoxic compound that has been isolated from the digestive glands of an edible mussel (*Mytilus galloprovincialis*). That was recently published by Fattorusso et al.<sup>70</sup> In that paper, MM calculations were initially performed to check the reliability of the NMR method with that particular substrate, and the stereochemistry was determined using the 9-AMA esters only after a positive result had been obtained.

### 3.3. Application to $\alpha$ -Chiral Tertiary Alcohols

Although the determination of the configuration of chiral secondary alcohols by NMR has been satisfactorily accomplished through the use of the various alternatives already discussed (see Section 3.1), a general methodology for chiral tertiary alcohols has not yet been established. This fact is mainly due to intrinsic problems associated with these substrates, such as difficulties in making derivatives (i.e., esters) in high yields and their unsuitable conformational characteristics. A few attempts have been made to find solutions to these problems but usually the

number of substrates studied is small and their structural variety is limited; therefore, the methods are applicable only to the cases reported.

#### 3.3.1. MTPA

The use of MTPA with tertiary alcohols<sup>71</sup> was explored for just two examples: pinan-2-ols **95.1** and **95.2** (see Figure 95).

A combination of MM2 calculations and NOE and anisotropic effects (measured as  $\Delta\delta^{SR}$  of the methyl groups) was used to predict the configuration of these substrates. The authors state that MTPA can be used in combination with conformational analysis; however, the method was not expanded to include other alcohols.

#### 3.3.2. Methoxy-(2-naphthyl)acetic Acid (2-NMA)

A method for the prediction of the absolute configuration of acyclic  $\alpha$ -methyl-substituted tertiary alcohols has been published and involves the use of methoxy-(2-naphthyl)acetic acid (2-NMA) as an auxiliary reagent.<sup>72</sup>

The method is based on an analysis of the NMR spectra of the 11 compounds of known configuration shown in Figure 96. According to the authors, the  $\Delta\delta^{RS}$  signs obtained are systematically distributed as positive and negative for substituents  $L_1$  and  $L_2$ . This arrangement can be represented by the model shown in Figure 97, and it was used by the authors for the assignment of configuration. The  $\beta$ -methylene and methyl protons directly bonded to the tertiary hydroxyl group should not be considered for the assignment.

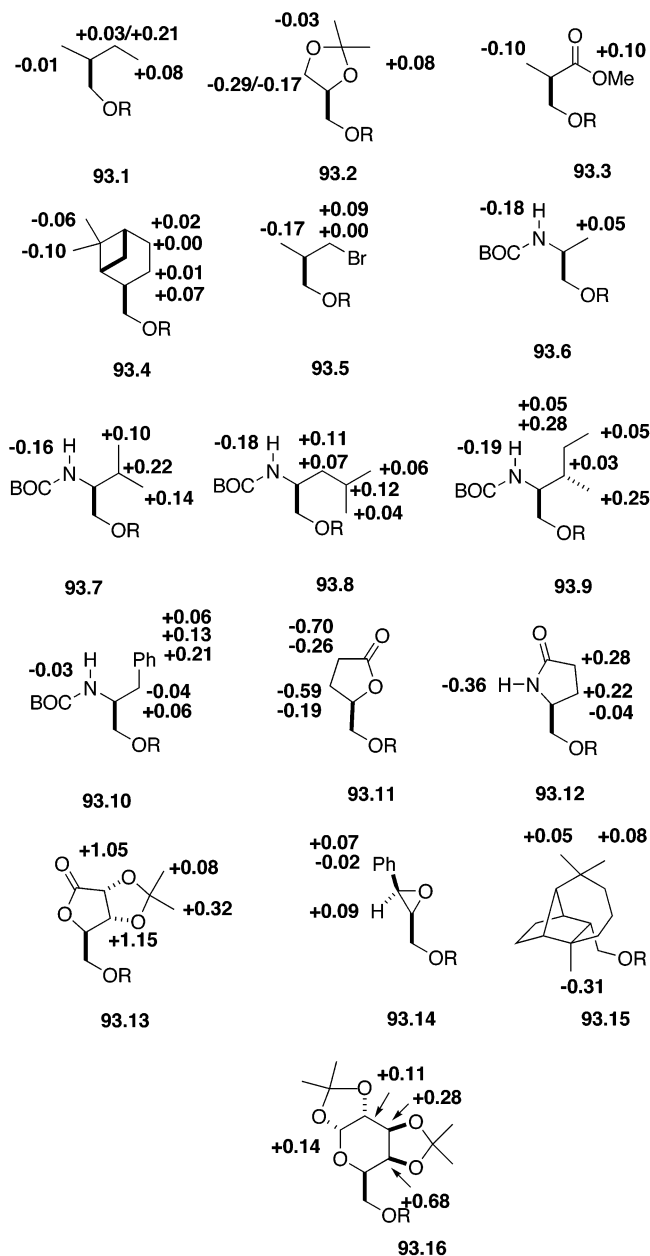


**Figure 93.**  $\Delta\delta^{RS}$  values for the 9-AMA esters of primary alcohols.

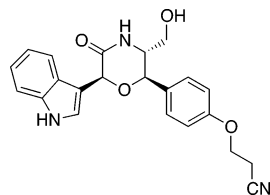


**Figure 94.** Structure of oxazin-1.

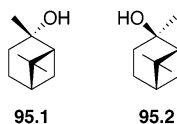


**Figure 95.**

Other drawbacks associated with this method are the low yields reported for the esterification (i.e., 27%) and the racemization problems that are encountered. MTPA and MPA were also tested; however, they resulted in smaller  $\Delta\delta$  values than those for 2-NMA.

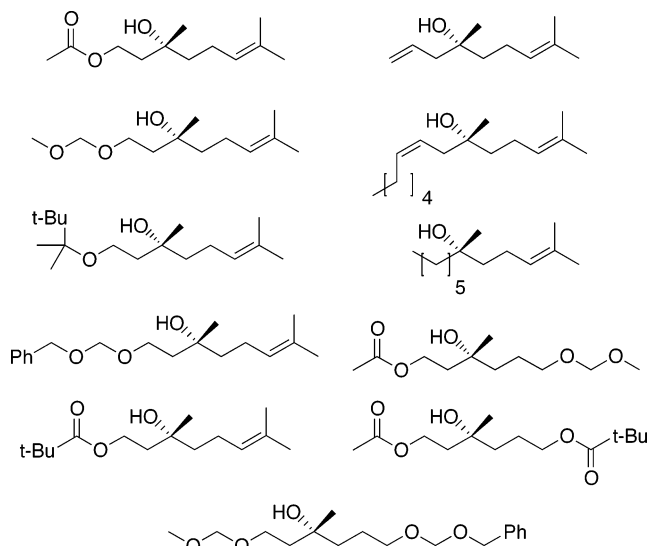


**Figure 96.**  $\alpha$ -Methyl-substituted tertiary alcohols used by Kobayashi et al.

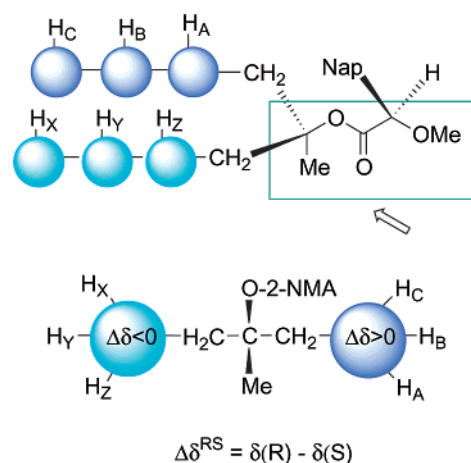


**Figure 97.** Empirical model to determine the absolute configuration of  $\alpha$ -methyl-substituted tertiary alcohols.

### 3.3.3. The Fucufuranoside Method

Kobayashi<sup>73</sup> applied a method that was devised for the determination of the absolute configuration of secondary alcohols to the series of six chiral tertiary alcohols (substituted with methyl and two methylene groups) shown in Figure 98. The method involves the derivatization of the alcohol as  $\beta$ -D- and  $\beta$ -L-fucufuranosides, comparison of the NMR spectra ( $^1\text{H}$  and  $^{13}\text{C}$ ) of the derivatives taken in pyridine- $d_5$ , and evaluation of the  $\Delta\delta$  values ( $\delta_L - \delta_D$ ) and signs for the proximate protons ( $^1\text{H}$  NMR) or  $\beta$ -carbons ( $^{13}\text{C}$  NMR).

The experimental data show that the  $\Delta\delta$  values are generally positive for the protons in the right-hand segment (Rr) and negative for those in the left-hand segment (Rl); however, in several cases, both positive and negative signs coexist on the same methylene group.

The  $\Delta\delta$  values from the  $^{13}\text{C}$  NMR study are positive for the right-hand  $\beta$ -carbon and negative for the left-hand  $\beta$ -carbon, except for the five-membered ring compound, which did not follow this trend.

These results can be interpreted on the basis of the model shown in Figure 99. This model does not have any proven conformational meaning, because NOE



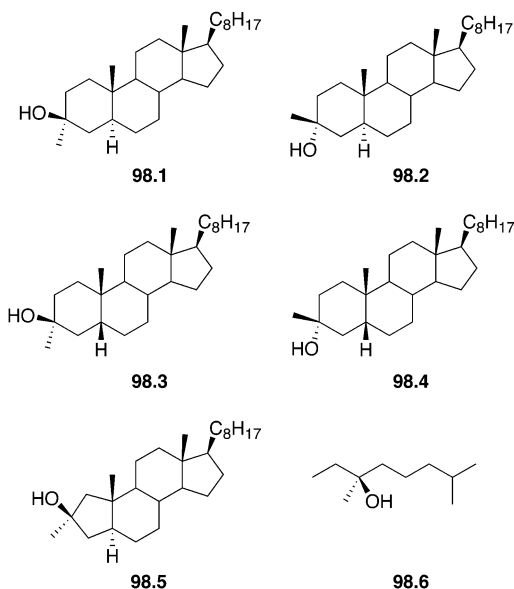


**Figure 98.** Tertiary alcohols used in this study.

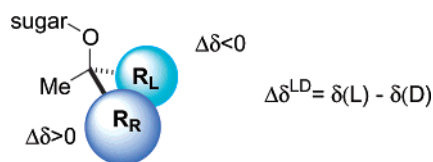


**Figure 99.** Models for assignment of tertiary alcohols as  $\beta$ -D- and  $\beta$ -L-fucofuranosides.

or low-temperature NMR studies or geometry calculations were not performed to establish the conformational characteristics of the derivatives.

Indeed, the author states that the method may not be valid for tertiary alcohols with more-complex substitution patterns. In addition, the very low yields obtained in the derivatization step (in the range of 2%–23%) or, in some cases, even the failure to obtain the fucofuranosides, represents a major limitation to the use of this method.

### 3.4. Application to $\alpha$ -Chiral Primary Amines

#### 3.4.1. MTPA

Another of the applications of “Mosher’s method” is the determination by  $^1\text{H}$  NMR spectroscopy of the

absolute configuration of primary amines<sup>8c,74</sup> that have a chiral center at the  $\alpha$ -position. The model used to correlate the stereochemistry with the chemical shifts is analogous to that proposed for secondary alcohols and, although a procedure based on  $^{19}\text{F}$  NMR studies of MTPA esters has been formulated for alcohols (Figure 8), a similar application with amines has very rarely been used.

The method is standard and involves the preparation of the corresponding MTPA amides from the two enantiomers of MTPA and the amine of unknown configuration. The NMR spectra of the two derivatives are then recorded and the differences in the chemical shifts ( $\Delta\delta^{SR}$ ) are calculated. Mosher proposed that the most-relevant conformer would be the one in which the  $\text{CF}_3$ , carbonyl, NH, and  $\text{C}(1')\text{H}$  groups are in the same plane, with the  $\text{CF}_3$  and the carbonyl units in a syn-periplanar disposition. In accordance with this model (see Figure 100), substituent  $\text{L}_2$  is shielded in the (*R*)-MTPA amide and substituent  $\text{L}_1$  is shielded in the (*S*)-MTPA amide. For an amine with the configuration shown in Figure 100c, substituent  $\text{L}_1$  has negative  $\Delta\delta^{SR}$  values and substituent  $\text{L}_2$  has positive values. In the case where the amine has the opposite configuration, as in Figure 100d, the signs are also opposite to those in the example in Figure 100c.

In an effort to establish the scope and limitations of this method, theoretical calculations (MM, semi-empirical AM1) and NMR studies (aromatic anisotropy increments, dynamic NMR) have recently been conducted.<sup>75</sup>

This conformational study showed that the main processes are those due to rotations around the  $\text{CO-NH}$ ,  $\text{C}\alpha\text{-CO}$ , and  $\text{C}\alpha\text{-Ph}$  bonds (see Figure 101). Rotation around the  $\text{CO-NH}$  bond generates two rotamers (*Z* and *E*). The *Z* rotamer is predominant, because of its greater stability, in terms of energy. Rotation around the  $\text{C}\alpha\text{-CO}$  bond produces the two usual *sp* ( $\text{CF}_3$  and carbonyl syn-periplanar) and *ap* ( $\text{CF}_3$  and carbonyl anti-periplanar) conformers. Rotation around the  $\text{C}\alpha\text{-Ph}$  bond results in three main orientations, with the phenyl group coplanar with either the  $\text{C}\alpha\text{-OMe}$ ,  $\text{C}\alpha\text{-CO}$ , or  $\text{C}\alpha\text{-CF}_3$  bonds.

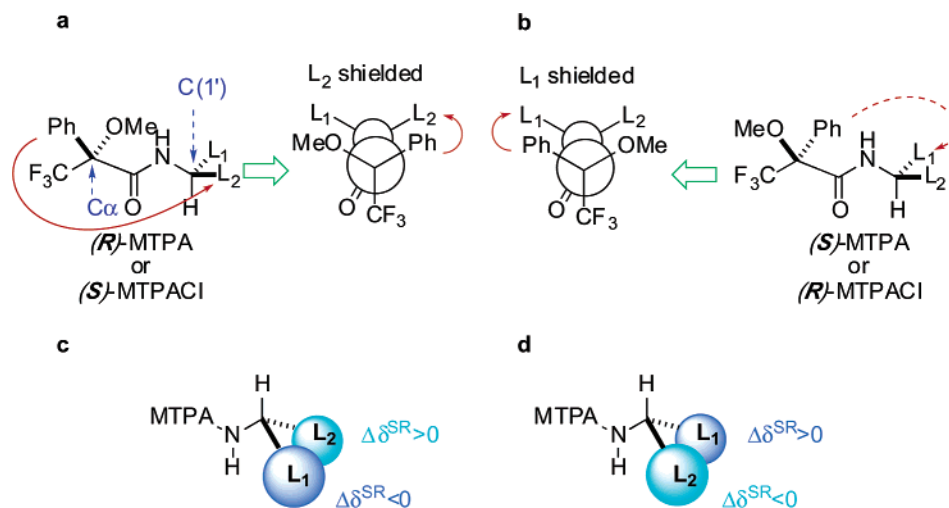


**Figure 100.** (a, b) Mosher’s model for the correlation of the configuration with the  $^1\text{H}$  NMR shifts and (c and d) expected signs of  $\Delta\delta^{SR}$ .

| Rotation around<br>C $\alpha$ -CO bond |    | Rotation around<br>C $\alpha$ -Ph bond | Conformer  | Character          |
|--|----|--|------------|--------------------|
|  |    | Fenil coplanar to                      |            |                    |
|  |    | C $\alpha$ -OMe                        | <b>sp1</b> | <b>shielding</b>   |
| CF <sub>3</sub> syn to CO              | sp | C $\alpha$ -CO                         | sp2        |                    |
|  |    | C $\alpha$ -CF <sub>3</sub>            | sp3        |                    |
|  |    | C $\alpha$ -OMe                        | <b>ap1</b> | <b>deshielding</b> |
| CF <sub>3</sub> anti to CO             | ap | C $\alpha$ -CO                         | ap2        |                    |
|  |    | C $\alpha$ -CF <sub>3</sub>            | <b>ap3</b> | <b>shielding</b>   |

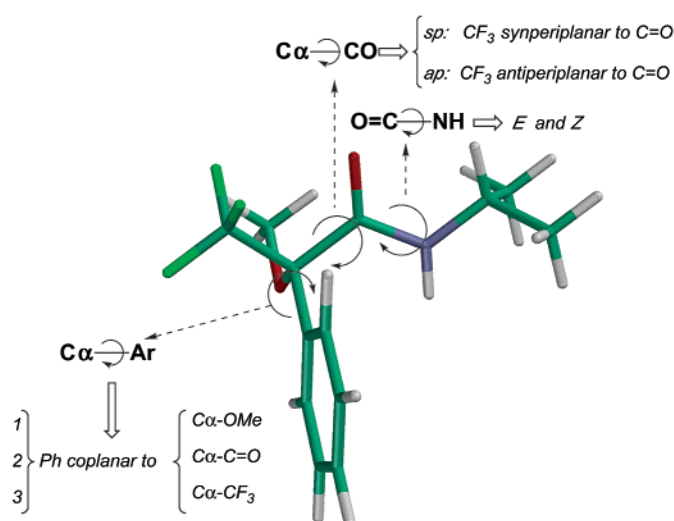


**Figure 101.** Generation of Z-conformers in MTPA amides and the most significant characteristics of each one.

The combination of these three orientations of the phenyl group with the two sp and ap conformers generates six possible situations (as in the case of esters).<sup>27</sup> These six possibilities can be reduced to just three (sp1, ap3, and ap1; see Figure 101)—as in MTPA esters<sup>27</sup>—on the basis of theoretical calculations (MM and AM1). The most stable conformer is sp1, with the other two conformers (ap3 and ap1) being energetically less stable (see Figure 102).

In the sp1 conformer, the CF<sub>3</sub> group is synperiplanar to the carbonyl and the phenyl ring is coplanar with the C $\alpha$ -OMe bond. Overall, this arrangement leads to selective shielding on one of the substituents (L<sub>1</sub>/L<sub>2</sub>) of the amine (see Figure 102a). In the other two conformers (ap1 and ap3), the CF<sub>3</sub> is anti-periplanar to the carbonyl group. However, in conformer ap1, the phenyl ring is coplanar with the C $\alpha$ -OMe bond, causing deshielding on one substituent of the amine (see Figure 102b), whereas in conformer ap3, the phenyl ring is coplanar to the C $\alpha$ -CF<sub>3</sub> bond, which produces shielding (see Figure 102c).

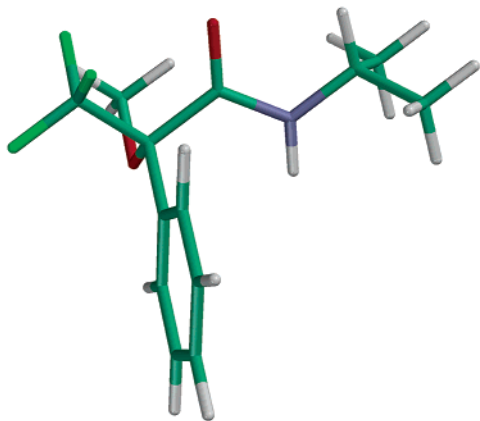
These shielding/deshielding effects were quantitatively demonstrated by calculating the contributions

of the aromatic ring to the chemical shifts (aromatic anisotropy increments) of each conformer.

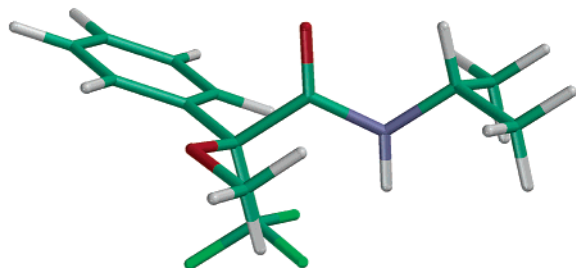
In the conformational equilibrium, each conformer plays a different role (shielding or deshielding) and the overall result is the weighted average among the conformer populations and their shielding/deshielding effects. From the NMR standpoint, the L<sub>1</sub> substituent of an (S)-MTPA amide is shielded in conformer sp1 (see Figure 103a), while substituent L<sub>2</sub> is virtually unaffected because it is deshielded in conformer ap1 and shielded in conformer ap3 (Figure 103a). The magnitude of the shielding/deshielding effects on substituent L<sub>2</sub> depends on the difference in the populations of the two conformers. Similarly, in the (R)-MTPA amide, substituent L<sub>2</sub> is shielded in conformer sp1 and substituent L<sub>1</sub> is almost unaffected (deshielded in conformer ap1 and shielded in conformer ap3) (Figure 103b).

The overall result is that the L<sub>1</sub> substituent is more shielded in the (S)-MTPA than in the (R)-MTPA amide. Conversely, substituent L<sub>2</sub> is more shielded in the (R)-MTPA than in the (S)-MTPA amide. When the differences in the chemical shifts are calculated for an amine with the configuration shown in Figure

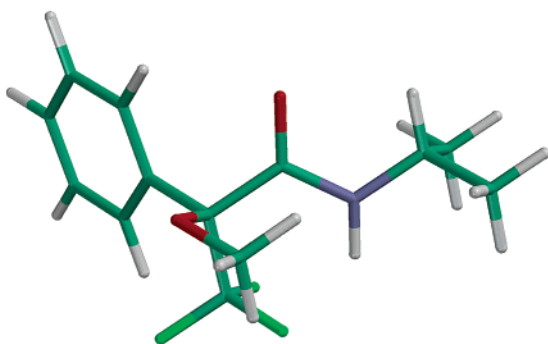
a) sp1 conformer



b) ap1 conformer



c) ap3 conformer

**Figure 102.** Main conformers for the MTPA amides.

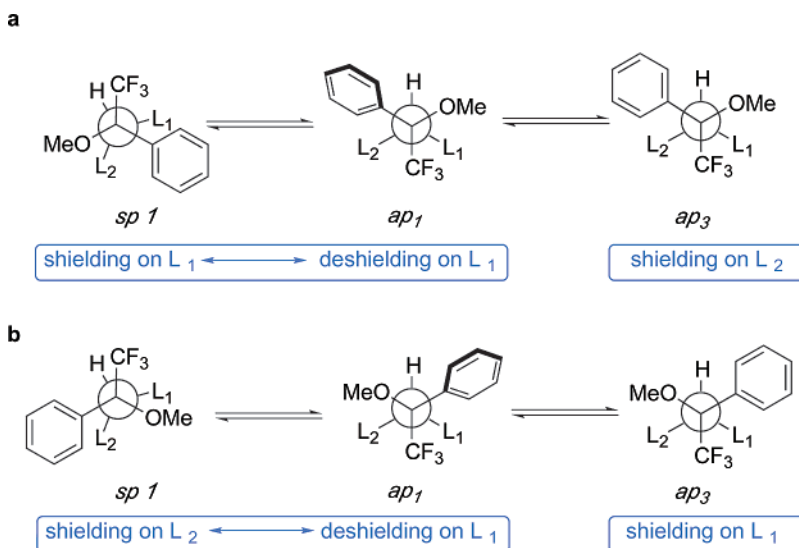
100c,  $\Delta\delta^{SR}$  has a negative value for substituent  $L_1$  and a positive value for substituent  $L_2$ . In the case where the configuration is opposite, so too are the signs for  $\Delta\delta^{SR}$  (see Figure 100d).

Further experimental evidence to support this equilibrium and the structures of the conformers was obtained from the study of the low-temperature  $^1\text{H}$  NMR spectra of the MTPA amides of (+)-bornylamine. The results (Figure 104a) are consistent with the previously discussed predictions and illustrate the effect of the phenyl ring on the substrate in each conformer.

Because of the greater significance of conformer sp1 in comparison to conformers ap1 and ap3, conformer sp1 can effectively be used as a correlation model for the assignment of the configuration of amines from the NMR spectra. This simplified model is shown in Figure 104b and is in full agreement with that originally proposed by Mosher (see Figure 100a). For instance, Me(10') is shielded by the phenyl group in the (*R*)-MTPA amide of (+)-bornylamine and H(6') is shielded in the (*S*)-MTPA amide, causing the  $\Delta\delta^{SR}$  sign to be positive for Me(10') and negative for H(6').

The reliability of this model for the prediction of the configuration was confirmed experimentally by comparing the NMR spectra of the MTPA amides derived from a series of  $\alpha$ -substituted primary amines of known absolute configuration.<sup>74,75</sup> The signs of  $\Delta\delta^{SR}$  are consistent with the model in all the examples studied, and a selection of data is shown in Figure 105.

The MTPA derivatives of alcohols<sup>27</sup> and amines<sup>75</sup> both have a conformational equilibrium that is considerably more complex than that of other reagents such as MPA (MTPA results in three main conformers with close populations instead of two<sup>29</sup>). However, there is a difference between MTPA esters and amides that is of significant practical importance: the major conformer in esters causes deshielding, whereas in amides, it causes shielding, and, therefore, larger  $\Delta\delta^{SR}$  values are obtained for amides than esters. For this reason, the use of MTPA as a CDA for the determination of the configuration of alcohols is frequently hampered by the small changes

**Figure 103.** Low-energy conformations of (a) (*S*)-MTPA and (b) (*R*)-MTPA, as obtained by MM and AM1 calculations.

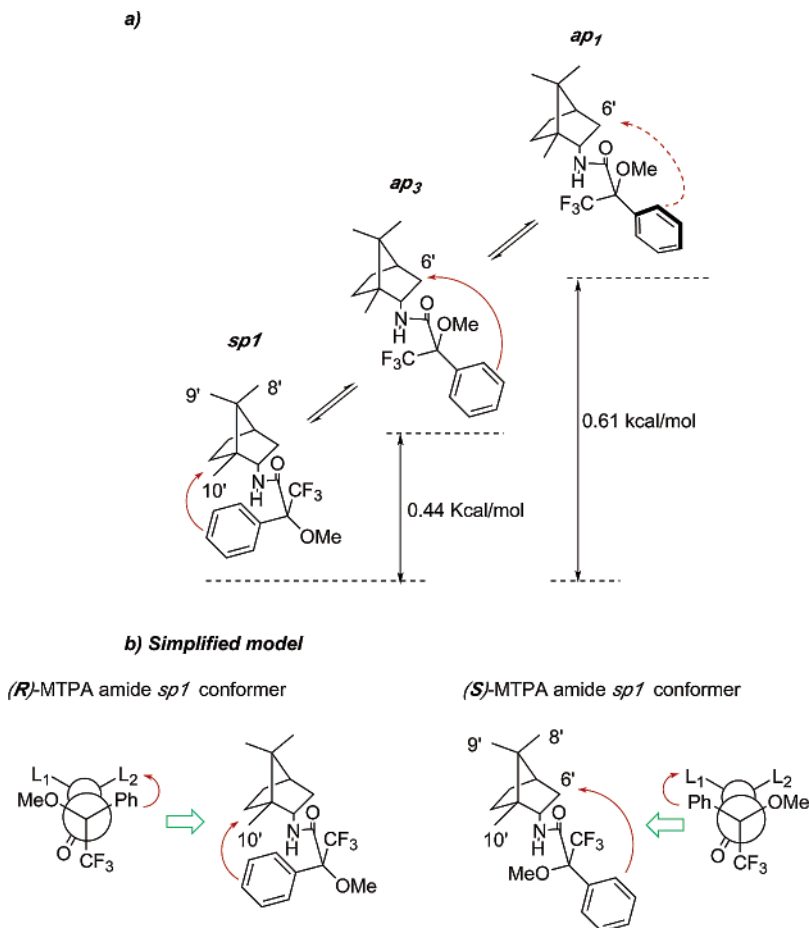


**Figure 104.** (a) Low-energy conformations of the (*R*)-MTPA amide of (+)-bornylamine. Solid arrows show shielding, and dashed arrows show deshielding effects. (b) Simplified models for (*R*)- and (*S*)-MTPA amides.

in shift obtained and the uneven distribution of  $\Delta\delta^{SR}$  signs;<sup>13,27</sup> such problems for MTPA amides have not been reported.

### 3.4.2. MPA

The application of MPA to the determination of the configuration of  $\alpha$ -substituted primary amines is a very recent development.<sup>76,77</sup> At present, there are two methods available for this reagent. The method described in this chapter involves the use of the two enantiomers of MPA,<sup>76a</sup> whereas only one enantiomer is necessary in the procedure described in section 4.2 of this review.<sup>77</sup>

The method consists of the derivatization of the amine with the two enantiomers of MPA, acquisition of the <sup>1</sup>H NMR spectra of the corresponding (*R*)- and (*S*)-MPA amides (preferably in a nonpolar solvent<sup>76a</sup>), and analysis of the  $\Delta\delta^{RS}$  parameters.

The  $\Delta\delta^{RS}$  signs for substituents  $L_1/L_2$  are correlated to the absolute configuration of the amine through out a nonempirical model, which has been established from a detailed study of aromatic shielding effects and structural calculations<sup>76a</sup> (molecular mechanics (MM), semiempirical (AM1, PM3) and ab initio), as well as by NMR experiments<sup>76a</sup> (low-temperature and dynamic NMR).

The conformational analysis shows that the main conformational processes involve rotations around the CO–NH and C $\alpha$ –CO bonds (see Figure 106). Two

Z and E rotamers result from rotation around the CO–NH bond, with the Z arrangement being the predominant one. The C $\alpha$ –CO rotation generates the two usual conformers for this type of system: sp (OMe and carbonyl in a syn-periplanar disposition) and ap (OMe and carbonyl in an anti-periplanar disposition) (Figure 106). In both the sp and ap forms, the OMe is anti, with respect to the C $\alpha$ –Ar bond, and the phenyl group is coplanar to the C $\alpha$ –H bond.

Theoretical calculations showed that the ap conformer has a lower energy than the sp conformer (this is opposite to the case for MPA esters, where sp is the most stable conformer). The evolution of the NMR spectra of the MPA amide of (+)-bornylamine at different temperatures confirmed these conformational characteristics.

The results of all these studies indicate that, in solution, the MPA amides exist in a conformational equilibrium composed of two main conformers: ap-Z (MeO and carbonyl, anti-periplanar) and sp-Z (MeO and carbonyl, syn-periplanar; carbonyl and C(1')H bond, syn-periplanar). In both cases, the methoxy group, the carbonyl group, the N–H bond, and the C $\alpha$ –H bond are in the same plane and the phenyl ring is almost coplanar to the C $\alpha$ –H bond (Figure 106).

Accordingly, in (*R*)-MPA amides, the  $L_2$  substituent is shielded by the phenyl ring in the ap conformer whereas substituent  $L_1$  is shielded in the sp con-

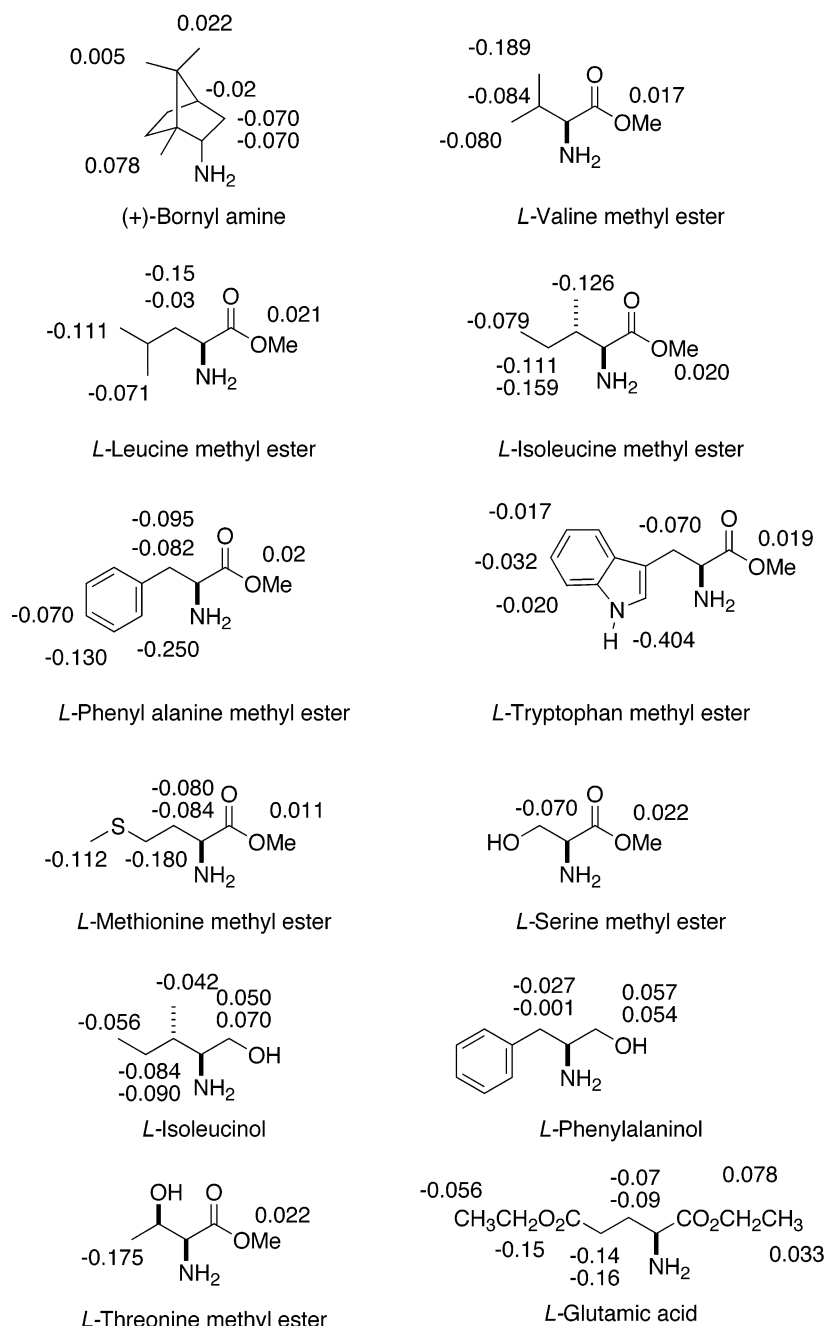


**Figure 105.**  $\Delta\delta^{SR}$  values (ppm,  $\text{CDCl}_3$ ) of the (*R*)- and (*S*)-MTPA amides of a selection of amines of known configuration.

former (Figure 107a). In the (*S*)-MPA amides, however, substituent  $L_1$  is shielded in the ap conformer and substituent  $L_2$  is shielded in the sp conformer (see Figure 107b). Given that the ap conformer is more populated than the sp conformer, the  $L_2$  substituent is more shielded in the (*R*)-MPA than in the (*S*)-MPA amides and, conversely, substituent  $L_1$  is more shielded in the (*S*)-MPA than in the (*R*)-MPA amides. Comparison of the spectra of the two derivatives of an amine with the configuration shown in Figure 107c shows that the  $\Delta\delta^{RS}$  value is positive for substituent  $L_1$  and negative for substituent  $L_2$  (with opposite signs for the enantiomeric amine) (see Figure 107d). In practice, this method effectively considers the ap conformer as a simplified model for the assignment of configuration of the amine by correlation of the  $\Delta\delta^{RS}$  signs with the configuration.

The reliability of the assignment obtained from the model shown in Figure 107c and d has been demonstrated experimentally with a series of amines of known absolute configuration (see Figure 108); in all cases, the signs of the  $\Delta\delta^{RS}$  values are consistent with the predictions.

**3.4.2.1. MPA versus MTPA.** When determining the configuration of a substrate, it is important to select the most suitable CDA available. In the case of amines, note that there are no significant differences in the magnitude of  $\Delta\delta$  obtained for MPA ( $\Delta\delta^{RS}$ ) and MTPA ( $\Delta\delta^{SR}$ ) amides, indicating that neither of these reagents has a clear advantage over the other<sup>75</sup> (see Figure 108). This situation may seem surprising initially, because the population of the predominant conformer in MTPA amides is smaller than that in MPA amides. However, in the former

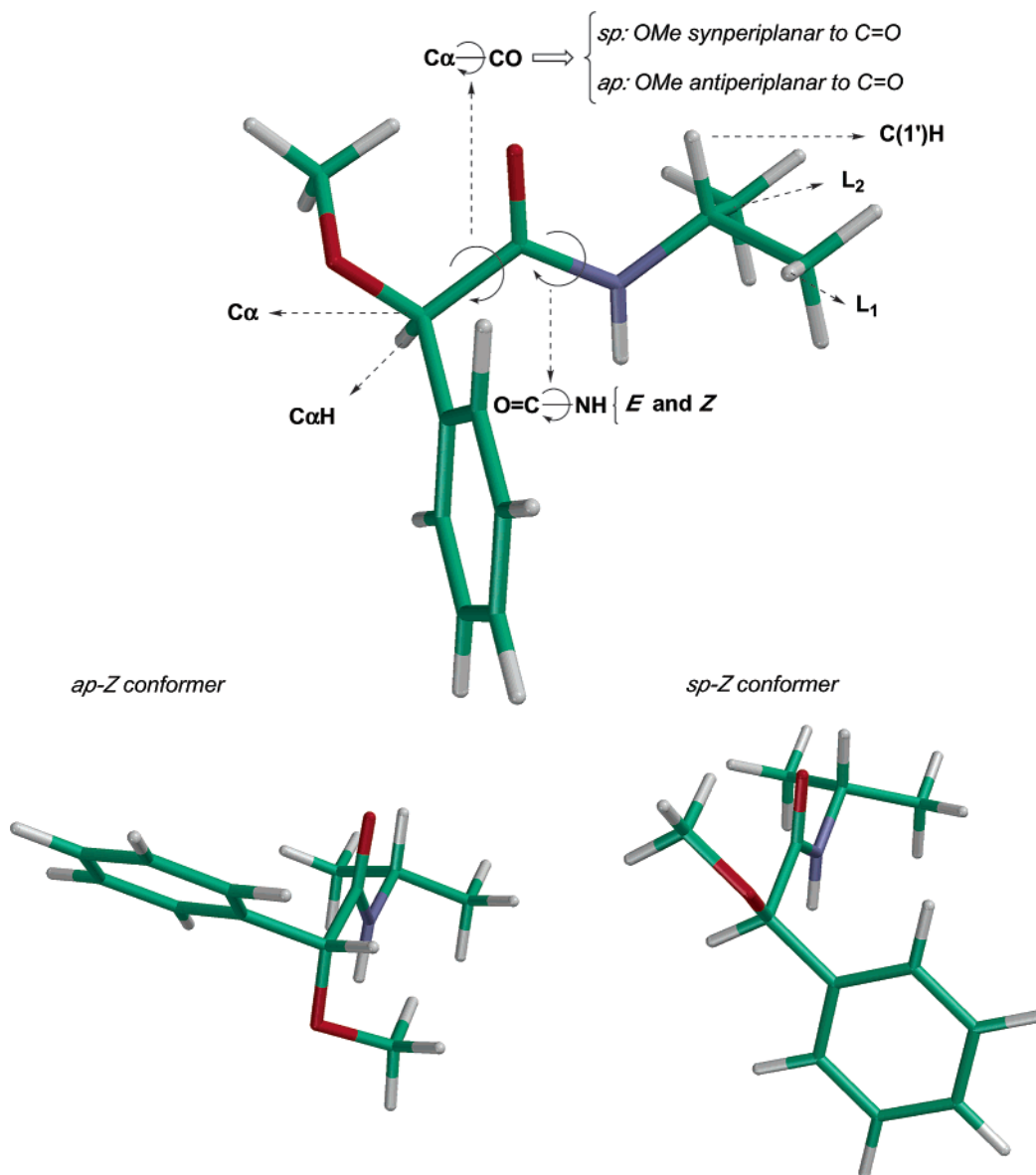


**Figure 106.** Generation and main conformers of MPA amides.

case, the phenyl ring is better orientated for shielding than in MPA amides and the combination of the two factors leads to similar shift changes.

**3.4.2.2. The Effect of the Polarity of the Solvent on the NMR of MPA Amides.** MM calculations on MPA amides revealed that the dipolar moment of the predominant ap-Z conformer is smaller than that of the sp-Z conformer.<sup>76a</sup> Thus, the population of ap-Z (and, therefore, the  $\Delta\delta^{RS}$  values) should increase if the polarity of the NMR solvent is reduced.

This proposal has been experimentally proven<sup>76a</sup> by acquiring NMR spectra in several solvents, which all showed the expected trend for  $\Delta\delta^{RS}$  values:  $\Delta\delta^{RS}_{CS_2} > \Delta\delta^{RS}_{CDCl_3} > \Delta\delta^{RS}_{(CD_3)_2CO}$  (see Figure 109). Therefore, one way to increase the efficacy of MPA as a CDA for amines (larger  $\Delta\delta^{RS}$  values) involves recording the spectra of the corresponding amides in nonpolar solvents such as  $CS_2$ .

A similar improvement in the  $\Delta\delta^{RS}$  data for MPA esters was obtained by reducing the temperature of the NMR probe. This technique was described in Section 3.1.2.8.

### 3.4.3. AMAAs

Other than MPA and MTPA, other arylmethoxyacetic acids with different aryl rings (9-AMA and 1-NMA) have been explored as CDAs for amines.<sup>76a</sup> The predominant conformer in the amides derived from both reagents was ap-Z (as in MPA amides). Despite the presence of an anthryl or naphthyl ring in these reagents, NMR experiments show that the  $\Delta\delta^{RS}$  values obtained for 9-AMA and 1-NMA amides are no higher than those obtained with MPA or MTPA. This is probably due to a lower population of the shielding conformer or to an unfavorable orientation of the aryl ring. In either case, the practical result is small  $\Delta\delta^{RS}$  values; therefore, the use of 9-AMA and 1-NMA as CDAs for amines does not provide any advantages over MTPA or MPA.

### 3.4.4. Boc-phenylglycine (BPG)

The use of Boc-phenylglycine (BPG; see Figure 110) as an auxiliary reagent<sup>78</sup> fills a gap that neither MTPA, MPA, nor the other AMAA reagents were able

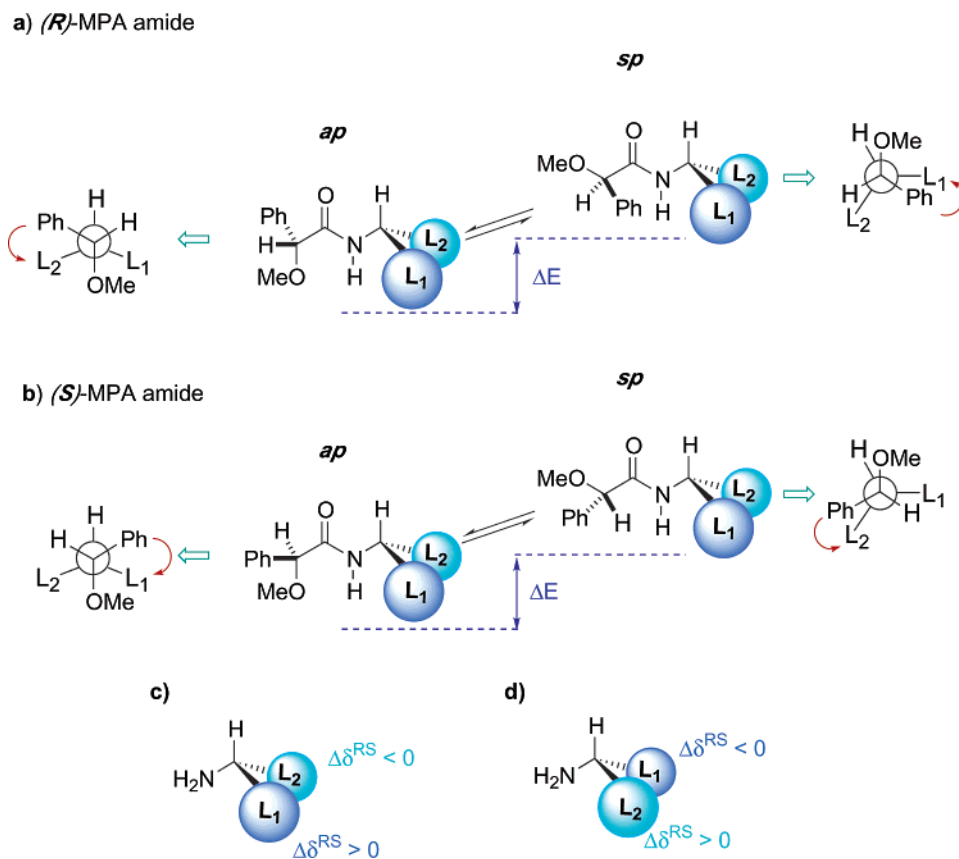


**Figure 107.** (a, b) Conformational equilibrium for MPA amides. (c, d) Prediction of  $\Delta\delta^{RS}$  signs.

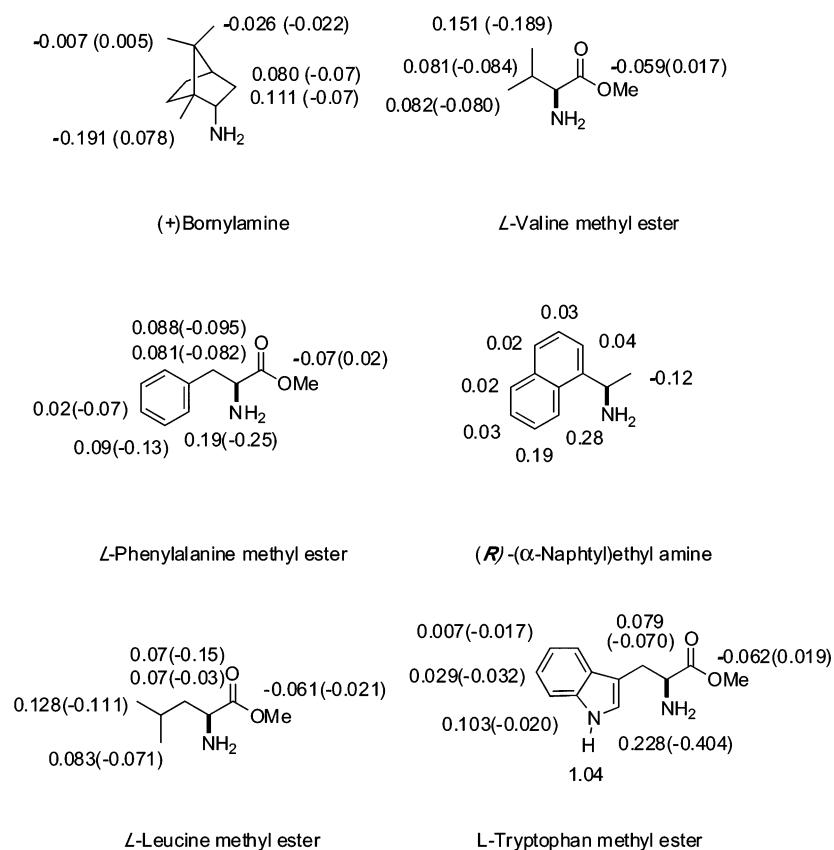


**Figure 108.** Selected  $\Delta\delta^{RS}$  values (ppm) obtained from the  $^1\text{H}$  NMR spectra of (*R*)- and (*S*)-MPA amides (in  $\text{CDCl}_3$ ) of the illustrated amines. For the sake of comparison,  $\Delta\delta^{SR}$  values obtained with MTPA are shown in parentheses.

to cover due to the small magnitude of the differences between the chemical shifts ( $\Delta\delta^{RS}$  or  $\Delta\delta^{SR}$ ) they generate.

The procedure consists of the derivatization of the amine of unknown configuration with the two enantiomers of BPG, recording of the  $^1\text{H}$  NMR spectra of

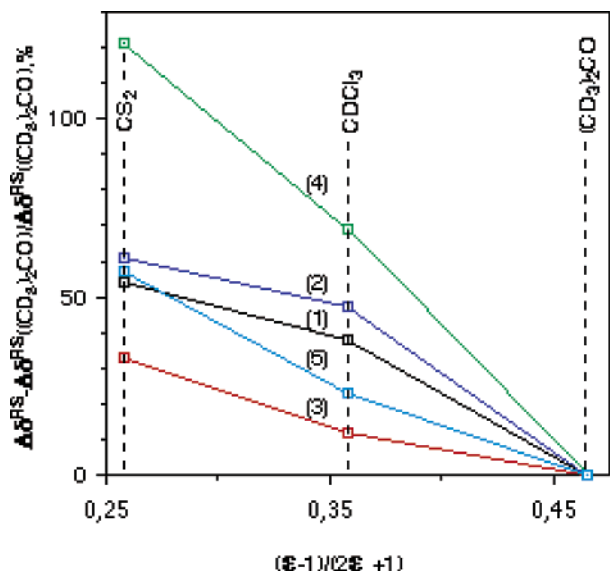


**Figure 109.** Plots showing the dependence of  $\Delta\delta^{RS}$  (expressed as a percentage of  $\Delta\delta^{RS}$  in  $(\text{CD}_3)_2\text{CO}$ ) versus the polarity of the solvent (as  $(\epsilon - 1)/(2\epsilon + 1)$ , where  $\epsilon$  is the dielectric constant): Line 1, Me(10') of (+)-bornylamine; Lines 2 and 3, H(3') and H(4') of L-valine methyl ester, respectively; and Lines 4 and 5, H(2') and H(7') of L-tryptophan methyl ester, respectively.

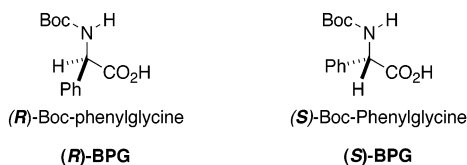


**Figure 110.** Structures of (*R*)- and (*S*)-BPG.

the corresponding diastereoisomeric BPG amides and measuring the differences in the chemical shifts ( $\Delta\delta^{RS}$ ) of substituents  $L_1/L_2$ . The signs of  $\Delta\delta^{RS}$  are then correlated with the absolute configuration by means of a nonempirical model that was established by detailed conformational analysis,<sup>78</sup> including MM and semiempirical (AM1) calculations, and experimentally proven by exhaustive NMR studies.

The main conformational processes involved are shown in Figure 111, and their study led to BPG amides being characterized as follows:

(a) In the amide bond (CO–NH), the *Z* isomer is more stable than the *E* isomer.

(b) Rotation around the  $\omega_1$  ( $\text{C}\alpha$ –CO) bond generates the common *sp* and *ap* conformations ( $\text{C}\alpha$ –H bond and carbonyl group, syn-periplanar and anti-periplanar, respectively).

(c) The phenyl group is coplanar with the  $\text{C}\alpha$ –H bond by rotation around  $\omega_2$  ( $\text{C}\alpha$ –Ph).

(d) The  $\text{C}\alpha$ –H, N–H, and C=O bonds have a tendency to remain coplanar, the  $\text{C}\alpha$ –H and N–H bonds ( $\omega_3$ ) have a tendency to remain in an anti disposition, and the N–H bond have a tendency to be in an anti disposition, with respect to the C=O bond ( $\omega_4$ ).

Both the theoretical calculations and the NMR studies revealed that the most important conformational process is the equilibrium between the *ap* and *sp* conformers, with the former being the most stable (see Figure 112).

In this way, substituent  $L_1$  is shielded by the phenyl group in the *ap* conformer and substituent  $L_2$  is shielded in the *sp* conformer in the case of (*R*)-BPG amides (see Figure 113a). Conversely, substituent  $L_2$  is shielded in the *ap* conformer and substituent  $L_1$  is shielded in the *sp* conformer in (*S*)-BPG amides (see Figure 113b). Because the *ap* population is larger than the *sp* population,  $L_1$  is the most shielded substituent in (*R*)-BPG amides and  $L_2$  is the most shielded substituent in (*S*)-BPG amides.

Thus, when the differences in chemical shifts are measured ( $\Delta\delta^{RS}$ ), a negative value is obtained for substituent  $L_1$  and a positive value is obtained for substituent  $L_2$  if the amine has the configuration shown in Figure 113c. Opposite signs are clearly obtained if the configuration of the amine is opposite (see Figure 113d).

This prediction has been experimentally proven in a series of amines of known absolute configuration and with a variety of structures (see Figure 114).

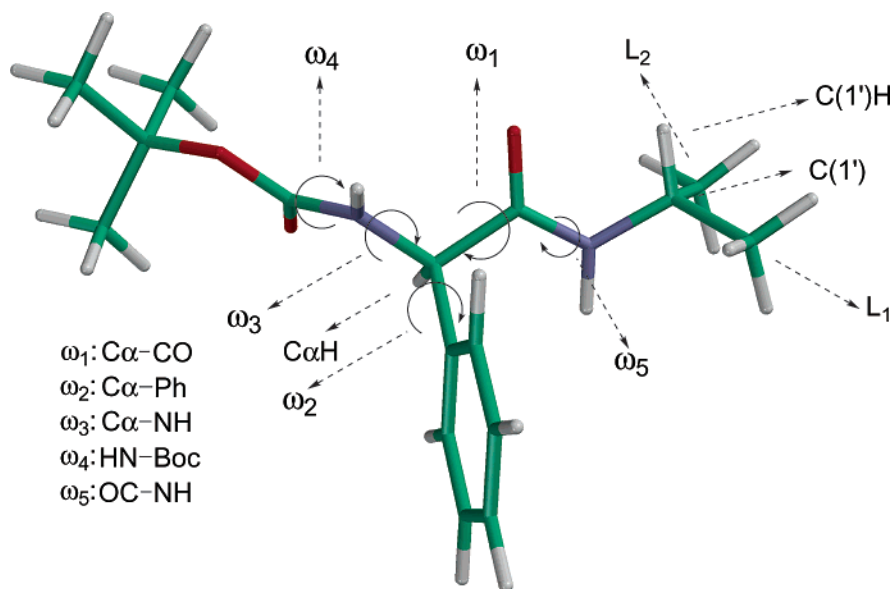


**Figure 111.** Generation of conformers of BPG amides.



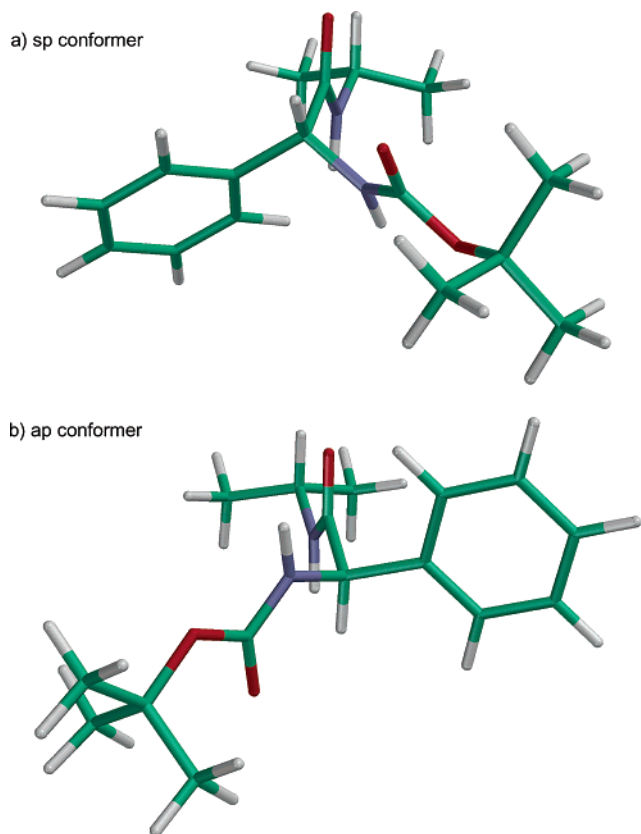


**Figure 112.** Main conformers of BPG amides: (a) *sp* conformer and (b) *ap* conformer.

The *ap* conformer is the major component in the mixture and, therefore, is the most significant, from the NMR standpoint. As such, it can be used as a simplified model to correlate the  $\Delta\delta^{RS}$  signs with the absolute configuration of the amines. This simplified model is shown in Figure 115 and can be used to place substituents  $L_1$  and  $L_2$  on the amine by simply considering the relevant  $\Delta\delta^{RS}$  signs.

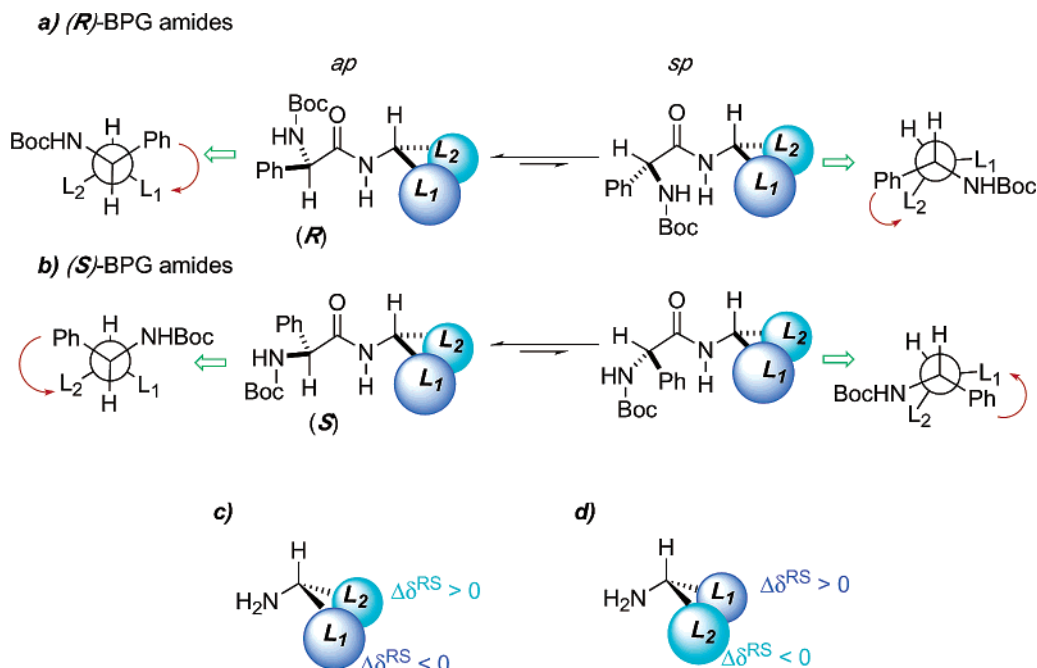


**Figure 113.** Conformational equilibrium in BPG amides.

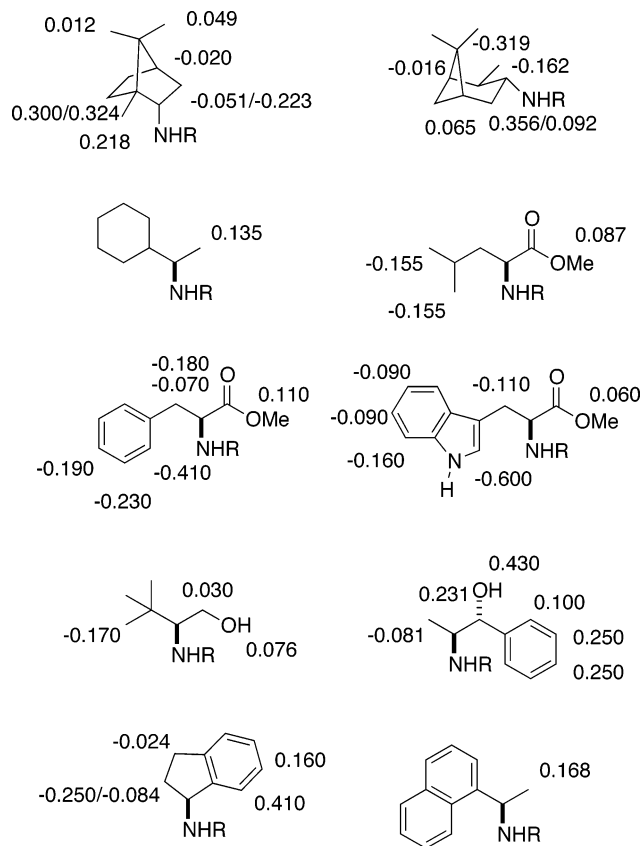


**Figure 114.** Selected  $\Delta\delta^{RS}$  values for (*R*)- and (*S*)-BPG amides.

For the sake of comparison, Figure 116 shows the  $\Delta\delta$  values observed in a selection of BPG ( $\Delta\delta^{RS}$ ), MPA ( $\Delta\delta^{RS}$ ), and MTPA ( $\Delta\delta^{SR}$ ) amides derived from amines of known configuration. The data show beyond doubt that BPG produces the largest values and, hence, the most-accurate assignments.

The reason for the advantage that is inherent in BPG systems, in comparison to the other reagents,

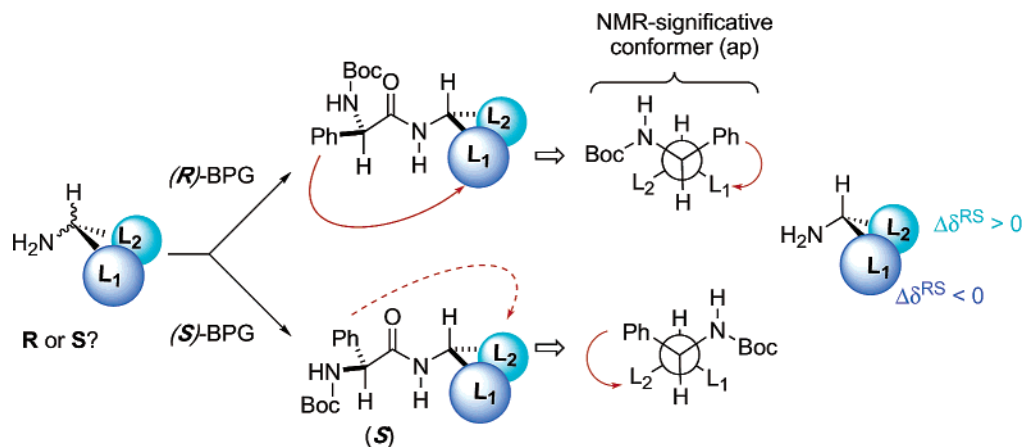


**Figure 115.** Simplified model for the assignment of the configuration of BPG amides.

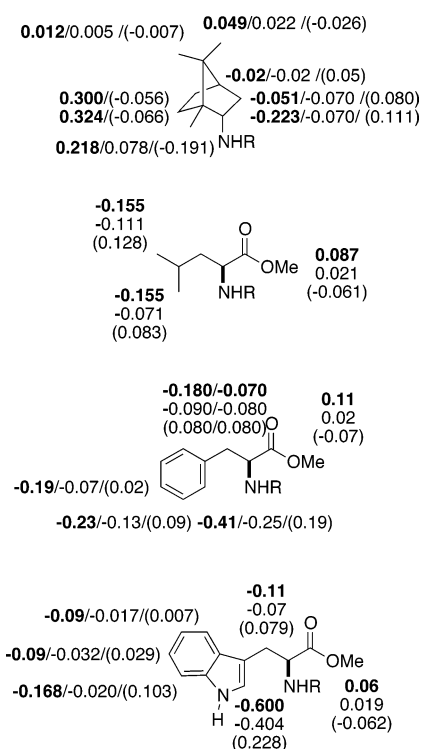


**Figure 116.** Comparison of the  $\Delta\delta$  values of BPG ( $\Delta\delta^{RS}$ ), MTPA ( $\Delta\delta^{SR}$ ), and MPA amides ( $\Delta\delta^{RS}$ ). Data for BPG given in boldface type, data for MTPA given in normal typeface, and data for MPA given in parentheses.

lies in the coexistence of two factors that only work together in BPG amides: (a) the excellent position of the phenyl group to transmit its shielding effect to substituents  $L_1/L_2$  of the amine in the most stable conformer (ap; see Figure 117a) and (b) a conformational equilibrium of just two conformers (sp/ap). The good orientation of the phenyl ring is also present in MTPA amides<sup>75</sup> (Figure 117c); however, its effect is reduced by a three-conformer composition. In MPA amides, the equilibrium is simple<sup>76</sup> but the orientation of the phenyl is not as good as that observed in the other two cases (see Figure 117b).

In conclusion, BPG has structural and conformational features that make it the reagent of choice for the assignment of the absolute configuration of primary amines. It is commercially available in its

two enantiomerically pure forms, and, in addition, it is cheaper than any of the alternative reagents.

### 3.4.5. Other Reagents

In addition to the reagents already described in this section, several other CDAs have been used with amines, and these compounds are discussed in this section.

Several methods and reagents are specifically not covered, because they have already been discussed in other sections (i.e., Helmchen's reagent<sup>44,45</sup> (PBA) and diazacyclophosphamides<sup>54</sup> are used for both alcohols and amines) or have been extensively described in other review articles<sup>4a</sup> (e.g., 2-[1-(9-anthryl)-2,2,2-trifluoroethoxy]acetic acid<sup>79</sup> (ATEA) and  $\alpha$ -methyl- $\alpha$ -methoxy-pentafluorophenylacetic acid<sup>80</sup> (MMPA)) for which no new relevant contributions have appeared since their last publication.

**3.4.5.1. 1-Fluoro-2,4-dinitrophenyl-5(*R,S*)-phenylethylamine [(*R,S*)-FDPEA].** This is the same reagent that is used in the difluoronitrobenzene method for the determination of the absolute configuration of secondary alcohols.<sup>52</sup> In its application to amines,<sup>81</sup> (*R*)- and (*S*)-FDPEA (Figure 118) are reacted with the amine of unknown configuration to give the corresponding diastereomers. On the basis of UV and NMR studies, a predominant conformation has been proposed that has the  $\alpha$ -protons of the amine and phenylethylamine moieties, as well as the phenyl H<sub>6</sub>, located in the same plane (see Figure 119a). In accordance with this model, in the (*R*)-FDPEA derivative, substituent  $L_2$  is shielded by the phenyl group of the phenylethylamine while  $L_1$  remains unshielded. On the other hand, in the (*S*)-FDPEA derivative, substituent  $L_1$  is shielded whereas  $L_2$  is not (Figure 119a). When the differences in the chemical shifts ( $\Delta\delta^{RS}$ ) are calculated for an amine with the configuration shown in Figure 119b, substituent  $L_2$  should show a negative  $\Delta\delta^{RS}$  value and substituent  $L_1$  should show a positive  $\Delta\delta^{RS}$  value.

Table 11 shows the  $\Delta\delta^{RS}$  values for the three FDPEA amides of known absolute configurations that have been used to validate the previously described predictions. However, despite the fact that the signs are as expected and the  $\Delta\delta^{SR}$  values are larger than those obtained with MTPA (included in Table 11 for comparison), the number of test com-

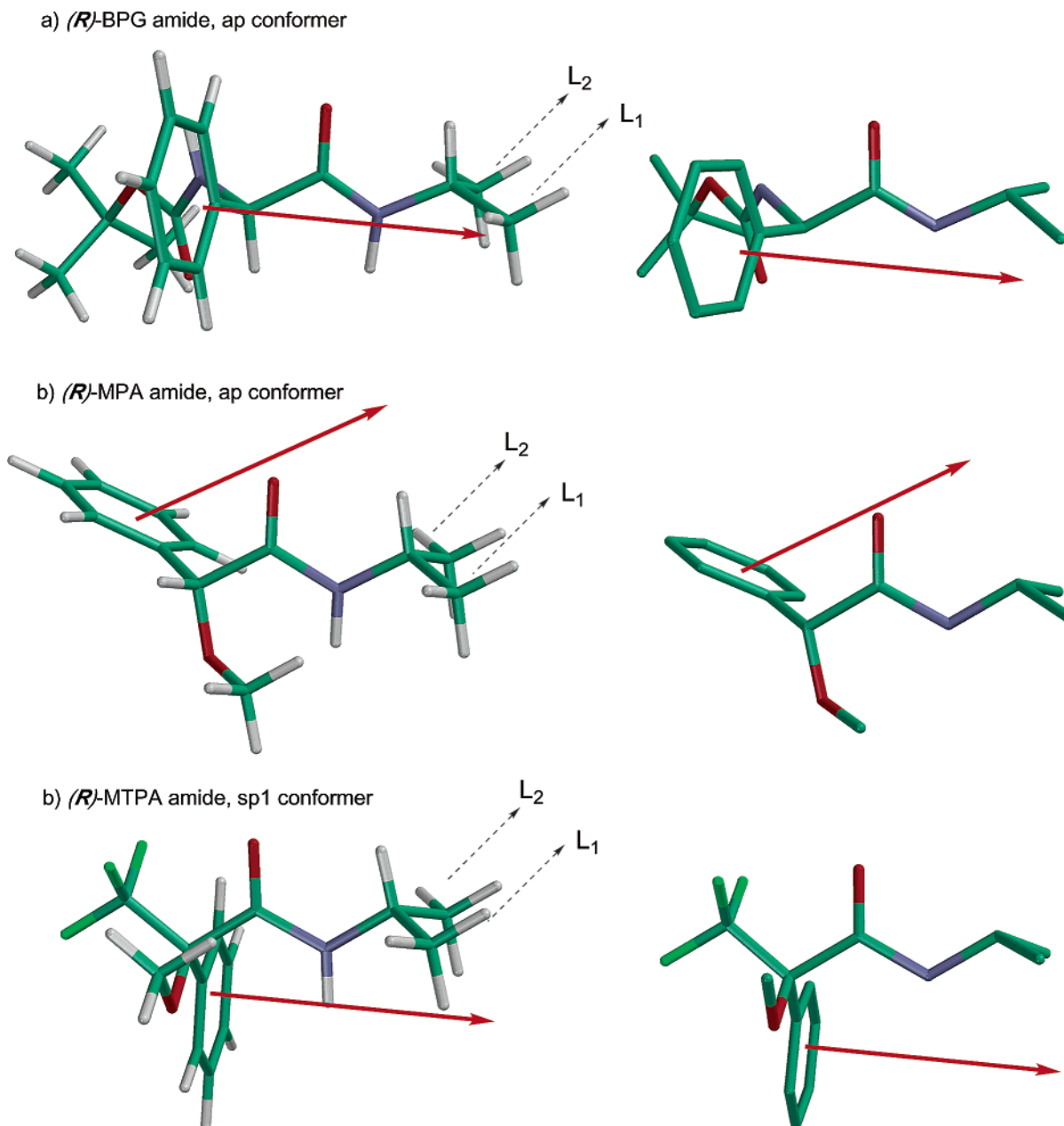


**Figure 117.** Main orientation of the phenyl ring and direction of maximum shielding in (a) BPG, (b) MPA, and (c) MTPA amides.

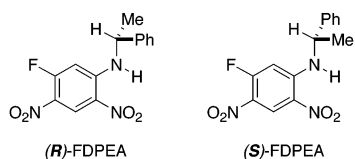


**Figure 118.** Structure of (*R*)- and (*S*)-FDPEA.

pounds is too small to recommend the method for application to amines in general.

Despite this limitation, the method has been used to determine the configuration of microginin (Figure 120), which is a natural product from cyanobacteria.<sup>81</sup>

**3.4.5.2. (*R*)-*O*-Aryllactic Acid (ROAL).** As discussed previously, many *O*-aryllactic acids have been used as derivatizing agents for the determination of the enantiomeric purity<sup>3a,60d</sup> of alcohols and amines by <sup>19</sup>F NMR, for the assignment of the absolute configuration of amines<sup>82</sup> and as solvating agents<sup>83</sup> in the determination of the enantiomeric purity of

amines. The *O*-aryllactic acids (ROAL) shown in Figure 121 have been proposed for the determination of the absolute configuration of  $\alpha$ -substituted primary amines, on the basis of theoretical and experimental studies.<sup>82</sup>

MM and semiempirical calculations, together with NMR data, suggest that the amides derived from the ROAL preferentially exist in the ap-Z conformation in solution. In this conformation, the aryl and carbonyl groups are anti-periplanar (Figure 122), as in MPA amides, but are different from the main conformation of their esters with secondary alcohols, where the C $\alpha$ -H and C=O bonds are syn.

According to this conformational model, the ROAL amide derived from an amine with the configuration shown in Figure 122a has substituent L<sub>1</sub> shielded while substituent L<sub>2</sub> is not. Conversely, if the amine had the configuration shown in Figure 122b, then the shielded group would be substituent L<sub>2</sub>.

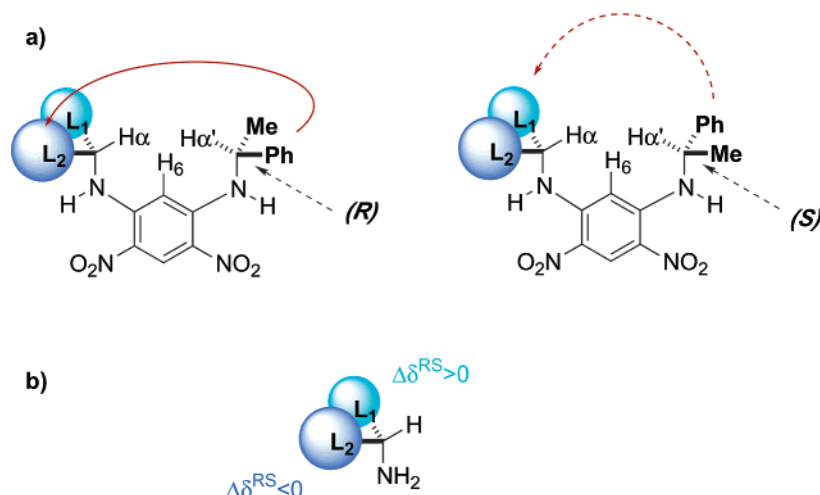


**Figure 119.** Model used to correlate the configuration with the  $^1\text{H}$  NMR shifts and  $\Delta\delta^{RS}$  signs.

**Table 11. Comparison of  $\Delta\delta$  Values between FDPEA and MTPA Amides**

| position                  | L-isoleucinol |         | L-phenylalaninol |         | D-phenylalaninol,<br>FDPEA |
|---------------------------|---------------|---------|------------------|---------|----------------------------|
|                           | FDPEA         | MTPA    | FDPEA            | MTPA    |                            |
| $\alpha$ -CH              | 0.0045        | -0.0420 | -0.0725          | 0.0400  | 0.0240                     |
| $\beta$ -CH               | 0.3120        | 0.0000  |                  |         |                            |
| $\beta$ -CH <sub>2</sub>  |               |         | 0.2410           | -0.0270 | -0.2880                    |
|                           |               |         | 0.2855           | -0.0010 | -0.3410                    |
| $\beta$ -CH <sub>3</sub>  | 0.2260        | -0.0420 |                  |         |                            |
| $\beta'$ -CH <sub>2</sub> | -0.43750      | 0.0500  | -0.4825          | 0.0570  | 0.4355                     |
|                           | -0.5085       | 0.0700  | -0.5360          | 0.0540  | 0.4880                     |
| $\gamma$ -CH <sub>2</sub> | 0.3910        | -0.0840 |                  |         |                            |
|                           | 0.3095        | -0.0900 |                  |         |                            |
| $\gamma$ -CH <sub>3</sub> | 0.2830        | -0.0560 |                  |         |                            |
| $\gamma$ -NH              | 0.0020        | -0.1420 | -0.0230          | 0.1210  | -0.0695                    |

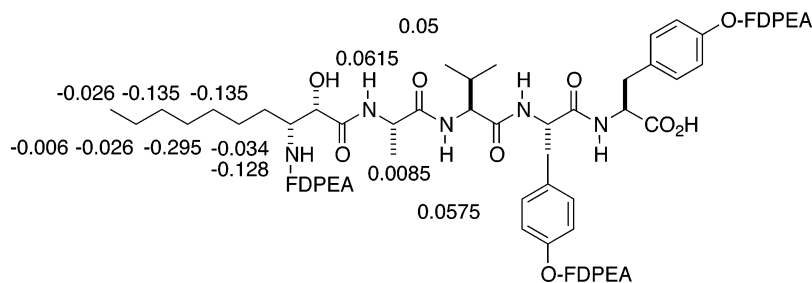


**Figure 120.**  $\Delta\delta^{RS}$  values for microginin-FDPEA.

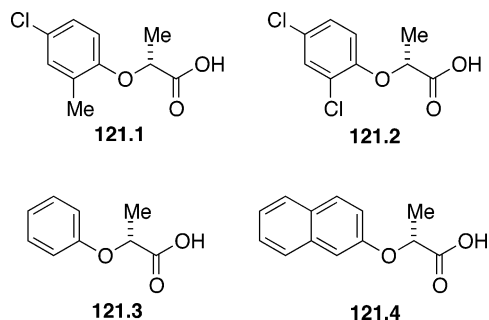


**Figure 121.** Structures of the *O*-aryllactic acids.

Therefore, determination of the configuration of  $\alpha$ -substituted primary amines or  $\alpha$ -amino acids is possible by comparison of the chemical shifts of the relevant substituents.

Experimental validation of the predictions given by this method was provided by the ROAL derivatives of the amines shown in Figure 123. The available  $\Delta\delta^{RS}$  data is presented in Table 12, and some

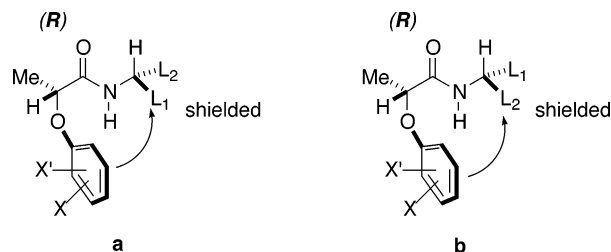


**Figure 122.** Model for the assignment of the configuration of (*R*)-*O*-aryllactic acid amides.

limitations are apparent: Only one acid (**121.1**) was tested with all the amines, whereas the others were tested with just one, two, or three amines.

In most cases, only the  $\Delta\delta$  values for one substituent (either  $L_1$  or  $L_2$ ) are reported. All the *O*-aryllactic acids described have the (*R*)-configuration (i.e., they are prepared from (*S*)-ethyl lactate) and examples of the application of both enantiomers of the reagent to one enantiomer of the amine have not been

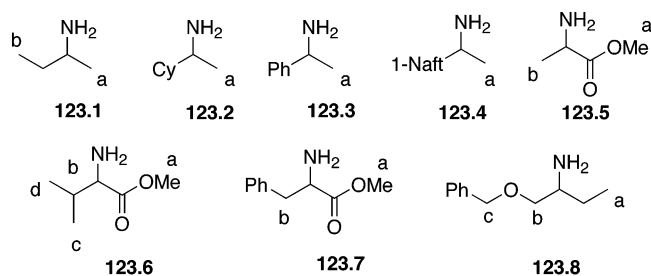


**Figure 123.** Structures of the amines used in this study.

**Table 12. Selected  $\Delta\delta$  Values for (*R*)-*O*-Aryllactic Acid Amides**

| ROAL  | amine | $\Delta\delta^a$ |             |       |      |
|-------|-------|------------------|-------------|-------|------|
|       |       | Ha               | Hb          | Hc    | Hd   |
| 121.1 | 123.1 | 0.09             | -0.15       |       |      |
| 121.3 |       | 0.11             | -0.21       |       |      |
| 121.4 |       | 0.04             | -0.25       |       |      |
| 121.1 | 123.2 | 0.08             |             |       |      |
| 121.1 | 123.3 | 0.08             |             |       |      |
| 121.2 |       | 0.07             |             |       |      |
| 121.3 |       | 0.10             |             |       |      |
| 121.4 |       | 0.11             |             |       |      |
| 121.1 | 123.4 | 0.10             |             |       |      |
| 121.1 | 123.5 | -0.05            | 0.08        |       |      |
| 121.1 | 123.6 | -0.08            | 0.09        | 0.18  | 0.07 |
| 121.3 |       | -0.11            | 0.1         | 0.24  | 0.22 |
| 121.1 | 123.7 | -0.06            | 0.06        |       |      |
| 121.1 | 123.8 | 0.13             | -0.18/-0.07 | -0.25 |      |

<sup>a</sup>  $\Delta\delta^{RS} = \delta^{RR} - \delta^{RS}$ .

performed. Thus, in its present form, this methodology can only be used when the two enantiomers of the chiral amine are available.

**3.4.5.3.  $\alpha$ -Cyano- $\alpha$ -fluoro-*p*-tolylacetic Acid (CFTA).**  $\alpha$ -Cyano- $\alpha$ -fluoro-*p*-tolylacetic acid (CFTA) has been described as a CDA for the determination of the absolute configuration of secondary alcohols<sup>61</sup> (by <sup>1</sup>H NMR) and e.e. calculation (by <sup>19</sup>F NMR). Its use for the determination of the absolute configuration of  $\alpha$ -amino esters by <sup>19</sup>F NMR has also been described<sup>84</sup> and is based on the study of the <sup>19</sup>F NMR spectra of the CFTA amides of a series of (*S*)-amino esters. The spectra of these compounds showed that the fluorine signals of the amides derived from (*R*)-CFTA ((*R,S*)-amides) resonate at higher field by 2–6 ppm, compared to those derived from (*S*)-CFTA ((*S,S*)-amides). Molecular orbital calculations<sup>84</sup> suggest a conformational equilibrium between two conformers: *ap* (the most stable; C $\alpha$ -F bond anti-periplanar to the carbonyl) and *sp* (both groups syn-periplanar) (Figure 124). The calculations also help to explain the shift of the fluorine signal to higher field in the *ap* conformer, with respect to the *sp*. The large difference in *ap/sp* populations between the (*R,S*)- and (*S,S*)-amides also helps to explain the fact that the fluorine signal resonates at higher field in the (*R,S*) compound than in the (*S,S*) compound.

Table 13 shows the NMR data obtained for CFTA and MTPA amides (included for comparative purposes). In all cases, the fluorine chemical shifts ( $\delta$ F) and their differences ( $\Delta\delta$ ) are coherent with the trends discussed, with larger  $\Delta\delta$  values obtained for the CFTA amides.

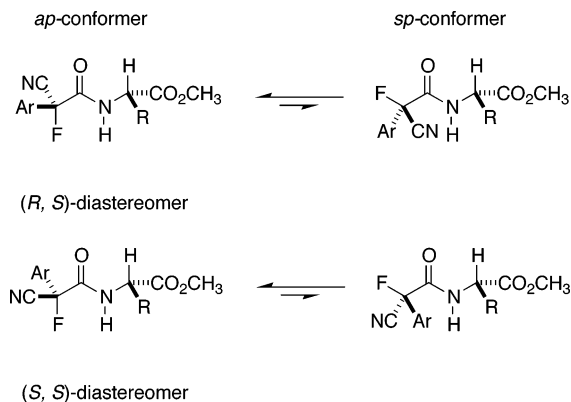


**Figure 124.** Conformational equilibria of CFTA (Ar = Ph) and CFTA (Ar = *p*-tol) amides.

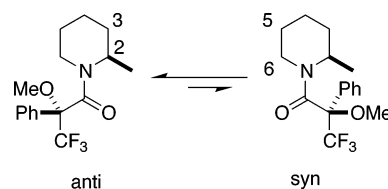
**Table 13.  $\Delta\delta$ F Values for CFTA and MTPA Amides**

| R  | CFTA        |             | MTPA             |                  |
|--|-------------|-------------|------------------|------------------|
|  | $\delta$ RS | $\delta$ SS | $\Delta\delta$ F | $\Delta\delta$ F |
| -Me  | -143.163    | -140.729    | -2.434           | -0.386           |
| -Et  | -143.839    | -140.843    | -2.996           | -0.369           |
| -iPr   | -144.578    | -140.948    | -3.630           | -0.327           |
| -iBu   | -145.578    | -141.676    | -4.074           | -0.171           |
| -iBu   | -143.761    | -140.061    | -3.700           | -0.373           |
| -CH(OBn)CH <sub>3</sub>  | -144.633    | -138.670    | -5.963           | -0.379           |
| -CH <sub>2</sub> CH <sub>2</sub> SCH <sub>3</sub>                                | -145.146    | -141.151    | -3.995           | -0.363           |
| -CH <sub>2</sub> CO <sub>2</sub> CH <sub>3</sub>                                 | -143.763    | -140.842    | -2.921           | -0.407           |
| -CH <sub>2</sub> CO <sub>2</sub> Bn  | -143.344    | -140.824    | -2.520           | -0.325           |
| -CH <sub>2</sub> CH <sub>2</sub> CO <sub>2</sub> Et                              | -144.771    | -140.507    | -4.264           | -0.389           |
| -CH <sub>2</sub> CH <sub>2</sub> CH <sub>2</sub> CH <sub>2</sub> NH <sub>2</sub> | -144.398    | -140.267    | -4.131           | -0.449           |
| -Bn  | -145.004    | -141.424    | -3.580           | -0.033           |
| -(3-Indolylmethyl)   | -144.798    | -140.398    | -4.400           | -0.044           |

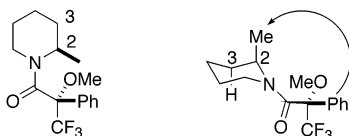
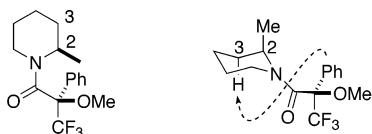
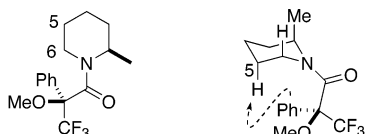
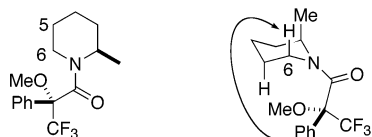
### 3.5. Application to Secondary Amines: MTPA

A procedure for the assignment of the absolute configuration of cyclic secondary amines with asymmetric carbons in the  $\alpha$ - or  $\beta$ -positions has recently been proposed by Hoyer et al.,<sup>85</sup> using MTPA as the CDA. This method is based on the standard comparison of the <sup>1</sup>H NMR spectra of the corresponding (*R*)- and (*S*)-MTPA amides; however, in this case, the foundations of the correlation between NMR shifts and configuration and the analysis of the spectra warrant a more detailed explanation.

In general, the <sup>1</sup>H NMR spectra of these MTPA amides show the presence of two rotamers around the amide bond (syn and anti; see Figure 125) that are in equilibrium. The signals of these rotamers can



**Figure 125.** Conformational equilibrium in the (*R*)-MTPA amide of (*R*)-2-methylpiperidine.

a) (*S*)-MTPA amide, syn conformerb) (*R*)-MTPA amide, syn conformerc) (*S*)-MTPA amide, anti conformerd) (*R*)-MTPA amide, anti conformer

**Figure 126.** (a, b) Syn and (c, d) anti rotamers for the (*S*)- and (*R*)-MTPA amides of (*R*)-2-methylpiperidine.

be identified because the populations of each are different, because of steric effects. The most abundant rotamer has the anti configuration when only one substituent is present.

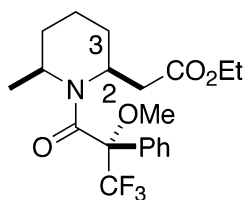
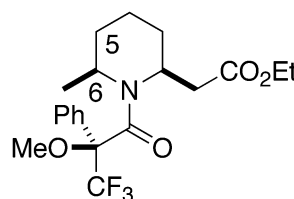
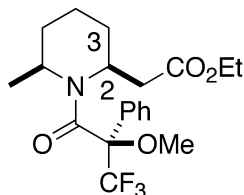
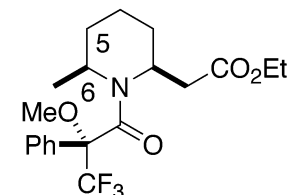
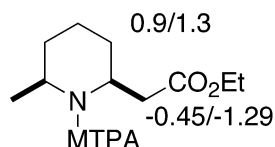
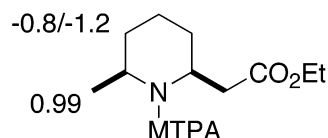
The differentiation between the spectra of the two rotamers is essential because, in this procedure, only the signals of the rotamer with the asymmetric carbon of the MTPA syn to the asymmetric carbon of the amine under examination should be considered.

For instance, in the assignment of the configuration of carbon-2 of (*R*)-2-methylpiperidine (Figure 125), only the signals due to the syn rotamer (Figure 126a,b) in the (*S*)-MTPA and the (*R*)-MTPA amides are relevant and only the  $\Delta\delta^{SR}$  values corresponding to these rotamers are valid for assignment purposes. In contrast, the anti conformers (Figure 126c, d) should not be considered.

The second requirement of this procedure is that only the chemical shifts of *axial* substituents in the aforementioned syn rotamer should be compared to obtain the  $\Delta\delta^{SR}$  value. This is due to the fact that the axial substituents are more exposed to the shielding/deshielding effects of the CDA.

Thus, in (*R*)-2-methylpiperidine, the resonances for the syn rotamer in the spectra of the (*S*)- and (*R*)-MTPA amides should be identified first and the signals due to the axial methyl group at C-2 and the axial proton at C-3 (Figure 126a and b) used to obtain the  $\Delta\delta^{SR}$  value.

In this situation, the axial methyl group is more shielded in the (*S*)-MTPA amide (Figure 126a) than in the (*R*)-MTPA amide (Figure 126b), and the H-3

a) (*S*)-MTPA amide, syn conformerd) (*S*)-MTPA amide, anti conformerb) (*R*)-MTPA amide, syn conformere) (*R*)-MTPA amide, anti conformerc)  $\Delta\delta^{SR}$  valuesf)  $\Delta\delta^{SR}$  values

**Figure 127.** (a, b) Syn and (c, d) anti rotamers for the (*S*)- and (*R*)-MTPA amides of (2*S*,6*S*)-(2-carbomethoxy-6-methyl)-6-methylpiperidine.

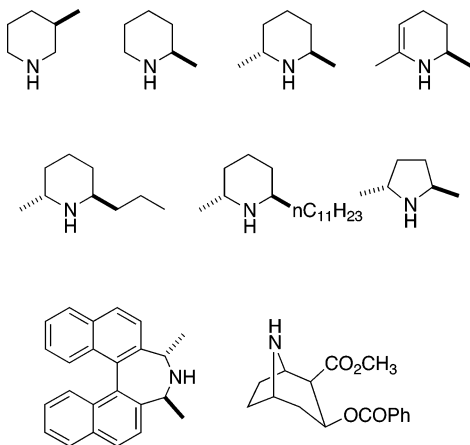


**Figure 128.** Cyclic secondary amines of known configuration examined by NMR of their MTPA amides.

proton is more shielded in the (*R*)-MTPA derivative (Figure 126b) than in the (*S*)-MTPA amide (Figure 126a). The resulting  $\Delta\delta^{SR}$  values are negative for the methyl at C-2 and positive for the proton at C-3. Conversely,  $\Delta\delta^{SR}$  signs will indicate the reverse configuration for the amine.

If the cyclic amine had more than one asymmetric C atom near the N atom, e.g., (2*S*,6*S*)-(2-carbomethoxymethyl)-6-methylpiperidine (Figure 127), the same principles would apply; however, the situation is more complex and the spectra of both the syn and anti rotamers should be considered.

For example, in the assignment of the absolute configuration at C-2, the NMR spectra of the axial groups in the syn conformers of the (*R*)- and (*S*)-MTPA amides should be examined (see Figure 127a, b). For the structure shown, the axial methylene at C-2 results in a negative  $\Delta\delta^{SR}$  value and the axial H atom at C-3 results in a positive  $\Delta\delta^{SR}$  value (see Figure 127c).

The assignment of the configuration at C-6 requires examination of the spectra of the axial groups in the anti rotamers (Figure 127 c,d) and, for the structure shown, the axial substituent at C-6 gives a positive  $\Delta\delta^{SR}$  and the axial hydrogen at C-5 a negative  $\Delta\delta^{SR}$  value (Figure 127f).

The generality of this correlation between the  $\Delta\delta^{SR}$  signs and the absolute stereochemistry has been tested with the cyclic secondary amines of known absolute configuration shown in Figure 128. In all cases, the signs are as expected from the stereochemistry and, therefore, the procedure can be used for the assignment of other amines.

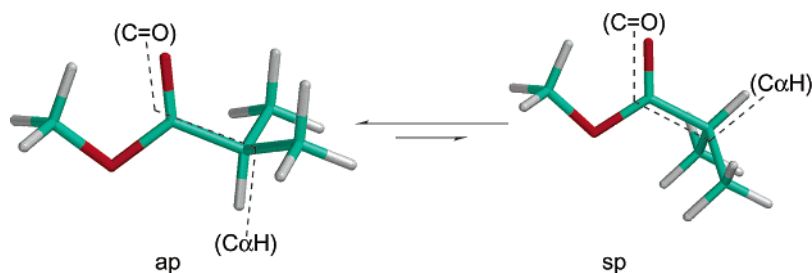
In addition, the absolute values obtained for  $\Delta\delta^{SR}$  are much larger than those observed for the MTPA esters or amides; this condition is probably related to the proximity of the groups under examination to the phenyl group and also to the favorable orientation of the phenyl ring for effective shielding.

### 3.6. Application to $\alpha$ -Chiral Carboxylic Acids

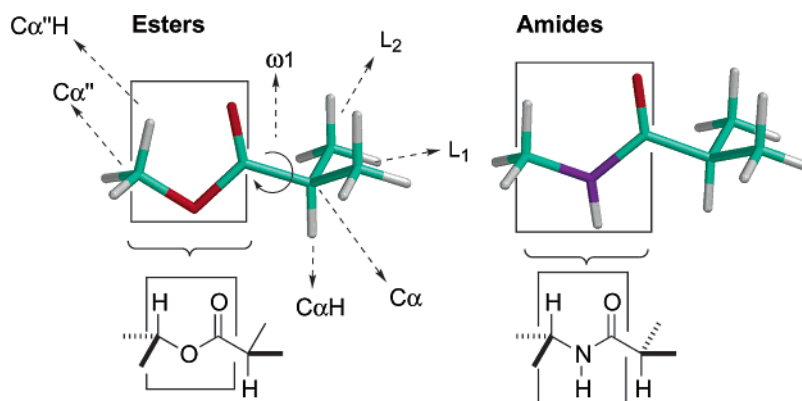
Carboxylic acids are frequently found in nature as optically active compounds with the chiral center at the  $\alpha$ -position, and general approaches for the determination of the absolute stereochemistry of these systems are rare.

An important decision that had to be made in the development of new reagents for this purpose concerned the selection of the type of bond used to link the auxiliary reagent to the substrate carboxylic acid. Several studies were undertaken for the purpose of obtaining suitable reagents, and ester<sup>29,30</sup> and amide<sup>75–78,86</sup> bonds seemed to be the most appropriate candidates.

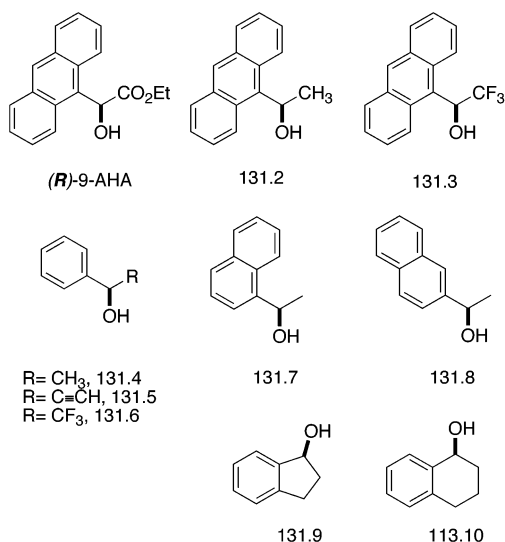
The main issue in relation to the selection of chiral reagents for the assignment of absolute configuration



**Figure 129.** Conformers ap and sp in carboxylic acids.



**Figure 130.** Conformational preference in the ester and amide bonds.

**Figure 131.**

of carboxylic acids is to demonstrate the existence of an NMR significant conformational preference that remains the same in the *R* and *S* derivatives and is independent of the nature of the carboxylic acid.

In accordance with previous experience, alcohols and amines can be considered potentially good candidates to that purpose.

To determine the conformational characteristics of carboxylic acids, molecular mechanics and semi-

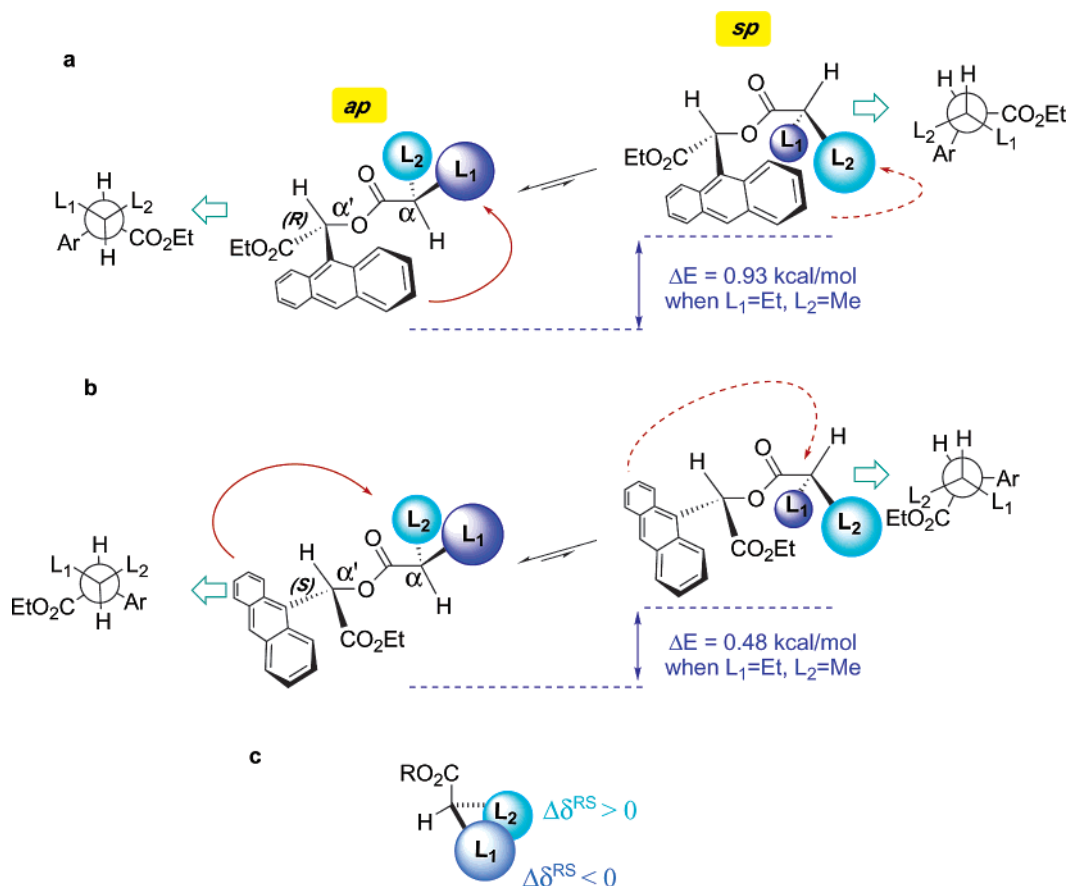
empirical calculations (AM1, PM3) on more than 20 carboxylic acids, and their methyl esters and methylamides, were performed<sup>87</sup> and showed that the main conformational process in all those compounds is the rotation around the  $\omega_1$  bond (Ca–C=O; see Figures 129 and 130). This generates two main conformers: *ap* (C $\alpha$ –H and C=O in anti-periplanar) and *sp* (syn-periplanar) (see Figure 129). In the case of the esters, the *ap* conformer is the more stable conformer; however, this preference is absent in amides.

In addition, it is known<sup>29</sup> that, although, in the esters, the (C=O)–O fragment has a clear preference for a *Z* orientation, the rotation around the (C=O)–NH fragment in amides is more complex<sup>75–78</sup> and ratios between the two main rotamers from 90:10 to 50:50 have been reported<sup>86</sup> (see Figure 130).

From that data, one can conclude that the ester bond is more convenient than the amide bond to link the auxiliary to the substrate, because the last one is conformationally less reliable and, as a consequence, the best auxiliary reagents for carboxylic acids should be found among secondary alcohols and not among amines.

### 3.6.1. Ethyl 2-(9-anthryl)-2-hydroxyacetate (9-AHA) and Related Aryl Alcohols

With that information on hand and using the AMAAs,<sup>29,30</sup> as models, many aryl alcohols have been evaluated as CDAs for  $\alpha$ -chiral carboxylic acids, using

**Figure 132.** Conformational equilibrium in the esters of (*R*)- and (*S*)-9-AHA with (a, b) an  $\alpha$ -chiral carboxylic acid and (c) predicted  $\Delta\delta^{RS}$  signs. Energies calculated by AM1 for (*S*)-2-methylbutiric acid.



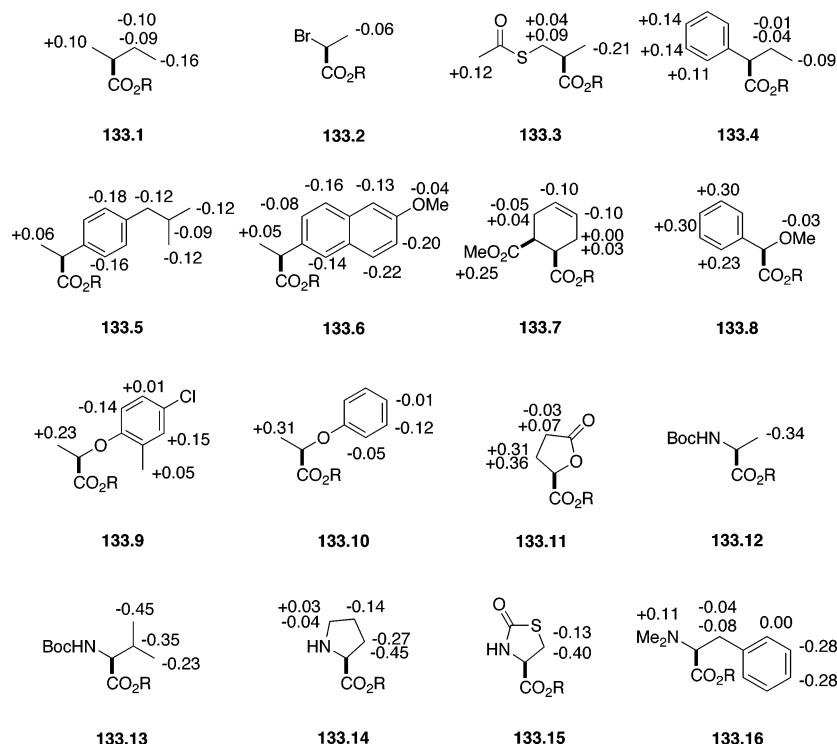


**Figure 133.**  $\Delta\delta^{RS}$  values for the 9-AHA esters of compounds **133.1**–**133.16**.

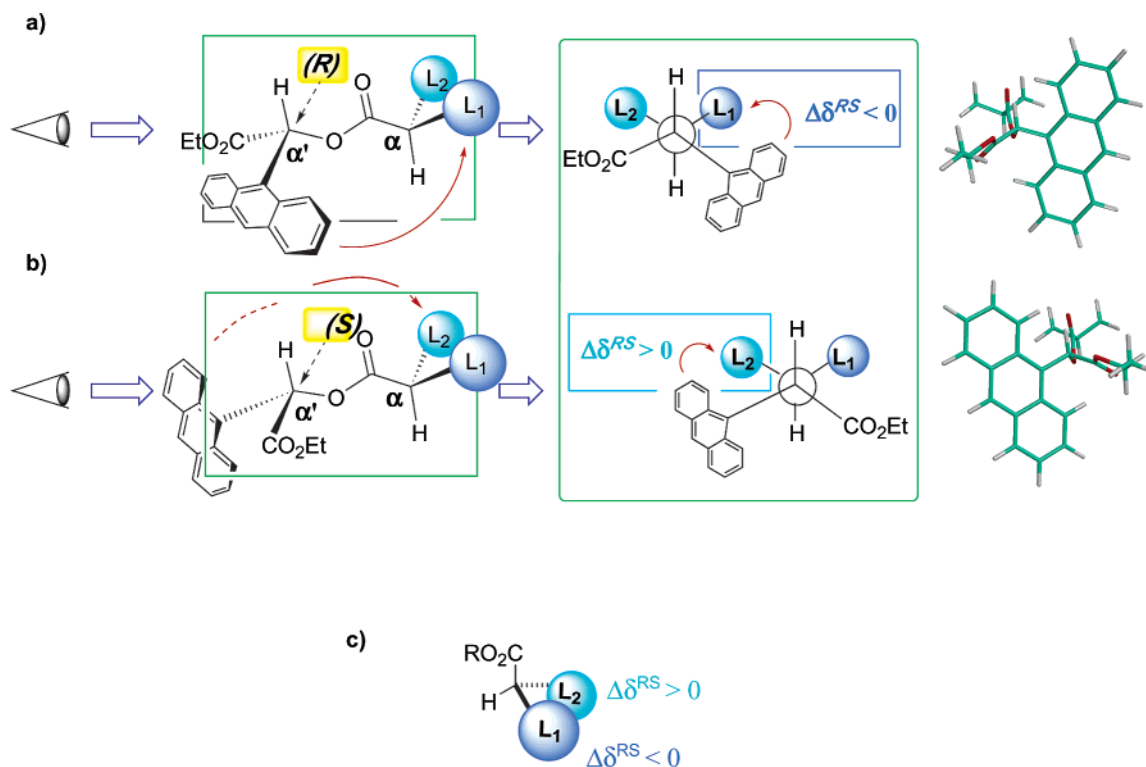


**Figure 134.** Conformational model for the determination of the absolute configuration of  $\alpha$ -chiral carboxylic acids by NMR of their 9-AHA esters.

(*S*)-2-methylbutyric acid as the model substrate. Their NMR showed that the higher  $\Delta\delta^{RS}$  values were obtained with ethyl 2-hydroxy-2-(9-anthryl) acetate (9-AHA; see Figure 131) as the auxiliary, and, therefore, 9-AHA was chosen for further studies as a CDA.

Theoretical and experimental studies showed the suitability of this reagent for the assignment of the

configuration of carboxylic acids: MM and AM1/PM3 methods were used to calculate the geometries and relative stabilities of the conformers of the 9-AHA esters; D NMR data were used to provide experimental evidence of the theoretical findings; and aromatic shielding effect.<sup>87</sup>

The studies previously described all established that the conformational composition of any ester of

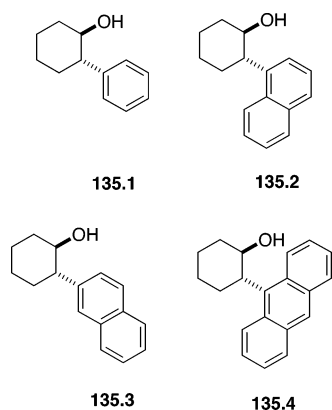


**Figure 135.** Structure of *trans*-aryl cyclohexanols.

9-AHA with an  $\alpha$ -chiral carboxylic acid is as represented in Figure 132: two main forms, *ap* (major) and *sp* (minor), are in conformational equilibrium. The  $L_1$  substituent in the (*R*)-9-AHA ester is shielded in the *ap* conformation, while the  $L_2$  substituent remains unaffected. In contrast, in the *sp* conformation, the  $L_2$  substituent is shielded while the  $L_1$  substituent remains unaffected (see Figure 132a). In the case of the (*S*)-9-AHA ester, substituent  $L_2$  is shielded in the *ap* conformation and substituent  $L_1$  is shielded in the *sp* conformation (see Figure 132b). Because the population of the *ap* conformer is higher than that of the *sp* conformer, substituent  $L_1$  is more shielded in the (*R*)-9-AHA ester than in the (*S*)-derivative ( $\Delta\delta^{RS} < 0$ ) and, conversely, substituent  $L_2$  is more shielded in the (*S*)-9-AHA ester than in the (*R*)-ester ( $\Delta\delta^{RS} > 0$ ). The signs of the  $\Delta\delta^{RS}$  values allow the assignment of the spatial position of substituents  $L_1/L_2$  by comparison of the  $^1\text{H}$  NMR spectra of both diastereoisomers (see Figure 132c).

Examination by  $^1\text{H}$  NMR spectroscopy of the (*R*)- and (*S*)-9-AHA esters of a large number of carboxylic acids of known absolute configuration and with a wide variety of structural features gave full experimental support to the aforementioned theory. The  $\Delta\delta^{RS}$  values shown in Figure 133 serve to illustrate two important facts. First, the distribution of the signs of  $\Delta\delta^{RS}$  shown in Figure 133 is perfectly homogeneous along the series and is consistent with both the absolute configurations of these compounds and the conformational composition shown in Figure 132.

Figure 134 shows the model for the assignment of the configuration of an acid of unknown configuration by comparison of the  $^1\text{H}$  NMR spectra of its (*R*)- and (*S*)-9-AHA esters. In this model, the *ap/sp* equilibrium is simplified by considering the dominant *ap* form (Figure 130) as the only relevant one and using this to fix the spatial location of substituents  $L_1$  and  $L_2$ . According to this model, the substituent that is more shielded in the (*R*)-9-AHA ester than in the (*S*)-9-AHA ester ( $\Delta\delta^{RS} < 0$ ) should be assigned as  $L_1$  in Figure 134c and, conversely, the substituent that is more shielded in the (*S*)-9-AHA ester than in the (*R*)-9-AHA ester ( $\Delta\delta^{RS} > 0$ ) corresponds to  $L_2$  (Figure

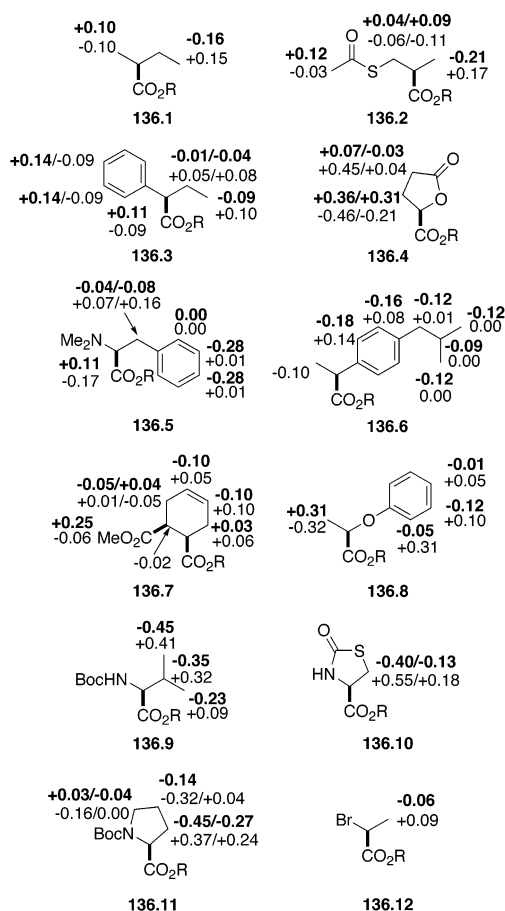


**Figure 136.**  $\Delta\delta^{RS}$  values for the esters of the carboxylic acids shown with *trans*-2-phenyl-1-cyclohexanol and 9-AHA. Data for 9-AHA given in boldface type.

134c). Identification of substituents  $L_1/L_2$  and their placement around the asymmetric center can then be directly obtained from the signs of  $\Delta\delta^{RS}$ , as shown in Figure 134.

### 3.6.2. Arylcyclohexanols

Other aryl alcohols different from the open-chain 1-aryl alcohols shown in Figure 131 also have been examined.<sup>87b</sup> Figure 135 shows their structures.

When the  $\Delta\delta^{RS}$  values obtained for the esters of the arylcyclohexanols **135.1–135.4** and a series of carboxylic acids of known absolute configuration are examined, it was observed that the commercially available (1*R*,2*S*)- and (1*S*,2*R*)-2-phenyl-1-cyclohexanol (**135.1**) gave  $\Delta\delta^{RS}$  values that were very similar to those obtained with 9-AHA. These data also indicate the following: (a) the signs of the shifts produced by **135.1** are regularly distributed in all the compounds examined ( $\Delta\delta^{RS}$  is positive for protons in substituent  $L_1$  and negative for protons in substituent  $L_2$ ); (b) the signs obtained are opposite to those obtained with 9-AHA (negative for substituent  $L_1$  and positive for substituent  $L_2$ ); (c) the absolute  $\Delta\delta^{RS}$  values obtained with **135.1** are, in all cases, similar to those produced by 9-AHA for protons near the chiral center. These facts indicate that both **135.1** and 9-AHA essentially show the same ability to

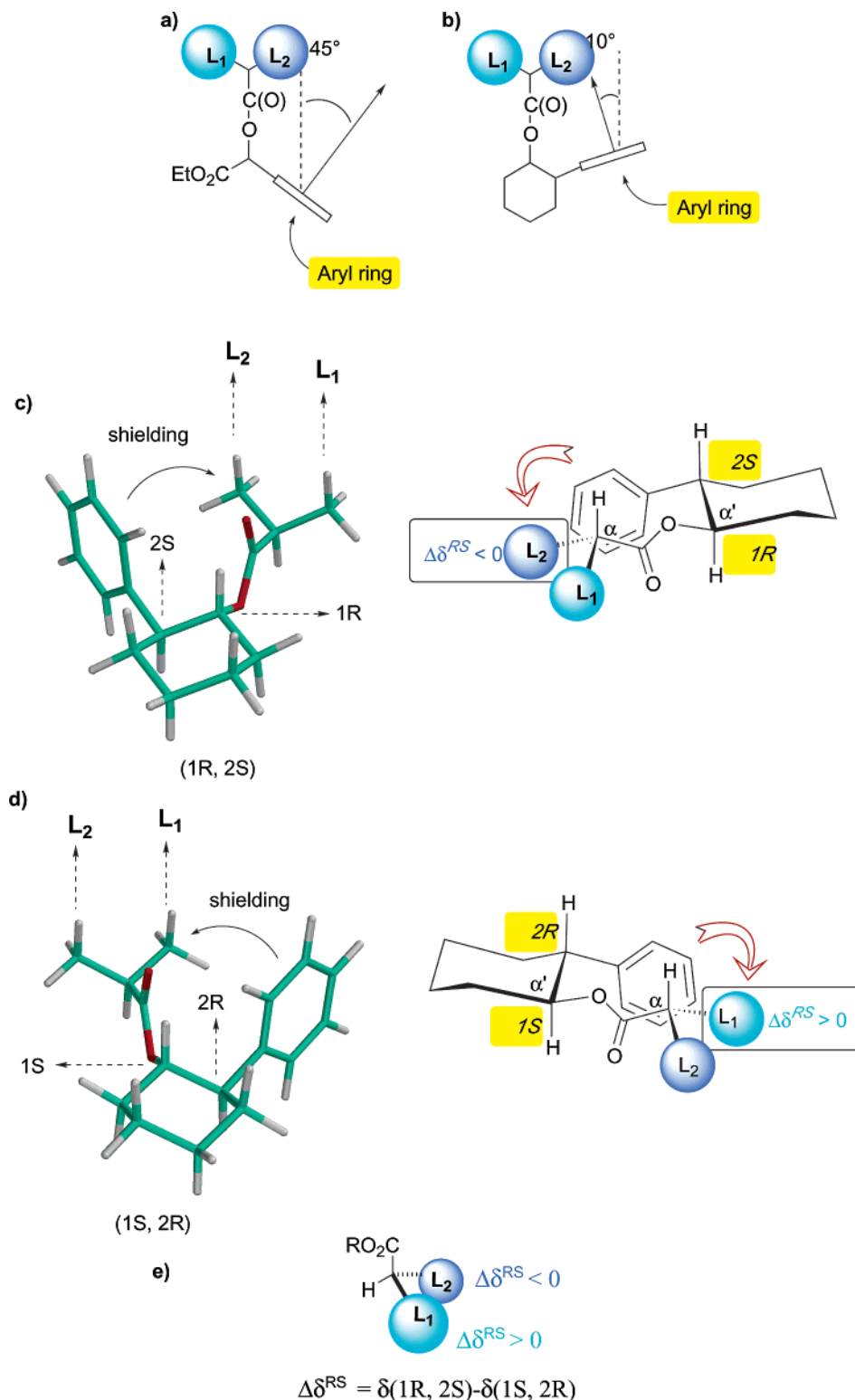


**Figure 137.** Representation of the direction of the maximum shielding in the esters of (a) 9-AHA and (b) **135.1**. Models for the determination of the absolute configuration on  $\alpha$ -chiral carboxylic acids by NMR of their *trans*-2-phenyl-1-cyclohexanol esters (c, d and e).

separate the resonances of the enantiomeric protons of the substrates (see Figure 136).

Aromatic shielding-effect calculations corroborated the shieldings obtained with this reagent. From a practical standpoint, **135.1** has an advantage over 9-AHA in that it is commercially available; on the other hand, the signals of 9-AHA in the NMR spectra

of its esters almost never overlap with those of the substrate, whereas the presence in **135.1** of numerous different protons is a clear limitation in this respect.

To analyze the role of the aryl ring in **135.1**, the possibility of increasing the  $\Delta\delta^{RS}$  values by changing the aromatic ring was explored and new reagents

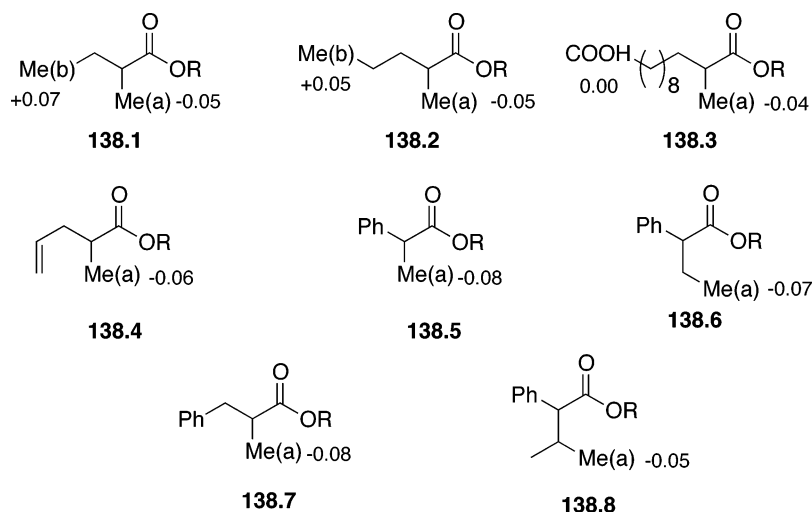


**Figure 138.**  $\Delta\delta^{SR}$  values obtained for enantiomeric mixtures of the acids shown, using (*S*)-methyl mandelate as the reagent (chemical shift of the (*S*)-acid-(*S*)-methyl mandelate minus that of the (*R*)-acid-(*S*)-methyl mandelate).

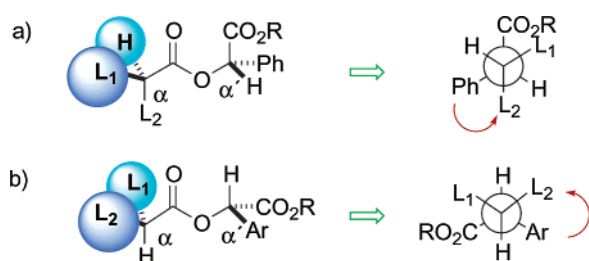


**Figure 139.** Simplified model for arylalkoxyacetic acid esters of a chiral acid according to (a) Tyrrel<sup>88</sup> and (b) Riguera.<sup>87</sup>

with 1-naphthyl, 2-naphthyl, and 9-anthryl rings (**135.2**, **135.3**, and **135.4**, respectively; see Figure 135) were synthesized and tested. Unfortunately, significant improvements in the  $\Delta\delta^{RS}$  values were not found when compared to **135.1**. The fact that compounds with naphthyl and anthryl rings do not produce higher shifts than **135.1**, which has a practically identical conformation, seems to be in conflict with data obtained for AMAA esters. Nevertheless, inspection of the structures of the esters of the arylcyclohexanols indicates that the direction of maximum shielding is focused on the area immediately surrounding the asymmetric C atom (Figure 137a,

b). Thus, when the phenyl group in the arylcyclohexanols is replaced by a larger aromatic system, the shielding area becomes very much larger and this should now affect not only the substituent on the same side ( $L_2$ ) but also the other substituent ( $L_1$ ), to some extent; therefore, on average, the  $\Delta\delta^{RS}$  values will not be as high as expected. In the case of phenylcyclohexanols, the focus of the shielding cone is so far away from the asymmetric center that even when its effect is greatly increased, it will never influence more than one substituent in each conformer.

Panels c–e in Figure 137 show a graphic summary that illustrates how the absolute configuration of an  $\alpha$ -chiral carboxylic acid can be deduced from the signs of the  $\Delta\delta$  values obtained from its esters with the two enantiomers of any *trans*-2-aryl-1-cyclohexanol.

### 3.6.3. (*S*)-Methyl Mandelate

Other than the auxiliary reagents described by Riguera's group in the preceding pages, very few papers have been devoted to the determination by NMR of absolute configuration of carboxylic acids. In one such example, however, (*S*)-methyl mandelate was tested as a chiral auxiliary with racemic and

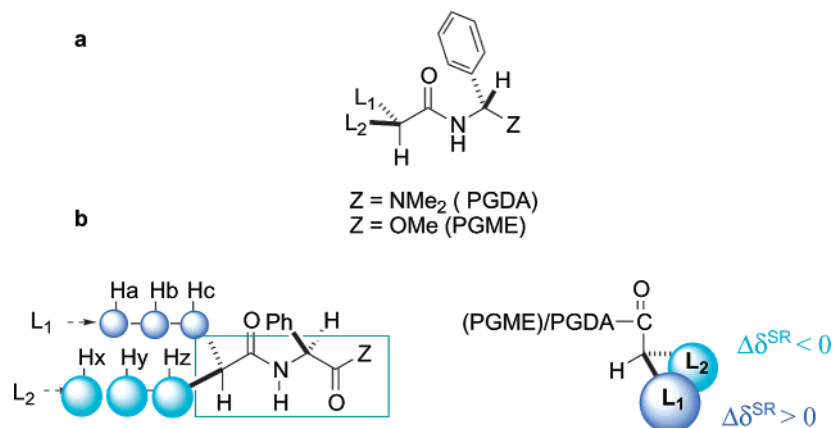


**Figure 140.** (a) Structure of PGDA and PGME amides and (b) empirical model for the assignment of the absolute configuration of carboxylic acids.

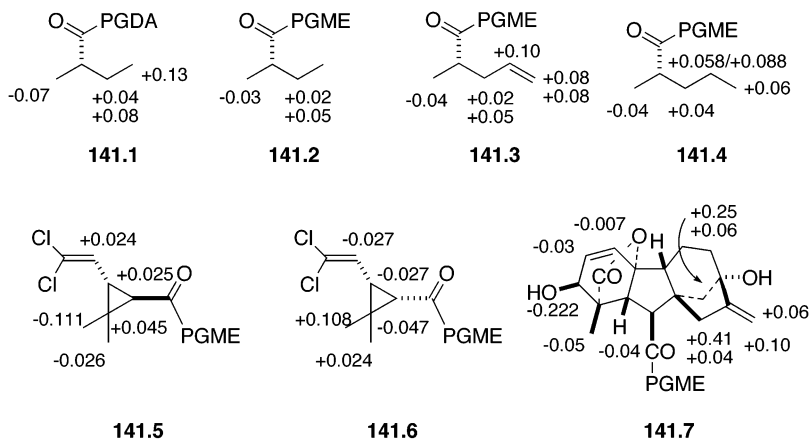


**Figure 141.**  $\Delta\delta^{SR}$  values for the PGDA and PGME amides of the carboxylic acids shown.

enriched mixtures of eight acids.<sup>88</sup> Although the number of chemical shifts reported was very limited (only the methyl groups labeled a and b in Figure 138), a coherent shift pattern, with a homogeneous distribution of signs for substituents  $L_1/L_2$  and useful  $\Delta\delta^{SR}$  values was obtained.

The results obtained on using (*S*)-methyl mandelate as the reagent were interpreted assuming a conformational equilibrium and preferred conformation ( $C_\alpha$ -H not coplanar with  $C=O$ , and  $L_2$  anti to the  $C=O$  group; see Figure 139) completely different from those described for the esters of 9-AHA (see Figures 132 and 134). Although this model can effectively be used to correlate the NMR shifts with the structure of the substrates, it is inconsistent with the well-documented coplanarity of  $C_\alpha$ -H with  $C=O$ , and therefore does not represent the real conformational composition of the compounds studied;<sup>29,75–78,87</sup> indeed, specific experimental data were not advanced to support the model. Therefore, the success of this model in the prediction of correct *R/S* configuration is purely accidental and can be explained because the spatial location of substituents  $L_1/L_2$ , relative to the aryl ring, is approximately the same as that if the model corresponding to 9-AHA (Figure 132) were considered.

### 3.6.4. Phenylglycine Dimethyl Amide (PGDA) and Phenylglycine Methyl Ester (PGME)

Phenylglycine dimethyl amide (PGDA) and phenylglycine methyl ester (PGME) were proposed by Kusumi and co-workers<sup>89</sup> as auxiliary reagents for  $\alpha$ -chiral carboxylic acids (Figure 140a). In this procedure, the acid of unknown configuration is condensed with the two enantiomers of the reagent and the  $\Delta\delta^{SR}$  values of substituents  $L_1/L_2$  are measured in the corresponding amides.

The empirical model shown in Figure 140b was proposed for the interpretation of the experimental data: substituents Hx, Hy, Hz, which correspond to  $L_2$ , are more shielded by the phenyl group in the (*S*)-PGDA (or (*S*)-PGDE) amides than in the (*R*)-amides, and the opposite case occurs for substituents Ha, Hb, Hc ( $L_1$ ). Thus,  $\Delta\delta^{SR}(L_2) < 0$  and  $\Delta\delta^{SR}(L_1) > 0$ .

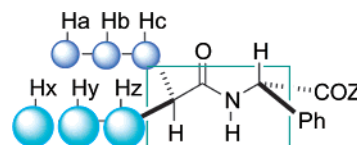


**Figure 142.** Alternative model for the assignment of the absolute configuration of carboxylic acids with PGDA or PGME.

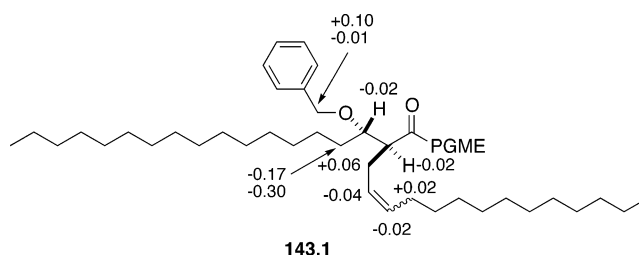


**Figure 143.**  $\Delta\delta^{SR}$  values for the PGME amides of compound **143.1**.

Although PGDA was tested with just one carboxylic acid of known absolute configuration (**141.1**; see Figure 141), and, therefore, its use as an auxiliary reagent for acids cannot be recommended, the reliability of the assignments produced using PGME was demonstrated with the series of carboxylic acids of known configuration shown in Figure 141.

An XRD study and NOE experiments were presented to support the model, although other studies have shown that, in solution, the  $C=O$ ,  $N-H$ , and  $C-H$  adopt a coplanar disposition.<sup>75–78</sup> If this is the case, then the model should be modified to the one shown in Figure 142, but this change does not affect either the shielding distribution or the configuration assigned, because the position of substituents  $L_1/L_2$ , relative to the phenyl group, is approximately the same in both cases.

When PGME was applied to compound **143.1** (Figure 143), an irregular distribution of  $\Delta\delta^{SR}$  signs was obtained<sup>90</sup> for several protons. The authors hypothesized that a phenyl-phenyl interaction could be the cause of this phenomenon, but when other substrates that contain phenyl groups were studied (Figure 144), the signs were as one would expect from the configuration of the substrates and no discrepancies were found. Steric hindrance or the effect of a

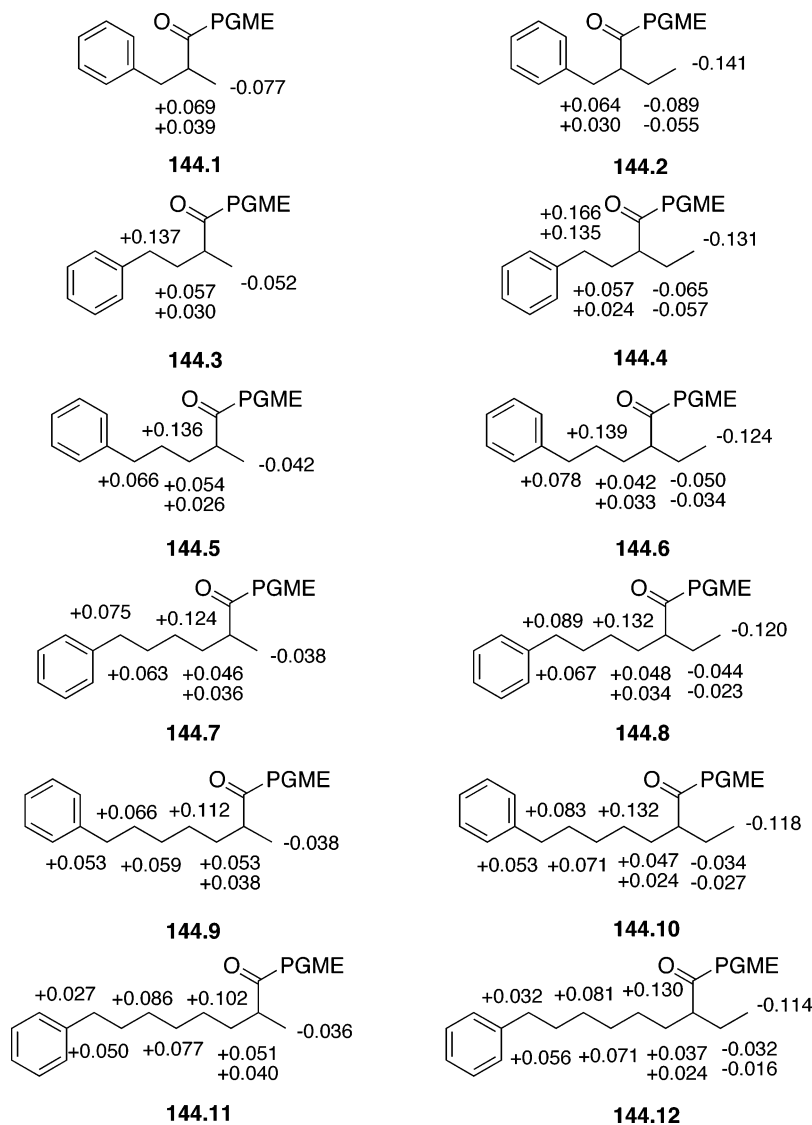


**Figure 144.**  $\Delta\delta^{SR}$  values for the amides of the carboxylic acids shown with PGME (obtained from the (*S*)-PGME amides of the racemic acids).

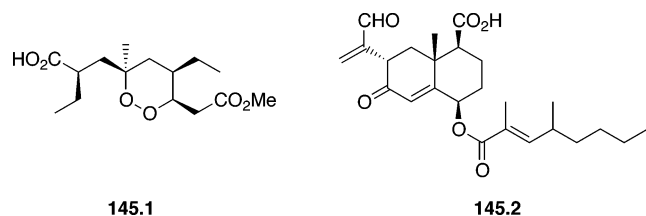


**Figure 145.**

nearly O atom were proposed as possible causes of the problem.

PGME has been used on several occasions to deduce the absolute configuration of natural products. Some examples in this field include the following: compound **145.1**, which is a degradation product from the marine cycloperoxide plakortin;<sup>91a</sup> the HIV-1 integrase inhibitor of microbial origin, integric acid<sup>91b</sup> **145.2** (Figure 145); and carboxyYTX, which is an analogue of yessotoxin, isolated from mussels.<sup>91c</sup>

More recently, PGME was applied to the assignment of the configuration of  $\alpha$ -oxy tertiary carboxylic acids<sup>92</sup> ( $\alpha$ -oxy- $\alpha,\alpha$ -disubstituted acetic acids). In these

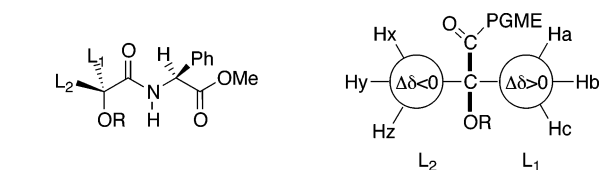


**Figure 146.** Empirical model for the assignment of the absolute configuration of  $\alpha$ -oxy- $\alpha,\alpha$ -disubstituted acetic acids with PGME.

cases, the empirical model shown in Figure 146 was proposed and several acyclic and cyclic  $\alpha$ -oxy-carboxylic acids of known absolute configuration, including some natural products, were used as substrates to prove the reliability of the procedure (Figure 147).

The method was first applied to determine the configuration at C-18 of polyether macrolide pectenotoxin-692a (**148.1**, Figure 148). The absolute configuration of lactone **148.2**, which is a derivative of tanikolide, isolated from cyanobacteria<sup>93</sup> was also assigned this way.

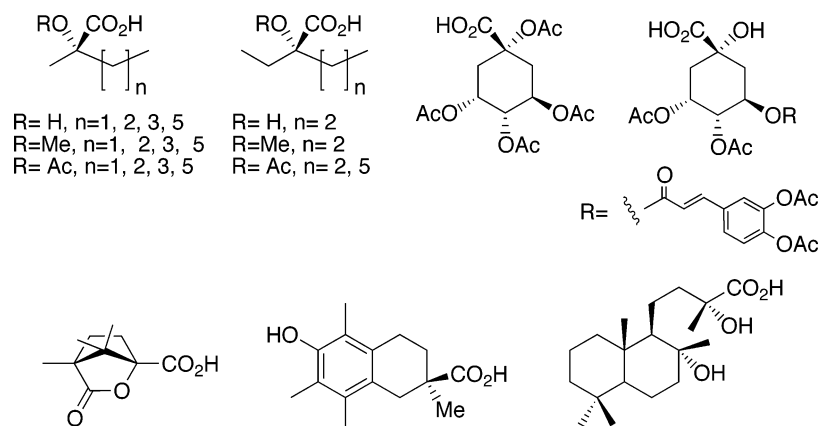


**Figure 147.**  $\alpha$ -Oxy- $\alpha, \alpha$ -disubstituted acetic acids studied with PGME.

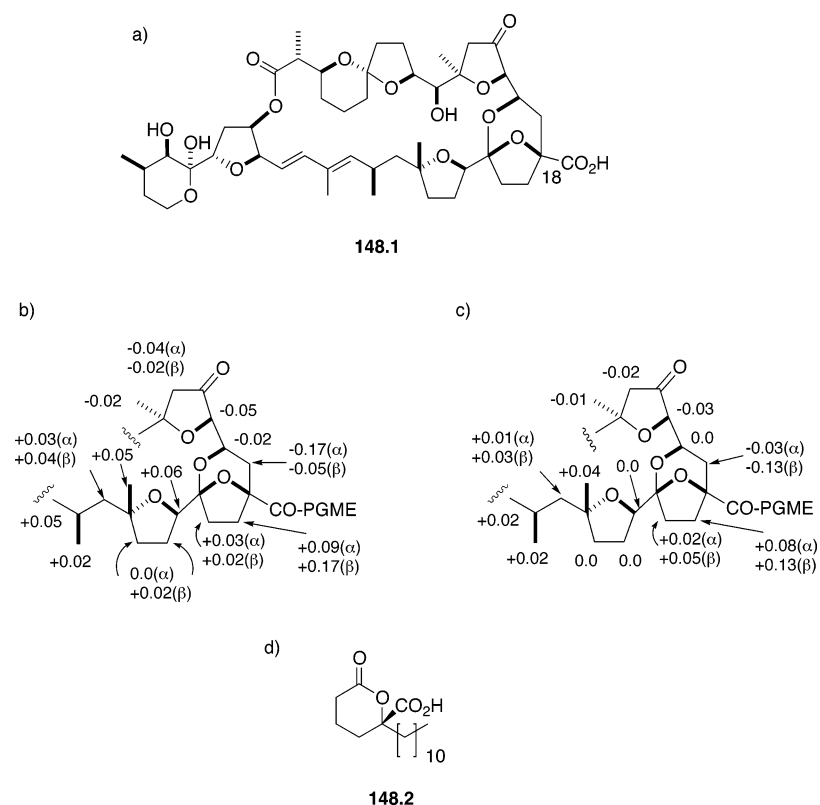


**Figure 148.** (a) Structure of Pectenotoxin-6, (b)  $\Delta\delta^{SR}$  values in  $\text{C}_5\text{D}_5\text{N}$ , (c)  $\Delta\delta^{SR}$  values in  $\text{CDCl}_3$ , and (d) structure of Tanikolide lactone.

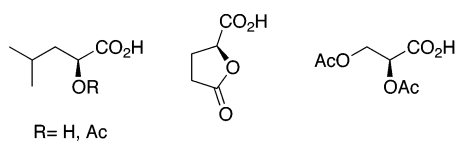


**Figure 149.**  $\alpha$ -Oxy- $\alpha$ -monosubstituted acetic acids studied with PGME.

The applicability of PGME to  $\alpha$ -oxy- $\alpha$ -monosubstituted acetic acids, using the empirical model proposed for  $\alpha$ -oxy- $\alpha, \alpha$ -disubstituted acetic acids in which one of the  $\alpha$ -substituents is a hydrogen, was also investigated.<sup>94</sup> Unfortunately, only four examples of known absolute configuration were used to support the reliability of this model (Figure 149).

In addition, Fusetani and co-workers<sup>95</sup> found that, when PGME was used for the study of the furoic acid

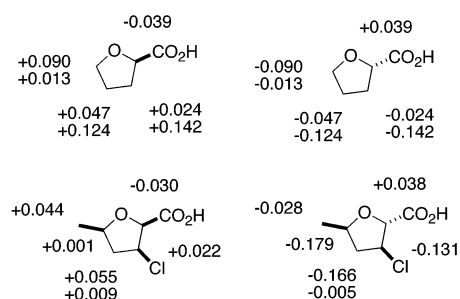


**Figure 150.**  $\Delta\delta$  values for furoic acid derivatives with PGME.

derivatives shown in Figure 150, the same  $\Delta\delta$  signs were obtained for all the relevant protons of the PGME amides. The model proposed by Kusumi is consistent with those results.

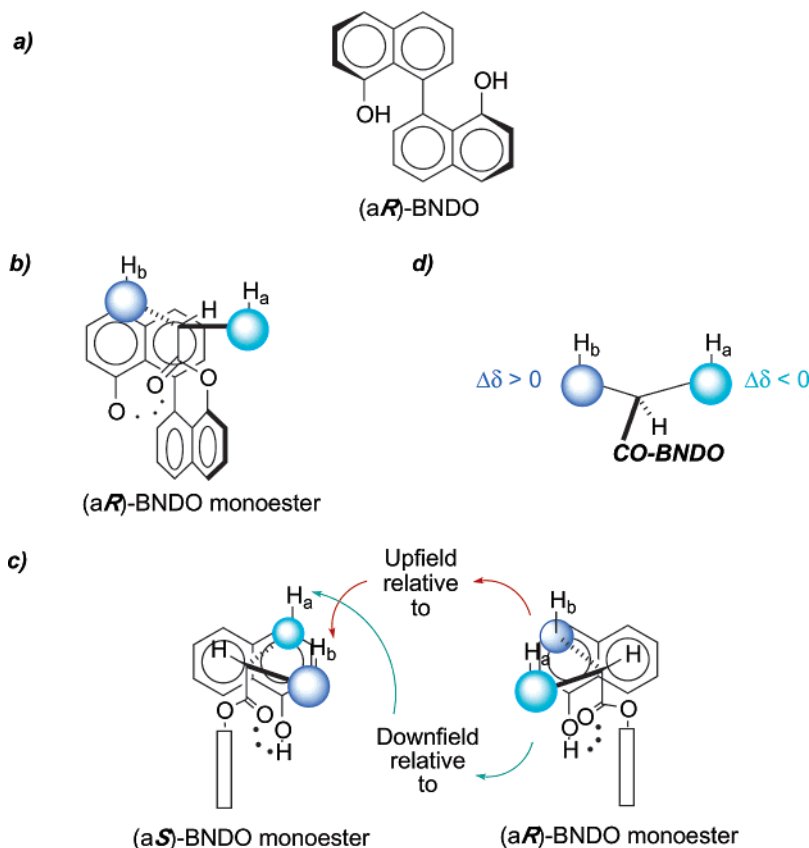


**Figure 151.** (a) Structure of (a*R*)-BNDO. (b) Ideal conformation of an (a*R*)-BNDO monoester. (c) Position of the acid substituents in the diastomeric esters. (d) Model for the assignment of configuration from the  $\Delta\delta$  values.

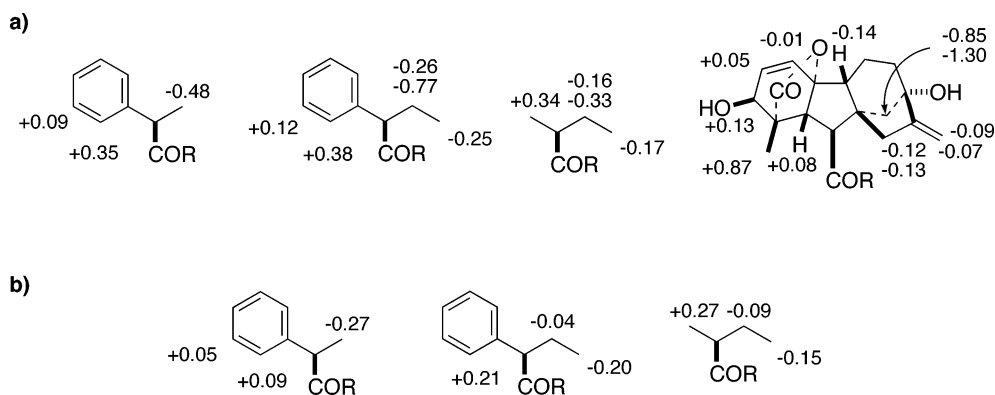


**Figure 152.** (a)  $^1\text{H}$   $\Delta\delta_{a.SaR}$  values for the BNDO esters of the carboxylic acids shown. (b)  $^{13}\text{C}$   $\Delta\delta_{a.SaR}$  values.

### 3.6.5. 1,1'-Binaphthalene-8,8'-diol (BNDO)

A completely different type of reagent was proposed in 1996 by Japanese workers<sup>96</sup> for the stereochemical assignment of carboxylic acids; this is 1,1'-binaphthalene-8,8'-diol (BNDO; see Figure 151a), which presents axial chirality and is available in the two enantiomeric forms.

Several acids of known absolute configuration were esterified with (a*R*)-, (a*S*)-, and/or racemic BNDO, and a method to predict the configuration was devised. The idealized conformation of a BNDO monoester is depicted in Figure 151b: The naphthalene rings are orthogonal, the carbonyl and the hydroxyl groups are syn, and the a proton is situated near the center of the facing naphthalene ring. Because of the effect of the aromatic ring, the signal

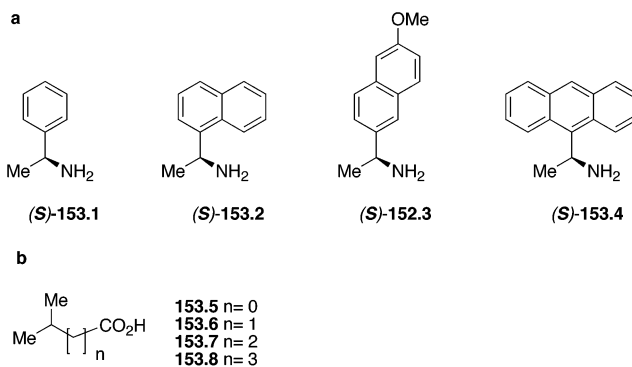


**Figure 153.**

due to  $H_a$  of the (a*R*)-BNDO monoester should appear downfield, relative to that in the (a*S*)-BNDO monoester. The reverse should hold true for  $H_b$



**Table 14.**  $\Delta\delta$  Values of the  $\beta$ -Methyl and Other Diagnostic Resonances in Diastereomeric Syn and Anti 1-Arylethylamides from 3-Methylcarboxylic Acids

|       |      | $\Delta\delta = \delta_{syn} - \delta_{anti}$ |        |                        |
|-------|------|---|--------|------------------------|
| R     | Ar   | $\Delta\delta_{C(3)-Me}$                      |        | $\Delta\delta_{other}$ |
| Me(5) | Ph   | +0.032  | -0.012 | H(5)                   |
|       | Ph   | +0.03   |        |                        |
|       | Ph   | +0.033  |        |                        |
|       | Ph   | +0.013  | -0.015 | OMe                    |
|       | Ph   | +0.030  | -0.019 | H(4)                   |
|       |      |   | -0.021 | H(5E)                  |
|       |      |   | -0.028 | H(5Z)                  |
|       | Ph   | +0.013  | -0.020 | H(4)                   |
|       |      |   | -0.048 | Me(6E)                 |
|       |      |   | -0.117 | Me(6Z)                 |
| Me(5) | 1-Np | +0.050  | -0.024 | H(5)                   |
|       | 1-Np | +0.050  |        |                        |
|       | 1-Np | +0.019  | -0.032 | OMe                    |
|       | 1-Np | +0.041  | -0.028 | H(4)                   |
|       |      |   | -0.050 | H(5E)                  |
|       |      |   | -0.042 | H(5Z)                  |
|       | 1-Np | +0.018  | +0.020 | H(4)                   |
|       |      |   | -0.062 | Me(6E)                 |
|       |      |   | -0.154 | Me(6Z)                 |

(Figure 151c). The chemical-shift difference was defined as  $\Delta\delta = \delta_{aS} - \delta_{aR}$ ; thus, in the model depicted in Figure 153d, positive and negative values are associated with the left- and right-hand sides of the substrate, respectively. Isobutyric acid and several derivatives were used for  $^1\text{H}$  NMR analyses to

confirm the preponderance of the ideal conformation in solution.

The  $^1\text{H}$   $\Delta\delta$  values for a very limited number (four) of chiral acids are shown in Figure 152a.  $^{13}\text{C}$   $\Delta\delta$  values for three of those compounds were also reported (Figure 152b).

### 3.7. Application to $\beta$ -Chiral Carboxylic Acids

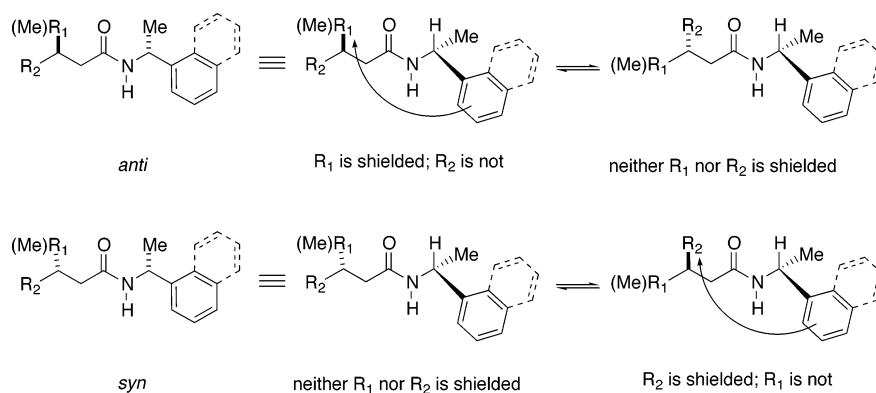
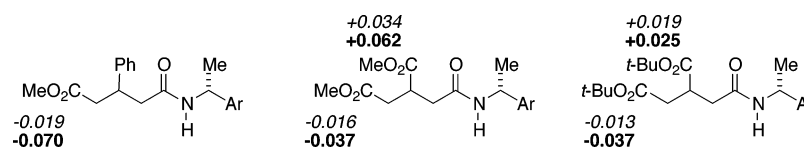
#### 3.7.1. Arylethylamines

Acyclic carboxylic acids containing remote stereocenters constitute a class of substrates for which methods to determine their configurations were also pursued. In fact,  $\beta$ -substituted acids represent a specific structural unit that is of interest in the context of natural products chemistry. Hoye et al.<sup>97</sup> chose the amide bond to link the reagent to the substrate and explored the use of 1-arylethylamines **153.1**–**153.4** as reagents (see Figure 153a).

These compounds were tested with the homologous series of acids **153.5**–**153.8** (see Figure 153b), using the signals of the methyl groups of the amides to assess the effectiveness of these systems as reagents. As expected, the anthryl derivative **153.4**, followed by the naphthyl derivative **153.2**, resulted in the largest shifts. Amines **153.1** and **153.2** are commercially available in optically pure form and were therefore adopted for further studies with a series of 3-substituted acids of known absolute configuration.

The results summarized in Table 14 show how the authors differentiate two stereochemical possibilities (defined as syn/anti, according to the relative orientation of the benzylic methyl group and the methyl substituent at C(3)) and calculate the parameter  $\Delta\delta$  (defined as the difference between the chemical shifts in the syn and anti diastereomers) for the  $\beta$ -methyl and other groups.

The data obtained show that the  $\beta$ -methyl groups are always more deshielded in the syn series than

**Figure 154.** Conformational model for the determination of the sign of  $\Delta\delta = \delta(\text{syn}) - \delta(\text{anti})$  of protons in  $R_1$  and  $R_2$ .**Figure 155.**  $\Delta\delta = \delta(\text{syn}) - \delta(\text{anti})$  values for amides from  $\beta$ -chiral acids with known relative configurations Ar = 1-Np data given in boldface type.

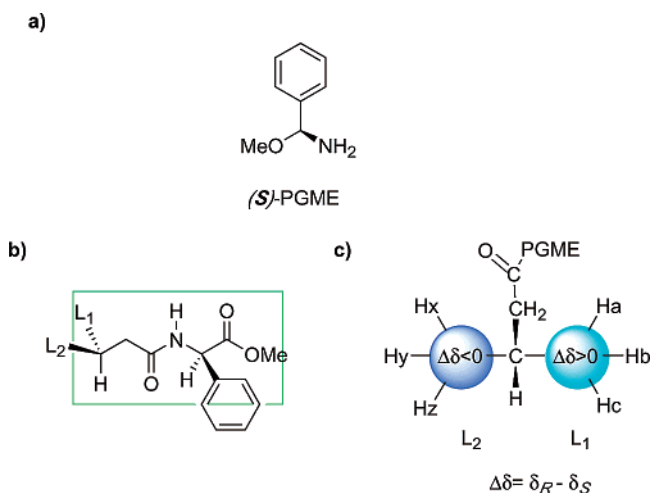


**Figure 156.** (a) Structure of (*S*)-PGME. (b) Suggested most stable conformation of a PGME amide. (c) Model for the assignment of the configuration.

in the anti series, whereas protons in the other  $\beta$ -substituent are more shielded in the syn isomers—with the exception of the vinylic H(4) proton in the last entry in Table 14.

A working model (Figure 154) based on the NMR results and routinely accessible calculations (AMBER force field, as implemented in the MacroModel software package) has been proposed. This model is based on two assumptions: (1) the predominant rotamer around the bond between the benzylic C atom and the N atom is that in which the benzylic proton is eclipsed with the carbonyl group, and (2) one of the two nonhydrogen substituents at C(3) occupies the anti position, relative to the carbonyl group.

In the case of the anti diastereomer, this situation results in preferential shielding of  $R_1$ , whereas preferential shielding of  $R_2$  should be observed in the syn diastereomer. As a consequence, the  $\Delta\delta$  values for protons in  $R_1$  are positive and those in  $R_2$  are negative.

The scope of this method/reagent was extended by the same authors to include carboxylic acids with substituents other than a methyl group at C(3), including the substrates shown in Figure 155 and six other examples of known absolute configuration

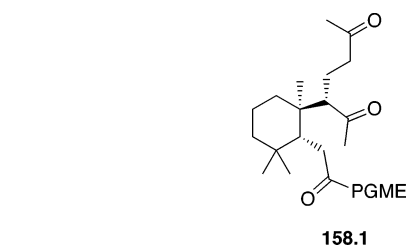


**Figure 158.**

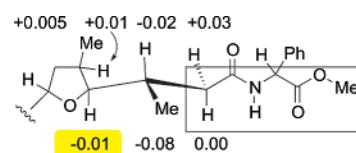


**Figure 159.** Proposed conformation for the PGME amides of the gambieric acids based on NMR analysis.  $\Delta\delta^{RS}$  (instead of  $\Delta\delta^{RS}$ ) values were reported; the inconsistent value is highlighted.

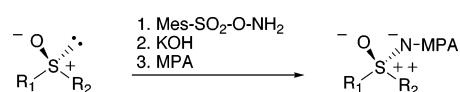


**Figure 160.** Formation of *N*-(methoxyphenylacetyl)sulfoximines from sulfoxides.

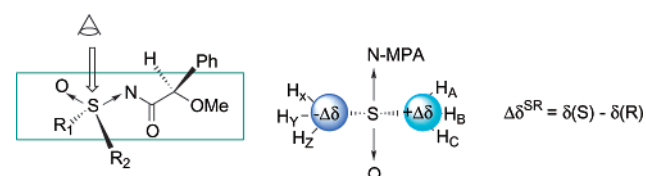


**Figure 161.** Model for the determination of configuration of *N*-(methoxyphenylacetyl)sulfoximines from sulfoxides.

taken from the literature. These studies confirmed the applicability of this method.<sup>98</sup>

### 3.7.2. PGME

Phenylglycine methyl ester (PGME; see Figure 156a), proposed by Kusumi et al.<sup>89</sup> for the determination of the configuration of  $\alpha$ -chiral carboxylic acids, has also been used with acids that have the chiral center at the  $\beta$ -position. The eight carboxylic acids of known configuration shown in Figure 157 were used as test compounds. The signs of the  $\Delta\delta^{RS}$  values of the corresponding PGME amides were coherent with their stereochemistry and the model outlined in Figure 156c.<sup>89b</sup>

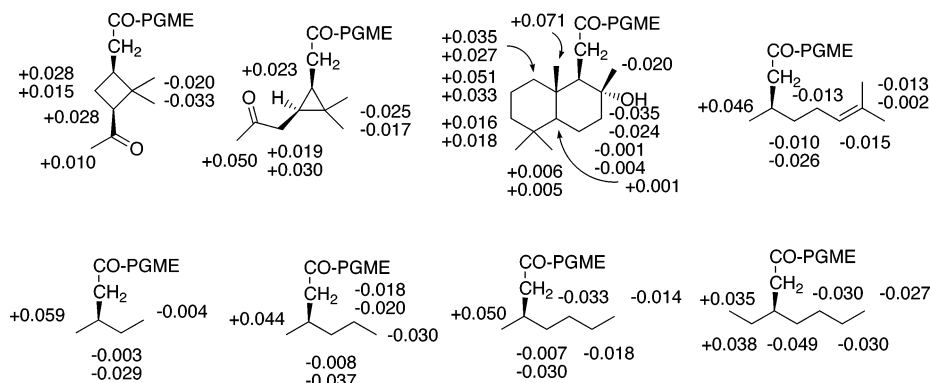


**Figure 157.**  $\Delta\delta^{RS}$  values for the amides of the  $\beta$ -chiral carboxylic acids tested with PGME.

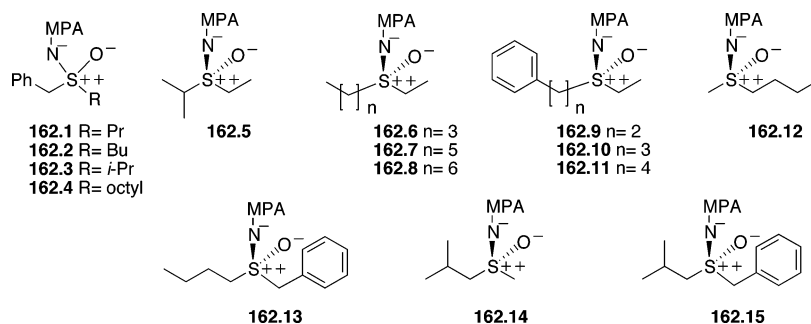


**Figure 162.** *N*-MPA-sulfoximides used in this study.

This situation is rationalized on the assumption that steric interactions cause the PGME amide of a

$\beta$ -chiral carboxylic acid to exist in essentially the conformation shown in Figure 156b. However, theo-

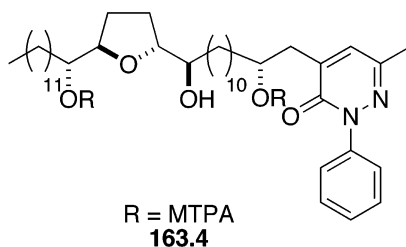
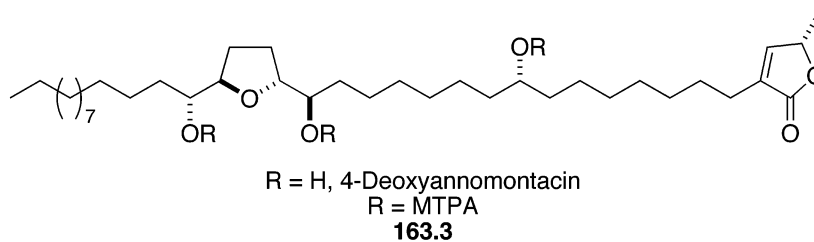
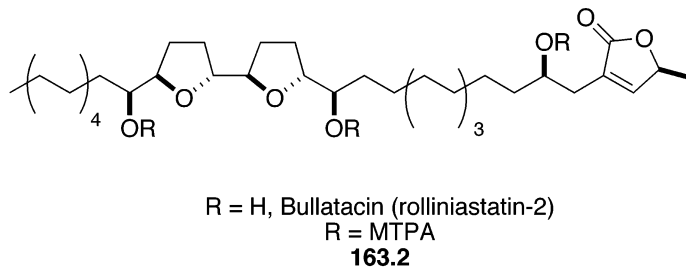
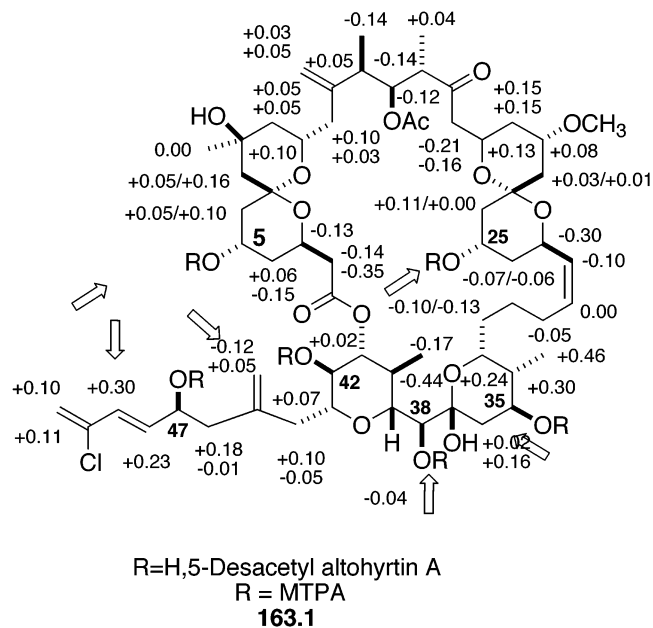


**Figure 163.** Polyhydroxylated compounds studied as MTPA esters.

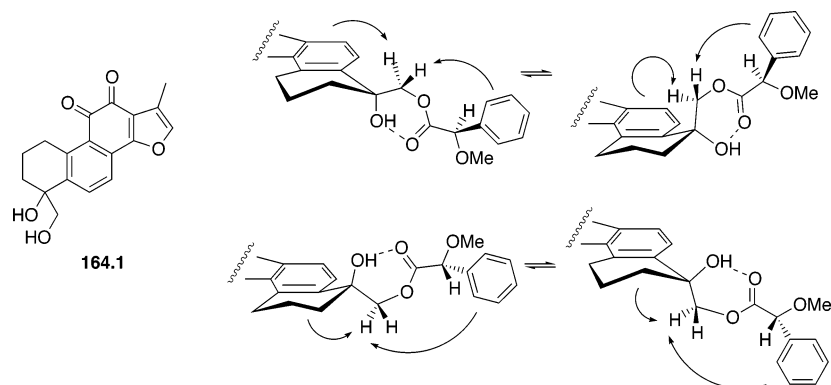


**Figure 164.** Analysis of the diastereomeric nonequivalence in the (*R*)-MPA esters of the enantiomers of tanshindiol (**164.1**). The shielding on the methylene protons is different in each case.

retical calculations were not performed to confirm this hypothesis.

This reagent/model was used to establish the stereochemistry of several natural products such as **158.1**, which is a degradation product from a diterpenoid isolated from an insect wax<sup>99a</sup> (see Figure 158) and the gambieric acids, which are polyethers isolated from marine dinoflagellates.<sup>99b</sup> In the latter case, the authors found it necessary to ensure that the proposed PGME model was acceptable for these compounds by performing a conformational analysis (NOE, HOHAHA). The resulting modified conformation is shown in Figure 159.

### 3.8. Application to Chiral Sulfoxides: MPA

A procedure for the determination of the absolute configuration of chiral sulfoxides has been developed<sup>100</sup> and requires the introduction of a chiral anisotropic moiety by transformation of the sulfoxides into *N*-(methoxyphenylacetyl)sulfoximines. The method consists of the amination of the sulfoxide with *O*-mesitylsulfonylhydroxylamine, which proceeds with complete retention of chirality at the S atom, followed by introduction of (*R*)- and (*S*)-MPA at the N atom (Figure 160).

Subsequent application of the empirical model shown in Figure 161 allows the configuration to be deduced on the basis of the  $\Delta\delta^{SR}$  values ( $\Delta\delta^{SR} = \delta(S) - \delta(R)$ ).

The utility of this model and the reliability of the configurational assignments are based on the coherence of the NMR data obtained for the MPA-derived sulfoximides shown in Figure 162, which are derived from eleven chiral sulfoxides of known absolute configuration (**162.5–162.15**). In addition, four racemic sulfoxides were derivatized with racemic MPA and the NMR data of the corresponding MPA-derived sulfoximides **162.1–162.4** were shown to produce shifts that apparently confirmed the model: the  $\Delta\delta$  signs are systematically arranged on both sides of the MPA plane, but the absolute configuration of each derivative was not available for proper validation.

### 3.9. Application to Chiral Polyhydroxylated Compounds

In many fields of chemistry—natural products, organic synthesis—researchers often must determine the absolute configuration of substrates that have several chiral centers and functional groups, such as polyols. Usually, when facing these situations through the use of the NMR methods, the direct application to polyalcohols of the models originally developed for monoalcohols was the solution that was used, without considering that such a solution could be highly inappropriate. This situation was exposed in a work<sup>13</sup> where several examples taken from the literature illustrate the magnitude and characteristics of the problem.

In those reports, attempts were made to assign the absolute configuration of all the asymmetric centers of a polyalcohol by application of the NMR method to the fully esterified derivatives with (*R*)- and (*S*)-MTPA; however, the  $\Delta\delta^{SR}$  data obtained generally did not allow a completely unambiguous assignment of configuration.

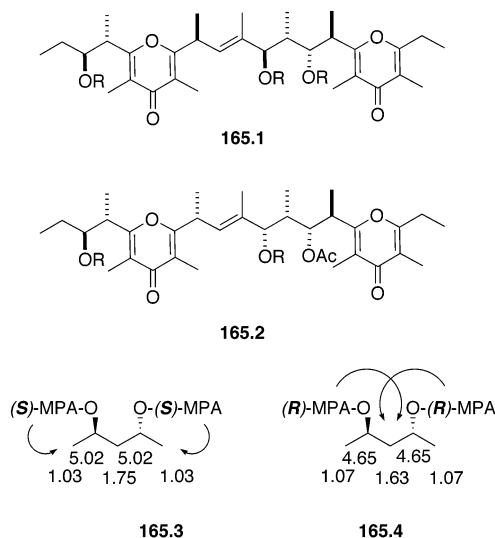


**Figure 165.** Polypropionate metabolites from the marine mollusk *Onchidium* sp. (**165.1** and **165.2**) and <sup>1</sup>H NMR chemical shifts of chiral bis-MPA esters of (*2R,4R*)-(-)-pentanediol, indicating the different shielding caused by the auxiliary reagents.

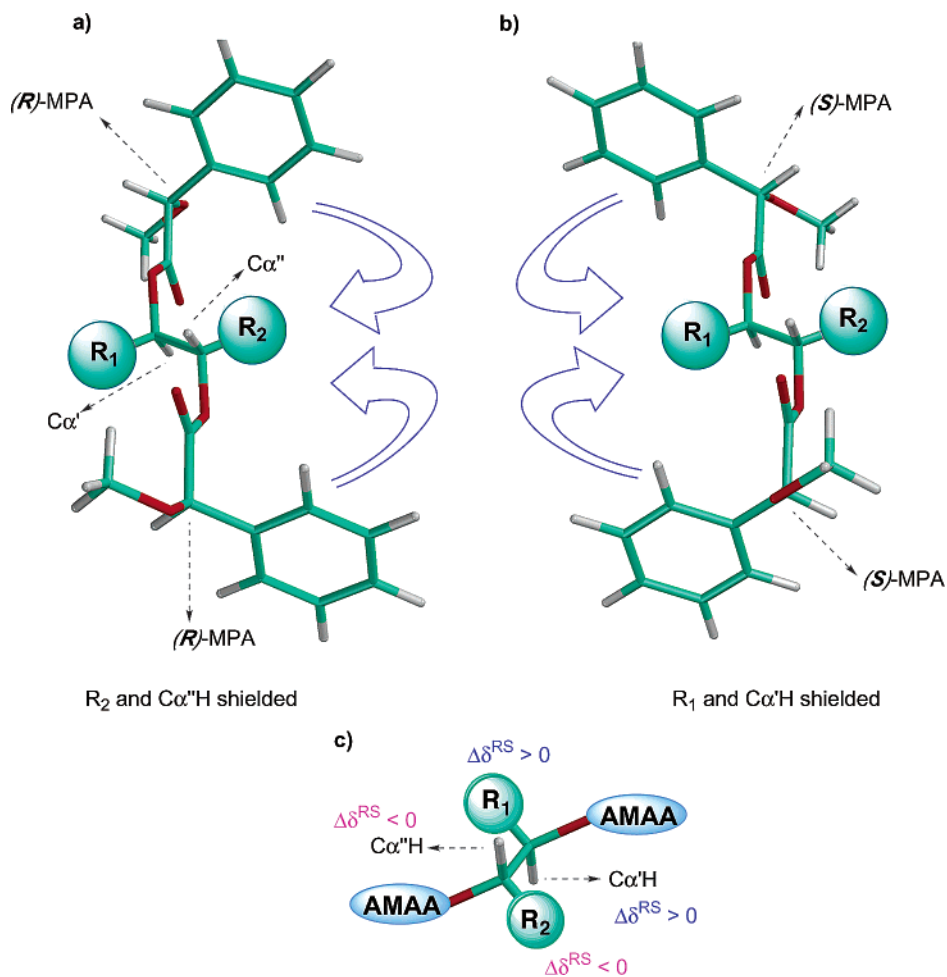


**Figure 166.** (*R*)- and (*S*)-MPA diester of an anti-1,2-diol and expected  $\Delta\delta^{RS}$  signs. Arrows show the shielding produced by the phenyl groups.

Figure 163 shows how the hexa-MTPA ester of 5-desacetylaltohyrtin A<sup>101</sup> (**163.1**) generates  $\Delta\delta$  values around C-5, C-35, C-38, C-42, and C-47 that do not present the necessary alternation of signs around substituents L<sub>1</sub>/L<sub>2</sub> and the same occurs with C-16, C-19, and C-24 of squamostatin D<sup>25b</sup> (**19.5**; see Figure 19). Other examples of this type include annonaceous acetogenins such as bullatacin<sup>12a,102a</sup> (rolliniastatin-2, **163.2**; see Figure 163), sootepensin A<sup>25a</sup> (**19.4**; see Figure 19), 4-deoxyannomontacin<sup>102b</sup> (**163.3**); a donaienin derivative<sup>102c</sup> (**163.4**); and sponge metabolites penaresidins<sup>23</sup> (**19.1** and **19.2**; see Figure 19).

This lack of homogeneity of the  $\Delta\delta^{SR}$  signs involves a clear risk of misassignment and means that, to some extent, the considerations known to be valid for monoesters are not fulfilled in those bis- or tris-MTPA esters. The aforementioned article<sup>13</sup> reminds us that the fundamentals of the NMR method are related to aromatic shielding, which is a through-space phenomenon that affects protons several bonds away from the hydroxylic C atom that has the auxiliary reagent. Therefore, the  $\Delta\delta^{SR}$  values observed in those polyderivatized compounds are, in fact, the result of the combined effects (shielding/deshielding) of all the MTPA phenyl rings and cannot be interpreted as if they were produced by just one phenyl group as in monofunctional compounds.

In practice, the assignment of the configuration of compounds that have several functional groups with the same reactivity (i.e. 2,3-pentanediol) can be addressed in two possible ways: either the appropriate protection/deprotection protocols are used to achieve selective derivatization of each hydroxyl group or, more simply, the two alcohol groups are derivatized together in a single reaction.

In the first case, the configuration at each asymmetric C atom is examined separately, using the models developed for monofunctional compounds; however, the protection/deprotection operations will be time- and sample-consuming and this is a significant drawback.

There could be special cases where the reactivity of the functional groups with the CDA is sufficiently different to achieve selective derivatization of one of the groups without protecting the other. One particularly noteworthy example of this situation using MPA as the reagent is represented by tanshindiol (**164.1**; see Figure 164), which is a plant metabolite that possesses vicinal primary and tertiary hydroxyl groups.<sup>103</sup> When both enantiomers of **164.1** were derivatized with (*R*)-MPA, single esters on the primary hydroxyl group were obtained and their NMR were used for the assignment on the basis of the models shown in Figure 164. Note that MPA is not a

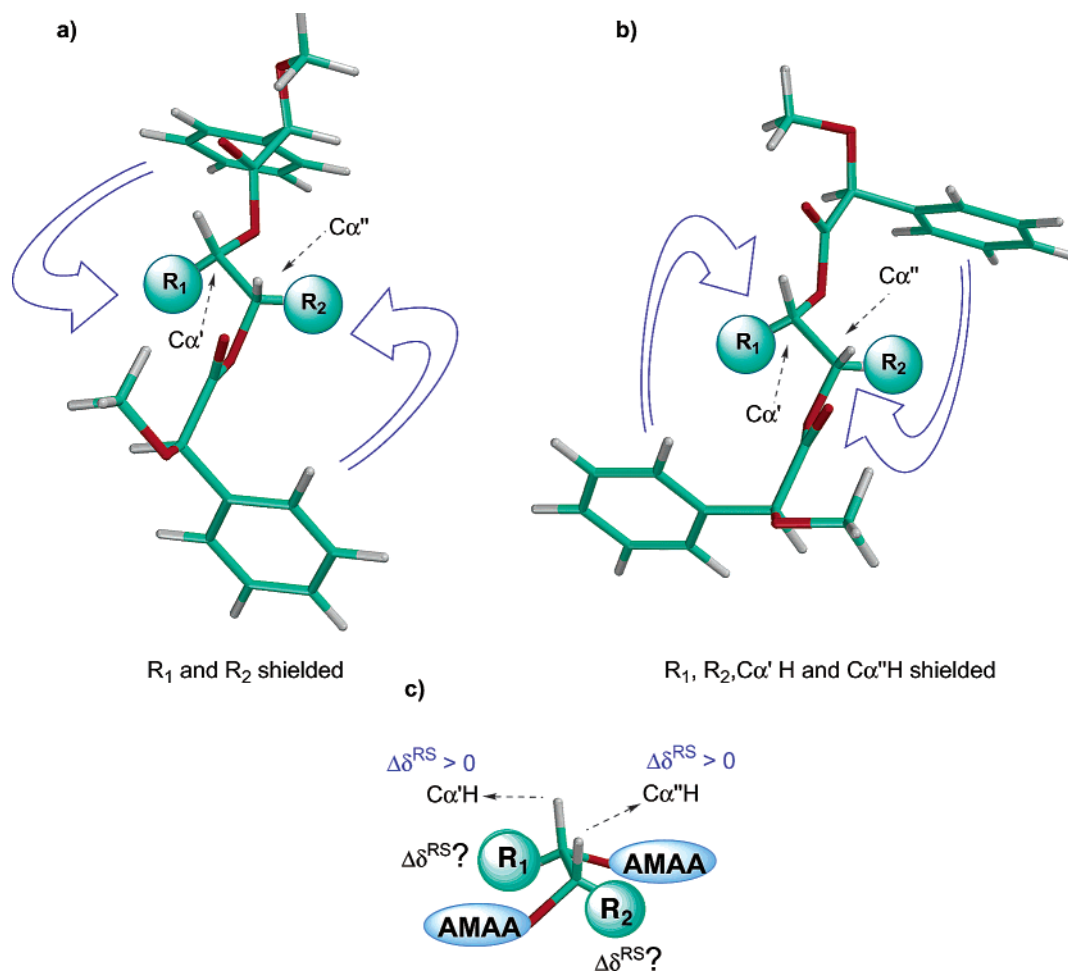


**Figure 167.** (*R*)- and (*S*)-MPA diester of a syn-1,2-diol, and expected  $\Delta\delta^{RS}$  signs. Arrows show the shielding produced by the phenyl groups.

reliable reagent for assignment of configuration of primary alcohols (see section 3.2 of this review) and that its application in the case of tanshindiol (**164.1**) is determined by the chelating ability of the tertiary hydroxyl group.

In the second and more general approach, the two functional groups are made to react with the auxiliary at the same time and the preparation of the bis derivatives is straightforward. However, as mentioned previously, the shifts observed in the NMR spectra of the fully derivatized compound (i.e., the bis-ester of the diol) cannot be interpreted using the models for monofunctional compounds. New and specific models that correlate the absolute stereochemistry of diols with the NMR spectra of their bis-AMAA esters have recently been described and will be presented in the next section of this review.

### 3.9.1. MPA and 9-AMA

The use of MPA on substrates that have several chiral hydroxyl groups was first described by Riguera et al.<sup>104</sup> in a study on polypropionate metabolites from the marine mollusk *Onchidium* sp. The configurations of the onchitriols **165.1** and **165.2** were established by comparison of the  $\Delta\delta^{RS}$  values of the bis-MPA esters with those of selected diols of known absolute configuration, such as (*2R,4R*)-(–)-pentanediol (Figure 165).

Years later, the correspondence between the absolute configuration of a series of diols of known configuration and the NMR spectra of their bis-AMAA derivatives was studied by the same group, and a general methodology to determine the configuration of 1,*n*-diols (1,2-diols, 1,3-diols etc.) from the NMR spectra of the bis esters was presented.<sup>105a</sup> In this procedure, the diol is fully esterified with the *R* and the *S* auxiliary (MPA or 9-AMA) and the  $\Delta\delta$  signs are interpreted as being the result of the combined action of the two auxiliary units.

This approach is based on the fact that the aromatic shielding is a through-space phenomenon; each reagent unit contributes to the chemical shift of a given proton in a different way (shielding or deshielding) and with a different strength, depending on the actual structure of the diol. As a consequence, the chemical shifts (and  $\Delta\delta^{RS}$  values) observed are the result of the additivity of the shielding/deshielding effects produced by all the auxiliary reagents present in the bis ester. This overall effect can be predicted for each stereochemical combination if the conformational composition of the AMAA esters is known. In fact, the predicted  $\Delta\delta^{RS}$  signs are fully in agreement with the experimental results for many diols of known absolute configuration.

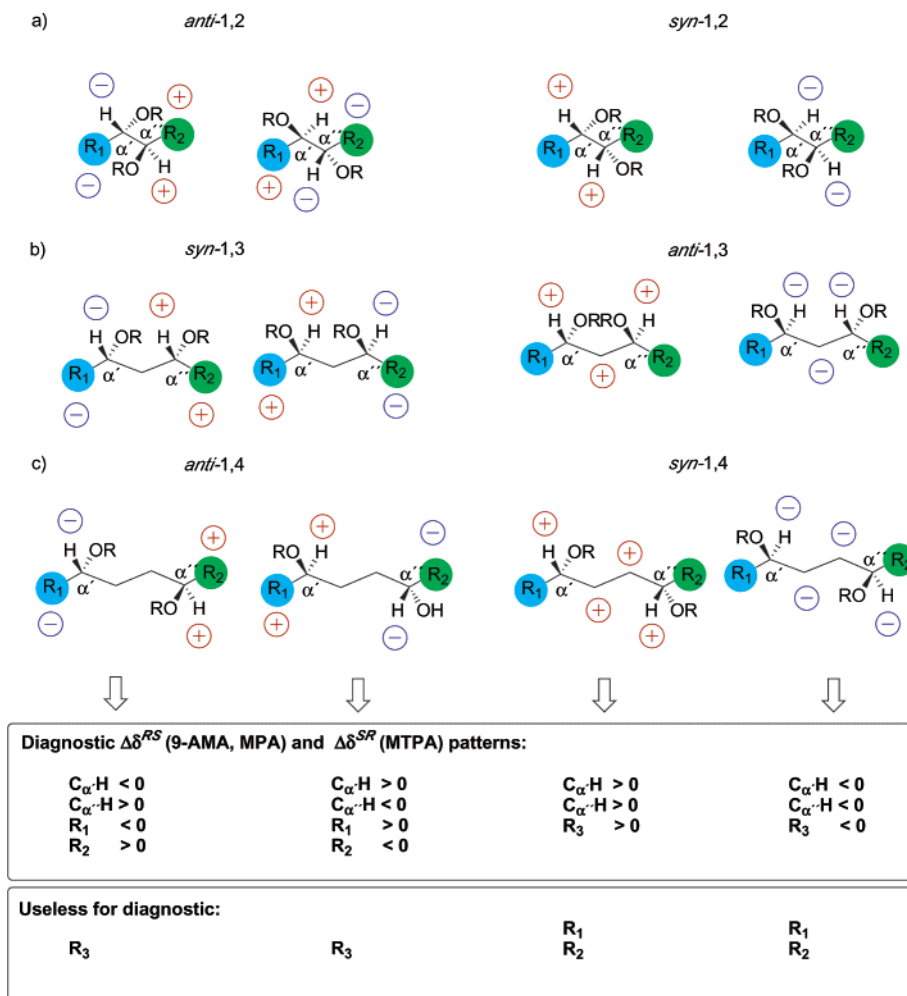


**Figure 168.** Diagnostic  $\Delta\delta^{RS}$  (9-AMA, MPA) and  $\Delta\delta^{SR}$  (MTPA) signs for the four stereoisomers of (a) 1,2-diols, (b) 1,3-diols and (c) 1,4-diols.  $R_3$  represents the substructure between the chiral centers in diols other than 1,2 systems.

Clearly, if the experimental  $\Delta\delta$  values were interpreted as if they were caused by just one reagent unit (and neglecting the effect of the other), using the models for monofunctional compounds, the resulting assignment may be incorrect.

If we consider the conformational characteristics of the AMAA esters of secondary alcohols previously discussed, and apply them to the case of a vicinal diol, the schematic diagrams that are presented in Figure 166 result.

In Figure 166a, the shielding/deshielding zones originated by the aryl group of an anti-1,2-diol derivatized as bis-MPA ester are presented: in the bis-(*R*)-MPA ester, the  $R_2$  group and  $C_{\alpha'}H$  are shielded, whereas in the bis-(*S*)-MPA ester, only the  $R_1$  group and  $C_{\alpha}H$  are shielded. Thus, negative  $\Delta\delta^{RS}$  ( $\delta^{R,R} - \delta^{S,S}$ ) values should be expected for  $R_2$ , and  $C_{\alpha'}H$ , and positive  $\Delta\delta^{RS}$  values are expected for  $R_1$ , and  $C_{\alpha}H$ . If the configuration of the diol were the opposite, the signs also would be opposite.

When a syn-1,2-diol is considered (Figure 167), caution must be taken into consideration, because only the signals due to the protons in  $\alpha$  positions are useful for assignment. Figure 167 shows that  $R_1$  and  $R_2$  are both shielded in the bis-(*R*)- and (*S*)-MPA

diester, which makes prediction of the sign of their  $\Delta\delta^{RS}$  values impossible. For its part, the  $C_{\alpha}H$  and  $C_{\alpha'}H$  are shielded only in the bis-(*S*)-MPA-diester; thus, a positive  $\Delta\delta^{RS}$  should be expected for both protons  $C_{\alpha}H$  and  $C_{\alpha'}H$ . Once again, if the configuration of the diol were the opposite, the signs also would be the opposite.

The same reasoning can be used to predict the distribution of the  $\Delta\delta^{RS}$  signs in other diols different than 1,2-diols. Figure 168 shows the distinctive  $\Delta\delta^{RS}$  patterns of the four stereoisomers of 1,2-, 1,3-, and 1,4-diols and constitutes a guide for the assignment of the configurations.

Note that, although for monofunctional compounds, the  $\Delta\delta^{RS}$  signs provide sufficient information to distinguish between the two enantiomers (*R* or *S*), in diols with two asymmetric centers, four stereochemical situations are possible (the syn and anti pairs: *RR*, *SS*, *RS*, or *SR*). In fact, four different combinations of shielding/deshielding effects—and, consequently, four different sets of  $\Delta\delta^{RS}$  signs—are predicted and experimentally obtained for those four stereochemical arrangements: one for each stereoisomer. Thus, the absolute configurations of the two chiral centers in any of the four stereochemical

combinations of the diol can be deduced from just the NMR of the corresponding bis-AMAA esters.

After the diol of unknown configuration has been derivatized with the two enantiomers of the reagent (MPA or 9-AMA), the  $\Delta\delta^{RS}$  values and signs of the bis esters are calculated in the usual manner. The next stage involves comparison of the signs of  $\Delta\delta^{RS}$  of the diagnostic signals  $C\alpha'H$  and  $C\alpha''H$  with those shown in Figure 168. If both the  $C\alpha'H$  and  $C\alpha''H$  have the same  $\Delta\delta^{RS}$  sign (either both positive or both negative), then the  $\Delta\delta^{RS}$  signs for  $R_3$  (but not for  $R_1/R_2$ ) should also be examined and all three signs should be compared with those of Figure 168 for assignment.

In case  $C\alpha'H$  and  $C\alpha''H$  present opposite  $\Delta\delta^{RS}$  signs (one positive and the other negative), the  $\Delta\delta^{RS}$  signs for  $R_1$  and  $R_2$  (but not for  $R_3$ ) then should be considered and all four signs should be compared with Figure 168 for assignment.

A selection of the diols of known absolute configuration that have been used to demonstrate these conclusions is shown in Figure 169 and includes 1,2- and higher-order diols as substrates and MPA, 9-AMA (**169.1**–**169.9**) and 2-NMA<sup>102a</sup> (**169.11** and **169.12**) as reagents.

Extension of this methodology to the assignment of nonsymmetrical 1,*n*-diols with two secondary (chiral) hydroxyl groups, or with primary and secondary (chiral) hydroxyl groups, as well as amino alcohols, has been conducted and shown to be successful.<sup>105b</sup>

### 3.9.2. MTPA

If the MTPA bis esters of the diols are submitted to the same analysis as the MPA esters, the resulting shielding/deshielding areas around the diol framework and the sign distributions are different from those obtained with MPA and AMAA. This is due to the diverse conformational composition of MTPA esters; however, from a practical standpoint, the same set of signs shown in Figure 168 for AMAA bis esters can be applied by simply using the experimental  $\Delta\delta^{SR}$  values of the MTPA esters as if they were  $\Delta\delta^{RS}$ . The data reported<sup>106</sup> for compound **169.10** serve to illustrate the application of this rule.

There are some examples in the literature of the application of MTPA to the assignment of configuration of diols where the NMR data are interpreted in a variety of ways. Interestingly, note that application of the general model of Figure 168 to the NMR data provided in those papers for the bis-MTPA esters lead, in all cases, to the correct assignment of absolute configuration giving further support to the generality of the models developed by Riguera's group.

Thus, Ichikawa and co-workers<sup>107</sup> studied the assignment of syn and anti diols by NMR of their MTPA esters; unfortunately, only a very small number of compounds (one syn (**170.1**) and two anti (**170.2** and **170.3**); see Figure 170) were examined (their

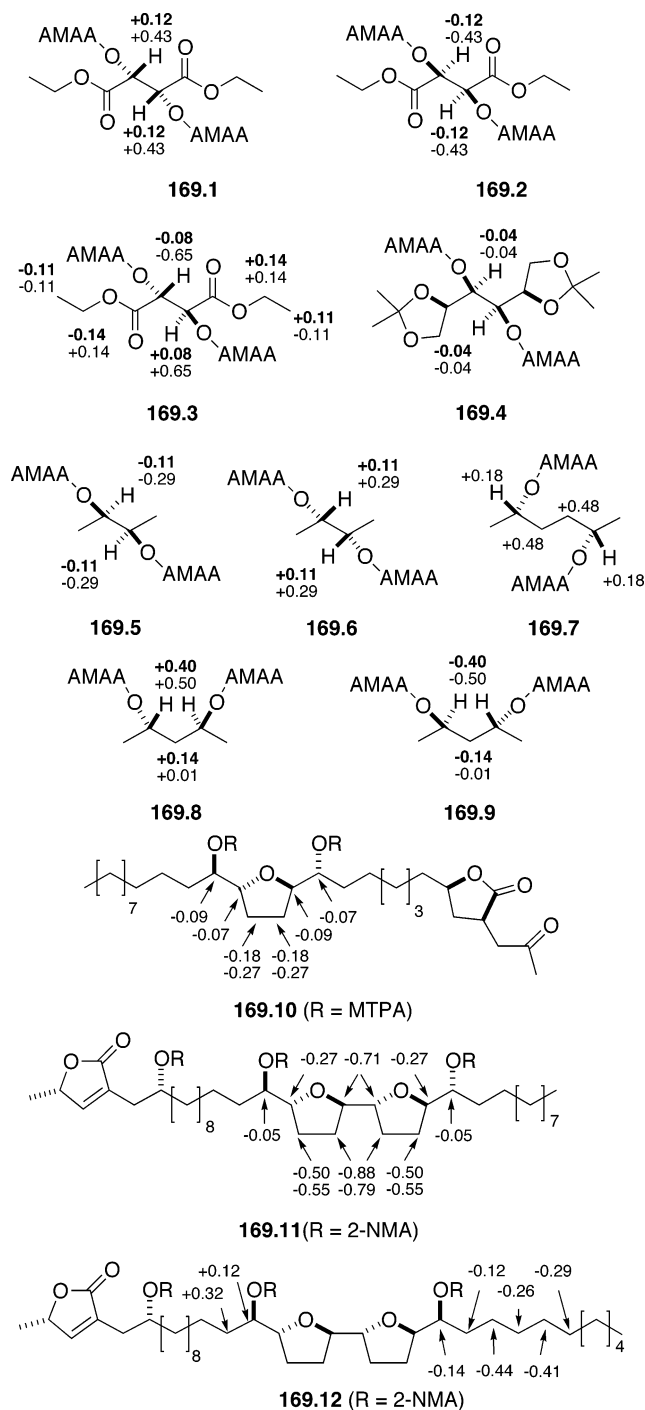


**Figure 169.** Structure and  $\Delta\delta^{RS}$  values obtained for bis-MPA, 9-AMA (**169.1**–**169.9**), 2-NMA (**169.11**–**169.12**), and MTPA (**169.10**). Data given in boldface type corresponds to that of MPA and data given in normal typeface correspond to that of 9-AMA.

configurations were not checked by independent methods: in two cases, the work was done with racemates and the  $\Delta\delta^{SR}$  values inferred from the (*R*)-MTPA derivatives).

According to the authors, the  $\Delta\delta^{RS}$  values of the protons on the asymmetric carbons and their vicinal C atoms are the only ones that can be considered for assignment purposes in the case of syn diols. The remainder protons should be neglected. This is related to the absence of the necessary homogeneity



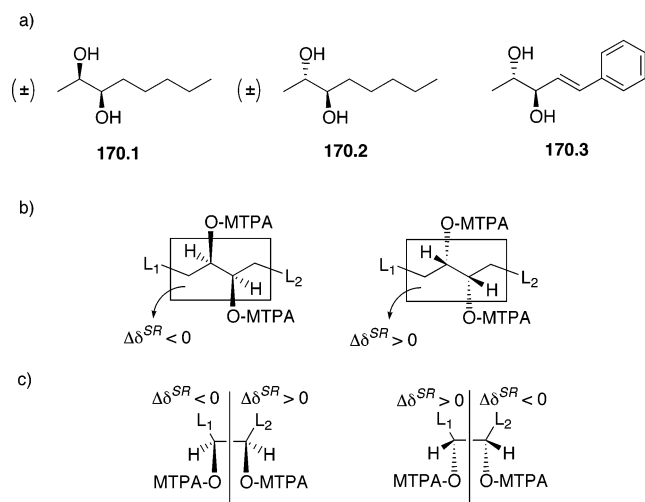


**Figure 170.** (a) Diols used in this study. Models for the determination of configuration of (b) *syn*- and (c) *anti*-1,2-diols with MTPA. Only protons inside the box fit the rule for *syn* diols.<sup>107</sup>

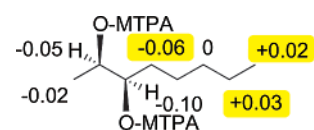


**Figure 171.**  $\Delta\delta^{SR}$  values for a *syn* diol. The lack of homogeneity in the signs obtained for a same L substituent are highlighted.

of  $\Delta\delta^{RS}$  signs in those protons in the *syn* diols (this is a requirement for reliable assignments frequently not fulfilled when MTPA is used as CDA; see Figure 171). A different model applies to *anti* diols (Figure 170).

In another paper<sup>108</sup> by the same group, the assignment by NMR of the bis-MTPA esters of diols that have aromatic groups was studied, as shown in Figure 172 (the inadequacy of MTPA as a reagent for alcohols that possess aromatic groups had already been noted by Ohtani<sup>17a</sup>). This study showed that, for the monoaromatic *anti*-glycols **172.1**, **172.2**, and **172.3**, the model showed in Figure 170 was operative but fail for the monoaromatic *syn*-glycol **172.4** and the bis-aromatic *syn*-glycol **172.5**. The fact that the method did work with the aliphatic *syn*-glycols **172.6** and **172.7** suggested that  $\pi$ - $\pi$  stacking could be the cause of the disagreement between the prediction and the experimental data.

Analysis of the NMR data, following the rules of Figure 168, shows discrepancies in the  $\Delta\delta^{SR}$  signs obtained for the protons at C $\alpha$  and C- $\alpha'$  of monoaromatic *syn*-glycol **172.4** and bis-aromatic *syn*-glycol **172.5**. This finding reinforces the idea that MTPA should not be recommended as CDA for the assignment of *syn*-glycols that possess aromatic groups nor for any diol of unknown relative configuration with aromatic groups.

In a more detailed and recent publication,<sup>109</sup> a series of 1,3-diols (see Figure 173) was studied as bis-MTPA esters and their NMR spectra analyzed in the

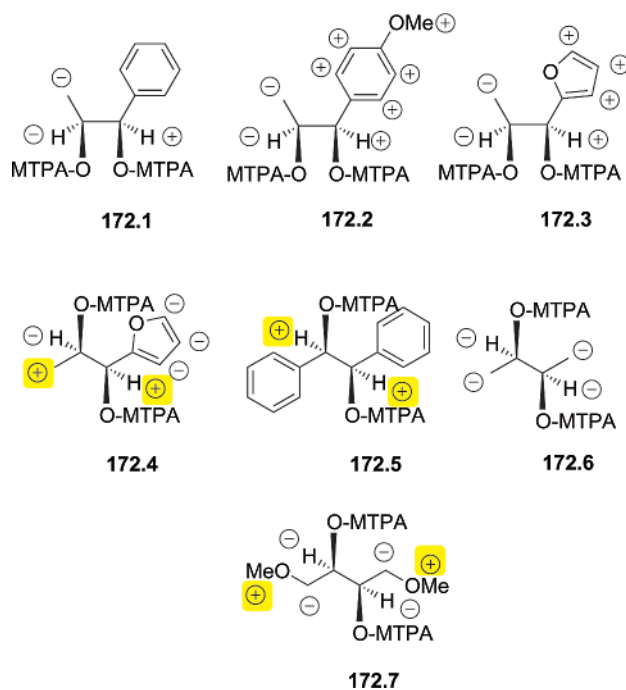


**Figure 172.**  $\Delta\delta^{SR}$  signs obtained from the bis-MTPA esters of glycols. Discrepancies with the models of Figure 170 are highlighted in **172.4**, **172.5**, and **172.7**.

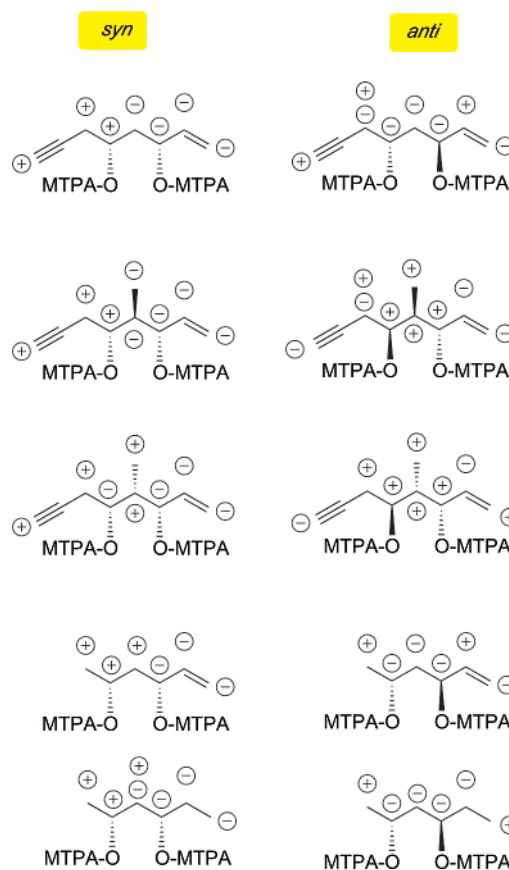


**Figure 173.** Experimental  $\Delta\delta^{SR}$  signs obtained for the bis-MTPA esters of the *syn*- and *anti*-cyclic 1,3-diols shown.

manner proposed by Riguera et al. for 1,*n*-diols. The authors concluded that the method was only applicable to *syn*-1,3-diols, where the values of substituents L<sub>1</sub> and L<sub>2</sub> are diagnostic (but not those of the

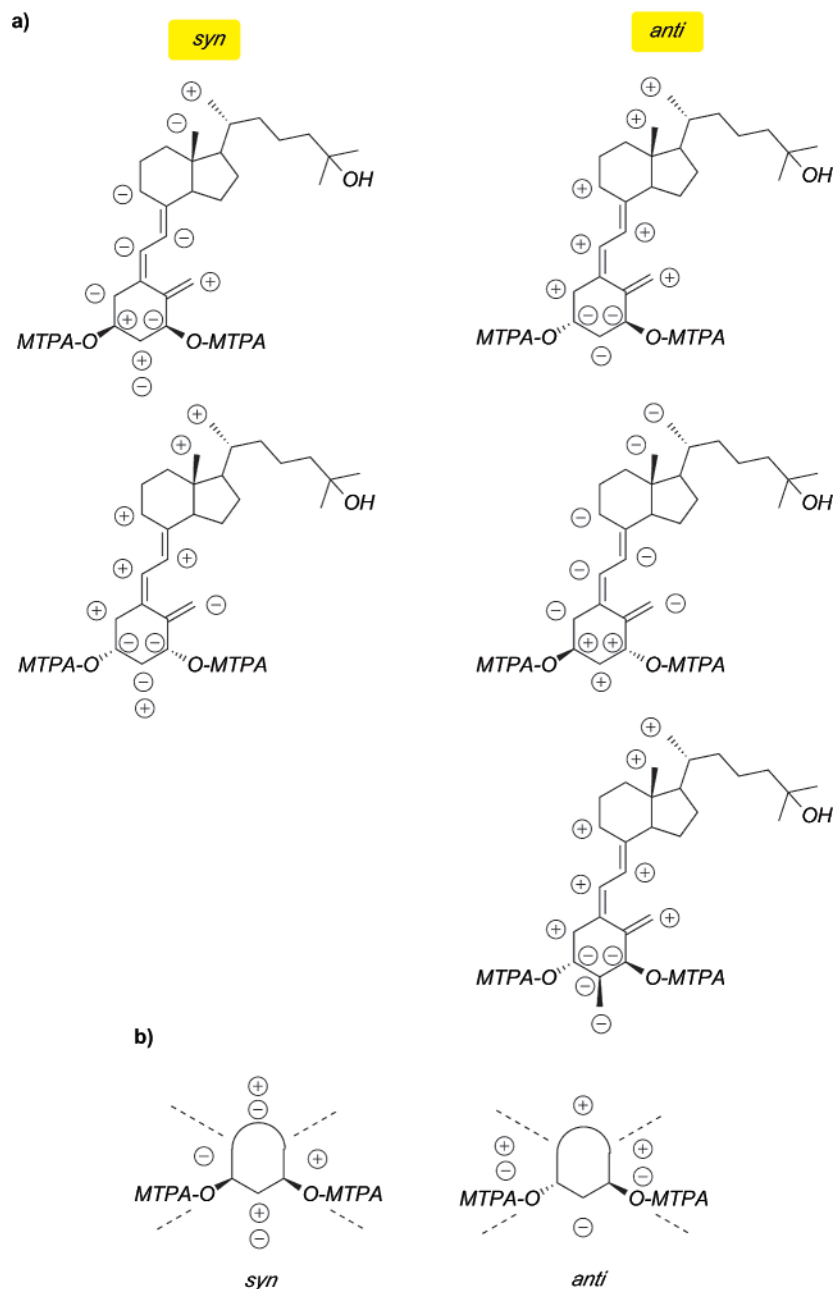


**Figure 174.** (a) Signs of the  $\Delta\delta^{SR}$  obtained for the bis-MTPA esters of *syn*- and *anti*-cyclohexane-1,3-diols used in this study, and (b) predicted  $\Delta\delta^{SR}$  values.

central part). They also state that it should not be applied to anti-1,3-diols, where substituents  $L_1/L_2$  cannot be considered and the central part is, in their opinion, not surely diagnostic. However, in all the cases, the  $\Delta\delta^{SR}$  signs obtained experimentally (Figure 173) are in full agreement with those predicted by Riguera's model for those configurations as shown in Figure 168.

In the same work, six-membered cyclic systems were examined and four zones with distinct  $\Delta\delta$  values, depending on the position around the ring, were proposed (see Figure 174). Five cyclohexane-1,3-diols derived from dihydroxyvitamin D<sub>3</sub> and with known absolute configuration were examined as bis-MTPA esters. Figure 174a shows the experimental  $\Delta\delta^{SR}$  sign distributions and Figure 174b shows the empirical models that have been used.

In the field of natural products, numerous examples can be found of the assignment of configuration by NMR of the bis- or tris-MTPA esters. Only in a few cases have the authors based their assignment on the use of simpler synthetic diols of known configuration as models for comparison. For example, Minale et al. determined the configuration of the side chains of marine polyhydroxysteroids<sup>110a</sup> such as **175.1** and **175.2**, using synthetic 2,3-dimethylpentane-1,2-diols and 2-methyl-3-ethylheptane-1,2-diols, respectively, as models.<sup>110b</sup>

The bis-MTPA derivatives of C27- and C29-alkane-6,8-diols (**175.3**; see Figure 175) were prepared in another report;<sup>110c</sup> however, their NMR data were used simply to discriminate among stereoisomers (in fact, only the small shifts at Me-1 were considered!) and the absolute configuration was not proposed.

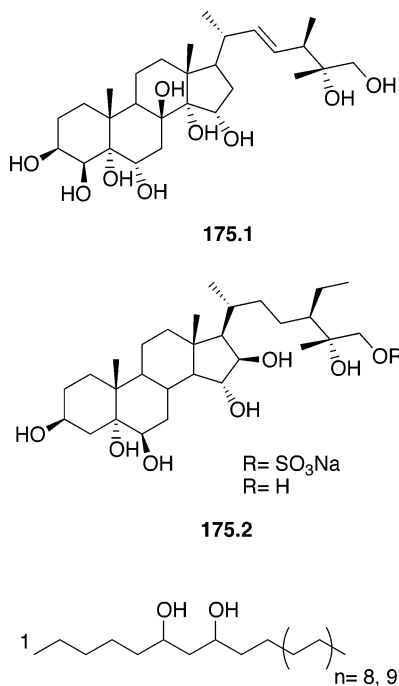


**Figure 175.** Natural products studied as MTPA esters.

#### 4. Methods Based on a Single Derivatization

As we have shown, all the procedures in the preceding pages involve the derivatization of the substrate with the two enantiomers of the reagent

and comparison of the NMR spectra of the corresponding diastereomeric derivatives. Nevertheless, recently, some effort has been devoted to methods that require the preparation of only one derivative. The existence of such a procedure would reduce the time and amount of sample necessary for the analysis by a factor of 2, because only one derivative and one derivatization step would be needed.

Two general approaches can be distinguished. The first applies to secondary alcohols and is based on extensive NMR data, indicating that, when a strong auxiliary reagent such as 9-AMA (but not MPA or MTPA) is used, comparison of the NMR spectra of the secondary alcohol with that of one of its 9-AMA esters (either the *R* or the *S*) allows the safe assignment of the absolute configuration of the alcohol. The procedure, which is summarized in Section 4.1.1, is based on the comparison of the chemical shifts of many secondary alcohols of known absolute configuration and the corresponding (*R*)- or (*S*)-9-AMA ester. A related method, which makes use of glycosylation shifts, is described in Section 4.1.2.

The other approach applies to secondary alcohols and primary amines. It consists on the controlled modification of the conformational equilibrium of the MPA esters and MPA amides and is based on our knowledge of the shielding/deshielding effects associated with each conformer.

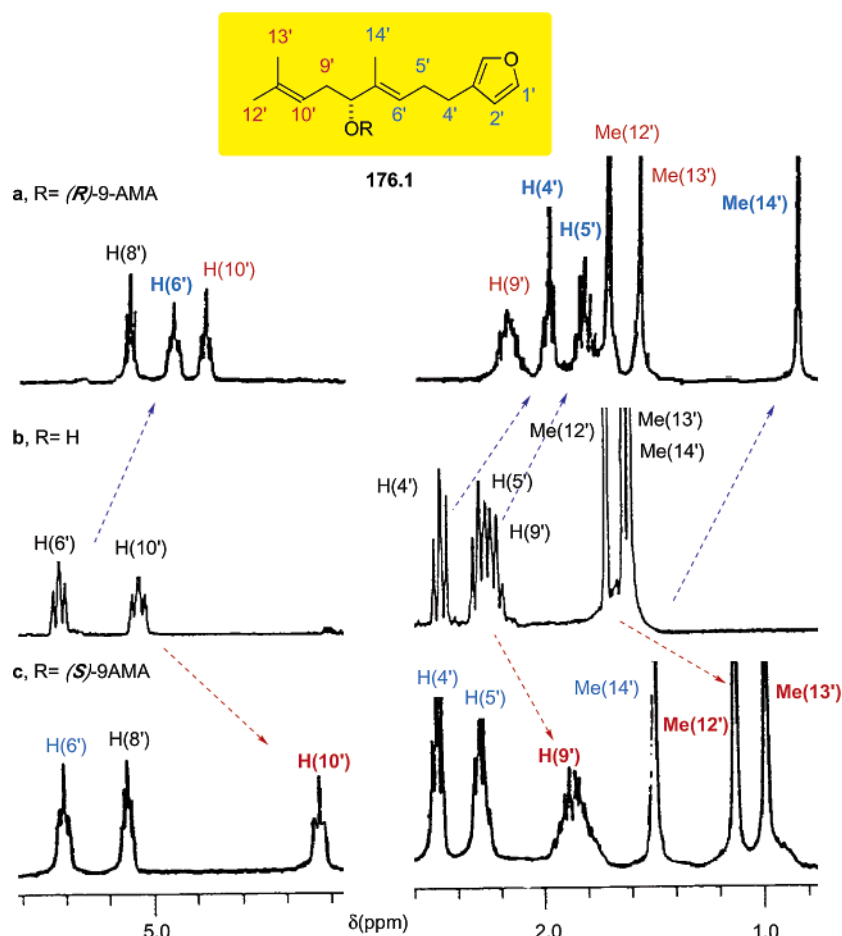


**Figure 176.** Partial <sup>1</sup>H NMR spectra (300 MHz) of (a) the (*R*)-9-anthrylmethoxyacetic acid ester of alcohol **176.1**; (b) alcohol **176.1**; (c) the (*S*)-9-anthrylmethoxyacetic acid ester of alcohol **176.1**.

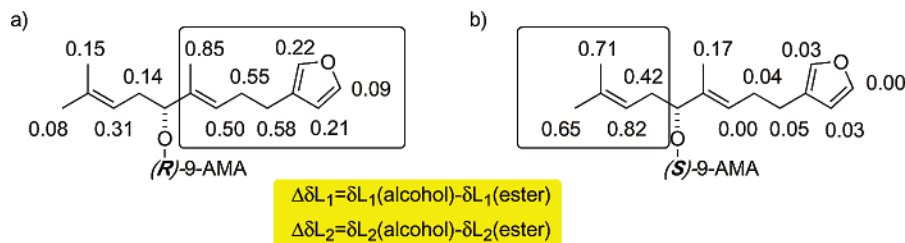


**Figure 177.** (a) Esterification shifts ( $\Delta\delta^{AR}$  values) measured for the (*R*)-9-AMA ester of **176.1**. (b) Esterification shifts ( $\Delta\delta^{AS}$  values) measured for the (*S*)-9-AMA ester. Larger shifts are highlighted.

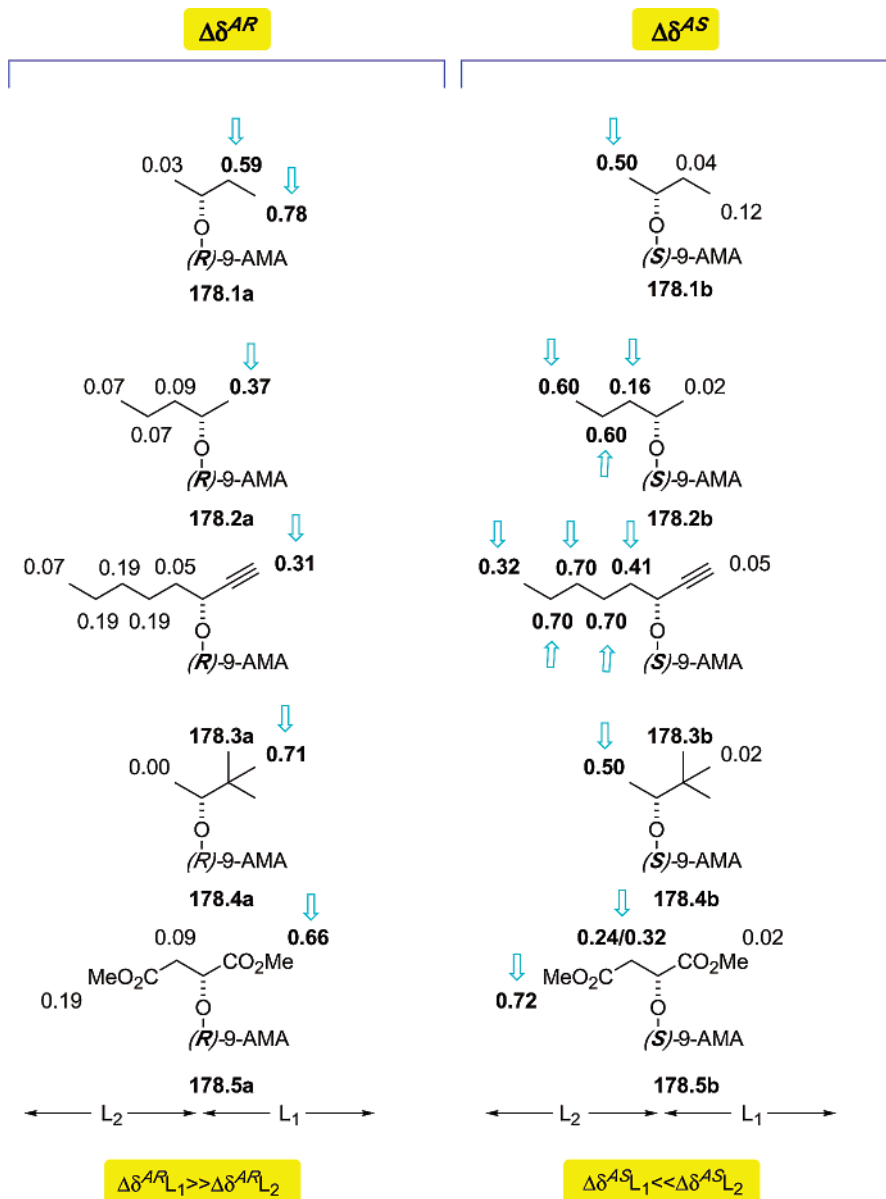


**Figure 178.**  $\Delta\delta^{AR}$  and  $\Delta\delta^{AS}$  values for (*R*) and (*S*)-9-AMA esters of alcohols **178.1–178.5**. (Larger values are given in boldface type.)

If the *sp/ap* conformer ratio is modified in a certain way (i.e., an increase of the *sp* conformer), the NMR spectra should translate such a change in ratio into a predictable modification in the chemical shifts associated with the substituents (i.e., greater population of the *sp* conformer in the (*R*)-MPA ester leads to greater shielding of substituent *L*<sub>1</sub> in the average spectrum). In this way, the spatial position of sub-

stituents *L*<sub>1</sub>/*L*<sub>2</sub>, with respect to the phenyl group of the auxiliary (absolute configuration known), can be determined by the NMR response to the disturbance in the equilibrium.

Two different procedures have been described to induce the conformational change:

(a) Modification of the equilibrium by reducing the temperature of the NMR probe. This approach has

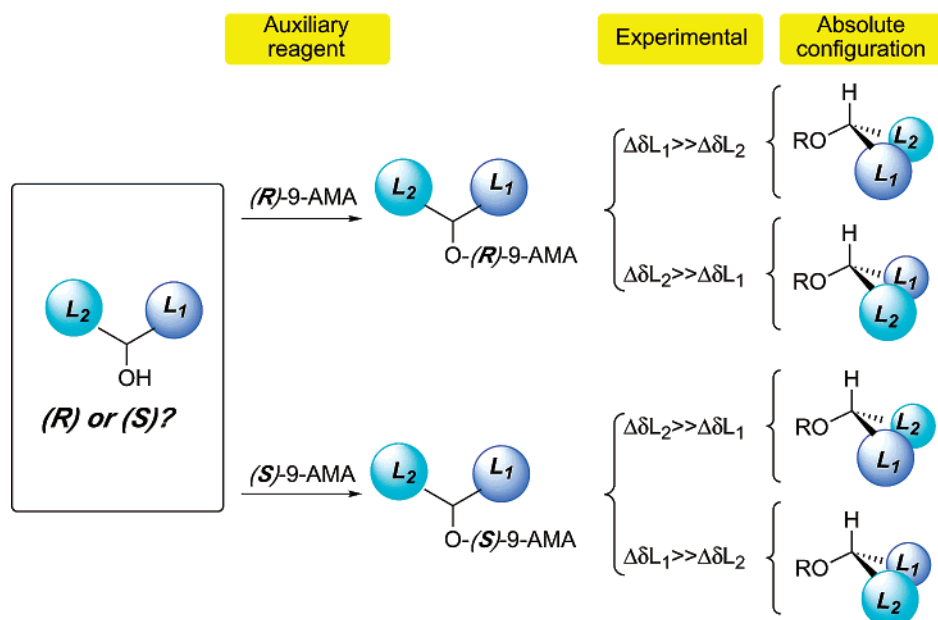


**Figure 179.** Diagram for the assignment of the absolute configuration of a secondary alcohol from  $\Delta\delta^{AR}$  or  $\Delta\delta^{AS}$  values.

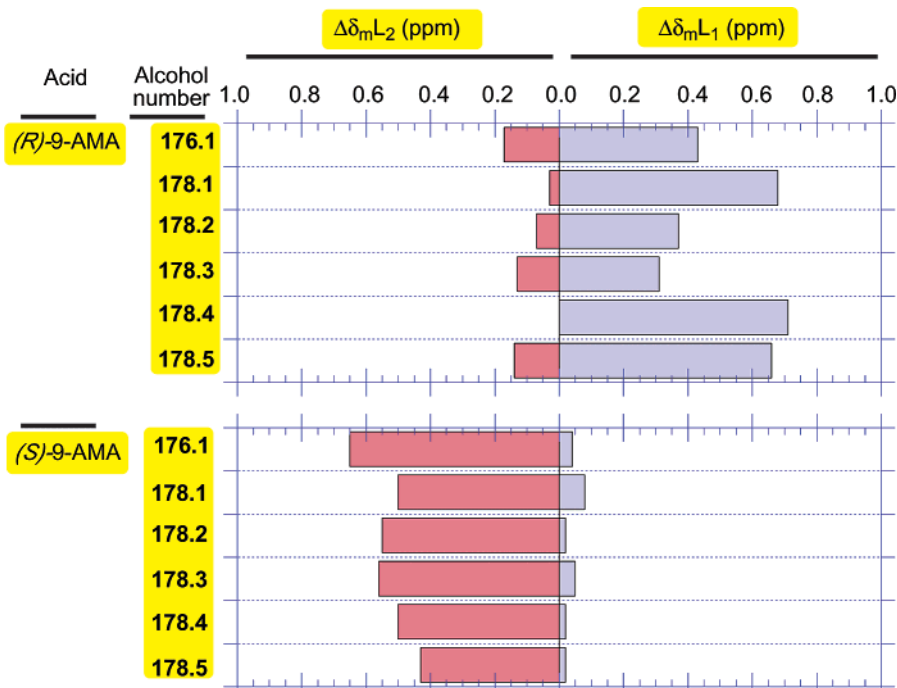


**Figure 180.** Esterification shifts for the (*R*)- and (*S*)-9-AMA esters of alcohols **176.1** and **178.1–178.6**, expressed as mean values ( $\Delta\delta_{mL_1}$  and  $\Delta\delta_{mL_2}$ ).

found application in the assignment of the absolute configuration of secondary alcohols using MPA as an auxiliary reagent (see Section 4.1.3).

(b) Modification of the equilibrium by selective chelation of one of the conformers. This procedure has been described for the assignment of secondary alcohols and primary amines using MPA as an auxiliary reagent and barium(II) salts as chelators (Sections 4.1.4 and 4.2, respectively).

#### 4.1. Application to $\alpha$ -Chiral Secondary Alcohols

##### 4.1.1. 9-AMA Esters: Esterification Shifts

A procedure for the assignment of the absolute configuration of secondary alcohols involving the

preparation of only one derivative has been recently presented by Riguera et al.<sup>35</sup> and consists of a comparison of the NMR spectrum of the alcohol with that of one of its esters prepared with either the (*R*)- or the (*S*)-9-AMA chiral auxiliary.<sup>29,30</sup> When the two resulting spectra are compared, the signals of substituents  $L_1$  and  $L_2$  can be easily distinguished, because the protons of one of those substituents (the one that is under the shielding cone of the anthryl ring in the derivative) move upfield in the 9-AMA ester, with respect to the free alcohol, whereas the protons of the other substituents (unaffected by the aromatic shielding) resonate at practically the same field in both the 9-AMA ester and in the free alcohol.

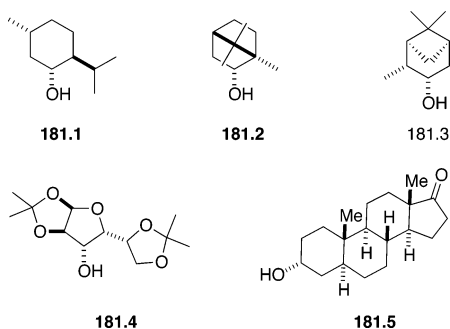


**Figure 181.** Cyclic alcohols studied with this method.

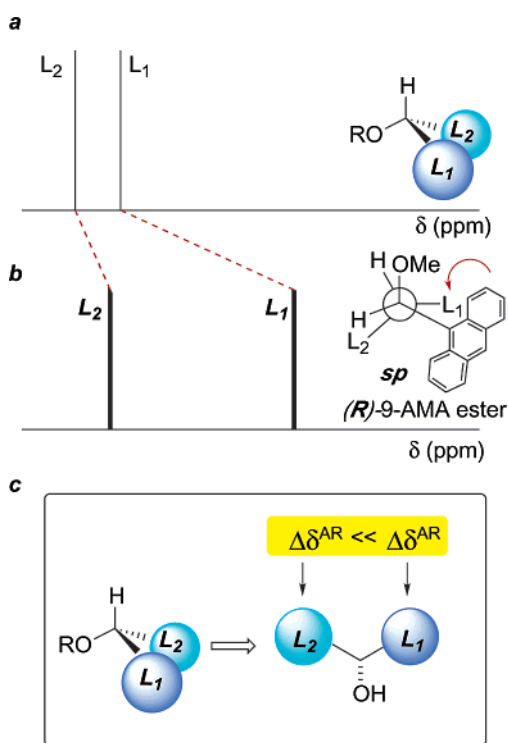


**Figure 182.** (a) <sup>1</sup>H NMR spectrum of a free alcohol. (b) <sup>1</sup>H NMR spectrum of its (*R*)-9-AMA ester. (c) Inferred absolute configuration from the  $\Delta\delta^{AR}$  values.

Consideration of the absolute configuration of the auxiliary reagent ((*R*)- or (*S*)-9-AMA) and the spatial location of its anthryl ring allows the placement of substituents L<sub>1</sub>/L<sub>2</sub> around the asymmetric C atom.

An example illustrating the esterification shifts observed in the marine metabolite<sup>40</sup> **176.1** is shown in Figure 176.

In the (*R*)-9-AMA ester (Figure 176a), H(6'), H(5'), and H(4') are intensely shielded, with respect to the same protons in the free alcohol (Figure 176b), while H(9'), H(10'), Me(12'), and Me(13') resonate at practically identical chemical shifts in the ester and in the alcohol (the opposite is observed in the (*S*)-9-AMA ester; see Figure 176c). These esterification shifts are quantitatively expressed for each individual proton as the difference between the chemical shift in the free alcohol and that in the ester ( $\Delta\delta^{AR}$  or  $\Delta\delta^{AS}$ , depending on which 9-AMA ester has been examined). Figure 177 shows the  $\Delta\delta^{AR}$  and  $\Delta\delta^{AS}$  values obtained for compound **176.1**.

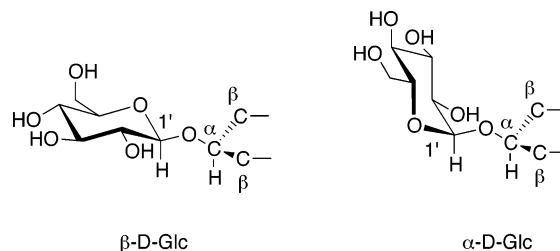


**Figure 183.** Glucosides studied by the procedure of glucosidation shifts in <sup>13</sup>C NMR.

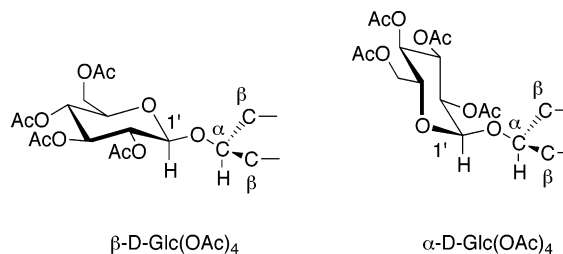


**Figure 184.** Tetra-*O*-acetylglucosides studied by the procedure of glucosidation shifts in <sup>1</sup>H NMR.

Several linear secondary alcohols of known absolute stereochemistry (Figure 178) have been examined in this way, and the results corroborate the existence of the aforementioned correlation between the spatial position of substituents L<sub>1</sub>/L<sub>2</sub> of the alcohol, the configuration of the auxiliary, and the NMR shifts.

Thus, in the (*R*)-9-AMA esters represented in Figure 178, the most intensely shielded protons are all located in the right-hand substituent (L<sub>1</sub>), whereas those that are only slightly shielded are located in the left-hand substituent (L<sub>2</sub>) ( $\Delta\delta^{AR}L_1 \gg \Delta\delta^{AR}L_2$ ): The reverse occurs in the (*S*)-9-AMA esters, where  $\Delta\delta^{AS}L_1 \ll \Delta\delta^{AS}L_2$ .

In this way, the configuration of a secondary alcohol such as *sec*-butanol (**178.1**) is *R* (as indicated in Figure 178) if the more intensely shielded protons in the (*R*)-9-AMA ester are in the right-hand side of the projection (i.e., the ethyl substituent) and those that are only very slightly shielded are on the left-hand side (i.e., the methyl substituent). This arrangement results in  $\Delta\delta^{AR}L_1 \gg \Delta\delta^{AR}L_2$ . The reverse ( $\Delta\delta^{AS}L_1 \ll \Delta\delta^{AS}L_2$ ) is observed when the enantiomeric reagent (*S*)-9-AMA is used and also when the configuration of the *sec*-butanol is *S* (opposite to that shown in Figure 178). A graphical resume for application of this procedure is shown in the model of Figure 179.

The plot shown in Figure 180 represents the intensity of the  $\Delta\delta$  parameter ( $\Delta\delta_m$ ) produced by 9-AMA on the alcohols **176.1** and **178.1–178.5**, and measured as mean values ( $\Delta\delta_m$ ) of all the protons in substituents L<sub>1</sub> and L<sub>2</sub> ( $\Delta\delta_{mL_1}$  and  $\Delta\delta_{mL_2}$ ).

Application of this methodology to cyclic alcohols is also possible, and compounds **181.1–181.5** (Figure 181) presented esterification shifts that were coherent with their stereochemistry and the model of Figure 179. The use of the mean values  $\Delta\delta_{mL_2}$  and

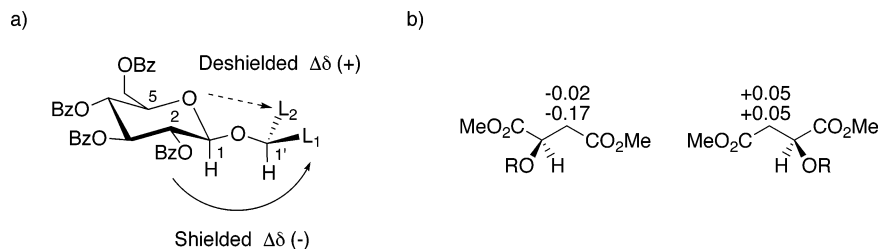


**Figure 185.** (a) Correlation model for secondary alcohols as  $\beta$ -D-glucopyranosides. (b)  $\delta D - \delta ROH$  values for dimethyl D- and L-malate (in ppm, at room temperature,  $CDCl_3$ ).

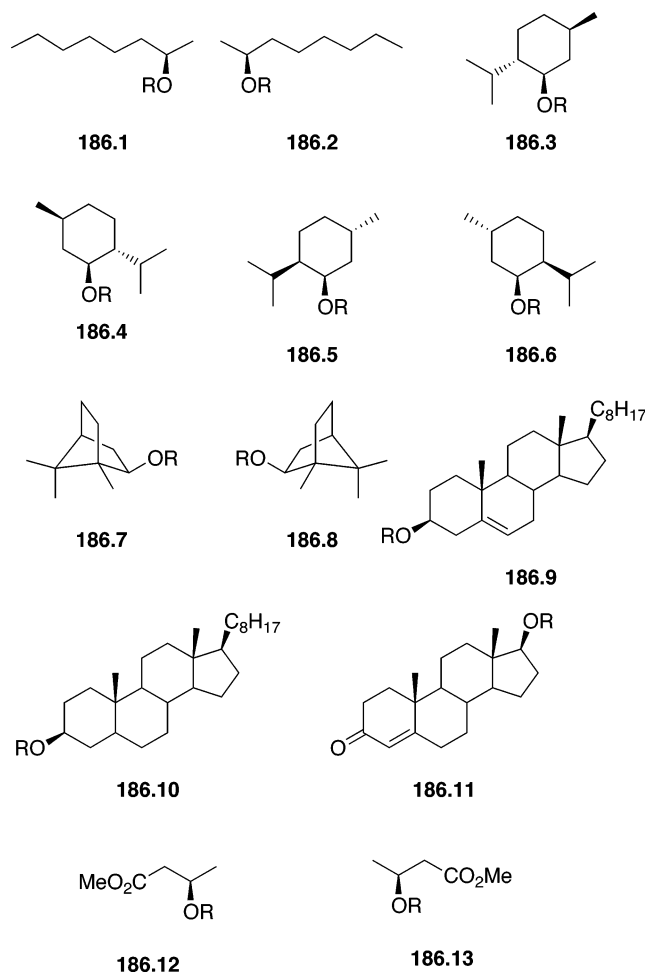


**Figure 186.** Alcohols of known configuration studied as  $\beta$ -D-glucopyranosides.

$\Delta\delta_{mL_1}$  is recommended for assignment of the configuration of these cyclic structures.

From a theoretical standpoint, the different esterification shifts observed for the shielded and non-shielded substituents are explained on the basis of the conformational composition and structure of the 9-AMA esters (see Figure 46 in Section 3.1.3). In the (*R*)-9-AMA ester of the alcohol of Figure 46, substituent  $L_1$  is located under the shielding cone of the anthryl ring of the reagent in the *sp* conformer, whereas in conformer *ap*, it is not shielded. The reverse holds for substituent  $L_2$  (shielded in the minor conformer *ap* and unaffected in *sp*) and, as a result, when one compares the spectrum of an alcohol in Figure 182a with that of its (*R*)-9-AMA derivative,

the signals for substituent  $L_1$  are shifted to a greater extent than those in  $L_2$  (Figure 182b).

In this way, the signals of the alcohol that are strongly shifted upfield upon esterification with (*R*)-9-AMA correspond to the protons that are located on the same side as the anthryl group in the *sp* conformer, i.e., the right-hand side of the asymmetric center in the projection shown (substituent  $L_1$  in Figure 182c). In turn, the protons that are slightly shielded (as they are not affected by the aryl group) are located on the left-hand side (substituent  $L_2$ , Figure 182c). The reverse holds for the (*S*)-AMA esters and also when the configuration of the alcohol is opposite.

Attempts to use auxiliary reagents other than 9-AMA for assignment of the configuration were unsuccessful. Thus, when the (*R*)- and (*S*)-MPA auxiliaries were tested with a wide range of substrates, the  $\Delta\delta^{AR}$  and  $\Delta\delta^{AS}$  obtained were very small and negative in some cases. As a consequence, the identification of substituent  $L_1$  or  $L_2$  by association with the shielded and nonshielded protons is not always possible; therefore, MPA cannot be recommended for this approach.

Similarly, 1- and 2-naphthylmethoxyacetic acids (1-NMA and 2-NMA, respectively) were assayed with linear secondary alcohols and did not give satisfactory results, although a limited approach based on certain empirical increment parameters has been proposed.<sup>111</sup>

#### 4.1.2. Glycosidation Shifts

**4.1.2.1. Glycosidation Shifts in  $^{13}C$  NMR.** A method for determining the absolute configuration of a secondary hydroxyl group based on characteristic glycosidation-induced shifts in  $^{13}C$  NMR spectroscopy was reported previously in the development of NMR methods for configurational assignment.<sup>55a,b</sup> The general strategy consists of several steps that include (a) measurement of the  $^{13}C$  NMR spectrum of the secondary alcohol (in pyridine-*d*<sub>5</sub>), (b) synthesis of the corresponding  $\beta$ -D- or  $\alpha$ -D-glucopyranosides (Figure 183), (c) measurement of the  $^{13}C$  NMR spectrum of either the  $\beta$ -D- or  $\alpha$ -D-glucopyranoside, (d) calculation of the glycosidation-induced shift variations for the anomeric carbon and for the  $\alpha$ - and  $\beta$ -carbons of the aglycone using the relations  $\Delta\delta(\text{anomeric carbon}, 1')$

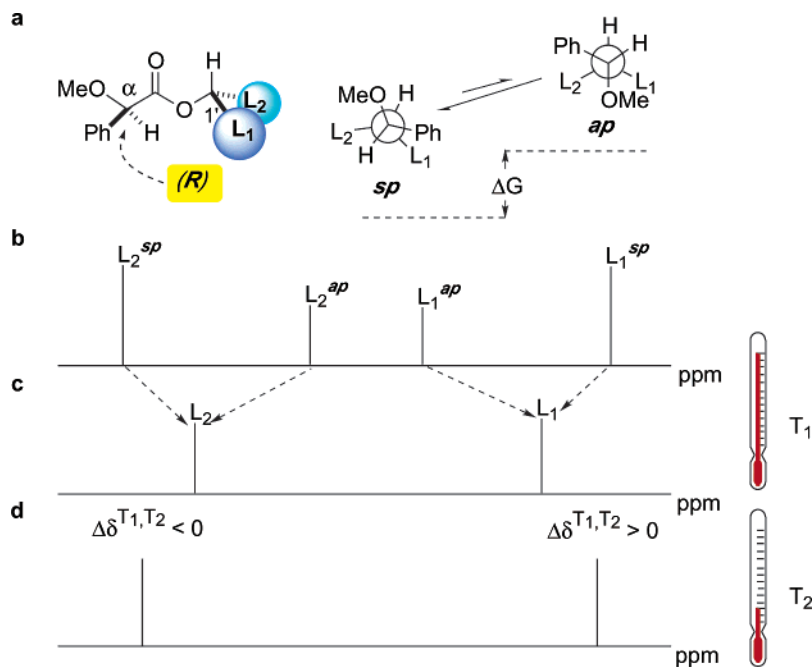


**Figure 187.** (a) Structure of the *sp* and *ap* conformers of an (*R*)-MPA ester. (b) Chemical shifts of substituents  $L_1$  and  $L_2$  in the *sp* and *ap* conformers. (c) Average chemical shifts of  $L_1$  and  $L_2$  at room temperature ( $T_1$ ). (d) Average chemical shifts of  $L_1$  and  $L_2$  at low temperature ( $T_2$ ).

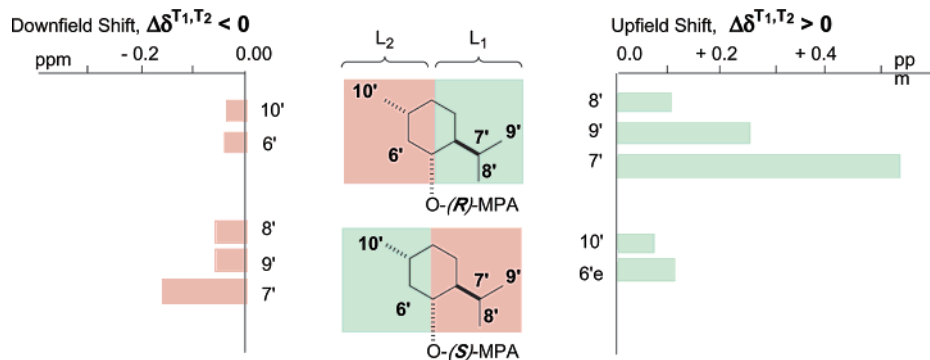


**Figure 188.** Distribution of shielded and deshielded areas in the (*R*)- and (*S*)-MPA esters of (-)-menthol and selected  $\Delta\delta^{T_1,T_2}$  values.

$= \delta(\text{alcoholic glucoside}) - \delta(\text{methyl glucoside})$  and  $\Delta\delta(\alpha\text{- and } \beta\text{-carbons}) = \delta(\text{alcoholic glucoside}) - \delta(\text{alcohol})$ , and (e) the absolute configuration of the alcohol is then determined by comparison of the  $^{13}\text{C}$  NMR chemical-shift changes with the glucosidation shifts of a series of secondary alcohols of known absolute configuration, classified according to their steric hindrance and degree of substitution in the C atoms next to the chiral center.

A caution note alerts the readers about the application of this procedure to sterically crowded alcohols.

**4.1.2.2. Tetra-*O*-acetyl- $\beta$ -glucosylates in  $^1\text{H}$  NMR.** The tetra-*O*-acetylglucosidation-induced  $^1\text{H}$  NMR shifts of a series of secondary alcohols were also found highly characteristic of their absolute configuration.<sup>55c</sup> Particularly important for the diagnostics were the protons of the aglycone attached to the C atoms at the  $\beta$ -position (see Figure 184), and accordingly, the tetra-*O*-acetylglucosidation-induced  $^1\text{H}$  NMR

shifts were calculated as follows:

$$\begin{aligned} \Delta\delta(\text{anomeric proton, } 1') &= \delta(\text{alcoholic glc-Ac4}) - \\ &\quad \delta(\text{methyl glc-Ac4}) \text{ for the sugar moiety} \\ \text{and} \\ \Delta\delta(\alpha\text{- and } \beta\text{-protons}) &= \delta(\text{alcoholic glc-Ac4}) - \\ &\quad \delta(\text{alcohol}) \text{ for the aglycone unit} \end{aligned}$$

As in the  $^{13}\text{C}$  NMR method, comparison of the values obtained with those of secondary alcohols of known configuration and different steric hindrance is necessary for assignment.

The same caution note that was mentioned previously applies when this procedure is intended for use with highly crowded alcohols.

**4.1.2.3. Tetra-*O*-benzoyl- $\beta$ -glucosylates in  $^1\text{H}$  NMR.** Another procedure based on the comparison of the NMR spectrum of the substrate with that of a



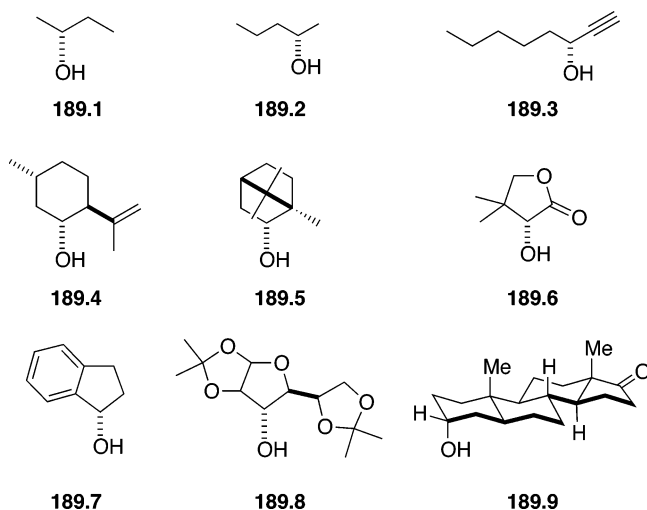


**Figure 189.** Secondary alcohols of known configuration studied through the low-temperature method.

single derivative of an auxiliary reagent, and closely related to the previous methods, has been described by Trujillo et al.<sup>56</sup> for the assignment of the configuration of alcohols.

In this procedure, the chiral alcohol is converted to the corresponding tetra-*O*-benzoyl- $\beta$ -glucoside by reaction with commercial 2,3,4,6-tetra-*O*-benzoyl- $\alpha$ -D-glucopyranosyl bromide in the presence of silver trifluoromethanesulfonate and 1,1,3,3-tetramethylurea. The <sup>1</sup>H NMR spectrum of the product is then compared with that of the free alcohol. The observed differences between the two spectra are caused by the anisotropic effect of the benzoyl groups and the

glycosylation-induced NMR shifts. This effect is quantified as the difference between the chemical shifts in the D-glucopyranoside derivative and the free alcohol ( $\Delta\delta = \delta D - \delta ROH$ ). The protons anti to the endocyclic glucopyranoside oxygen (O-5) are shielded due to the effect of the benzoyl group at C-2 (negative  $\Delta\delta$ ), whereas protons syn to that O atom show positive  $\Delta\delta$  values, because of their proximity to O-5, as shown in the model of Figure 185a. Figure 185b shows experimental  $\Delta\delta$  values that fit the model for an enantiomeric pair of alcohols.

Other alcohols of known absolute configuration that have been used to assess the viability of this methodology are shown in Figure 186. In some cases, the  $\Delta\delta$  signs are opposite to those expected (for instance, in compounds **186.1**, **186.5**, **186.11**, and **186.13**); however, the authors state that the configuration can still be deduced if all the other protons are considered. However, in case of doubt, they recommend that a double-derivatization procedure be used (formation of both the D- and L-benzoylglucopyranosides) and the larger  $\delta D - \delta L$  values considered (Section 3.1.4.7) rather than  $\delta D - \delta ROH$ . Attempts to assign the configuration of the alcohol using the  $\delta D - \delta ROH$  shift of the H atom at the chiral center (C1') alone did not give successful results.

#### 4.1.3. Low-Temperature NMR of MPA Esters

As mentioned previously, reducing the temperature of the equilibrium should lead to an increase in the population of the most stable conformer. In the case

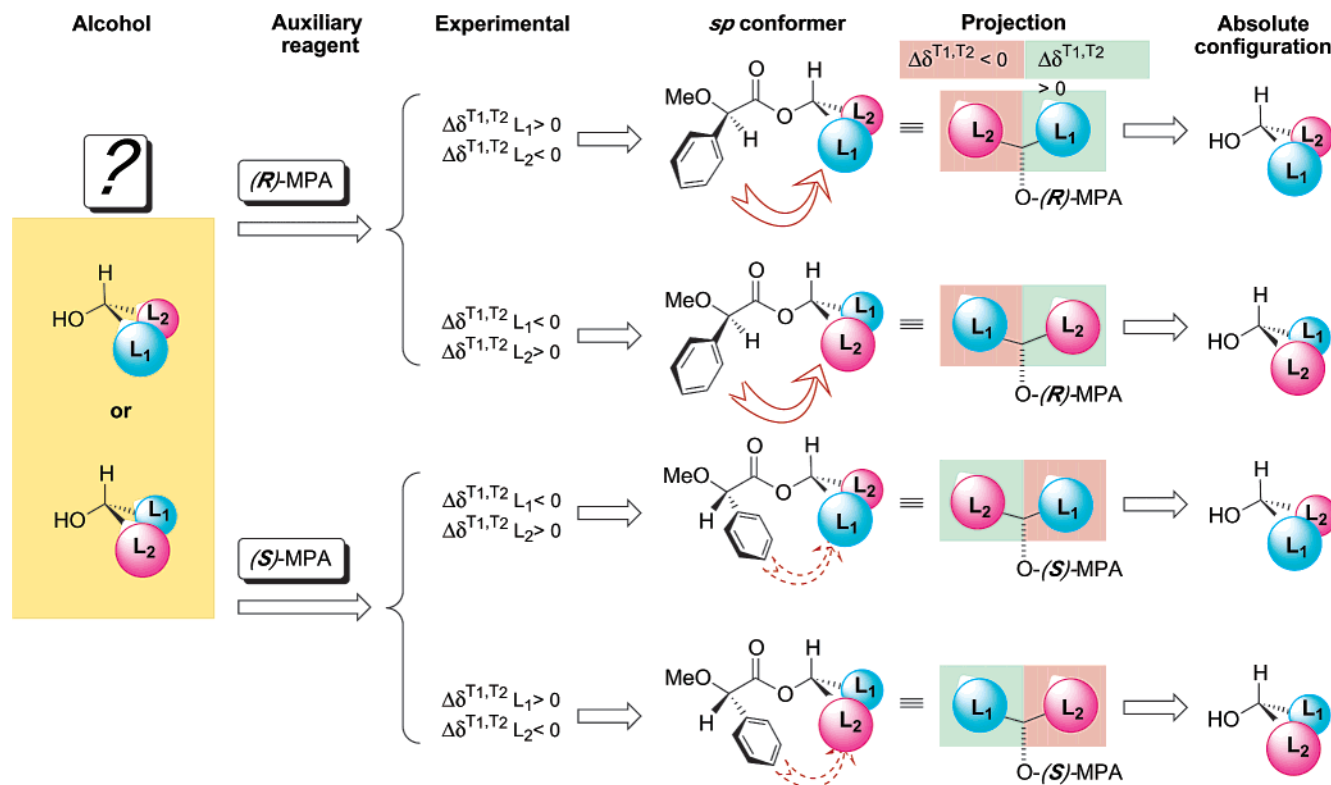


**Figure 190.** Diagram to deduce the absolute configuration of an alcohol from the experimental  $\Delta\delta^{T_1,T_2}$  signs of either its (*R*)- or (*S*)-MPA ester.

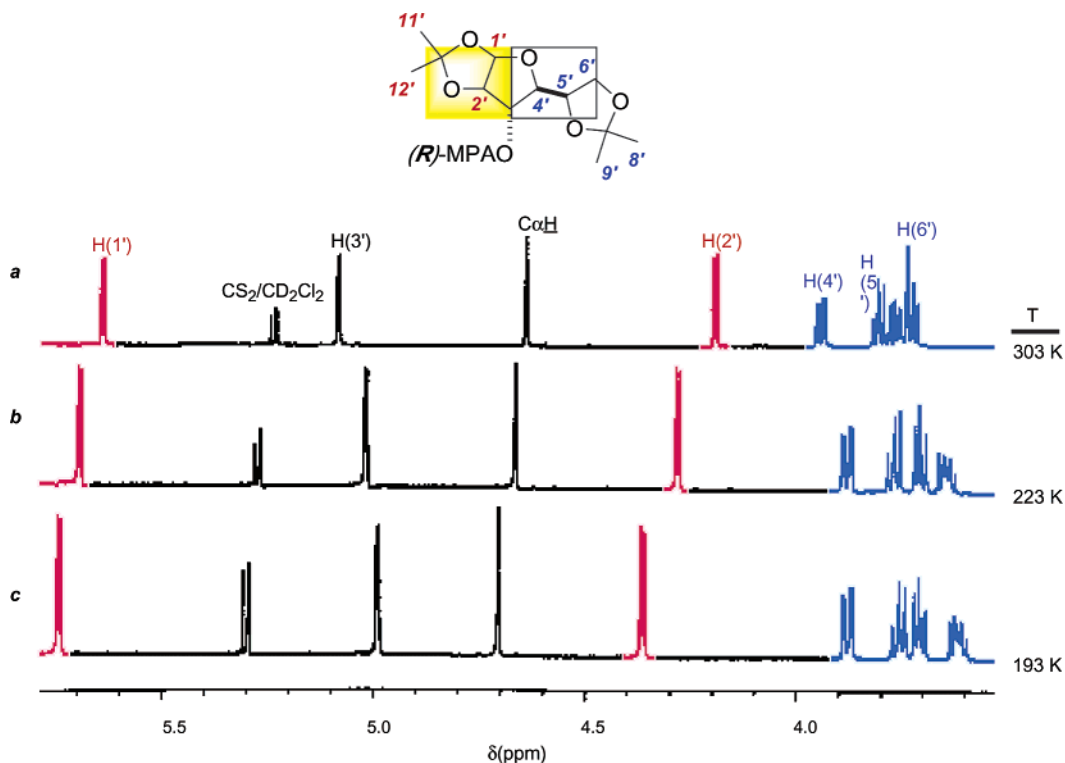


**Figure 191.** Partial spectra of the (*R*)-MPA ester of diacetone-*D*-glucose at (a) 303, (b) 223, and (c) 193 K in  $\text{CS}_2/\text{CD}_2\text{Cl}_2$ .

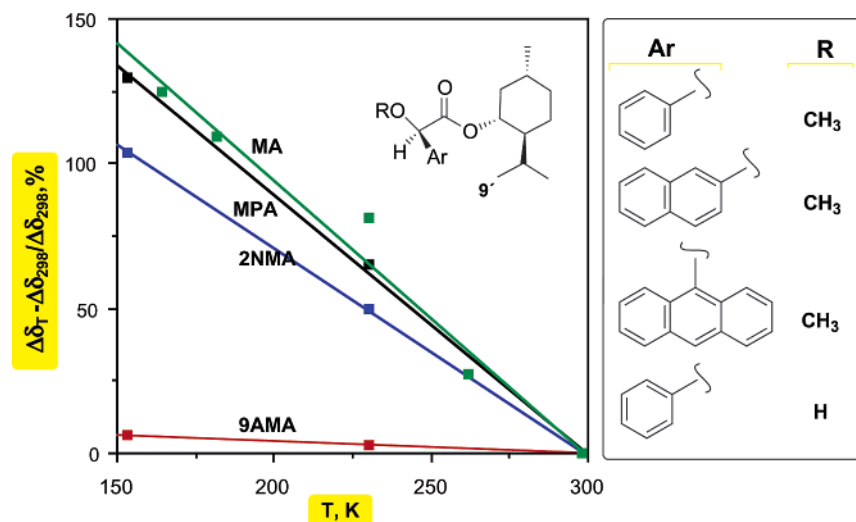


**Figure 192.** Plot of the proportional increase of  $\Delta\delta^{RS}$  with decreasing probe temperature  $T$  (in K) for the Me(9) group of (–)-menthyl esters of arylmethoxyacetic acids.

of MPA esters, this is the *sp* conformer and, therefore, greater shielding of the substituent located on the same side as the Ph group in the (*R*)-MPA ester is expected. The practical application of this approach requires the preparation of a single MPA ester (either the *R* or the *S* derivative) and comparison of two  $^1\text{H}$  NMR spectra taken at two sufficiently different temperatures.<sup>112</sup> The differences in chemical shifts are now measured as  $\Delta\delta^{T_1T_2}$  (the chemical shift at the higher temperature  $T_1$  minus that at the lower temperature  $T_2$ ) and obey the scheme shown in Figure 187, where, at lower temperature, the signal for substituent  $L_2$  moves to lower field and that of substituent  $L_1$  to higher field. The sign of this

parameter is positive for substituent  $L_1$  (the group located on the same side as the Ph ring) and negative for substituent  $L_2$  (the group located on the other side) and provides the configurational information.

Several alcohols of known absolute stereochemistry have been used to demonstrate the general applicability of this phenomenon. Figure 188 shows the shielded and deshielded areas in the MPA esters of (–)-menthol. Other alcohols that have been tested are shown in Figure 189. From a practical standpoint, it seems that temperatures lower than  $-70^\circ\text{C}$  are not necessary, and, therefore, the commonly used  $\text{CDCl}_3$  or a  $\text{CS}_2/\text{CD}_2\text{Cl}_2$  (4:1) mixture can be used as the NMR solvent. The scheme shown in Figure 190

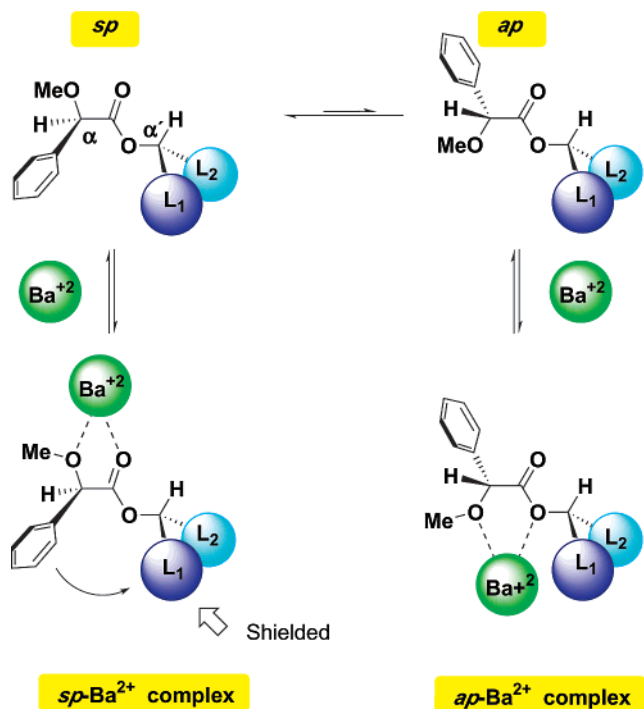


**Figure 193.** Formation of  $Ba^{2+}$  complexes of the (*R*)-MPA ester of a chiral secondary alcohol. The population of the *sp* form increases by formation of the most stable *sp*- $Ba^{2+}$  complex, so the signals for substituent  $L_1$  shift to higher field.

outlines the steps that should be followed for the application of this methodology using either the (*R*)- or (*S*)-MPA derivative.

Figure 191 shows the actual spectra of the (*R*)-MPA ester of diacetone-D-glucose, taken at 303, 223, and 193 K, and illustrates the upfield and downfield shifts of the protons situated on the shielded and non-shielded areas around the chiral center.

Curiously, when the usually more efficient reagent 9-AMA was used instead of MPA, no improvement in the  $\Delta\delta^{T_1 T_2}$  values was observed and this is related to the different *sp/ap* ratio present in the two

reagents.<sup>29,30</sup> In fact, the study of the sensitivity of chemical shifts, relative to changes in the temperature, for the esters of (–)-menthol with several reagents (Figure 192) shows that the  $\Delta\delta^{RS}$  values of MA, MPA, and 2-NMA esters increase steadily at lower temperatures whereas those of the 9-AMA esters remain practically constant. This is because in the first case there is a progressive shift of the equilibrium toward the most stable *sp* conformer whereas, in the 9-AMA esters, the *sp/ap* ratio is at room-temperature already shifted toward the *sp* and there is little place for further displacement.

#### 4.1.4. Complexation of MPA Esters with Barium(II)

A second procedure devised for the controlled shift of the conformational equilibrium in AMAA derivatives consists of the addition of a metal salt that is capable of stabilizing a certain conformer by complexation. Approaches for secondary alcohols<sup>113</sup> and primary amines are described in the literature. In both cases, MPA was used as the auxiliary reagent and barium(II) as the chelating agent.

The conformational equilibrium for the MPA esters of chiral alcohols is outlined in Figure 193. The addition of the  $Ba^{2+}$  salt (i.e.,  $Ba(ClO_4)_2$ ) to the NMR tube containing either the (*R*)- or (*S*)-MPA ester in  $MeCN-d_3$  causes the spectra to change in a way that is practically identical to that observed in the low-temperature experiments, indicating that the conformational changes introduced are similar (i.e., there is an increase in the population of the *sp* conformer). In fact, in addition to  $^1H$  NMR evidence,  $^{13}C$  NMR and CD experiments, together with high-level *ab initio* Hartree–Fock (HF) and density functional theory (DFT) calculations, also prove that the  $Ba^{2+}$  atom becomes strongly bonded to the O atoms of the C=O and MeO groups, therefore leading to an increase in the stability and population of the *sp* form (see Figure 194).

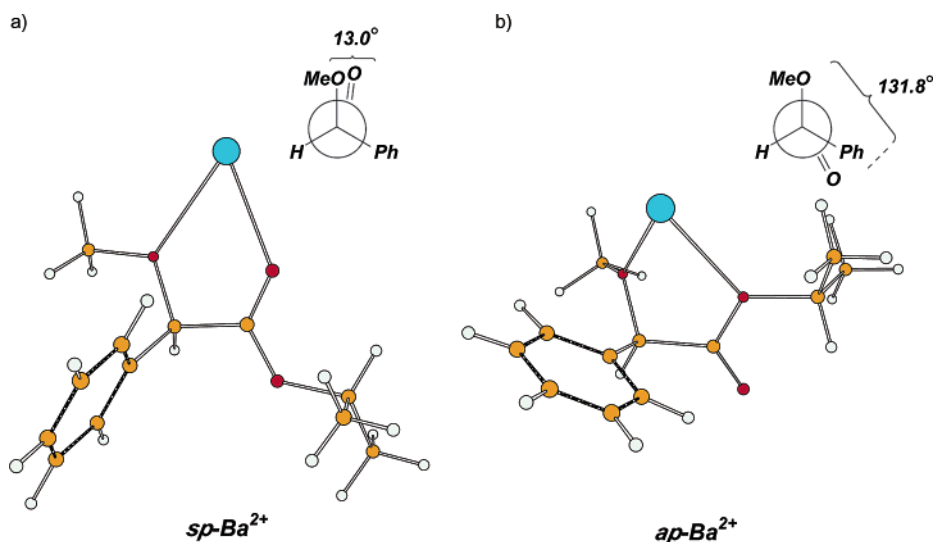


**Figure 194.** HF optimized geometries for the (a) *sp*- $Ba^{2+}$  and (b) *ap*- $Ba^{2+}$  conformers of the (*R*)-MPA ester of 2-propanol. The *sp*- $Ba^{2+}$  geometry is more stable than that of *ap*- $Ba^{2+}$ , by 13.9 kcal/mol.

Several other ions have been investigated but the results are not as good; even the  $\text{Mg}^{2+}$  ion, which is well-known for its superior ability to complex with oxygen donors, produces lower shifts than the  $\text{Ba}^{2+}$  ion. The reasons for this apparent incoherence were highlighted by *ab initio* studies, which showed that, in these cases, powerful solvent–cation interactions are operative and, thus, make these metals less suitable, because of strong solvation by the solvent MeCN. The importance of the  $\text{Ba}^{2+}/\text{MeCN}-d_3$  pair is therefore a key aspect in this method.

From the standpoint of the application of this procedure to the assignment of absolute configuration, only one derivative should be prepared (with either the *R* or *S* auxiliary) and two NMR spectra should be taken: one of the derivative alone and the other after the addition of  $\text{Ba}^{2+}$  ions. The shifts produced are expressed as  $\Delta\delta^{\text{Ba}} = \delta(\text{MPA ester}) - \delta(\text{MPA ester} + \text{Ba}^{2+})$  and should be positive for one of the substituents and negative for the other. Figure 195 shows the values obtained for some representative examples of known absolute configuration that have been used to test the coherence, reliability, and scope of this approach.

The scheme shown in Figure 196 illustrates graphically the steps that should be followed for the assignment of the absolute configuration of a secondary alcohol by this procedure.

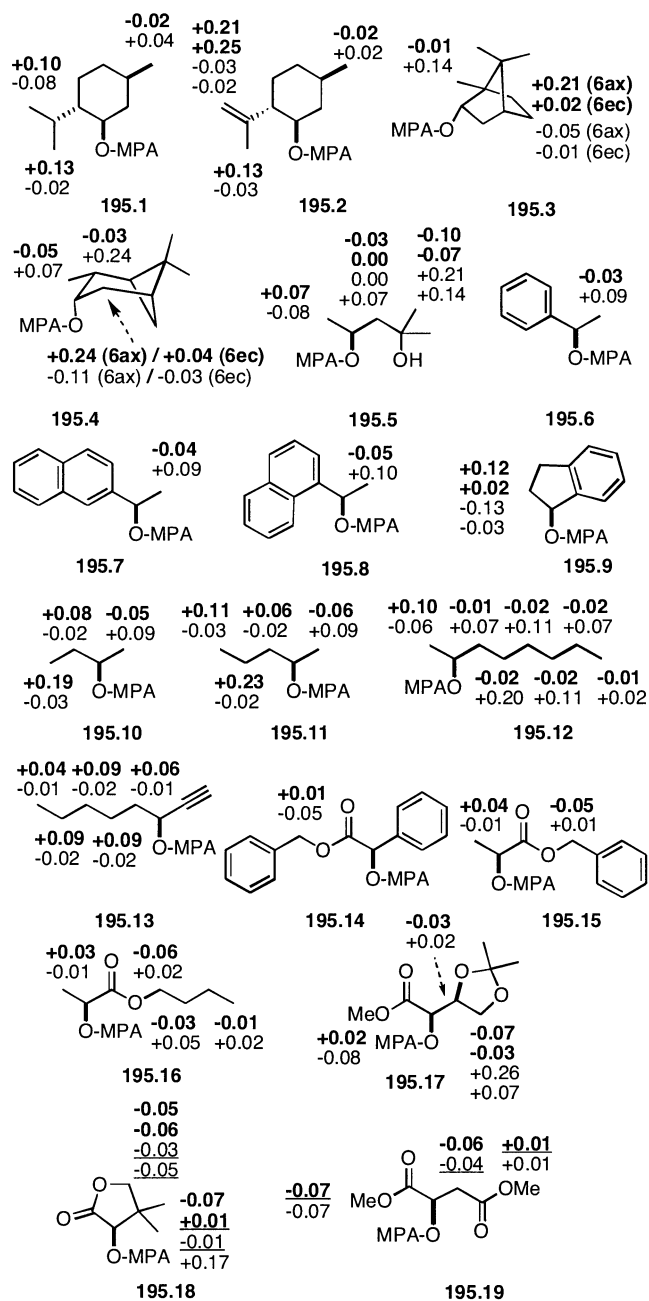
In regard to the limitations of this method, there is an obvious drawback in terms of those substrates in which substituents  $L_1/L_2$  contain functional groups that are able to complex with the  $\text{Ba}^{2+}$  ion. In these cases, there is no guarantee that the general conformational scheme shown in Figure 193 is still operative, and, therefore, safe assignment of the substrate cannot be assured. Examples where competitive chelation occurs because of the presence of extra carbonyl groups (i.e., **195.18** and **195.19** in Figure 195) have been described.<sup>113</sup>

The actual spectra of the (*R*)-MPA ester of diacetone-D-glucose before and after the addition of  $\text{Ba}^{2+}$  ions are shown in Figure 197. Comparison with the spectra for the same compound taken at different temperatures (Figure 191) illustrates the similarity in the shifts generated by both procedures because of the increase in the population of the most stable *sp* conformers.

#### 4.2. Application to $\alpha$ -Chiral Primary Amines: Complexation of MPA Amides with Barium(II)

In a similar way, the absolute configuration of  $\alpha$ -chiral primary amines can be deduced from the NMR complexation effect produced by the addition of a  $\text{Ba}^{2+}$  salt on a single MPA amide, prepared from either (*R*)- or (*S*)-MPA.<sup>77</sup>

In this case, the summarized conformational equilibrium is shown in Figure 198 for an (*R*)-MPA amide. The most stable conformer, in the absence of



(*R*)-MPA (bold), (*S*)-MPA (plain), anomalous signs (underlined)

**Figure 195.** Selected  $\Delta\delta^{\text{Ba}}$  values (in ppm) obtained from the  $^1\text{H}$  NMR spectra of the (*R*)- and (*S*)-MPA esters of structurally representative chiral esters.

any chelating agent, is the *ap* form, where the  $L_2$  substituent is shielded by the phenyl ring of the reagent. Upon addition of a  $\text{Ba}^{2+}$  salt (e.g.,  $\text{Ba}(\text{ClO}_4)_2$ ) to the NMR tube containing the MPA amide (MeCN- $d_3$  as the solvent), changes in the NMR chemical shifts are observed, indicating that the equilibrium is being shifted to the *sp* form ( $L_1$  is now the shielded group). The changes in the chemical shifts of  $L_1$  and  $L_2$  are expressed as  $\Delta\delta^{\text{Ba}} = \delta(\text{MPA amide} + \text{Ba}^{2+}) - \delta(\text{MPA amide})$  and are positive for one substituent and negative for the other. (See Figure 199.)

The scheme shown in Figure 200 illustrates graphically the steps that should be followed for the assignment of the absolute configuration of a primary

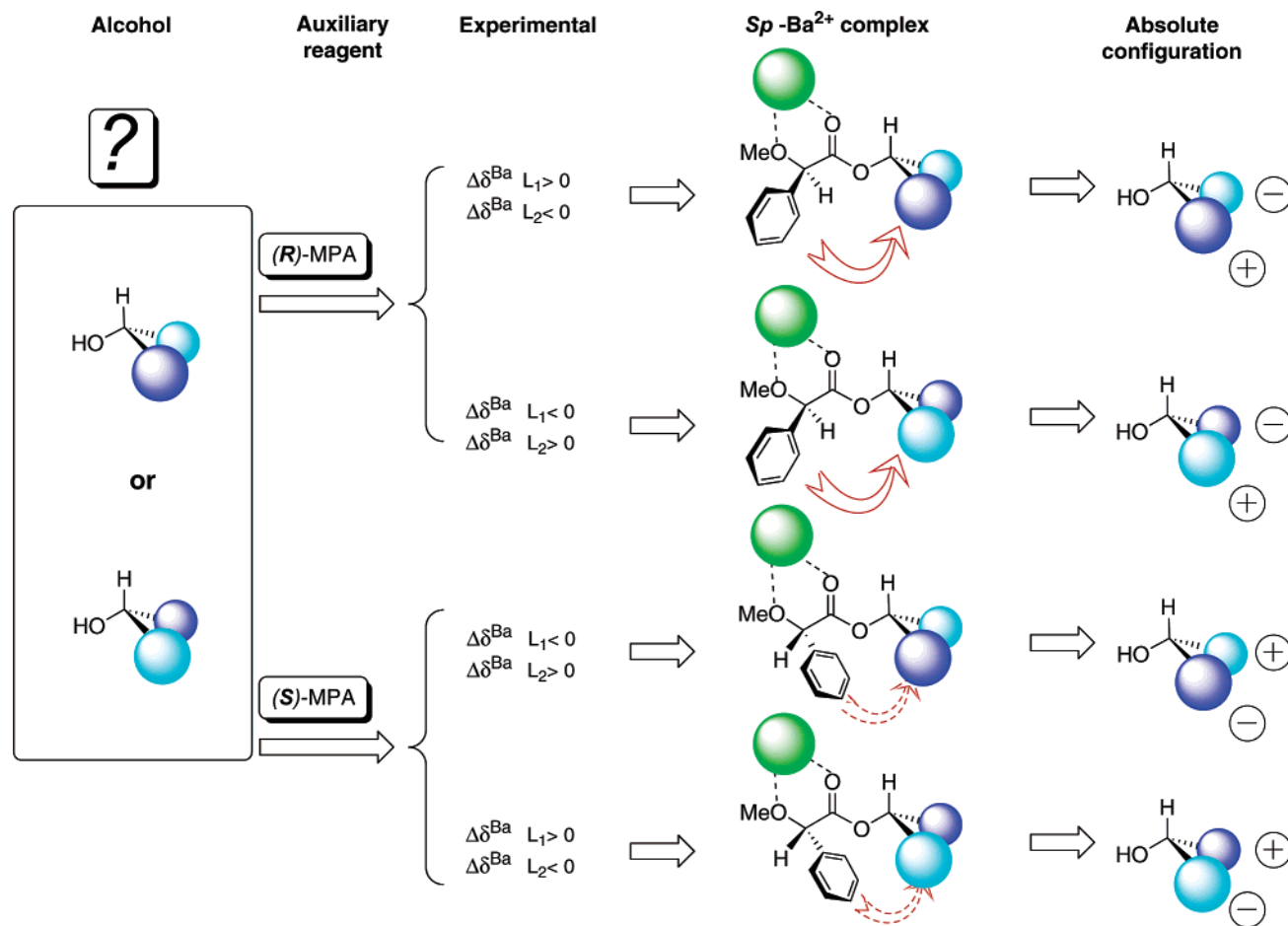


**Figure 196.** Diagram to deduce the absolute configuration of a chiral secondary alcohol from the  $\Delta\delta^{\text{Ba}}$  experimental values of one ester (either the (*R*)- or the (*S*)-MPA derivative).

amine by this method. Figure 201 shows the changes produced in the spectra of the (*R*)-MPA amide of L-valine methyl ester upon the addition of Ba(ClO<sub>4</sub>)<sub>2</sub>.

As discussed previously for MPA esters, amines that have functional groups in substituents L<sub>1</sub>/L<sub>2</sub> that are able to complex with the Ba<sup>2+</sup> ion should not be assigned by this method. 4-Oxo- $\alpha$ -amino acids, such as **202.1** (see Figure 202), are good examples that show the effect of such competitive chelation.<sup>114</sup>

## 5. New Trends

### 5.1. Hyphenated High-Pressure Liquid Chromatography (HPLC) NMR–MS Techniques for Automatization and Microscale Analysis

The development of hyphenated techniques for rapid separation of mixtures and spectroscopic analysis of its components is a topic of great interest, particularly when the amount of sample is limited and the need for automatization is high. This is the case for high-pressure liquid chromatography nuclear magnetic resonance-mass spectroscopy (HPLC NMR–MS), which has been shown to be extremely useful in certain pharmaceutical and medical applications.

Quite recently, Riguera et al. reported<sup>115</sup> that the derivatization of mixtures of enantiomeric secondary alcohols with 9-AMA, followed by tandem HPLC NMR, allows the separation of the enantiomers, the

evaluation of their enantiomeric excess, and the assignment of their absolute configuration at the microscale level and in a single operation.

Two different cases can be distinguished:

(a) If the absolute configuration of each enantiomer in a mixture (including racemic ones) is to be determined, the mixture is derivatized with either (*R*)- or (*S*)-9-AMA, according to standard procedures. The mixture of 9-AMA esters is submitted to HPLC NMR and comparison of the <sup>1</sup>H NMR spectra of the two HPLC peaks allows the assignment of the configuration based on the shielding/deshielding effects caused in substituents L<sub>1</sub>/L<sub>2</sub> by the auxiliary reagent of known configuration (see Figure 203 and Section 3.1.3).

(b) If assignment of the absolute configuration of a single enantiomer is the objective, then the alcohol is derivatized with a 3:1 mixture of (*R*)- and (*S*)-9-AMA. The unequal mixture of 9-AMA esters is subjected to HPLC NMR and the spectra of both peaks are compared, taking into consideration that the major component of the mixture corresponds to the (*R*)-ester and the minor component corresponds to the (*S*)-ester (see Figure 204).

In both cases,  $\ll 1$  mg of the alcohol is needed for derivatization and no more than 10–15  $\mu\text{g}$  of the mixture of 9-AMA esters, dissolved in acetonitrile-

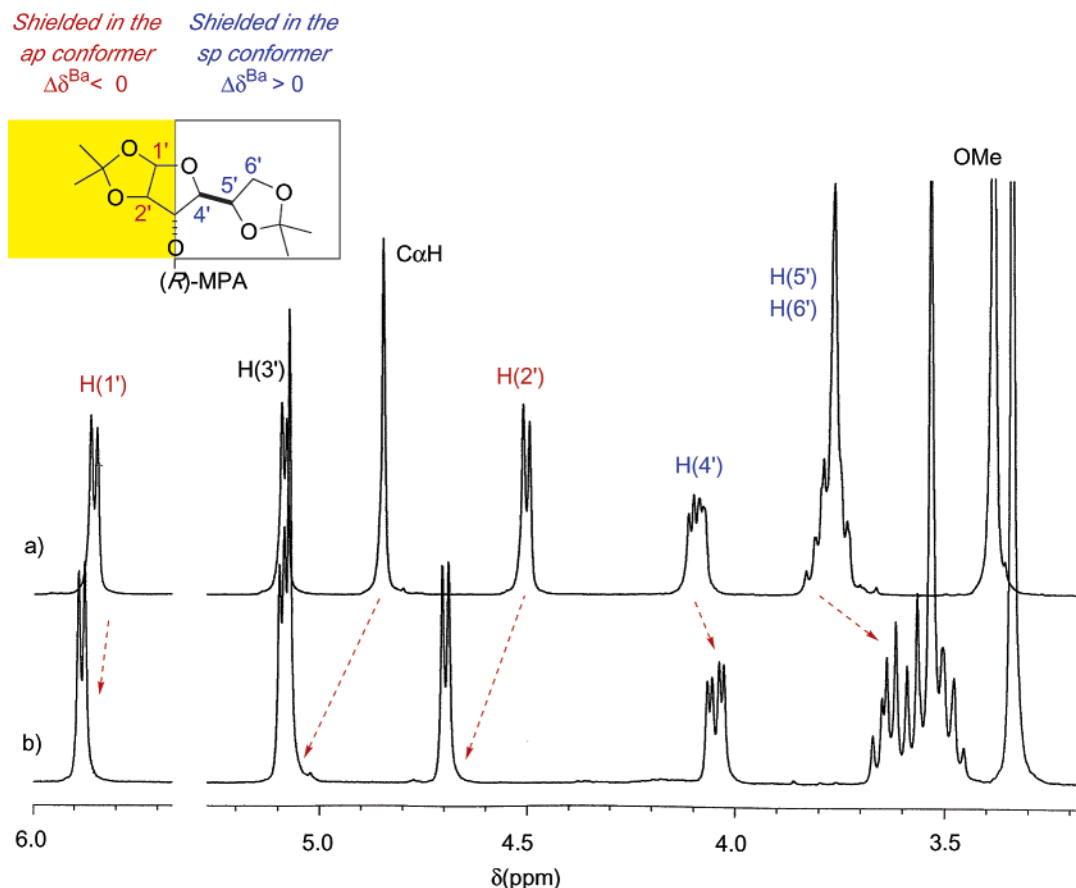


**Figure 197.** Partial  $^1\text{H}$  NMR spectra (250 MHz) for the (*R*)-MPA ester of diacetone-D-glucose (a) before and (b) after the addition of  $\text{Ba}^{2+}$ .

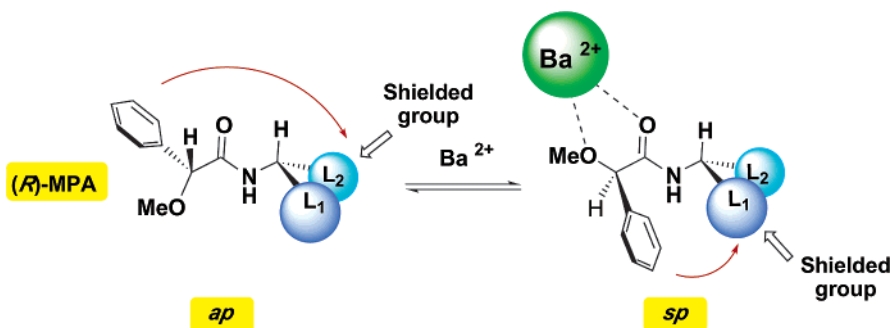


**Figure 198.** Main conformers present in the equilibrium of (*R*)-MPA amides in the absence and presence of a barium(II) salt.

$d_3$ , are injected onto a standard reverse phase column eluted with acetonitrile- $d_3$ /deuterium oxide/formic acid mixtures.

The generality of this approach, including the reliability of the NMR data obtained in acetonitrile- $d_3$ /deuterium oxide/formic acid mixtures instead of deuteriochloroform, was demonstrated by its successful application to the secondary alcohols of known absolute configuration (205.1–205.18, shown in Figure 205, including saturated, unsaturated, aromatic, acyclic, and cyclic compounds).

The authors also mention that if actual isolation of the 9-AMA esters of the enantiomeric alcohols is needed for preparative purposes or else, higher loading can be obtained when the HPLC separation is performed with normal-phase HPLC and provides

experimental conditions and many examples of such separation.

The number and structural variety of the alcohols that have been used to validate the procedure indicate beyond doubt that this methodology is quite general for secondary alcohols and that it can be used in the analytical and semipreparative scales. The simplification involved in the use of the same auxiliary reagent for both the HPLC separation and the NMR configurational assignment, and its implementation in directly coupled HPLC NMR should be extremely useful for the automatization of many processes involving optically active compounds. HPLC NMR has been recently used to purify and analyze the two MTPA esters of a very small sample of a natural product.<sup>116</sup>

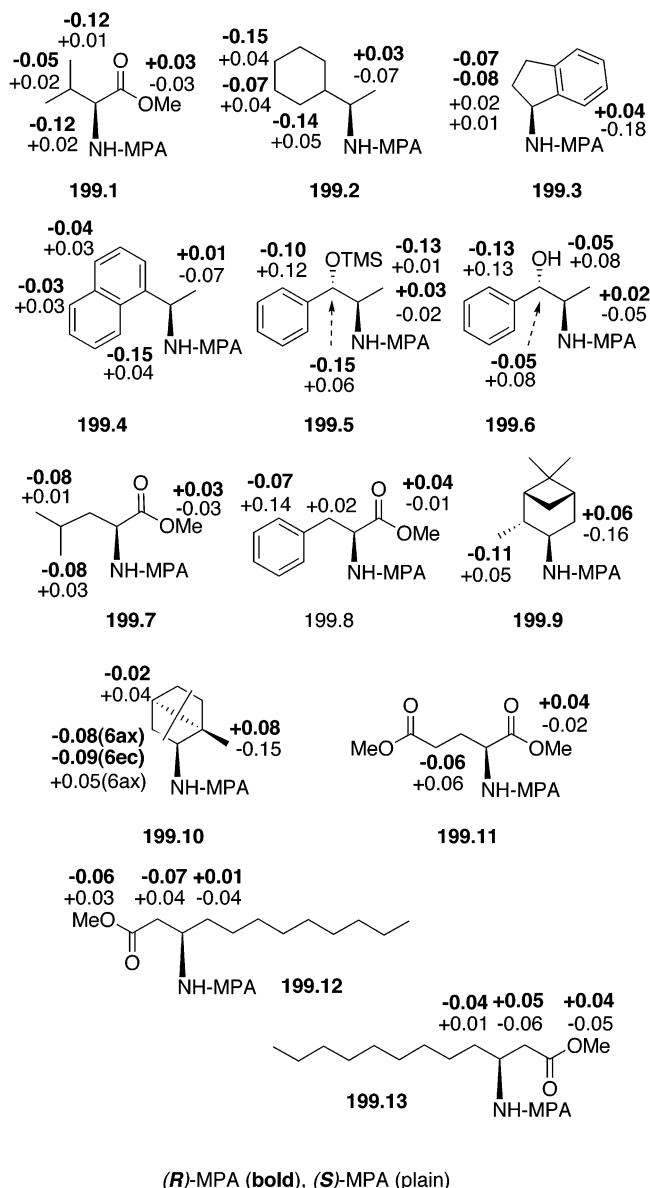


**Figure 199.** Selected  $\Delta\delta^{\text{Ba}}$  values (given in ppm) obtained from the  $^1\text{H}$  NMR spectra of the (*R*)- and (*S*)-MPA amides of structurally representative chiral amines.

## 5.2. Resin-Bound Auxiliaries: The “Mix and Shake” Method

In the search for new ways to simplify the configurational assignment by NMR, a new procedure that allows determining the absolute configuration in just few minutes and without any type of separation, workup, or manipulation being needed has been recently presented.<sup>117</sup> In this approach, the required derivative/s are prepared by simply mixing a solid matrix-bound auxiliary reagent (i.e., MPA, MTPA, or BPG) with the chiral substrate (i.e., a primary amine or a secondary alcohol) directly in the NMR tube and the NMR spectra of the resulting derivatives are obtained without any further manipulation after a few minutes.

The key for the success of this methodology lies in the linking of the auxiliary reagent to the solid matrix through a mixed anhydride group, which allows the auxiliary reagent moiety to act as an electrophile toward the chiral substrate and permits the solid resin to be the leaving group, liberating the ester or amide derivative into the solution (see Figure 206).

Resins containing either a single enantiomer or mixtures of both enantiomers of MPA, MTPA, and BPG, linked through anhydride groups, were prepared from commercial carboxypolystyrene and used to derivatize alcohols and amines. The reaction is performed directly in the NMR tube, in  $\text{CD}_3\text{CD}_2$ , and takes from 5 min (with primary amines) to a few hours (with secondary alcohols), depending on the substrate. After that time, the spectra are recorded as usual, the resin that remains in the tube causes no interference at all, and the assignment of absolute configuration is conducted from the  $\Delta\delta^{\text{RS}}$  signs using the corresponding configurational models (see Section 3 of this review).

The resulting spectrum is sufficiently clean to allow assignment of the absolute stereochemistry at the

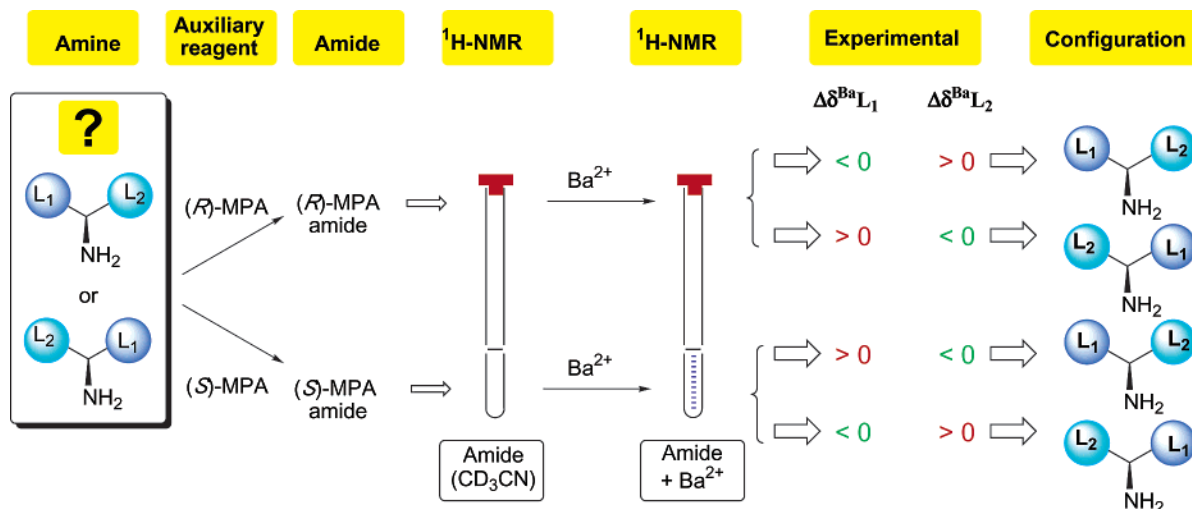


**Figure 200.** Diagram to deduce the absolute configuration of a chiral primary amine from the experimental  $\Delta\delta^{\text{Ba}}$  signs, from either the (*R*)- or (*S*)-MPA amide.

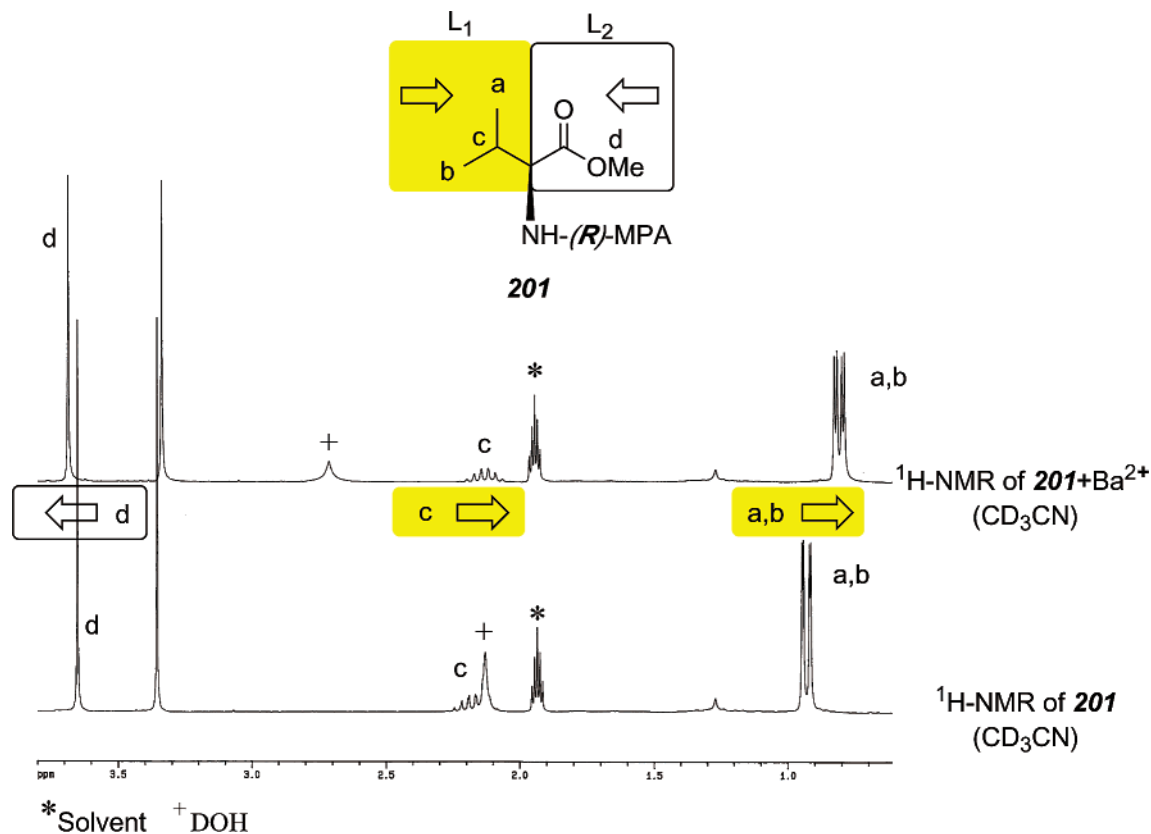


**Figure 201.** Partial <sup>1</sup>H NMR spectra of the (*R*)-MPA amide of L-valine methyl ester in the presence (upper) and absence (bottom) of barium perchlorate. The observed shifts are highlighted.

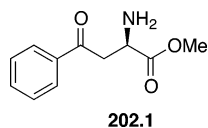


**Figure 202.**

microscale level (<0.5 mg of substrate). In fact, if a 1:2 (*R*)/(*S*)-MPA resin is used, the assignment can be performed in a single operation and by taking just one spectrum because the different ratios of the NMR signals of the two diastereomeric MPA derivatives

(those of the (*R*)-MPA derivative are half the size of those for the (*S*)-derivative) allow the upfield/downfield shifts ( $\Delta\delta^{RS}$ ) to be measured.

Another successful adaptation that makes the usual double derivatization (with (*R*)- and (*S*)-MPA) and recording of two spectra unnecessary is the method based on the complexation of MPA esters or amides with the Ba<sup>2+</sup> ion (see Section 4 of this review). This approach can also be performed directly in the NMR tube with a resin-bound MPA (single enantiomer) in CD<sub>3</sub>CN, although formation of the

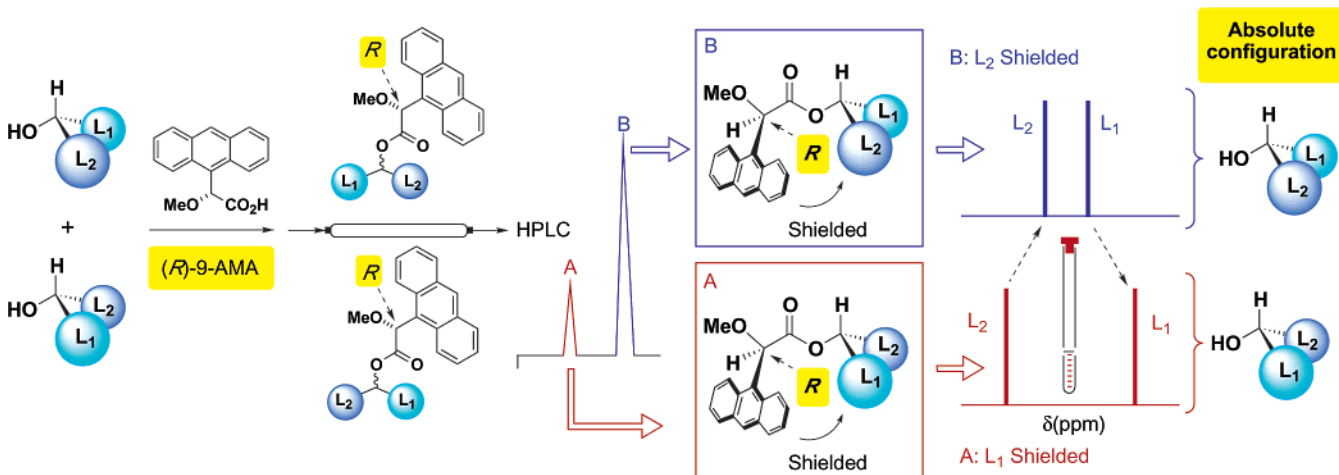


**Figure 203.** Enantioresolution and assignment of the absolute configuration of the enantiomers of a chiral secondary alcohol by tandem HPLC NMR of its (*R*)-9-AMA esters (the assignment is the opposite if (*S*)-9-AMA is chosen as the reagent).



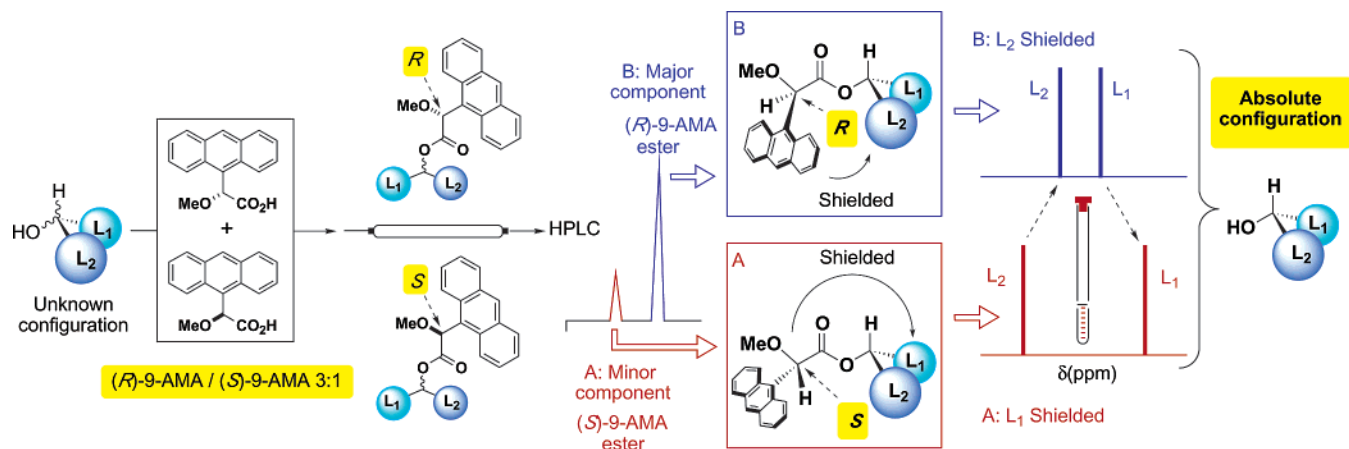


**Figure 204.** Assignment of the absolute configuration of a chiral secondary alcohol by derivatization with a (*R*)-9-AMA/*(S)*-9-AMA 3:1 mixture followed by tandem HPLC NMR of the diastereomeric esters.

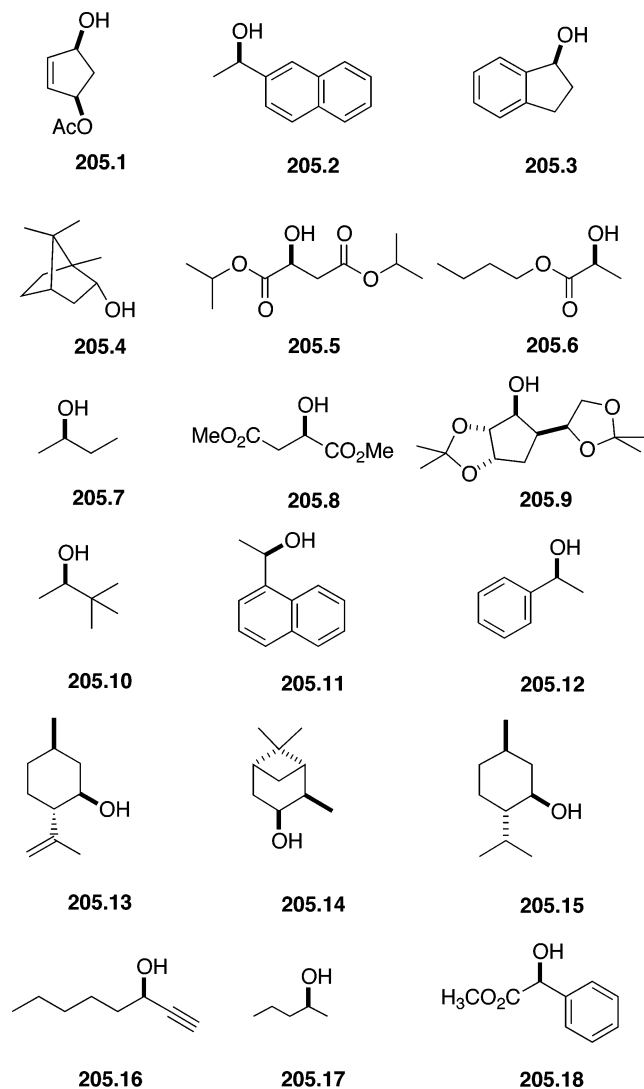


**Figure 205.** Chiral alcohols studied by this method.

derivative in this solvent takes longer time (~90 min) than in  $\text{Cl}_3\text{CD}$ .

A precedent of this methodology can be found in the preparation of a ROMPgel support of activated Mosher ester (MTPA) as a means to performing the purification free synthesis of MTPA amides by the Barrett group.<sup>118</sup>

## 6. Concluding Remarks: A Critical Assessment

The interest of researchers on the use and discovery of procedures for the determination of absolute configuration of organic compounds by NMR is evidently originated by the economy and simplicity of the methods and the wide availability of NMR equipments in all laboratories. These advantages explain the very large number of papers published on this topic that are either devoted to the proposal of new chiral-derivatizing agents (CDAs) or mentioning their application to the configurational assignment of a certain substrate. It is among those working in the field of natural products—plagued with small samples difficult to crystallize—where the application of these techniques is more appreciated and the highest number of papers is found, the same as for those working in the synthesis of chiral compounds.

Nevertheless, the fact that, using these NMR methods, the absolute configuration is determined in solution and that conformational and other structural information related to the through-space anisotropic effect of the reagent is also obtained, wide their applications to other fields.

There are also many publications that have proposed new CDAs; however, researchers should be aware that the reliability of the NMR assignment depends very much on the number and structural variety of the substrates of known absolute configuration that have been used as test compounds to validate the procedure/reagent. Consequently, of the many reagents and procedures described in this review, only a few can be considered to produce reliable assignments, because, in many cases, the number of test compounds is so small that no general behavior can be deduced from the data available.

In the past few years, the experimental data has been frequently complemented with theoretical work (conformational analysis, energy minimization, shielding-effect calculations) and this certainly provided supplementary support to the method/reagent in-

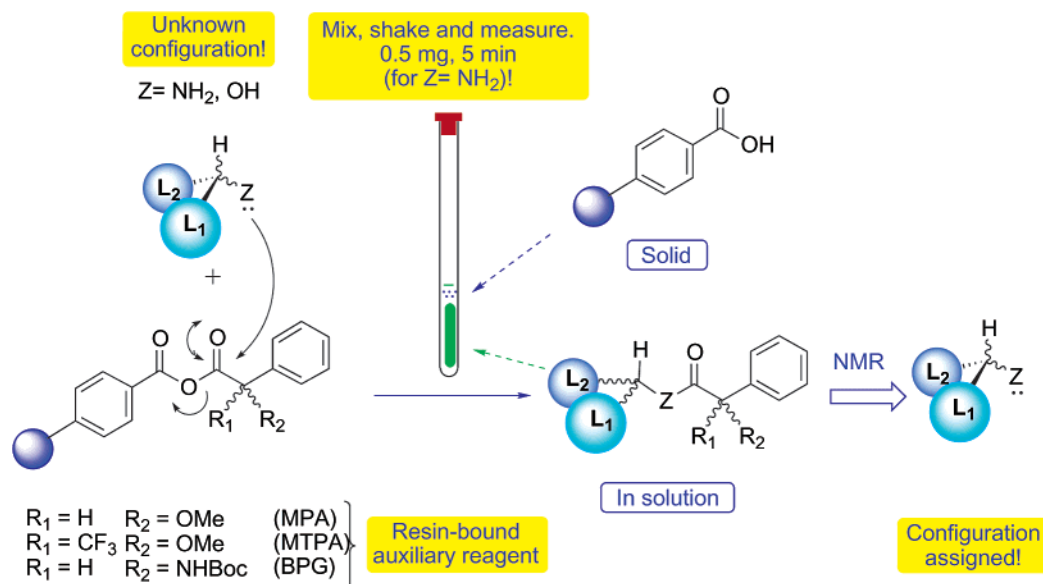


**Figure 206.** MPA, MTPA, and BPG resins used in this “mix and shake” methodology.

involved; however, these calculations also showed that the differences in energy between the derivatives are frequently so small that calculations can in no way replace the use of a collection of compounds of known absolute configuration and representative structures as a test compounds.

In regard to the substrates investigated, most of the efforts have been directed to monofunctional compounds. Secondary alcohols and primary amines have been the most frequently investigated, and although other functional groups were also studied, those remain the most amenable to assignment by NMR procedures. Quite recently, an extension of the procedure to diols has been described, which will surely open the way to the assignment by NMR of other polyfunctional compounds.

Although many procedures that are based on the use of NMR of nucleus different from <sup>1</sup>H (i.e., <sup>19</sup>F, <sup>13</sup>C) have been described and recommended on the basis of the simplified NMR spectra obtained, the low sensitivity of those nuclei to the anisotropic effects produced by the CDA originate very small shifts that overcome that advantage. Nevertheless, the simplification of the spectra renders those reagents very useful when the enantiomeric excess of a mixture (but not the configurational assignment of each enantiomer), is the objective.

Other than papers directed to widen the scope of functional groups amenable to be studied by the NMR procedure, in the past few years, some efforts have been described to simplify the method and reduce the amount of sample. In the classical approach, the chiral substrate should be transformed to two diastereomeric derivatives and their NMR compared. Simplified methods have been described for assignment of the configuration of alcohols and amines that require the preparation of only one derivative and represent evident practical advantages, particularly when only a very small amount

of substrate sample is available. In a paper recently published, the enantioresolution of secondary alcohols (either an unequal or racemic mixture of enantiomers) and the assignment of the absolute configuration of the enantiomers is achieved in a single operation and with just a few micrograms of substrate by tandem HPLC NMR of the 9-AMA derivatives. In another publication by the same group, the simplification of the methodology is attained using solid matrix-bound auxiliaries that allow the derivatization to happen in the NMR tube and within a few minutes. In this way, the NMR spectra can be obtained after just mixing the resin and the substrate without other operations being necessary.

In summary, NMR procedures for assignment of the absolute configuration have evolved in a few decades from the original “Mosher’s method” to a mature field, where a “menu” containing a large number of CDAs is available for the study of different substrates using a variety of approaches. New exciting advances will undoubtedly emerge in the future.

## 7. Acknowledgment

The authors are grateful to Ministerio de Ciencia y Tecnología and Xunta de Galicia for financial support (currently through Grant Nos. BQU2002-01195 and PGIDT02BTF20902PR) and to their co-workers, who have contributed to many of the articles described herein.

## 8. References

- (1) (a) Nakanishi, K.; Berova, N.; Woody, R. W. *Circular Dichroism: Principles and Applications*; VCH Publishers: New York, 1994. (b) Polavarapu, P. L. *Chirality* **2002**, *14*, 768. (c) Wang, F.; Wang, Y.; Polavarapu, P. L.; Li, T.; Drabowicz, J.; Pietrusiewicz, K. M.; Zygo, K. *J. Org. Chem.* **2002**, *67*, 6539. (d) Constante, J.; Hecht, L.; Polavarapu, P. L.; Collet, A.; Barron, L. D. *Angew. Chem., Int. Ed. Engl.* **1997**, *36*, 885.
- (2) Weisman, G. R. Nuclear Magnetic Resonance Analysis Using Chiral Solvating Agents. In *Asymmetric Synthesis*; Morrison, J. D., Ed.; Academic Press: New York, 1983; Vol. 1, p 153.

- (3) (a) Parker, D. *Chem. Rev.* **1991**, *91*, 1441. (b) Rothchild, R. *Enantiomer* **2000**, *5*, 457. (c) Finn, M. G. *Chirality* **2002**, *14*, 534.
- (4) (a) Rinaldi, P. L. *Prog. Nucl. Magn. Spectrosc.* **1982**, *15*, 291. (b) Yamaguchi, S. Nuclear Magnetic Resonance Analysis Using Chiral Derivatives. In *Asymmetric Synthesis*; Morrison, J. D., Ed.; Academic Press: New York, 1983; Vol. 1, p 125.
- (5) Fraser, R. R. Nuclear Magnetic Resonance Analysis Using Chiral Shifts Reagents. In *Asymmetric Synthesis*; Morrison, J. D., Ed.; Academic Press: New York, 1983; Vol. 1, p 173.
- (6) (a) Seco, J. M.; Quiñoá, E.; Riguera, R. *Tetrahedron: Asymmetry* **2001**, *12*, 2915. (b) Uray, G. In *Houben-Weyl Methods in Organic Chemistry*; Helchen, G., Hoffmann, R. W., Mulzer, J., Schaumann, E., Eds.; Thieme: Stuttgart, New York, 1996; Vol. 1, p 253. (c) Eliel, E. L.; Wilen, S. H.; Mander, L. N. *Stereochemistry of Organic Compounds*; Wiley-Interscience: New York, 1994; p 221.
- (7) (a) Raban, N.; Mislow, K. *Tetrahedron Lett.* **1965**, 4249. (b) Raban, N.; Mislow, K. *Topics in Stereochemistry*; Allinger, N. L., Eliel, E. L., Eds.; Wiley-Interscience: New York, 1967; Vol 2, p 199. (c) Jacobus, J.; Raban, N.; Mislow, K. *J. Org. Chem.* **1968**, *33*, 1142.
- (8) (a) Dale, J. A.; Mosher, H. S. *J. Am. Chem. Soc.* **1968**, *90*, 3732. (b) Dale, J. A.; Dull, D. L.; Mosher, H. S. *J. Org. Chem.* **1969**, *34*, 2453. (c) Dale, J. A.; Mosher, H. S. *J. Am. Chem. Soc.* **1973**, *95*, 512. (d) Sullivan, G. R.; Dale, J. A.; Mosher, H. S. *J. Org. Chem.* **1973**, *38*, 2143.
- (9) (a) Joshi, B. S.; Pelletier, S. W. *Heterocycles* **1999**, *51*, 183. (b) Joshi, B. S.; Newton, M. G.; Lee, D. W.; Barber, A. D.; Pelletier, S. W. *Tetrahedron Asymmetry* **1996**, *7*, 25.
- (10) Kusumi, T.; Ohtani, I. Determination of the Absolute Configuration of Biologically Active Compounds by the Modified Mosher's Method. In *The Biology-Chemistry Interface*; Cooper, R., Snyder, J. K., Eds.; Marcel Dekker: New York, 1999; pp 103.
- (11) Pehk, T.; Lippmaa, E.; Loop, M.; Paju, A.; Borer, B. C.; Taylor, R. J. K. *Tetrahedron: Asymmetry* **1983**, *4*, (7), 1572.
- (12) (a) For compound **9.1**, see ref 8a. (b) For compounds **9.2–9.6**, see Ohtani, I.; Kusumi, T.; Kashman, Y.; Kakisawa, H. *J. Am. Chem. Soc.* **1991**, *113*, 4092. (c) For compound **9.7**, see Rieser, M. J.; Hui, Y.; Rupprecht, J. K.; Kozlowski, J. F.; Wood, K. V.; McLaughlin, J. L.; Hanson, P. R.; Zhuang, Z.; Hoye, T. R. *J. Am. Chem. Soc.* **1992**, *114*, 10203.
- (13) Seco, J. M.; Quiñoá, E.; Riguera, R. *Tetrahedron: Asymmetry* **2000**, *11*, 2781.
- (14) (a) Inouye, Y.; Ohtani, I.; Kusumi, T.; Kashman, Y.; Kakisawa, H. *Chem. Lett.* **1990**, 2073. (b) Ohtani, I.; Kusumi, T.; Kashman, Y.; Kakisawa, H. *J. Org. Chem.* **1991**, *56*, 1296.
- (15) Kusumi, T.; Fujita, Y.; Ohtani, I.; Kakisawa, H. *Tetrahedron Lett.* **1991**, *32*, (25), 2923.
- (16) (a) Ohtani, I.; Kusumi, T.; Ishitsuka, M. O.; Kakisawa, H. *Tetrahedron Lett.* **1989**, *30*, (24), 3147. (b) Kusumi, T.; Hamada, T.; Ishitsuka, M. O.; Ohtani, I.; Kakisawa, H. *J. Org. Chem.* **1992**, *57*, 1033.
- (17) (a) Ohtani, I.; Hotta, K.; Ichikawa, Y.; Isobe, M. *Chem. Lett.* **1995**, 513. (b) Kubo, I.; Jamlamadaka, V.; Kamikawa, T.; Takahashi, K.; Kusumi, T. *Chem. Lett.* **1996**, 441.
- (18) Banskota, A. H.; Tezuka, Y.; Tran, K. Q.; Tanaka, K.; Saiki, I.; Kadota, Sh. *J. Nat. Prod.* **2000**, *63*, 57.
- (19) (a) For compound **15.1**, see Suzuki, M.; Takahashi, Y.; Matsuo, Y.; Guiry, M. D.; Masuda, M. *Tetrahedron* **1997**, *53*, 4271. (b) For compound **15.2**, see Ninomiya, M.; Hirohara, H.; Onishi, J.; Kusumi, T. *J. Org. Chem.* **1999**, *64*, 5436. (c) For compound **15.3**, see Amico, V.; Piatelli, M.; Bizzini, M.; Neri, P. *J. Nat. Prod.* **1997**, *60*, 1088. (d) For compound **15.4**, see Shi, X.; Attygalle, A. B.; Livio, A.; Hao, M. H.; Meinwald, J.; Dharmaratne, H. R. W.; Wanigasekera, A. P. *J. Org. Chem.* **1998**, *63*, 1233. (e) For compound **15.5**, see Reese, M. T.; Gulavita, N. K.; Nakao, Y.; Hamann, M. T.; Yoshida, W. Y.; Coval, S. J.; Scheuer, P. J. *J. Am. Chem. Soc.* **1996**, *118*, 11081.
- (20) (a) For compound **16.1**, see Tsuda, M.; Endo, T.; Kobayashi, J. *J. Org. Chem.* **2000**, *65*, 1349. (b) For compound **16.2**, see Kobayashi, J.; Shimbo, K.; Sato, M.; Shiro, M.; Tsuda, M. *Org. Lett.* **2000**, *2*, 2805. (c) For compound **16.3**, see Zhang, Y. J.; Tanaka, T.; Iwamoto, Y.; Yang, C. R.; Kouno, I. *Tetrahedron Lett.* **2000**, *41*, 1781. (d) For compound **16.4**, see Bode, H. B.; Zeeck, A. *J. Chem. Soc., Perkin Trans. 1*, **2000**, 323. (e) For compounds **16.5** and **16.6**, see Jansen, R.; Kunze, B.; Reichenbach, H.; Hofle, G. *Eur. J. Org. Chem.* **2000**, 913.
- (21) (a) For compound **17.1**, see Kim, J. W.; Shin, K.; Furihata, K.; Hayakawa, Y.; Seto, H. *J. Org. Chem.* **1999**, *64*, 153. (b) For compound **17.2**, see Takada, N.; Suenaga, K.; Zheng, S.; Cheng, H.; Uemura, D. *Chem. Lett.* **1999**, 1025. (c) For compound **17.3**, see Tsuda, M.; Endo, T.; Kobayashi, J. *Tetrahedron* **1999**, *55*, 14565. (d) For compound **17.4**, see Ohta, T.; Uwai, K.; Kikuchi, R.; Nozoe, S.; Oshima, Y.; Sasaki, K.; Yoshizaki, F. *Tetrahedron* **1999**, *55*, 12087. (e) For compounds **17.5** and **17.6**, see Gavagnin, M.; Napoli, A.; Cimino, G.; Iken, K.; Avila, C.; García, F. J. *Tetrahedron: Asymmetry* **1999**, *10*, 2647. (f) For compound **17.7**, see Takada, N.; Sato, H.; Suenaga, K.; Arimoto, H.; Yamada, K.; Ueda, K.; Uemura, D. *Tetrahedron Lett.* **1999**, *40*, 6309. (g) For compound **17.8**, see Cheng, X. C.; Jensen, P. R.; Fenical, W. *J. Nat. Prod.* **1999**, *62*, 605.
- (22) (a) For compound **18.1**, see Shigemori, H.; Tenna, M.; Shimazaki, K.; Kobayashi, J. *J. Nat. Prod.* **1998**, *61*, 696. (b) For compounds **18.2** and **18.4**, see Golakoti, T.; Ogino, J.; Heltzel, C. E.; Husebo, T. L.; Jensen, C. M.; Larsen, L. K.; Patterson, G. M. L.; Moore, R. E.; Mooberry, S. L.; Corbett, T. H.; Valeriotte, F. A. *J. Am. Chem. Soc.* **1995**, *117*, 12030. (c) For compound **18.3**, see Dromer, P. G.; Smith, A. B. *Tetrahedron Lett.* **1992**, *33*, 1717. (d) For compound **18.5**, see Tanahashi, T.; Takenaka, Y.; Nagakura, N.; Nishi, T. *J. Nat. Prod.* **1999**, *62*, 1311. (e) For compound **18.6**, see Harrigan, G. G.; Luesch, H.; Yoshida, W. Y.; Moore, R. E.; Nagle, D. G.; Biggs, J.; Park, P. U.; Paul, V. *J. Nat. Prod.* **1999**, *62*, 464. (f) For compound **18.7**, see Moore, B. S.; Chen, J. L.; Patterson, M. L.; Moore, R. E. *Tetrahedron* **1992**, *48*, 3001.
- (23) Kobayashi, J.; Tsuda, M.; Cheng, J.; Ishibashi, M.; Takikawa, H.; Mori, K.; *Tetrahedron Lett.* **1996**, *37*, 6775.
- (24) Tomoda, H.; Nishida, H.; Kim, Y. K.; Obata, R.; Sunazuka, T.; Omura, S. *J. Am. Chem. Soc.* **1994**, *116*, 12097.
- (25) (a) For compound **19.4**, see Sinz, A.; Matusch, R.; Kämpchen, T.; Fiedler, W.; Schmidt, J.; Santisuk, T.; Wangcharoentrakul, S.; Chaichana, S.; Reutrakul, V. *Helv. Chim. Acta* **1998**, *81*, 1608. (b) For compound **19.5**, see Shimada, H.; Nishioka, S.; Singh, S.; Sahai, M.; Fujimoto, Y. *Tetrahedron Lett.* **1994**, *35*, 3961.
- (26) (a) Takagi, Y.; Nakatani, T.; Itoh, T.; Oshiki, T. *Tetrahedron Lett.* **2000**, *41*, 7889. (b) Kelly, D. R. *Tetrahedron: Asymmetry* **1999**, *10*, 2927.
- (27) Latypov, Sh.; Seco, J. M.; Quiñoá, E.; Riguera, R. *J. Org. Chem.* **1996**, *61*, 8569.
- (28) (a) Trost, B. M.; Belletire, J. L.; Goldleski, P. G.; McDougal, P. G.; Balkovec, J. M.; Baldwin, J. J.; Christy, M.; Ponticello, G. S.; Varga, S. L.; Springer, J. P. *J. Org. Chem.* **1986**, *51*, 2370. (b) Trost, B. M.; Curran, D. P. *Tetrahedron Lett.* **1981**, *22*, (49), 4929. (c) Trost, B. M.; O'Krongly, D. O.; Belletire, J. L. *J. Am. Chem. Soc.* **1980**, *102*, 7595.
- (29) Latypov, Sh. K.; Seco, J. M.; Quiñoá, E.; Riguera, R. *J. Org. Chem.* **1995**, *60*, 504.
- (30) Seco, J. M.; Quiñoá, E.; Riguera, R. *Tetrahedron* **1997**, *53*, 8541.
- (31) (a) For compound **33.1**, see Zhou, B. N.; Baj, N. J.; Glass, T. E.; Malone, S.; Werkhoven, M. C. M.; Troon, F.; Wisse, J. H.; Kingston, D. G. I. *J. Nat. Prod.* **1997**, *60*, 1287. (b) For compound **33.2**, see Harrison, B.; Crews, P. *J. Nat. Prod.* **1998**, *61*, 1033. (c) For compound **33.3**, see Gupta, S.; Krasnoff, S. B.; Renwick, J. A. A.; Roberts, D. W. *J. Org. Chem.* **1993**, *58*, 1062. (d) For compound **33.4**, see Adamczeski, M.; Quiñoá, E.; Crews, P. *J. Org. Chem.* **1990**, *55*, 240. (e) For compound **33.5**, see Ulubelen, A.; Gören, N.; Jiang, T. Y.; Scott, L.; Ramomojy, M. T.; Snyder, J. K. *Magnetic Resonance in Chemistry* **1995**, *33*, 900. (f) For compound **33.6**, see Wang, G. Y. S.; Crews, P. *Tetrahedron Lett.* **1996**, *37*, (45), 8145. (g) For compound **33.7**, see Wilson, K. E.; Burk, R. M.; Biftu, T.; Ball, R. G.; Hoogstenn, K. *J. Org. Chem.* **1992**, *57*, 7151. (h) For compound **33.8**, see Gupta, S.; Pleser, G.; Nakajima, T.; Hwang, Y. S.; *Tetrahedron Lett.* **1994**, *35*, 6009. (i) For compound **33.9**, see Alvi, K. A.; Rodríguez, J.; Diaz, M. C.; Moretti, R.; Wilhelm, R. S.; Lee, R. H.; Slate, D. L.; Crews, P. *J. Org. Chem.* **1993**, *58*, 4871. (j) For compound **33.10**, see Vázquez, M. J.; Quiñoá, E.; Riguera, R.; Martín, A. S.; Darias, J. *Liebigs Ann. Chem.* **1993**, 1257. (k) For compound **33.11**, see Galinis, D. L.; Wiemer, D. F. *J. Org. Chem.* **1993**, *58*, 7804.
- (32) Fernández, E.; Ley, S. V. *Chemtracts* **1999**, *12*, 539.
- (33) Seco, J. M.; Latypov, Sh. K.; Quiñoá, E.; Riguera, R. *Tetrahedron Lett.* **1994**, *35*, 2921.
- (34) (a) Chatainer, I.; Lebreton, J.; Durand, D.; Guingant, A.; Villiéras, J. *Tetrahedron Lett.* **1998**, *39*, 1759. (b) Parve, O.; Aidnik, M.; Lille, U.; Martin, I.; Vallikivi, I.; Vares, L.; Pehk, T. *Tetrahedron: Asymmetry* **1998**, *9*, 885.
- (35) Seco, J. M.; Quiñoá, E.; Riguera, R. *Tetrahedron* **1999**, *55*, 569.
- (36) (a) Kusumi, T.; Takahashi, H.; Fukushima, T.; Asakawa, Y.; Hashimoto, T.; Kan, Y.; Inouye, Y. *Tetrahedron Lett.* **1994**, *35*, (25), 4397. (b) Kusumi, T.; Takahashi, H.; Hashimoto, T.; Kan, Y.; Asakawa, Y. *Chem. Lett.* **1994**, 1093. (c) Kimura, M.; Kunoki, A.; Sugai, T. *Tetrahedron: Asymmetry* **2002**, *13*, 1059.
- (37) (a) Kouda, K.; Ooi, T.; Kaya, K.; Kusumi, T. *Tetrahedron Lett.* **1996**, *37*, (35), 6347. (b) Kouda, K.; Kusumi, T.; Ping, X.; Kan, Y.; Hashimoto, T.; Asakawa, Y. *Tetrahedron Lett.* **1996**, *37*, (26), 4541.
- (38) Seco, J. M.; Latypov, Sh. K.; Quiñoá, E.; Riguera, R. *Tetrahedron: Asymmetry* **1995**, *6*, 107.
- (39) Latypov, Sh. K.; Galiullina, N. F.; Aganov, A. V.; Kataev, V. E.; Riguera, R. *Tetrahedron* **2001**, *57*, 2231.
- (40) Lenis, L. A.; Ferreira, M. J.; Debitus, C.; Jiménez, C.; Quiñoá, E.; Riguera, R. *Tetrahedron* **1998**, *54*, 5385.
- (41) (a) For details on compounds **48.1–48.13**, see ref 30. (b) For details on compounds **49.6** and **49.7**, see ref 36a. (d) For details on compound **49.8**, see Watanabe, K.; Tsuda, Y.; Yamane, Y.; Takahashi, H.; Iguchi, K.; Naoki, H.; Fujita, T.; Van Soest, R. W. M. *Tetrahedron Lett.* **2000**, *41*, 9271. (e) For details on compounds **49.9** and **49.10**, see ref 37a.

- (42) (a) For details on compounds **51.1**–**51.3**, see Abad, J. L.; Fabriás, G.; Camps, F. *J. Org. Chem.* **2000**, *65*, 8582. (b) For details on compounds **51.4** and **51.5**, see ref 37b.
- (43) Horeau, A. *Tetrahedron Lett.* **1961**, 506.
- (44) (a) Helmchen, G.; Ott, R.; Sauber, K. *Tetrahedron Lett.* **1972**, 3873. (b) Helmchen, G. *Tetrahedron Lett.* **1974**, 1527.
- (45) (a) Helmchen, G.; Völter, H.; Schüle, W. *Tetrahedron Lett.* **1977**, 1417. (b) Helmchen, G.; Schmierer, R. *Angew. Chem., Int. Ed. Engl.* **1976**, *15*, 703.
- (46) (a) Niederer, D.; Tamm, C.; Zurcher, W. *Tetrahedron Lett.* **1992**, *33*, (28), 3997. (b) Augustiniak, H.; Irschik, H.; Reichenbach, H.; Hofle, G. *Liebigs Ann.* **1996**, 1657. (c) Oh, H.; Gloer, J. B.; Shearer, C. A. *J. Nat. Prod.* **1999**, *62*, 497. (d) Tang, Y. Q.; Sattler, I.; Grabley, S.; Feng, X. Z.; Thiericke, R. *Nat. Prod. Lett.* **2000**, *14*, 341.
- (47) Arnone, A.; Bernardi, R.; Blasco, F.; Cardillo, R.; Resnati, G.; Gerus, I. I.; Kukhar, V. P. *Tetrahedron* **1998**, *54*, 2809.
- (48) Nadkarni, P. J.; Sawant, M. S.; Trivedi, G. K. *Tetrahedron Asymmetry* **1995**, *6*, (8), 2001.
- (49) (a) Harada, N.; Watanabe, M.; Kuwahara, S.; Sugio, A.; Kasai, Y.; Ichikawa, A. *Tetrahedron: Asymmetry* **2000**, *11*, 1249. (b) Fujita, T.; Kuwahara, S.; Watanabe, M.; Harada, N. *Enantiomer* **2002**, *7*, 219. (c) Ichikawa, A.; Hiradate, S.; Sugio, A.; Kuwahara, S.; Watanabe, M.; Harada, N. *Tetrahedron: Asymmetry* **1999**, *10*, 4075. (d) Ichikawa, A.; Hiradate, S.; Sugio, A.; Kuwahara, S.; Watanabe, M.; Harada, N. *Tetrahedron: Asymmetry* **2000**, *11*, 2669. (e) Ichikawa, A.; Ono, H.; Hiradate, S.; Watanabe, M.; Harada, N. *Tetrahedron: Asymmetry* **2002**, *13*, 1167.
- (50) (a) Goto, J.; Hasegawa, M.; Nakamura, S.; Shimada, K.; Nambara, T. *J. Chromatogr.* **1978**, *152*, 413. (b) Goto, J.; Hasegawa, M.; Nakamura, S.; Shimada, K.; Nambara, T. *Chem. Pharm. Bull.* **1977**, *25*, 847.
- (51) (a) Fukushi, Y.; Yajima, C.; Mizutani, J. *Tetrahedron Lett.* **1994**, *35*, (4), 599. (b) Fuhushi, Y.; Yajima, C.; Mizutani, J. *Tetrahedron Lett.* **1994**, *35*, (50), 9417. (c) Latypov, Sh.; Aganov, A. V.; Tahara, S.; Fukushi, Y. *Tetrahedron* **1999**, *55*, 7305.
- (52) Harada, K.; Shimizu, Y.; Kawakami, A.; Fujii, K. *Tetrahedron Lett.* **1999**, *40*, 9081.
- (53) Latypov, S. K.; Riguera, R.; Smith, M. B.; Polivkove, J. *J. Org. Chem.* **1998**, *63*, 8682.
- (54) Oshikawa, T.; Yamashita, M.; Kumagai, S.; Seo, K.; Kobayashi, J. *J. Chem. Soc., Chem. Commun.* **1995**, 435.
- (55) (a) Seo, S.; Tomita, Y.; Tori, K.; Yoshimura, Y. *J. Am. Chem. Soc.* **1978**, *100*, 3331. (b) Seo, S.; Tomita, Y.; Tori, K.; Yoshimura, Y. *J. Am. Chem. Soc.* **1980**, *102*, 2512. (c) Faghieh, R.; Fontaine, C.; Horibe, I.; Imamura, P. M.; Lukacs, G.; Olesker, A.; Seo, S. *J. Org. Chem.* **1985**, *50*, 4918.
- (56) Trujillo, M.; Morales, E. Q.; Vázquez, J. *J. Org. Chem.* **1994**, *59*, 6637.
- (57) Kobayashi, M. *Tetrahedron* **1997**, *53*, 5973.
- (58) (a) Noe, C. E. *Chem. Ber.* **1982**, *115*, 1591. (b) Noe, C. E.; Knollmuller, M.; Oberhauser, B.; Steinbauer, G.; Wagner, W. *Chem. Ber.* **1986**, *119*, 729. (c) Noe, C. E.; Knollmuller, M.; Steinbauer, G.; Jangg, E.; Vollenkle, H. *Chem. Ber.* **1988**, *121*, 1231.
- (59) Takeuchi, Y.; Itoh, N.; Satoh, T.; Koizumi, T.; Yamaguchi, K. *J. Org. Chem.* **1993**, *58*, 1812.
- (60) (a) Apparu, M.; Tiba, Y. B.; Léo, P. M.; Hamman, S.; Coulombeau, C. *Tetrahedron: Asymmetry* **2000**, *11*, 2885. (b) Barrelle, M.; Boyer, L.; Fong, J. C.; Hamman, S. *Tetrahedron: Asymmetry* **1996**, *7*, 1961. (c) Barrelle, M.; Hamman, S. *J. Chem. Res., Synop.* **1990**, 100. (d) Heumann, A.; Faure, R. *J. Org. Chem.* **1993**, *58*, 1276. (e) Takahashi, T.; Fukuishima, A.; Tanaka, Y.; Takeuchi, Y.; Kabuto, K.; Kabuto, C. *Chem. Commun.* **2000**, 788.
- (61) Weibel, D. B.; Walker, T. R.; Schroeder, F. C.; Meinwald, J. *Org. Lett.* **2000**, *2*, 2381.
- (62) (a) Yasuhara, F.; Yamaguchi, S. *Tetrahedron Lett.* **1977**, 4085. (b) Yamaguchi, S.; Yashuara, F.; Kabuto, K. *Tetrahedron* **1976**, *32*, 1363. (c) Yamaguchi, S.; Yashuara, F. *Tetrahedron Lett.* **1977**, 89.
- (63) (a) Sugimoto, Y.; Tsuyuki, T.; Moriyama, Y.; Takahashi, T. *Bull. Chem. Soc. Jpn.* **1980**, *53*, 3723. (b) D'Auria, M. V.; Minale, L.; Pizza, C.; Riccio, R.; Zollo, F. *Gazz. Chim. Ital.* **1984**, *114*, 469. (c) Bruno, I.; Minale, L.; Riccio, R.; La Barre, S.; Laurent, D. *Gazz. Chim. Ital.* **1990**, *120*, 449. (d) Tachibana, K.; Sakaitani, M.; Nakanishi, K. *Tetrahedron* **1985**, *41*, 1027.
- (64) D'Auria, M. V.; De Riccardis, F.; Minale, L.; Riccio, R. *J. Chem. Soc., Perkin Trans. 1*, **1990**, 2889.
- (65) Finamore, E.; Minale, L.; Riccio, R.; Rinaldo, G.; Zollo, F. *J. Org. Chem.* **1991**, *56*, 1146.
- (66) (a) De Riccardis, F.; Minale, L.; Riccio, R.; Giovannitti, B.; Iorizzi, M.; Debitus, C. *Gazz. Chim. Ital.* **1993**, *123*, 79. (b) De Rosa, S.; Milone, A.; Crispino, A.; Jaklin, A.; De Giulio, A. *J. Nat. Prod.* **1997**, *60*, 462. (c) Shigemori, H.; Sato, Y.; Kagata, T.; Kobayashi, J. *J. Nat. Prod.* **1999**, *62*, 372. (d) Tsuda, M.; Endo, T.; Kobayashi, J. *J. Org. Chem.* **2000**, *65*, 1349. (e) Kubota, T.; Tsuda, M.; Kobayashi, J. *J. Org. Chem.* **2002**, *67*, 1651.
- (67) Ramón, D. J.; Guillena, G.; Seebach, D. *Helv. Chim. Acta* **1996**, *79*, 875.
- (68) Ferreiro, M. J.; Latypov, Sh. K.; Quiñoá, E.; Riguera, R. *Tetrahedron: Asymmetry* **1996**, *7*, 2195.
- (69) Latypov, Sh. K.; Ferreiro, M. J.; Quiñoá, E.; Riguera, R. *J. Am. Chem. Soc.* **1998**, *120*, 4771.
- (70) Ciminiello, P.; Dell'Aversano, C.; Fattorusso, E.; Forino, M.; Magno, S.; *Tetrahedron* **2001**, *57*, 8189.
- (71) Izumi, S.; Moriyoshi, H.; Hirata, T. *Bull. Chem. Soc. Jpn.* **1994**, *67*, 2600.
- (72) Takahashi, H.; Kato, N.; Iwashima, M.; Iguchi, K. *Chem. Lett.* **1999**, 1181.
- (73) Kobayashi, M.; *Tetrahedron* **1998**, 10987.
- (74) Kusumi, T.; Fukushima, T.; Ohtani, I.; Kakisawa, H. *Tetrahedron Lett.* **1991**, *32*, 2939.
- (75) Seco, J. M.; Latypov, Sh. K.; Quiñoá, E.; Riguera, R. *J. Org. Chem.* **1997**, *62*, 7569.
- (76) (a) Latypov, Sh. K.; Seco, J. M.; Quiñoá, E.; Riguera, R. *J. Org. Chem.* **1995**, *60*, 1538. (b) Trost, B. M.; Bunt, R. C.; Pulley, S. R. *J. Org. Chem.* **1994**, *59*, 4202.
- (77) López, B.; Quiñoá, E.; Riguera, R. *J. Am. Chem. Soc.* **1999**, *121*, 9724.
- (78) Seco, J. M.; Quiñoá, E.; Riguera, R. *J. Org. Chem.* **1999**, *64*, 4669.
- (79) Pirkle, W. H.; Simmons, K. A. *J. Org. Chem.* **1981**, *46*, 3239.
- (80) (a) Polh, L. R.; Trager, W. F. *J. Med. Chem.* **1973**, *16*, 475. (b) Valente, E. J.; Polh, L. R.; Trager, W. F. *J. Org. Chem.* **1980**, *45*, 543.
- (81) Harada, K.; Shimizu, Y.; Fujii, K. *Tetrahedron Lett.* **1998**, *39*, 6245.
- (82) Chinchilla, R.; Falvello, L. R.; Nájera, C. *J. Org. Chem.* **1996**, *61*, 7285.
- (83) Chinchilla, R.; Falvello, L. R.; Nájera, C.; Yus, M. *Tetrahedron: Asymmetry* **1995**, *6*, 1877.
- (84) Fujiwara, T.; Omata, K.; Kabuto, K.; Kabuto, C.; Takahashi, T.; Segawa, M.; Takeuchi, Y. *Chem. Commun.* **2001**, 2694.
- (85) (a) Hoye, T. R.; Renner, M. K. *J. Org. Chem.* **1996**, *61*, 8489. (b) Hoye, T. R.; Renner, M. K. *J. Org. Chem.* **1996**, *61*, 2056.
- (86) (a) Stewart, W. E.; Siddall, T. H. *Chem. Rev.* **1970**, *70*, 517. (b) Jacobus, J.; Jones, T. B. *J. Am. Chem. Soc.* **1970**, *92*, 4583.
- (87) (a) Ferreiro, M. J.; Latypov, S. K.; Quiñoá, E.; Riguera, R. *Tetrahedron: Asymmetry* **1997**, *8*, 1015. (b) Ferreiro, M. J.; Latypov, S. K.; Quiñoá, E.; Riguera, R. *J. Org. Chem.* **2000**, *65*, 2658.
- (88) Tyrrell, E.; Tsang, M. W. H.; Skinner, G. A.; Fawcett, J. *Tetrahedron* **1996**, *52*, 9841.
- (89) (a) Nagai, Y.; Kusumi, T. *Tetrahedron Lett.* **1995**, *36*, 1853. (b) Yabuuchi, T.; Kusumi, T. *J. Org. Chem.* **2000**, *65*, 397.
- (90) Yabuuchi, T.; Ooi, T.; Kusumi, T. *Chirality* **1997**, *9*, 550.
- (91) (a) Cafieri, F.; Fattorusso, E.; Tagliatalata-Scafati, O. *Tetrahedron* **1999**, *55*, 7045. (b) Singh, S. B.; Zink, D.; Polishook, J.; Valentino, D.; Shafiee, A.; Silverman, K.; Felock, P.; Teran, A.; Vilella, D.; Hazuda, D. J.; Lingham, R. B. *Tetrahedron Lett.* **1999**, *40*, 8775. (c) Ciminiello, P.; Fattorusso, E.; Forino, M.; Poletti, R.; Viviani, R. *Eur. J. Org. Chem.* **2000**, 291.
- (92) (a) Sasaki, K.; Satake, M.; Yasumoto, T. *Biosci., Biotechnol., Biochem.* **1997**, *61*, 1783. (b) Yabuuchi, T.; Kusumi, T. *J. Org. Chem.* **2000**, *65*, 397.
- (93) Singh, I. P.; Milligan, K. M.; Gerwick, W. H. *J. Nat. Prod.* **1999**, *62*, 1333.
- (94) Yabuuchi, T.; Kusumi, T. *J. Org. Chem.* **2000**, *65*, 397.
- (95) Sata, N. U.; Wada, S.; Matsunaga, S.; Watabe, S.; van Soest, R. W. M.; Fusetani, N. *J. Org. Chem.* **1999**, *64*, 2331.
- (96) Fukushi, Y.; Shigematsu, K.; Mizutani, J.; Tahara, S. *Tetrahedron Lett.* **1996**, *37*, 4737.
- (97) Hoye, T. R.; Koltun, D. O. *J. Am. Chem. Soc.* **1998**, *120*, 4638.
- (98) Hoye, T. R.; Hamad, A.-S. S.; Koltun, D. O.; Tennakoon, M. A. *Tetrahedron Lett.* **2000**, *41*, 2289.
- (99) (a) Toki, M.; Ooi, T.; Kusumi, T. *J. Nat. Prod.* **1999**, *62*, 1504. (b) Morohashi, A.; Satake, M.; Nagai, H.; Oshima, Y.; Yasumoto, T. *Tetrahedron* **2000**, *56*, 8995.
- (100) Yabuuchi, T.; Kusumi, T. *J. Am. Chem. Soc.* **1999**, *121*, 10646.
- (101) Kobayashi, M.; Aoki, S.; Kitagawa, I. *Tetrahedron Lett.* **1994**, *35*, 1243.
- (102) (a) Duret, P.; Waechter, A.; Figadère, B.; Hocquemiller, R.; Cavé, A. *J. Org. Chem.* **1998**, *63*, 4717. (b) Alali, F.; Zeng, L.; Zhang, Y.; Ye, Q.; Hopp, D. C.; Schewedler, J. T.; McLaughlin, J. L. *Bioorg. Med. Chem.* **1997**, *5*, 549. (c) Jiang, Z.; Yu, D.-Q. *J. Nat. Prod.* **1997**, *60*, 122.
- (103) Lee, J.; Li, J.-H.; Oya, S.; Snyder, J. K. *J. Org. Chem.* **1992**, *57*, 5301.
- (104) Rodriguez, J.; Riguera, R.; Debitus, C. *J. Org. Chem.* **1992**, *57*, 4624.
- (105) (a) Seco, J. M.; Martino, M.; Quiñoá, E.; Riguera, R. *Org. Lett.* **2000**, *2*, 3261. (b) Authors' laboratory; unpublished results.
- (106) Woo, M. H.; Cho, K. Y.; Zhang, Y.; Zeng, L.; Gu, Z.-M.; McLaughlin, J. L. *J. Nat. Prod.* **1995**, *58*, 1533.
- (107) (a) Ichikawa, A.; Takahashi, H.; Ooi, T.; Kusumi, T. *Biosci., Biotechnol., Biochem.* **1997**, *61*, 881. (b) Ichikawa, A. *Enantiomer* **1997**, *2*, 327.
- (108) Ichikawa, A. *Enantiomer* **1998**, *3*, 255.

- (109) Konno, K.; Fujishima, T.; Liu, Z.; Takayama, H. *Chirality* **2002**, *13*, 72.
- (110) (a) Riccio, R.; Santaniello, M.; Greco, O. S.; Minale, L. *J. Chem. Soc., Perkin Trans. 1* **1989**, 823. (b) De Riccardis, F.; Izzo, I.; Iorizzi, M.; Palagiano, E.; Minale, L.; Riccio, R. *J. Nat. Prod.* **1996**, *59*, 386. (c) Ukiya, M.; Akihisa, T.; Motohashi, S.; Yasukawa, K.; Kimura, Y.; Kasahara, Y.; Takido, M.; Tokutake, N. *Chem. Pharm. Bull.* **2000**, *48*, 1187.
- (111) Yamase, H.; Ooi, T.; Kusumi, T. *Tetrahedron Lett.* **1998**, *39*, 8113.
- (112) (a) Latypov, S. K.; Seco, J. M.; Quiñoá, E.; Riguera, R. *J. Am. Chem. Soc.* **1998**, *120*, 877. (b) Williamson, R. T.; Boulanger, A.; Vulpanovici, A.; Roberts, M. A.; Gerwick, W. H. *J. Org. Chem.* **2002**, *67*, 7927.
- (113) García, R.; Seco, J. M.; Vázquez, S. A.; Quiñoá, E.; Riguera, R. *J. Org. Chem.* **2002**, *67*, 4579.
- (114) Earle, M. A.; Hultin, P. G. *Tetrahedron Lett.* **2000**, *41*, 7855.
- (115) Seco, J. M.; Tseng, L. H.; Godejohann, M.; Quiñoá, E.; Riguera, R. *Tetrahedron: Asymmetry* **2002**, *13*, 2149.
- (116) Guilet, D.; Guntern, A.; Ioset, J.-R.; Queiroz, E. F.; Ndjoko, K.; Foggín, C. M.; Hostettmann, K. *J. Nat. Prod.* **2003**, *66*, 17.
- (117) Porto, S.; Durán, J.; Seco, J. M.; Quiñoá, E.; Riguera, R. *Org. Lett.* **2003**, *5*, 2979.
- (118) Arnauld, T.; Barrett, A. G. M.; Hopkins, B. T.; Zécri, F. *Tetrahedron Lett.* **2001**, *42*, 8215.

CR000665J

